THE FREE RADICAL POLYMERIZATION OF METHYL METHACRYLATE TO HIGH CONVERSIONS

BY

STEPHEN THOMAS BALKE, B. Eng.

A Thesis

Submitted to the Faculty of Graduate Studies

in Partial Fulfilment of the Requirements

for the Degree

Doctor of Philosophy

McMaster University

August 1972

DOCTOR OF PHILOSOPHY (1972)
(Chemical Engineering)

McMASTER UNIVERSITY,
Hamilton, Ontario

TITLE : The Free Radical Polymerization of Methyl Methacrylate to High Conversions

AUTHOR : Stephen Thomas Balke

B.Eng.(Chem.) (Royal Military College)

SUPERVISOR : Professor A. E. Hamielec

NUMBER OF PAGES : I-135, II-96, III-39

SCOPE AND CONTENTS :

This dissertation describes an investigation into the free radical batch polymerization of methyl methacrylate to high conversion. The overall objective was to develop a kinetic model to accurately predict conversion and molecular weight distribution for the polymerization. The dissertation is divided into three self-contained parts.

Part I describes the development and testing of the kinetic model. New gel permeation chromatograph (GPC) data interpretation methods (developed in Part II), the free volume concept of diffusion theory, and newly obtained isothermal kinetic data, are combined with computer implemented optimization techniques, to show that classical kinetics apply to high conversions.

Part II details the development of three new GPC interpretation techniques. The two most recent are evaluated in Part I. The third has been used by other workers. Other interpretation methods are also evaluated and discussed.

Part III describes the development of a high shear concentric cylinder viscometer and its use with Newtonian standards. This is a prelude to future studies in polymer rheology and polymerization under shear conditions.

ACKNOWLEDGEMENTS

The author wishes to express his gratitude and appreciation to those who contributed to this study. In particular, he is indebted to:

His research director, Dr. A. E. Hamielec, for his enthusiasm, interest and guidance throughout the work.

The members of the Ph.D. Supervisory Committee: Dr. A. J. Yarwood and Dr. W. K. Lu for their advice and encouragement.

The Chemical Engineering Department, McMaster University for providing the necessary enthusiastic environment and adequate finances to accomplish the research.

Dr. S. P. Sood and Dr. A. W. T. Hui for their helpful discussions regarding high vacuum technology.

Dr. J. H. Duerksen for providing blueprints for the high shear concentric cylinder viscometer.

S. K. Vig for performing some of the GPC analyses.

Xerox Corporation, and in particular, Dr. J. C. Goldfrank, for providing time and resources to permit rapid completion of the thesis.

Mrs. Wendy Coniglio for her careful and thoughtful work in typing this dissertation.

Finally, to my wife, Madeleine, for her perpetual, and very necessary, understanding attitude.

TABLE OF CONTENTS

THE FREE RADICAL POLYMERIZATION
OF
METHYL METHACRYLATE
TO
HIGH CONVERSIONS

TABLE INDEX

FIGURE INDEX

INTRODUCTION

Polymer technology has developed tremendously in the past three decades, as the uses of polymers in society have multiplied. Nevertheless, the technology in the processing of polymers remains empirical. The basic reason for this, is that not only are many important fundamental properties of these materials very difficult to measure, but the reaction mechanisms and flow behavior in processing which yield these qualities are very complex.

The aim of the chemical engineer working in the polymer area is to treat only those parts of the mechanism which are essential to obtaining a product with desired physical properties. In order to recognize and so simplify the situation in a reasonable way, today's chemical engineer in polymers requires a broad background in the polymer area. The scope of this research project was chosen with this requirement in mind.

The advent of the high speed computer and of new analytical instruments have greatly assisted the scientific approach over the purely empirical approach in the engineering of polymers. Methods of applying these new aids to the problems involved urgently require further exploration and development on a broad front. The overall objective of this work was to help satisfy this need by investigating, under the general title, "The Free Radical Polymerization of Methyl Methacrylate to High Conversions", three related areas: Polymerization Kinetics, Gel Permeation Chromatography, and High Shear Viscometry.

The dissertation is divided into three parts, one corresponding to each of the above areas. Part I, the main concern of the polymer chemist, describes the development of polymerization kinetics to high conversions. Part II, the main concern of the analytical chemist, describes the development of Gel Permeation Chromatography as an extremely useful analytical instrument for polymers. Part III, the main concern of the polymer rheologist, describes development of a high shear viscometer as a prelude to polymer rheology and polymerization kinetics under shear conditions.

PART I

DEVELOPMENT OF POLYMERIZATION KINETICS

1. Introduction

The more fundamental polymer properties often of importance to the chemical engineer are concentration, molecular weight distribution, branching and stereoregularity. These are the result of the elementary reactions occurring in polymerization and their respective rates. In transient (batch) free radical vinyl polymerization much work has been done to establish the reaction mechanism at low conversions (less than 10%). However, there are still considerable disagreements between laboratories. Beyond low conversions, diffusion control of some reactions in the mechanism coupled with experimental difficulties has severely hindered progress in kinetic modelling.[1,2,3]

This study involved the theoretical and experimental investigation of the transient bulk free radical polymerization of methyl methacrylate (MMA) to high conversions using conditions of interest to industry (high initiator concentrations and high temperatures). In the following sections the conventional kinetic model is described. Experimental methods of obtaining rate data along with ways of applying the model to this data so as to predict conversion and molecular weight distribution are developed and evaluated.

2. Literature Review--The Conventional Kinetic Model for Free Radical Polymerization

2.1 Description

A general description of the conventional kinetic model for free radical polymerization is as follows:

Reaction Step		Reaction
Initiation	(I-1)	$\text{Initiation} \rightarrow R_1^o$
Propagation	(I-2)	$R_r^o + M \xrightarrow{k_p} R_{r+1}^o$
Transfer	(I-3)	$R_s^o + X_r \xrightarrow{k_{fx}} P_s + X_r^o$
Reinitiation by Transfer Radicals	(I-4)	$X_r^o + M \xrightarrow{k_{px}} R_r^o$
Termination	(I-5)	$R_r^o + R_s^o \xrightarrow{k_{tc}} P_{r+s}$
	(I-6)	$R_r^o + R_s^o \xrightarrow{k_{td}} P_r + P_s$
Terminal Double Bond Polymerization	(I-7)	$P_r + R_s^o \xrightarrow{k_p^*} R_{r+s}^o$

where R_r^o is a free radical of chain length r, P_r is a dead polymer molecule of chain length r. M is monomer. X_r, the transfer agent in bulk polymerization, may be monomer, initiator, or polymer (for all but the latter, the R_r^o produced by (I-4) is considered R_1^o).

It should be noted that the initiation step of the model is very general, and both type of initiation, as well as its efficiency (i.e. the fraction of free radicals produced by the initiator which actually initiate polymer chains) are included in one parameter, I. The rate of consumption of monomer by the reactions determine the conversion. The concentration of dead polymer of each chain length, together, determine the molecular weight distribution.

2.2 The Polymerization of Methy Methacrylate

2.2.1 Initiation

2.2.1.1 Thermal Initiation

This reaction is favored by high temperatures, but is generally considered only 1% as fast as styrene thermal polymerization.[1,4] However, the actual mechanism is considered unknown. Reproducible rates have proven difficult to obtain because of the influence of trace impurities.

2.2.1.2 Chemical Initiation

The initiator used in this study, Azobisisobutyronitrile (AIBN), is a popular one.[1-3] The first order decomposition constant (k_d) of AIBN in low viscosity solvents has been determined by many workers using such methods as nitrogen evolution and U.V. absorption. Values agree within about 10%.[5] (i.e. 95% of the measurements fall within $\pm$ 10% of the mean value). Recently[6-8] k_d has been found to decrease as viscosity increases in contrast to other studies.[9]

The initiator efficiency of AIBN has been determined by numerous methods which compare the number of chains initiated with the number of free radicals produced.[1-4] Values of .5 to .7 were obtained at 50°C to 77°C and at low viscosity. As viscosity increases, Messerle[6-8] by direct measurement and Nishimura,[10] Robertson,[11] Hui,[12] and Duerksen[13] by progressively more sophisticated extraction of the value from the kinetic model found the efficiency to decrease.

2.2.2 Propagation

The propagation reaction of MMA is

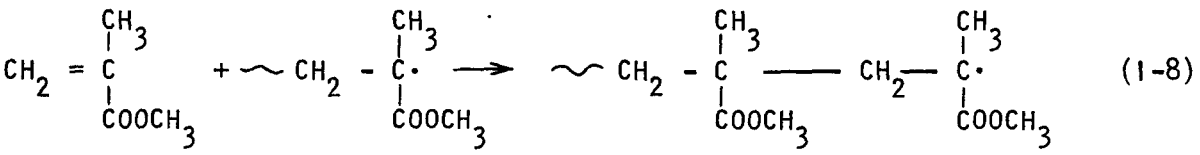

(I-8)

The propagation reactions determine the stereoregularity of the resulting polymer. This is discussed in Appendix I-A.

Several techniques have been applied to MMA polymerization to extract rate constants at low conversion. Usually two different experiments are performed which give some ratio of k_p to k_t so that together the individual values of the rate constants can be determined.[1-4] The rotating sector method combined with rate of initiation measurement has been used by several workers.[5] Experimental error leads values of k_p to k_t to sometimes differ by a factor of five between laboratories. Measurements of the pre-effect and the post-effect in photopolymerization by measurement of shrinkage, index of refraction, temperature or intrinsic viscosity have been made, with similar results.[5]

At about 55 to 70% conversion the propagation reaction becomes diffusion controlled.[14] A maximum limiting conversion[15-18] is reached which depends on temperature and which indicates that propagation has completely ceased because of the high viscosity.

2.2.3 Termination

The termination reaction is the most studied in the model because: one of two termination reactions, combination (Equation (I-9)) and disproportionation (Equation (I-10)), may predominate depending on conditions[4] and; termination contributes heavily to the extreme acceleration of rate of

polymerization observed to commence at about 20% conversion.[14,19]

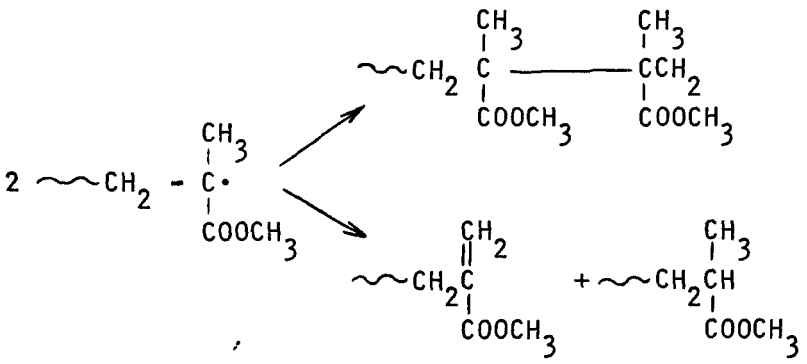

(I-9)

(I-10)

Because PMMA has five hydrogen atoms available for disproportionation, and because a strained bond is formed if combination occurs due to the two bulky groups in proximity to each other, it is considered likely that disproportionation is predominant at higher temperatures.[4] However, despite many studies,[1-4] the relative importance of disproportionation and combination is still uncertain. The presence of transfer reactions and inaccuracies in experimental technique are the main reasons for the lack of agreement.

Low conversion values of k_t have been determined by assuming either combination or disproportionation alone was operating and using rotating sector or unsteady state methods.[5] High conversion k_t values have been obtained with values of initiator efficiency from kinetic equations.[11] As conversion, and hence viscosity, increases, k_t decreases. This decrease while the value of k_p remains constant results in the sudden high rate of reaction at about 20% conversion which is known as the "Viscosity" or "Trommsdorf" or "Gel" effect. This cause for the acceleration has been shown by using different temperatures,[20] employing lower viscosity solvents,[21] adding preformed polymer to the monomer,[22] and by applying low conversion kinetic schemes.[23-26]

Theoretical attempts to predict the variation of k_t with viscosity and its variation with chain length have centered about the Smoluchowski Equation (derived from a simple mass balance and extended by North),[14] and the Rabinowitch Equation[27] (derived by assuming reactant molecules undergo disconnected jump displacements). Allen[28] pointed out serious limitations in both these approaches, in that the first is based on a non-existent concentration gradient, and the second is applicable only where all the molecules are of the same size and shape. Attempts were made to use the equations to predict the viscosity at which acceleration of rate should begin.[15,29,30] Both North[31] and Patrick[32] have shown that the viscosity of a polymer solution is not an indication of the diffusion process except at very low concentrations because of entanglement effects. Other evidence also dictates against the attempts to predict viscosity and indicates that the termination reaction is diffusion controlled even at zero conversion.[14]

By measuring self and mutual diffusion coefficients with k_t, North[33] showed that the termination mechanism depended on the diffusion of the active chain ends out of the polymer coil rather than a translational diffusion of the center of gravity of the chain.

Termination by primary radicals is favored by high viscosities, low temperatures and high initiator concentrations.[4] Baldwin[34] showed that under favorable conditions it could be very significant in MMA polymerization. Chain length dependence and primary radical termination is discussed further in Appendix I-B.

2.2.4 Transfer and Terminal Double Bond Polymerization

Transfer depends on the bond strengths of the carbon hydrogen bonds available and on the stability of the resulting free radical.[4] Transfer rate constants are generally evaluated by application of the kinetic model at low conversions and measurement of number average molecular weight, rate of polymerization, initiator and monomer concentration.[1-5]

Transfer to MMA is less than to styrene.[5] Transfer to AIBN is generally considered negligible.[5] Recently Smith and May,[35,36] using GPC, and Pryor[37] radioactive tracer methods, have disagreed with all previous workers by postulating significant transfer to AIBN. At least in Smith's case this can easily be attributed to inaccurate GPC analysis.

Transfer to middle functional groups in the polymer chain is the reaction considered to be responsible for any branching in PMMA.[38] Crosslinking results if branched molecules combine (but not if they disproportionate). At low conversions transfer to polymer is insignificant because of the negligible quantity of polymer present. Ultracentrifuge measurements[39,40] and solubility[41] indicated that high conversion PMMA could be branched. Pyrkov et. al.[42] showed that transfer to polymer might result in fracture of the chain and then a number of other reactions were possible. Tasset et. al.[43] showed that such fracture could be induced in PMMA.

Schulz and Henrici Olive[44-46] studied transfer to polymer at low conversions by adding characterized oligomer to the reaction mixture. Morton[47] carried out a similar procedure. More recently, Krause et. al[38] fractionated high conversion PMMA and calculated Zimm's "g factor", both from light scattering (radius of gyration) data, and by intrinsic viscosity

measurements. These investigations[38,44-47] showed that high conversion PMMA is likely linear ($C_p \approx 2.2 \times 10^{-5}$), and that impurities in the chain which can lead to branching sites, can be removed through distillation of the original monomer.

Transfer to a polymer group at the end of a chain, or polymerization commencing at a chain end double bond, resulting from disproportionation ("terminal double bond polymerization") or transfer to monomer, may not cause the formation of a branched molecule, but could result in an appreciable increase in molecular weight averages with conversion at high conversion. This was shown by Graessley et. al.[48,49] for vinyl acetate polymerization. Schulz and Henrici Olive[44-46] applied the Mayo equation to MMA polymerization in the presence of oligomers of known but different degrees of polymerization and concluded that the end groups of the polymer molecule were more reactive in transfer than the center groups. No estimate of the importance of terminal double bond polymerization for MMA has been published. However, it is evident that the importance of both of the above reactions depend upon the concentration of suitable end groups. High molecular weights and linear molecules would tend to decrease their importance. Furthermore, if the reactions often involve the ends of long chain linear molecules they are likely subject to retardation by diffusion control as are the termination reactions.

Transfer to polymer or terminal double bond polymerization are very difficult reactions to account for, either theoretically or experimentally[49] when polymer concentration depends on termination as well as transfer. In the mathematics of the model they couple the free radical and the dead polymer mass balances. Experimentally, estimation of branching is a complex

analytical problem. Progress has been made by Graessley et. al.[48,49] through investigating reaction conditions which emphasize the importance of transfer reactions. Mathematical methods (notably the Method of Continuous Variables [50-52]) can provide solution techniques for more complex kinetics. The analytical difficulties associated with determining branching are a main obstacle to consideration of the transfer to polymer reaction in a kinetic study. The classical approach using intrinsic viscosity based on Zimm's theoretical development has been hampered by polydispersity effects and shear rate effects on intrinsic viscosity.[38,53] Use of the GPC in combination with other instruments at present provide a potentially useful approach.[54-57]

2.3 The Rate of Polymerization of Methyl Methacrylate

The prediction of conversion at any time for the polymerization naturally must be based on a prediction of the rate of polymerization. In low conversion studies, two characteristics of the rate are well known.[1-3] If monomer concentration change is negligible, the rate is proportional to the square root of the initiation rate. If initiator efficiency, initiator concentration, k_t (or, more generally the total free radical concentration) and k_p remain constant, then rate is first order with respect to monomer.

The following equations for the rate of polymerization (R_p) are then usually employed:

$$R_p = k_p R^o M \qquad (I\text{-}11)$$

$$= k_p \sqrt{\frac{I}{k_t}} M \qquad (I\text{-}12)$$

where R^o is the total free radical concentration (moles/ℓ) and M is monomer concentration (moles/ℓ).

If the initiator decomposition is considered first order and if the efficiency of initiating new chains is f then

$$I = 2fk_d c_o \exp(-k_d t) \qquad (I-13)$$

where c_o is the initial initiator concentration (moles/ℓ) and t is reaction time (sec).

Therefore at small times:

$$\frac{R_p}{c_o^{\frac{1}{2}}} = K_1 M \qquad (I-14)$$

where $K_1 = \sqrt{\frac{2fk_d}{k_t}} k_p$ $((\ell/\text{mole})^{\frac{1}{2}}\text{sec}^{-1})$

Values of K_1 are tabulated in the literature,[2] and are summarized in the Arrhenius plot (Fig. I-1).

For the variable volume reaction, if volume change is considered proportional to conversion X (the weight of polymer produced divided by the weight of polymer plus monomer present), then K_1 can be obtained by plotting $\ell n(1-X)$ versus t and dividing the slope by $c_o^{\frac{1}{2}}$.[58]

The initial increase followed by a decrease in rate of conversion with time was considered by North et. al.[33] to be greater than that attributable to the consumption of monomer. They suggest that this could be due to a solvent effect which affects the segmental diffusion of the growing polymer chain end so as to cause an increase in the k_t value.

The onset of the "gel effect" is marked by an auto-acceleration of rate. Because of the exothermic nature of the reaction ($\Delta H = -12.9$ kcal/mole),[4] much of the kinetic data for the bulk reaction in the literature is nonisothermal beyond low conversions.[18,59] The significance of tempera-

ture rise during the gel effect on the measured conversion is unknown, although it has been blamed for poor reproducibility.[59]

Although, as mentioned above, rate of polymerization can be determined easily from conversion versus time data at low conversions, by the usual integral analysis for a first order reaction, differentiation of the data at higher conversions is the usual procedure for determination of polymerization rates. However, the shape of the curve combined with experimental error in conversion determination make this procedure of dubious value. In fact, by using a differential scanning calorimeter for direct isothermal rate measurement, Horie et. al.[18] have recently shown that the rate versus conversion curves, rather than being uniformly parabolic in shape as previously believed, have a significant shoulder at high conversion which increased as reaction temperature decreased and could be qualitatively explained by diffusion control of termination. They also review other instruments which could be used for isothermal rate measurement.

Thus, prediction of conversion versus time data during the gel effect without direct rate measurement is likely best accomplished by using a semi empirical equation, which does not require differentiation of experimental conversions.

The equation of Sawada[60] is the one used in this work. By assuming the concentration of radicals proportional to the monomer concentration consumed after the gel effect begins, that the effective monomer concentration is reduced by the limiting conversion reached, and that the effect of shrinkage is negligible, he obtained

$$\frac{dX}{dt} = k_p k\ (X-b)(a-X) \qquad (I-15)$$

where X is conversion during the gel effect

$(= (M_o - M)/M_o)$

b is the conversion at the onset of the gel effect

a is the limiting conversion

k is an empirical constant (moles/ℓ)

which when integrated yields

$$X = \frac{[a \exp((a-b)(k_p kt + c_1)) + b]}{[1 + \exp((a-b)(k_p kt + c_1))]} \qquad (I-16)$$

Horie et. al.[18] showed that the limiting conversions that they measured in PMMA polymerization could be related to the glass transition temperature of the system by using equations from the free volume theory of diffusion.[61] The two important relationships involved are the effect of molecular weight of a polymer on its glass transition temperature (T_{gp}) derived by Fox and Flory:[61]

$$T_{gp} = T_{g\infty} - \frac{2\rho\bar{N}\theta}{\alpha_p \bar{M}} \qquad (I-17)$$

where $T_{g\infty}$ = glass transition temperature of the polymer with infinite molecular weight (^oC)

ρ = density of the polymer (g/cm^3)

$\bar{N}$ = Avogadro's number (6.023×10^{23} (g mole)$^{-1}$)

α_p = the difference between the volume expansion coefficient in the melt and in a glassy state (^oC)$^{-1}$

θ = contribution of the chain end to the free volume $(cm)^3$

$\bar{M}$ = molecular weight of polymer

and the glass transition temperature of a polymer monomer mixture, derived by Kelley and Bueche[61]

$$Tg = \frac{\left\{ \alpha_p \phi_p T_{gp} + \alpha_m (1-\phi_p) T_{gm} \right\}}{\left\{ \alpha_p \phi_p + \alpha_m (1-\phi_p) \right\}} \qquad (I-18)$$

where ϕ is the volume fraction in the system and "p" and "m" represent polymer and monomer, respectively. Horie et. al.[18] recommend that the following numerical values of the various parameters be used:

ρ = 1.1 (g/cm^3)

θ = 80.*10^{-24} $(cm)^3$

α_p = 0.48*10^{-3} $(^oC)^{-1}$

$T_{g\infty}$ = 114. (^oC)

T_{gm} = -106. (^oC)

α_m = 1.*10^{-3} $(^oC)^{-1}$

The above equation for T_g was obtained by assuming the additivity of free volume per cm^3 (V_f) (volume fraction available for molecular movement) of monomer and polymer. That is:

$$V_f = V_{fp} * \phi_p + V_{fm} \phi_m \qquad (I-19)$$

$$= \left[0.025 + \alpha_p (T-T_{gp})\right] \phi_p + \left[0.025 + \alpha_m (T-T_{gm})\right] \phi_m \qquad (I-20)$$

At the glass transition temperature ($T = T_g$) the free volume V_f is considered to be 0.025 so then Equation (I-20) becomes Equation (I-18).

Horie et. al. set T_g in Equation (I-18) equal to the polymerization temperature (T) and, using M_v calculated from intrinsic viscosity in Equation (I-17) to obtain T_{gp}, they calculated ϕ_p corresponding to this

temperature T. This ϕ_p was found to be the limiting volume fraction (limiting conversion) obtained at T.

2.4 The Molecular Weight Distribution of Polymethyl Methacrylate

At low conversions (< 10%) the molecular weight distribution of polymethyl methacrylate is known to be unimodal and to be generally in agreement with the conventional kinetic model, the distribution being "the most probable". The success of various investigators in fitting of both molecular weight averages[1-3] and the results of an early GPC study [36] substantiate this observation.

In data treatment the consumption of monomer is generally neglected and the equations used to express the experimental molecular weight distribution and/or molecular weight averages are for instantaneously produced polymer (Equations (I-58 to 60) in Appendix I-B). The parameters usually considered most pertinent to the molecular weight distribution and tabulated in the literature[1-5] are: A' $(\equiv \frac{1}{2}(1+\lambda)\frac{k_{td}}{k_p^2}$ (where $\frac{k_{td}}{k_{tc}} = \frac{\lambda}{1-\lambda}$)), C_m $(\equiv \frac{k_{fm}}{k_p})$, C_c $(\equiv \frac{k_{fc}}{k_p})\frac{C}{M}$ (where C is initiator concentration). The latter two quantities are difficult to determine accurately because they are small and easily affected by analysis error (notably error in Mn). In the temperature range 50-90°C, C_m is approximately $1.*10^{-5}$, and C_c is likely small for AIBN.[5] Literature values of A' are summarized in an Arrhenius plot (Figure I-2).[2] The gentle curvature of the data was attributed to the difference in activation energy between combination and disproportionation.[2] However, since much of the data were obtained in large ampoules, it is likely that nonisothermal effects contributed to the curvature.

At higher conversions there has been long disagreement in the literature over whether the molecular weight distributions are unimodal[73,74] or multimodal.[22,75,76,59,36] Analytical difficulties and nonisothermal reaction conditions heavily contribute to the problem. Errors in experimental analysis can yield multimodal curves[77] or can hide minor peaks.[78] The effect of a rise in temperature on the molecular weight distribution during the gel effect is unknown.

The kinetic mechanism required to obtain a multimodal distribution is uncertain. Pyrkov et. al.[42] stated that multimodal distributions are the result of two different kinetic mechanisms. Marshall[79] indicated that at high conversions kinetics became extremely complicated by a change in the termination mechanism. Zeman[52] obtained bimodal distributions using a monomer termination mechanism in a mathematical development.

3. Application of the Conventional Kinetic Model to Methyl Methacrylate Polymerization

3.1 The Model for Batch Bulk Free Radical Polymerization

Assumptions used and pertinent steps in the derivation of the equations are outlined in Appendix I-B. The final equations are those often used to interpret data at low conversion.[3] The dimensionless parameters originated more recently.[80] The emphasis in this study was on development and evaluation of techniques of extending this previous work for the polymerization of methyl methacrylate to high conversion.

Application of the model to prediction of conversion involves the extension of the conventional low conversion model to as high conversions as possible. During the gel effect Sawada's equation was applied to the data. The glass transition temperature of the system was calculated

using the free volume theory and used to predict limiting conversion. Free volume was also considered as a means of predicting the onset of the gel effect.

Application of the model to the molecular weight distribution (MWD) data involves the use of the dimensionless parameters. These parameters not only simplify the model but a characteristic of them not used before is that they permit one to study MWD without use of a measured rate of polymerization (R_p). (R_p is difficult to measure accurately during the gel effect).

The instantaneous weight fraction of polymer of chain length r is:

$$W_r = \tau\,(\tau+\beta)(r\phi_1{}^r) + \tfrac{1}{2}\beta\,(\tau+\beta)^2\,(r^2\phi_1{}^r) \qquad (I\text{-}21)$$

where $\alpha = \dfrac{k_{td}}{k_p{}^2}\dfrac{R_p}{M^2} = \dfrac{k_{td}}{k_p{}^2}\dfrac{dX}{dt}\dfrac{(1+\epsilon X)}{M_o(1-X)^2} = \alpha_1\dfrac{(1+\epsilon X)}{(1-X)^2}$

$$\beta = \frac{k_{tc}}{k_p{}^2}\frac{R_p}{M^2} = \frac{k_{tc}}{k_p{}^2}\frac{dX}{dt}\frac{(1+\epsilon X)}{M_o(1-X)^2} = \beta_1\frac{(1+\epsilon X)}{(1-X)^2}$$

$$\tau = \alpha + \frac{k_{fm}}{k_p} = \alpha + C_m$$

$$\phi_1 = \frac{1}{1+\beta+\tau}$$

where r is chain length and α, β, and τ are the dimensionless parameters referring to disproportionation, combination and transfer to monomer respectively.

Published literature (Section 2.2.4) and experimental data obtained (Section 3.4.5.2 in particular) led to both transfer to polymer and terminal double bond polymerization being excluded from the model.

The method used to obtain the cumulative differential distribution was to simply sum the instantaneous distributions, each weighted by the weight fraction it contributes to the total distribution.

That is at conversion X_n

$$W_{r\ CUM} = \sum_{i=1}^{n} \frac{X_i - X_{i-1}}{X_n} W_{r_{i-\frac{1}{2}}} \tag{I-22}$$

or

$$W_{r\ CUM} = \frac{\int_0^X W_r dX}{X} \tag{I-23}$$

The molecular weight averages were similarly calculated:

$$\frac{1}{M_n} = \sum_{i=1}^{n} \frac{X_i - X_{i-1}}{X_n} \frac{1}{M_{n_{i-\frac{1}{2}}}} \tag{I-24}$$

$$Mw = \sum_{i=1}^{n} \frac{X_i - X_{i-1}}{X_n} Mw_{i-\frac{1}{2}} \tag{I-25}$$

At low conversions, where the rate constants are unknown but constant, and rate of polymerization is known, each dimensionless variable includes only one unknown parameter, $\frac{k_{td}}{k_p^2}$ for example.

At higher conversions both rate constants and rate of polymerization are unknown functions of conversion and so each dimensionless variable may contain more than one unknown parameter.

3.2 Determination of Kinetic Model Parameters Using GPC Data

The development of new techniques for using GPC in kinetic studies is detailed in Part II of this thesis. A brief outline will be presented here, with emphasis on methyl methacrylate polymerization.

It should be noted at the outset that the conventional GPC chromatogram F(v) is a sensitive reflection of the molecular weight distribution of the sample injected. The distribution involved is differential with respect to molecular weight (since each area slice F(v)dv is proportional to the weight of polymer between retention volume v and v+dv) but it is cumulative with respect to conversion (because the sample contains polymer formed at all conversions up to the conversion at which it was obtained). When chromatograms, or molecular weight distributions, are mentioned in this dissertation it is this conventional one that is referred to unless otherwise stated. The subject of distributions is discussed in Appendix II-A. The chromatograms dealt with in this thesis are summarized in Table I-29. It can be seen that actually F(v), $F_N(v)$ and $F_c(v)$ all reflect the molecular weight distribution mentioned above, whereas $\Delta F(v)$ and $\Delta F_N(v)$ reflect a molecular weight distribution which is not only differential with respect to molecular weight but also differential with respect to conversion (i.e. an "instantaneous distribution").

Previous to this study, GPC has been mainly used to obtain molecular weight averages for kinetic studies.[12,13] May[36] considered the whole molecular weight distribution, but was effectively hindered by the relatively unrefined state of both GPC and the numerical techniques employed. Duerksen[13] and Hui[12] presented molecular weight distributions, but numerical instabilities in the resolution correction method used caused bimodal and even multimodal peaks to appear. These artificial peaks misled Ito[81] who attributed them to primary radical termination.

Three useful methods of using GPC in kinetic studies were developed in this research. One of these, the "Method of Molecular Weight Averages" is a resolution correction method, which although not easily applicable to methyl methacrylate polymerization (because of the broad chromatograms obtained and the lack of monodisperse standards for resolution calibration) and not used in this kinetic study, has already been used in a study of polystyrene kinetics to complete conversion.[82] It is particularly suitable for use with the Method of Moments where theoretical molecular weight averages are calculated as a function of conversion. The other two more recent methods "The Method of Chromatogram Heights" and "The Method of Differential Chromatograms" were used to determine kinetic parameters here. They are ideally suited when GPC chromatograms are very broad even when measured molecular weight averages are not highly reproducible.

The adequacy of both of these latter methods is due to the reproducibility and accuracy of central chromatogram heights. The tails (or more generally, the lower heights) of the chromatogram are poor in reproducibility for reasons associated with the GPC and with polymerization kinetics of the sample. Baseline drift (usually due to small temperature fluctuations in the refractometer detector) and axial dispersion (more particularly concentration effects) contribute significantly to poor accuracy in tail heights. The mechanism of the polymerization kinetics can yield a polymer with a long tail in the molecular weight distribution so rapidly that reproducibility of the formation of the tail is poor.

The reproducibility of the molecular weight averages calculated from a GPC chromatogram is directly dependent on the significance of the

lower heights of the chromatogram in calculation of the average. The equation used to calculate molecular weight averages is the ratio of weighted integrals of the heights over the whole curve (ref. Equation (II-4) Part II).

The significance of the lower heights on the average thus depends on the length of the tail of the chromatogram, the calibration curve of the GPC and the moments used in calculation of the average. The steeper the calibration curve and the higher the moments involved, the greater will be the dependence of an average on the tail heights.

The accuracy of the chromatogram (i.e. how well it reflects the true molecular weight distribution of the polymer) depends on GPC calibration, and the correction for imperfect resolution used (the correction for the instrument's inability to separate the sample into separate peaks, one for each molecular weight present). GPC calibration for PMMA was done using two different methods as outlined in Part II. Resolution correction was accomplished taking due cognizance of the effect of imperfect resolution on the GPC chromatogram. This latter subject is described in some detail in Part II. The pertinent facts regarding GPC imperfect resolution will be repeated below.

Axial dispersion is the source of GPC imperfect resolution. A chromatogram corrected for axial dispersion is always taller and narrower in shape than the uncorrected chromatogram. That is, the heights along the sides of the chromatogram near the inflection points are the least affected by imperfect resolution. The wider the chromatogram, the less the chromatogram heights change with axial dispersion. However, the molecular weight

averages, being integrals over the whole curve, and weighted by the inaccurate chromatogram tail heights are affected as much for narrow chromatograms as for broad. In addition, the correction to the molecular weight averages for imperfect resolution is very difficult to establish for broad chromatograms.

3.2.1 The Method of Chromatogram Heights

The "Method of Chromatogram Heights" involves calculating the theoretical chromatogram ($F_N(v)_{MODEL}$, Table I-29) from the molecular weight distribution given by the model and comparing the side heights with the experimental chromatogram ($F_N(v)$) heights similarly located. The unknown parameters in the model are varied using optimization routines until the best agreement is reached. In the present case, at low conversions this can be a three variable search (if C_m, α_1, and β_1 are considered unknown and significant), a two variable search (if only α_1 and β_1 are considered) or even a single variable search (for α_1 if transfer to monomer and termination by recombination are insignificant compared to termination by disproportionation). At higher conversions, multivariable searches are required as each of the dimensionless variables become unknown functions of conversion.

It should be noted that the parameter estimates obtained either by this method or the next mentioned "Method of Differential Chromatograms", are a direct reflection, not only of the model with its assumptions, but also of the relative importance given different chromatogram heights and the actual heights used. This is discussed in Appendix I-C.

3.2.2 The Method of Differential Chromatograms

This method also uses central chromatogram heights. However, the difference is that the chromatograms used in the search ($\Delta F_N(v)$ and $\Delta F_N(v)_{MODEL}$, Table I-29) represent only the polymer produced during a finite time increment and not from time zero. They are therefore approximately "instantaneous".

The main object of this method is to show if the model can be made to fit the data in a reasonable way and to give first approximations to the unknown rate parameters. It is particularly useful at high conversions where the dependence of the parameters on conversion are unknown.

3.3 Experimental

3.3.1 Reagents and Analytical Techniques

The initiator, AIBN, (Eastman Organic Chemicals) was recrystallized twice and sometimes three times from absolute methanol. The methyl methacrylate was provided by Rohm and Haas and contained 10 ppm monomethyl ether of hydroquinone (MEHQ). This inhibitor was removed by distillation under reduced pressure, with sulfur to eliminate polymerization in the reboiler, using a four foot glass column packed with glass cylinders and employment of a high reflux ratio. The distillate was tested by nitrosation of the hydroquinone. Comparison was made with an undistilled sample. Absence of any brown coloration indicated removal of the inhibitor.[83-86] A variety of GPC runs which included injection of monomer indicated no high molecular weight impurities in the monomer.

Conversion was determined by dissolving a known weight of the reaction mixture in acetone, adding MEHQ as inhibitor, later precipita-

ting the polymer in a 20 fold excess of methanol, drying the precipitate at 50°C under vacuum, and weighing. An estimate of low molecular weight loss in this procedure was obtained by injecting the reacted monomer polymer mixture directly into the GPC. Molecular weight distribution information was obtained by analyzing selected samples by GPC. A few high resolution NMR measurements were obtained to give estimates of tacticity of the polymer produced.

3.3.2 Apparatus and Procedure

Several types of glass ampoules were used. They are shown in Figure I-3. Types 1 to 3 are the conventional straight tube ampoule although of much smaller diameters than is usual. Type 4 is a dilatometer ampoule (only the 2 mm O.D. part finally contained reactant--degassing was done in the lower bulb). Type 5 was used as an alternate to Type 3. Type 6 was a double graft ampoule used to examine the effect of temperature by having the reaction conducted in two different surface area to volume ratios. Types 7 and 8 were similar to Types 2 and 3 except that a side arm was provided to permit entry and sealing of a thermocouple. The general procedure was as follows:

1. Washing: The ampoules (open at both ends) were immersed 48 hours in chromic acid, flushed with distilled water, stored under distilled water for 24 hours, flushed with distilled water, immersed in acetone and dried in an oven at 100°C for 4 hours. After removal from the oven the ampoules were sealed at the bottom by using an oxy-methane torch (after this, thermocouples were sealed into the ampoule at the side arm of Types 7 and 8 using "Epoxy Resin" or "Dow Corning Glass and

Ceramic Adhesive" with only occasional complete success (refer to Section 3.4.2). Ampoules were then placed on a glass vacuum system, evacuated and tested for leaks.

2. Reactant Preparation

Catalyst was weighed and added to a weighed amount of monomer. To eliminate reactant preparation as a source of error large batches were prepared when required and stored under air in sealed ampoules in liquid nitrogen. Eight preparations were used in the study.

3. Filling Procedure

A syringe or glass capillary was used to fill ampoules.

4. Degassing

The ampoules were immediately placed on the vacuum system[82] and degassed by four successive freeze-thaw cycles using liquid nitrogen and a pressure of 10^{-6} mm mercury. They were maintained at below room temperature at all times and exposure to bright light was avoided.

5. Sealing of Ampoules

Ampoules were first sealed off from the vacuum system, while the monomer was under liquid nitrogen, by applying the oxy-methane torch to the ampoule just below the ground glass joint. All were then stored under liquid nitrogen. For ampoules Type 1, 2, 3, 7 and 8 all sealing was thus concluded. Types 4, 5 and 6 were allowed to thaw previous to use and then immediately inverted and the reactant easily shaken from the degassing reservoir at the bottom to the bottom of the narrower part of the ampoule. Quantities of reactant

were chosen so that the ampoule was approximately 3/4 full at room temperature. The reactant in latter types was then cooled (but not frozen, or cracking of the glass at the end seal opposite the reservoir would result). The reservoir was then removed by sealing the ampoule at the reservoir-ampoule joint. Once so sealed, these types were reacted immediately, as outlined in the next step of the procedure.

6. Ampoule Reactions

The ampoules were immersed suspended by a copper wire in a water bath maintained to $\pm$ .01^{o}C by a mercury themoregulator and an electric heater. After reaction for a certain period an ampoule was quickly removed and quenched in liquid nitrogen. Rapid action and accurate timing was necessary in immersion and quenching. The reactant was then either removed directly (usually conversions above 80%) or dissolved out of the broken ampoule with acetone. Conversion was calculated as the weight of precipitated polymer from a known weight of monomer polymer reactant mixture.

7. Shrinkage Measurement

The decrease in level of the monomer was followed in the Type 4 ampoules in the initial phase of the study (50^{o}C work) by surrounding the ampoule in the bath with a graduated burette segment. Later (for 70^{o} and 90^{o}C work) a traveling microscope was used. Measurements were stopped when the first bubble of nitrogen was noticed and towards the conclusion of the study the point at which clinging to the walls of the tube became significant was noted.

8. Storage of Samples

Precipitated polymer was stored in individual bottles in the dark at room temperature. Monomer polymer mixtures were stored in small capped vials which were placed in batches of 4 or 5 in sealed 12 inch O.D. glass tubes immersed in liquid nitrogen or a dry ice acetone mixture. A note of caution here: in two cases where liquid nitrogen was used the tube cracked and permitted atmospheric air to condense inside. Violent pressure explosions resulted when the tube was removed from the liquid nitrogen and placed at room temperature. This possibility was foreseen in time to contain the explosions and so avoid damage.

3.3.3 Experimental Design

The experimental conditions used were those of interest to industry. At 50°C, .3, .391 and .5 weight % AIBN concentrations were used. At 70°, .3 and .5 weight % and at 90°C, 0% (thermal polymerization) .3 and .5 weight % AIBN were used. All reaction conditions except those for thermal polymerization were carried to limiting conversions.

The number allocated to a sample refers to the group to which the sample belonged for degassing on the vacuum system. The letter is for identification purposes only and does not indicate reaction time. Reproducibility studies were adequately randomized. Runs used for dilatometer data only are not listed in tables but only on Figures I-6 to I-10.

Several experiments and analyses were replicated or at least duplicated. Figure I-4 shows the site of the main replicates. Only a few molecular weight distribution measurements at 50°C beyond low conversion

could be performed due to the instability of the high angstrom styragel GPC columns (ref. Part II) so molecular weight distributions corresponding to the main replicates could be obtained only at 90°C, 0.5 weight % AIBN, 45% conversion level. This was a good test of the reproducibility since at this level the reaction rate is extremely fast and the gel effect is just beginning. Shrinkage measurements were all made with one or more replicates.

3.4 Results and Discussions

3.4.1 Reproducibility

The reproducibility of gravimetrically determined conversion is shown in Table I-1 and a good indication of variation over all of the conditions and ampoule sizes used may be seen from Figures I-4,5 and Tables I-3 to 10. These data show that these conversion data were generally better than 1% in reproducibility, although errors of about 5% were possible during an extreme gel effect, such as that at 240 min., 50°C and 0.5% AIBN or at low conversion where quantities of material available from small ampoules yielded very small quantities of polymer. Dilatometer results are shown in Figures I-6 to I-12. Despite the variety of reaction conditions and continual improvement of technique,results all appear to be better than 1% in reproducibility.

The reproducibility of molecular weight distribution data included three separate considerations: molecular weight averages (of general interest since they can be determined by many other instruments besides GPC and since many physical properties correlate with them), normalized chromatogram heights (for use in "The Method of Chromatogram Heights") and, the

product of normalized chromatogram heights and gravimetrically determined conversion (the heights used to obtain differential chromatograms for "The Method of Differential Chromatograms"). These reproducibilities are shown in Table I-2 and Figure I-13 respectively. Further indication of reproducibility over the whole range of conditions can be gained from Table I-11 to 17 and Figures I-16 to 19. The errors introduced by GPC analysis without the error introduced by using samples from different ampoules are shown in Part II.

From all of this data it is evident that the expected results were obtained (ref. Section 3.2). The central chromatogram heights are highly reproducible whereas the tails of the chromatogram are poor in reproducibility. The molecular weight averages (particularly those involving high moments of the distribution) can be very poor in reproducibility, or very good, depending on the significance of the lower heights in the calculations. Mw and higher averages are 19% or worse in Table I-2(1) whereas Mn is reasonable (5.2%). The reproducibility of all molecular weight averages is quite good for Table I-2(2).

3.4.2 Isothermal Conditions

Attempts to measure temperature directly using thermocouples were unsuccessful. Air leaks at sealed entrance of the thermocouple to the ampoule and reaction of the thermocouple insulation with the monomer were the main obstacles. However, these approximate measurements as well as elementary heat balance considerations indicated that a rise of $6^{o}C$ at the center of a 5 mm O.D. (surface to volume ratio of 1.63) was possible during the gel effect at $90^{o}C$. In a 3 mm O.D. ampoule the rise was only about $1^{o}C$.

Preceeding the gel effect, the temperature in a 5 mm O.D. ampoule was about 1 ^{o}C higher than the bath temperature whereas in a 3 mm O.D. ampoule temperature was less than 0.1^{o}C higher than the bath temperature.

The best check on whether the data were in fact sufficiently isothermal to avoid undesirable temperature effects on conversion or molecular weight distribution was to use ampoules of different surface area to volume ratios or composite ampoules (Type 6 Figure I-3). GPC analysis of the reaction mixtures (unprecipitated) and gravimetric analyses were performed. The results are shown in Tables I-3 to I-17 and indicate that reaction conditions were sufficiently isothermal for our purposes and that surface effect on reaction was unimportant.

3.4.3 The Molecular Weight Distribution of PMMA

Although the qualitative variation of the conversion with time is well known, as has already been pointed out, the shape of the molecular weight distribution of PMMA at conversions beyond the gel effect has been the subject of disagreement for more than twenty years. Part of this difficulty lies in the various ways of presenting a molecular weight distribution which in turn reflect the various ways of obtaining them. A discussion of this is presented in Part II, Appendix IA. The type of distribution directly reflected by the conventional GPC chromatogram is detailed in Section 3.2.

This study has provided considerable evidence that the molecular weight distribution of the PMMA samples produced here at high conversion is bimodal. It agrees with some recent unpublished work of Kawasaki.[87] Here samples were actually obtained through the gel effect and the growth

of the high molecular weight peak observed beginning just after the onset of the acceleration in rate of polymerization. This distinctive trend with conversion essentially eliminates many other possible causes for bimodal chromatograms. Room temperature polymerization [36] would cause the second peak to be observable at very low conversions. Axial dispersion or some other GPC phenomenon (such as negative adsorption mentioned by Yamada et. al.)[88] cannot be the cause because of the methods of GPC calibration and interpretation used (ref. Part II). Mathematical instabilities resulting from resolution correction methods which have misled previous investigators[81] have been investigated and avoided by development of new methods. Crystallinity can affect GPC chromatograms with PVC as shown previously.[89] To ensure that this was not the case for PMMA one bimodal sample was heated in THF solution to 90°C for 10 minutes prior to injection. No effect was observed on the resulting chromatogram. Some samples were analyzed by NMR and found to be of expected tacticity. According to the literature, crystallization of PMMA produced at these temperatures does not occur.[90-92]

Finally, the appearance of the second peak was well explained by the production of linear high molecular weight polymer resulting from diffusion control of termination by disproportionation. The developments leading to this explanation are detailed in the following sections. However, it is interesting to note here that there is a striking resemblance of the chromatogram shapes obtained in this study to the rate curves of Horie et. al.[18] at the same temperatures. A resemblance might be expected because of the integral equation (Equation (I-23)). The rate of polymerization enters this equation in a similar way to that in which the function W(y) enters

Tung's axial dispersion equation (Part II Equation (II-12)). There is always a strong resemblance between W(y) and F(v) in that equation.

3.4.4 Model Application to the Onset of the Gel Effect

3.4.4.1 Conversion

Rate of polymerization showed a first order dependence on monomer concentration to quite high conversions. Tables I-3 to I-10 and Figures I-4 and I-5 show the result and the pseudo-first order rate constants obtained by a least squares fit of ln (1-X) versus time.

Figure I-1 shows that excellent agreement with the literature was obtained when K_1 (Equation (I-14)) was calculated from these rate constants. By least squares $\ln K_1 = 30.13-9.63\cdot(10^3/T)$. This demonstrates that rate is both first order with respect to monomer and proportional to the square root of the initiator concentration.

Table I-28 shows the results of calculating conversion from the area under the GPC PMMA peak knowing the weight of monomer-polymer mixture injected. Results agree with those determined gravimetrically.

Free volume was examined as a possible indicator of the gel effect. By definition,free volume is a measure of voids or holes in the liquid that permit movement of molecules. At the glass transition temperature the free volume is about .025. Free volume above .025 is attributed to thermal expansion in excess of the van der Waals expansion (the increase due to increase of amplitude of vibration of segments). It became obvious that molecular weight plays an insignificant part in calculation of free volume at each conversion if the molecular weights are not too low while the conversion is not too high (all experiments conducted in this study). Figure I-14 demonstrates this more quantitatively.

Free volume was calculated from conversion and reaction temperature by assuming $T_g = T_{g\infty}$ (i.e. no influence of molecular weight). It is evident (Tables I-3 to I-10) that the gel effect consistently starts at a free volume of approximately 0.15 if the onset of the gel effect is defined as that conversion at which rate of polymerization deviates from a first order dependence on monomer concentration (i.e. the conversion given by the Sawada constant "b"). The accuracy of prediction of the gel effect using free volume depends on the change of free volume over the conversion increment 20 to 40% (the range of conversion at the onset of the gel effect) and the accuracy with which the free volume can be estimated. The free volume change for these conditions is about .155 to .100 and the conversion replicates indicate that free volume can be determined to about .002. Thus it appears that it might be a useful indication of the onset and development of the gel effect with conversion.

3.4.4.2 Molecular Weight Distribution

The proportionality constant, ε, for relating shrinkage to conversion was calculated from the slope of plots of percent shrinkage versus conversion. Results are shown in Table I-25 along with values calculated using estimates of polymer and monomer density. They are generally higher than the latter values. Two likely reasons for this are that the latter values assume both that the volumes are additive and that the proportionality is valid to 100% conversion. The effect of the difference in these values on predicted molecular weight distributions is small.

The kinetic model was applied to the experimental data using each of the two new GPC methods previously outlined for methyl methacrylate polymerization. MWD's at low conversions were all unimodal.

Using the Method of Chromatogram Heights and, in turn, a three, two and finally a single variable search on all of the low conversion GPC data it was determined that molecular weight distribution was controlled by termination by disproportionation with combination and transfer to monomer playing an insignificant role. Results of the single variable search are shown in Table I-18-24 where uncorrected GPC molecular weight averages are compared with the model. Figure 15 shows a typical theoretical and experimental low conversion chromatogram.

Generally the molecular weight averages are in close agreement with the model values with the exception of some cases where the search gives a higher Mn value than found by GPC. The theoretical chromatograms are always higher and narrower than the experimental chromatograms. All of these results are well explained by general considerations of imperfect resolution of the GPC (i.e. the inability of the instrument to separate each molecular weight in the sample sufficiently to yield a separate chromatogram peak for each). Usually a series of 7 or 9 GPC columns were used. With this many columns in series,uncorrected molecular weights would be expected to require a relatively small correction for imperfect resolution (Mn is likely approximately 10 to 15% too low and Mw about 5% too high (ref. Figures II-13 and II-14). The perfectly resolved sample chromatogram heights would be made taller and narrower with resolution correction with the change in shape depending on the breadth of the molecular weight distribution and the magnitude of axial dispersion in the GPC. In other words, the α_1 values found in the search are considered valid. This is discussed more fully in Part II.

The quantity A' ($= \frac{1}{2}(1 + \lambda)\frac{k_{td}}{k_p^2}$, where λ is unity here (no combination)) was extracted from α_1 obtained in the single variable search and plotted with the literature values in Figure I-2. Values at 70°C and 90°C are slightly higher than the few values available from the literature. They provide a better straight line extrapolation from the literature low temperature values and, as already mentioned, unlike the literature values, are free of nonisothermal effects.

The Arrhenius relation obtained (In Figure I-2: : $\ell nA' = -4.609 + 2.960\ (10^3/T)$ and $E_A = 5.88$ Kcal/mole) was used to calculate Mn and Mw assuming A' to be independent of conversion. These are shown in Figures I-16 to I-19 as conventional kinetics. At low conversions, agreement is generally reasonable. At high conversions the molecular weights predicted are much too low because of the onset of diffusion control of termination which results in a lowering of k_{td} and hence A' with conversion.

At low conversions the Method of Differential Chromatograms is not very useful because the low conversion GPC chromatograms ($F_N(v)$) are the same as the differential chromatograms ($\Delta F_N(v)$). The results of a single variable search on the differential chromatograms is shown in Figure I-20 to I-23.as circles in the center of horizontal bars indicating the conversion range of each differential chromatogram. They are slightly lower than those obtained by the former method.

3.4.5 Model Application After the Onset of the Gel Effect

3.4.5.1 Conversion

As is evident from Table I-3 to 10 and Figures I-4 and I-5 the Sawada Equation fits much of the accelerated rate data well. Fitting was

accomplished as described previously with the value "b" (conversion at the onset of the gel effect) as the value of conversion at a free volume of 0.151 and the value "a" (limiting conversion) the value at a free volume of 0.025. Generally a free volume of 0.025 is reached soon after the gel effect so the glass transition temperature is a good indication of the immediate limiting conversion. Apparently long times permitted van der Waals contraction and so free volume decreased to less than 0.025 for the final limiting conversion.

3.4.5.2 Molecular Weight Distribution

At low conversions the Method of Differential Chromatograms was not really needed because, before the onset of diffusion control, the rate constants are true constants, so that the GPC chromatogram can be used directly as an instantaneous molecular weight distribution. However, beyond low conversion, the method was invaluable. The kinetic model used is the same as that used at low conversions. Only initiation, propagation, and termination by disproportionation were considered important. The GPC chromatograms obtained provided the main reason for this assumption.

Figures I-24 to I-27 show the cumulative chromatograms at different conversions for polymerizations at 70 and 90°C. They indicate that after an initial spike of high molecular weight polymer is formed, lower molecular weight polymer is produced. Furthermore, differential chromatograms obtained were generally unimodal (the occasional bimodality was attributed to too large a conversion differential). In accordance with the trend of the cumulative chromatograms, the differential chromatograms produced were initially at low molecular weights, later at high molecular weights,

and finally at low molecular weights again. These results showed that both transfer to polymer and terminal double bond polymerization were likely not significant, since both of these would cause the molecular weights produced to increase at all conversions. Transfer to monomer or to catalyst could likely not produce such a large amount of high molecular weight polymer.

Attempts to guess the functional form for α_1 as it varied with conversion and to then apply the Method of Chromatogram Heights directly, all had very limited success. The Method of Differential Chromatograms was applied and a single variable search for α_1 was made to match each differential chromatogram. An example of the differential chromatograms obtained with the search is shown in Figure I-28. A least squares fit was then made of the α_1 found by the search. The two fits used of each set of α_1 data were of the following form: (Note: values of α_1 estimated at zero conversion were used in the least squares fit).

$$\text{FIT \#1} \quad \alpha_1 = \text{EXP}\ (A + B\ X + CX^2) \tag{I-26}$$

$$\text{FIT \#2} \quad \alpha_1 = \text{EXP}\ (A + B\ X + CX^2 + DX^3) \tag{I-27}$$

The actual coefficient values obtained are shown in Table I-26. The functions are plotted in Figures I-20 to 23 and results of their use to obtain chromatograms and molecular weight averages over the whole range of conversion at 70 and 90°C are shown in Figures I-16 to 19 and I-29, 30. Although the few high conversion samples injected into the GPC obtained by reactions at 50°C could not be analyzed (their high molecular weight tails were beyond the range of GPC resolution) they show a similar chromatogram shape to those obtained at high conversion and 70°C.

It is evident from these results that the simple Method of Differential Chromatograms gives good approximations to the molecular weight distribution throughout the whole conversion range. Mn is generally close to the GPC value. Chromatogram shape is most often close to the true shape except at the onset of the gel effect where the high molecular weight tail is not produced rapidly enough by the model. This latter point is directly reflected in the values of Mw obtained.

The Method of Chromatogram Heights was then applied. Each of the two fits (Equations (I-26) and (I-27)) were used in turn as first approximations in a two and a three variable search for the coefficients of X. The functions obtained are plotted in Figures I-20 to 23. Actual coefficient values are listed in Table I-26. Use of these functions to obtain chromatograms and molecular weight averages is shown in Figures I-16 to 19 and I-29, 30. There is, with the exception of 70°C, 0.3% AIBN data, some noticeable improvement, particularly in Mw.

Values of α throughout the whole conversion range were calculated from the α_1 functions obtained by the three variable search ($\alpha = \frac{k_{td}}{k_p^2}\frac{R_p}{M^2} = \frac{1}{M_o}\frac{k_{td}}{k_p^2}\frac{dX}{dt}\frac{(1+\varepsilon X)}{(1-X)^2} = \alpha_1\frac{(1+\varepsilon X)}{(1-X)^2}$) and are shown in Figure I-31. It is evident that α is an order of magnitude higher than the literature value of C_m because of monomer consumption, despite the fact that α_1 decreases to much lower values due to diffusion control of k_{td}. After a conversion of about 75% there is a significant increase in α indicating that the instantaneous molecular weight averages are falling appreciably near complete conversion.

Figure I-31 (the variation of α with conversion), Figures I-20 to 23 (the variation of α_1 with conversion) and Figures I-24 to 27 (cumulative chromatograms-the weight of each chain length produced as a function of

conversion) provide considerable evidence that conventional kinetics used for many years at low conversions can be successfully applied to higher conversions if variation of rate constants, changing rate of polymerization, and consumption of monomer are taken into account. α_1 decreases with conversion as k_{td} is decreased by diffusion control. The increase of dX/dt tempers the effect of the decrease of k_{td} on α_1, but not until after an initial "spike" of high molecular weight material has formed (this is the part of the kinetic data not well predicted by the simple functions of α_1 assumed). α shows a final increase at high conversions because of monomer depletion. Figures I-24 to 27 show that a small amount of medium molecular weight polymer is produced at the end of the polymerization as a consequence of this. It is worth reiterating that analysis of branching by Graessley et. al.[48,49] shows that Mn and Mw increase significantly with conversion when transfer to polymer and terminal double bond polymerization are important. The fact that the "instantaneous" molecular weight averages fall with conversion suggests that these reactions are not significant and PMMA produced is likely linear.

Figure I-32 shows the results of an attemp*ed general correlation for the effect of conversion on α_1. This correlation is a plot of $\frac{\alpha_1}{(\alpha_1)_{x=0}}$ calculated from the results of the three variable search for polymerizations with .3 and .5 wt.% AIBN at both 70 and 90°C. The correlation is quite good down to a free volume of about 0.05. This is equivalent to a conversion of about 75 to 80%. The scatter at lower free volumes may be due to a reduction in k_p which would have the effect of increasing the ratio $\frac{\alpha_1}{(\alpha_1)_{x=0}}$.

This general correlation could be used in the following manner if, for example, the molecular weight distribution at 80°C for a conversion of 75% using 0.4 wt.% AIBN is required. First V_f is calculated as a function of conversion neglecting the effect of polymer molecular weight (Equation (I-20)) with $T_{gp} = T_{g\infty}$). The generalized plot, Figure I-32, is now used to obtain $\frac{\alpha_1}{(\alpha_1)_{x=0}}$ as a function of conversion. $(\alpha_1)_{x=0}$ can be obtained from Figure I-2 after an estimate of K_1 is obtained from Figure I-1. Molecular weight distribution calculation is then a straight forward integration using Equation (I-23).

4. Summary

A review of the literature indicated that conventional kinetics might be applicable to the polymerization of methyl methacrylate throughout the whole range of conversion if the rate constants were permitted to vary with conversion (due to diffusion control of the reactions) in a correct manner. It was also evident that, despite its long history (the polymer was synthesized in the 1920's), experimental difficulties, along with a complex polymerization mechanism, caused much of the literature data to be of doubtful validity and conclusions based on these data were uncertain.

Experimental techniques were herein developed based principally on the use of gel permeation chromatography and applied to obtain isothermal kinetic data for the polymerization over a difficult range of reaction conditions (high rates and conversions) of interest to industry. Conventional kinetics were treated in a new and general way to derive the usual equations phrased in terms of dimensionless groups which effectively separated the problem of molecular weight distribution prediction and conversion prediction.

New GPC data treatment techniques were developed and linked to computer optimization routines to obtain model parameters for molecular weight distribution prediction. The free volume theory of diffusion was found useful for predicting the onset of diffusion control and limiting conversion as well as for providing a basis for correlating a dimensionless kinetic parameter with conversion at different temperatures and initiator concentrations. Conversion prediction was accomplished with the use of a low conversion model (involving a rate first order with respect to monomer) combined with the Sawada equation.

At low conversions, experimental data were well fit and results were shown to agree with literature values. At higher conversions predictions were generally satisfactory with the exception of the prediction of the initial high molecular weight spike at the onset of the gel effect. This is likely attributable to the simple variation of α_1 with conversion permitted in the fitting of molecular weight data.

5. Conclusions

(1) Considerable evidence indicates that conventional kinetics apply at high conversions with the appropriate diffusion controlled termination constant. Instantaneous molecular weight distributions were generally in agreement with conventional kinetics.

(2) Molecular weight distributions are unimodal at low conversion and bimodal at high conversions for these reaction conditions. This is attributed to a change in the termination constant with diffusion control.

(3) The generalized correlation of the parameter $\frac{\alpha_1}{(\alpha_1)_{x=0}}$ versus free volume provides a means of predicting apriori the effect of diffusion control on molecular weight distribution of PMMA.

(4) New methods of extracting kinetic parameters from GPC data: The Method of Chromatogram Heights and the Method of Differential Chromatograms, developed in Part II have proven to be useful methods of employing GPC chromatograms to obtain kinetic parameters at high conversions where termination reactions are diffusion controlled.

(5) Free volume for the reaction mixture is almost independent of polymer molecular weight and it can be estimated from temperature and conversion for a monomer-polymer mixture. It provides both an estimate of the onset of the gel effect and the initial limiting conversion (conversion continues to increase and after a very long time occurs at a somewhat decreased free volume).

(6) Rate of polymerization is first order in monomer within experimental error up to approximately a free volume of 0.15.

(7) The Sawada equation correlates conversion data reasonably well during the gel effect.

(8) New ampoule techniques and GPC analysis of monomer-polymer mixtures permitted isothermal kinetic data (conversion, molecular weight distribution and shrinkage data) to be obtained and the validity of precipitation methods to be checked.

6. Recommendations

(1) The applicability of conventional kinetics with the assumptions used here should be more fully explored using more accurate rate of polymerization data (the use of a differential scanning calorimeter should permit this).

(2) Analysis of monomer polymer mixtures by GPC to obtain conversion should be further investigated. There is potential here to significantly reduce analysis time and thus permit more comprehensive kinetic studies particularly at high conversions.

(3) The use of free volume to correlate diffusion control of the termination reactions should be further explored in an attempt to obtain a universal correlation for all polymer systems.

7. Nomenclature

a	limiting conversion (free volume = .025)
AIBN	azobisisobutyronitrile
A'	rate constant ratio (= $0.5(1.+\lambda)k_{td}/k_p^2$) ($\ell$ sec/mole)
b	conversion at the onset of the gel effect (free volume = .151)
c	initiator concentration (moles/ℓ)
c_o	initial initiator concentration (moles/ℓ)
C_m	rate constant ratio (= k_{fm}/k_p)
C_c	rate constant ratio (= k_{fc}/k_p)
C_p	rate constant ratio (= k_{fp}/k_p)
A,B,C,D	coefficients of polynomial expressing α_1 as a function of X
c_1	empirical constant in Sawada Equation
f	initiator efficiency
F(v), $F(v)_{MODEL}$	GPC chromatogram (Table I-29): experimental and model predicted values
$\bar{F}(v)$	mean value of F(v)
$F_N(v)$	normalized GPC chromatogram (Table I-29) experimental and model
$F_N(v)_{MODEL}$	predicted values

$F_C(v)$, $F_C(v)_{MODEL}$ — cumulative GPC chromatogram (Table I-29) experimental model predicted values

I — rate of initiation (g mole/ℓ sec)

k — empirical constant in Sawada Equation (moles/ℓ)

$k_d, k_{fx}, k_p, k_{px}, k_{p\ isotactic}, k_{p\ syndiotactic}, k_p^*, k_{td}, k_{tc}$ — various rate constants in kinetic model (dimensions of k_d are $(sec)^{-1}$; all others are (ℓ/mole sec))

k_t — termination rate constant $(= k_{tc} + k_{td})$ (ℓ/mole sec)

k_{pr} — propagation rate constant for radicals of chain length r

k_{trs} — termination rate constantfor radicals of chain length r and s

K_1 — rate constant ratio $\left(= \sqrt{\frac{2fk_d}{k_t}}\, k_p\right)$ $(\ell/mole)^{\frac{1}{2}} sec^{-1}$)

M — monomer concentration (moles/ℓ)

M^o — concentration of free radicals produced by transfer to monomer (moles/ℓ)

M_o — initial concentration of monomer (moles/ℓ)

$\bar{M}$ — some average molecular weight

Mn_i, Mw_i — number and weight average molecular weights of instantaneously produced polymer

Mn, Mw, Mv, Mz	number, weight, viscosity and z average molecular weights which include all polymer produced up to conversion X
$Mn(h)$, $Mw(h)$	GPC average molecular weights corrected for symmetrical axial dispersion
$Mn(\infty), Mw(\infty), Mz(\infty), P(\infty)$	GPC average molecular weights and polydispersity calculated assuming infinite resolution
Mn_{MODEL}, Mw_{MODEL}	molecular weight averages predicted by kinetic model
N	critical chain length indicating longest mobile chains
$\bar{N}$	Avogadro's Number $(g\ mole)^{-1}$
$O_1(\alpha), O_2(\alpha)$	objective functions
P_r	concentration of dead polymer of chain length r (g mole/ℓ sec)
r	chain length
r_{N_i}	number average chain length of instantaneously produced polymer
R^o	total free radical concentration (moles/ℓ)
R_r^o	concentration of free radicals of chain length r (moles/ℓ)
R_p	rate of polymerization (moles/ℓ sec)
R	molar gas constant
T	temperature (^oC or ^oK)

t	time (min) or (sec)
T_{gp}	glass transition temperature of polymer (^{o}C)
T_{g}	glass transition temperature of polymer-monomer mixture (^{o}C)
$T_{g\infty}$	glass transition temperature of polymer of infinite molecular weight (^{o}C)
T_{gm}	glass transition temperature of monomer (^{o}C)
V_{f}	free volume for molecular movement per cm^3 of total volume
V_{fp}	free volume occupied by polymer per cm^3 of total volume
V_{fm}	free volume occupied by monomer per cm^3 of total volume
V	volume of reactants at conversion X
V_{o}	initial volume of reactants
$W(r)dr$ or W_{r}	weight fraction of molecules between chain length r and r+dr instantaneously produced
$W(r)_{CUM}dr$ or W_{rCUM}	weight fraction of molecules between chain length r and r+dr produced up certain conversion X
$W(y)$	GPC chromatogram corrected for the effect of axial dispersion
X	conversion
X_{r}	concentration of transfer agent (moles/ℓ)
Z	ratio of free radicals of chain length less than or equal to N to total free radical concentration

Greek Symbols

α	$k_{td} R_p / k_p^2 M^2$
α_1	$\frac{1}{M_o} \frac{dX}{dt} \frac{k_{td}}{k_p^2}$
α^*	$Z\alpha$
α_m	difference between volume expansion coefficient of monomer in the melt and in a glassy state $(^oC)^{-1}$
α_p	difference between volume expansion coefficient of polymer in the melt and in a glassy state $(^oC)^{-1}$
β	$k_{tc} R_p / k_p^2 M^2$
β_1	$\frac{1}{M_o} \frac{dX}{dt} \frac{k_{tc}}{k_p^2}$
$\Delta F(v)$, $\Delta F(v)_{MODEL}$	differential chromatograms: experimental and model
$\Delta F_N(v)$, $\Delta F_N(v)_{MODEL}$	normalized differential chromatograms: experimental and model
ϵ	volumetric expansion coefficient - Eqn. (I-64)
ζ	proportionality constant - Eqn. (I-33)
θ	contribution of chain end to the free volume $(cm)^3$
$\bar{\theta}_i$, θ_{MAX_i}, θ_{MIN_i}, θ_{N_i}, θ_i	symbols for parameter values in Eqns. (I-65) and (I-66)

λ	rate constant ratio $(\frac{k_{td}}{k_{tc}} = \frac{\lambda}{1-\lambda})$
λ_r, λ_s	components of a chain length dependent termination rate constant k_{trs}
ρ	density of the polymer (g/cm^3)
σ	probability of a new link having the same configuration as the preceeding link
τ	$\nu + (k_{fm}/k_p)$
ϕ_1	$1/(1+\beta+\tau)$
ϕ_2	$\frac{R_p}{k_p M} (Z(2-Z)\ \alpha + Z\ (2-Z)\ \beta + C_m)/(1+\tau+\beta)$
ϕ_3	$1./(1+\beta Z+\nu Z+C_m)$
ϕ_p	volume fraction of polymer
ϕ_m	volume fraction of monomer

8. References

1. Odian, G.,
"Principles of Polymerization"
McGraw-Hill Book Company, New York, (1970).

2. Bagdasar'yan, Kh. S.,
"Theory of Free-Radical Polymerization",
Israel Program for Scientific Translations, Jerusalem, (1968).

3. Bamford, C. J., Barb, W. G., Jenkins, A. D., Onyon, P. F.,
"The Kinetics of Vinyl Polymerization by Radical Mechanisms"
Butterworths, London, (1958).

4. Lenz, R. W.,
"Organic Chemistry of Synthetic High Polymers",
Interscience Publishers, New York, (1967).

5. Brandrup, J., Immergut, E. H.,
"Polymer Handbook"
Interscience, New York, (1966).

6. Rafikov, S. R., Messerle, P. Y., Gladyshev, G. P., Shafranskaya, I. B.,
J. Polymer Sci., B5, 715 (1967).

7. Messerle, P. Y., Gladyshev, G. P.,
Polymer Sci. USSR, 8, 2006 (1966).

8. Messerle, P. Y., Rafikov, S. R., Gladyshev, G. P.,
Dokl. Phys. Chem., 166, 7 (1966).

9. De Schriver, F., Smets, G.,
J. Polymer Sci., A1, 4, 2201 (1966).

10. Nishimura, N.,
Bul. Chem. Soc. Jap., 34, 1158 (1961).

11. Robertson, E. R.,
Trans. Faraday Soc., 52, 426 (1956).

12. Hui, A. W. T.,
"Free Radical Polymerization of Styrene in a Batch Reactor Up to High Conversion",
M. Eng. Thesis, McMaster University, Hamilton, Ontario, (1967).

13. Duerksen, J. H.,
"Free Radical Polymerization of Styrene in Continuous Stirred Tank Reactors",
Ph.D. Thesis, McMaster University, Hamilton, Ontario, (1968).

14. North, A. M.,
"Diffusion Control of Homoeneous Free Radical Reactions",
Progress in High Polymers, 2, Iliffe, (1968).

15. Schulz, G. V.,
Z. Physik Chem. N.F., 8, 290 (1956).

16. Burnett, G. M., Duncan, G. L.,
Makromol. Chem., 51, 154 (1962).

17. Burnett, G. M., Loan, L. D.,
Collect. Czechoslov. Chem. Commun., 22, 113 (1957).

18. Horie, K., Mita, I., Kambe, M.,
J. Polymer Sci., A-1, 6, 2663 (1968).

19. Gladyshev., G. P.,
Rus. Chem. Rev., 35, (1966).

20. Norrish, R. G. W., Smith, R. R.,
Nature, London, 150, 336 (1942).

21. Schulz, G. V., Harborth, G.,
Makromol. Chem., 1, 106 (1947).

22. Trommsdorff, E., Kohle, H., Lagally, P.,
B.I.O.S. 363.

23. Matheson, M. S., Auer, E. E., Bevilacqua, E. B., Hart, E. J.,
J. Am. Chem. Soc., 71, 497 (1949).

24. Hayden, P., Melville, H. W.,
J. Polymer Sci., 43, 201 (1960).

25. Bengough, W. I., Melville, H. W.,
Proc. Roy. Soc., A249, 445 (1959).

26. Fujii, S.,
Bull. Chem. Soc. Jap., 27, 238 (1954).

27. Rabinowitch, E., Wood, W. C.,
Trans. Faraday Soc., 32, 1381 (1936).

28. Allen, P. E. M., Patrick, C. R.,
Makromol. Chem., 72, 106 (1964).

29. Vaughan, M. F.,
Trans. Faraday Soc., 48, 576 (1952).

30. Vaughan, M. F.,
J. Appl. Chem., 2, 422 (1952).

31. North, A. M.,
Makromol. Chem., 49, 241 (1961).

32. Patrick, C. R.,
Makromol. Chem., 43, 248 (1961).

33. North, A. M., Reed, G. A.,
Trans. Faraday Soc., 57, 859 (1961).

34. Baldwin, M. G.,
J. Polymer Sci., A1, 3209 (1963).

35. Smith, W. B.,
ACS Polymer Preprints, 11, #2 1109 (1970).

36. May, J. A.,
"Polymer Studies by Gel Permeation Chromatography",
Ph.D. Thesis, Texas Christian University, Fort Worth, Texas, (1968).

37. Pryor, W. A., Fiske, T. R.,
Macromol., 2, 62 (1969).

38. Krause, S., Cohn-Ginsberg, E.,
J. Polymer Sci., A2, 1393 (1964).

39. Eriksson, A. F.,
Svensk. Kem. Tidskr., 68, 301 (1956).

40. Eriksson, A. F.,
Acta Chem. Scand., 10, 378 (1956).

41. Riddle, E. H.,
"Monomeric Acrylic Esters"
Reinhold, New York, (1954).

42. Pyrkov, L. M., Frenkel, S. Y.,
Rus. Chem. Rev., 32, 140 (1963).

43. Tasset, G., Smets, G.,
J. Polymer Sci., 12, 517 (1954).

44. Schulz, G. V., Henrici, G., Olive, S.,
J. Polymer Sci., 17, 45 (1955).

45. Schulz, G. V., Henrici, G., Olive, S.,
Z. Elektrochem., 60, 296 (1956).

46. Henrici-Olive, V. G. Schulz, G. V.,
Makromol. Chem., 23, 207 (1957).

47. Morton, M., Piirma, I.,
J. Am. Chem. Soc., 80, 5596 (1958).

48. Graessley, W. W., Uy, W. C., and Gandhi, A.,
I.&E.C. Fund., 8, 696 (1969).

49. Nagasubramanian, K., and Graessley, W. W.,
Chem. Eng. Sci., 25, 1549 (1970).

50. Zeman, R. J., Amundson, N. R.,
Chem. Eng. Sci., 20, 331 (1965).

51. Zeman, R. J., Amundson, N. R.,
AIChE Journal, 4, 297 (1963).

52. Zeman, R. J., Amundson, N. R.,
Chem. Eng. Sci., 20, 637 (1965).

53. Miller, M. L.,
"The Structure of Polymers",
Reinhold Publishing Corp., New York, (1966).

54. Drott, E. E., Mendelson, R. A.,
Proceedings 6th International GPC Seminar, Miami Beach, (1968).

55. Drott, E. E., Mendelson, R. A.,
Proceedings 5th International GPC Seminar, London, (1968).

56. Drott, E. E.,
Proceedings 4th International GPC Seminar, Miami Beach, (1967).

57. Tung, L. H.,
J. Polymer Sci,. A-2, 9, 759 (1971).

58. Levenspiel, O.,
"Chemical Reaction Engineering",
John Wiley & Sons, Inc., New York, (1965).

59. Smets, G., Musquelier, C., Van Tornout, F.,
Bull, Soc. Chim. Belg., 57, 493 (1948).

60. Sawada, H.,
J. Polymer Sci., B1, 305 (1963).

61. Bueche, F.,
"Physical Properties of Polymers",
Interscience Publishers, John Wiley & Sons, New York, (1962).

62. Arnett, L.,
J. Am. Chem. Soc., 74, 2027 (1952).

63. Obrien, J., Gornick, F.,
J. Am. Chem. Soc., 77, 4757 (1955).

64. Bonsal, E., Valentine, L., Melville, H.,
Trans. Faraday Soc., 48, 763 (1952).

65. O'Driscoll, K., Tobolsky, A.,
J. Coll. Sci., 11, 244 (1956).

66. Bevington, J., Melville, H., Taylor, R.,
J. Polymer Sci., 12, 449 (1952), 14, 463 (1954).

67. Nandi, U., Palit, S.,
J. Polymer Sci., 17, 65 (1955).

68. Ferington, T., Tobolsky, A.,
J. Coll. Sci., 10, 536 (1956).

69. Tobolsky, A., Baysal, B.,
J. Polymer Sci., 11, 471 (1953).

70. Saha, N., Nandi, U., Palit. S.,
J. Chem. Soc., 427, (1956).

71. Saha, N., Nandi, U., Palit, S.,
J. Chem. Soc., 7, (1958).

72. Mackay, M., Melville, H.,
Trans. Faraday Soc., 45, 323 (1949).

73. Harris, I., Miller, R. G. J.,
J. Polymer Sci., 7, 377 (1950).

74. Billmeyer, F. M., Stockmayer, W. H.,
J. Polymer Sci., 5, 121 (1950).

75. Kinell, P. O.,
Acta Chem. Scand., 1, 832 (1947).

76. Ericksson, A. F.,
Acta Chem. Scand., 3, 1 (1949).

77. Flory, P. J.,
"Principles of Polymer Chemistry",
Cornell University, New York, (1953).

78. Smith, D. A.,
"Addition Polymers: Formation and Characterization",
Plenun, New York, (1968).

79. Marshall, I., ref. Harris et. al. (Ref. 73).

80. Hui, A. W. T., Hamielec, A. E.,
J. Appl. Polymer Sci., 16, 749 (1972).

81. Ito, K.,
J. Polymer Sci., A-1, 7, 2995 (1969).

82. Hui, A. W. T.,
"Kinetics of Free Radical Polymerization of Styrene to Complete Conversion",
Ph.D. Thesis, McMaster University, Hamilton, Ontario, (1970).

83. "Removal of Inhibitors from Ethylenically Unsaturated Monomers",
U.S. Patent 3,247,242 to Rohm & Haas.

84. Johnson, B. P., Critchfield, F. M.,
Anal. Chem., 33, 910 (1961).

85. "Analytical Methods for the Acrylic Monomers",
Rohm & Haas, Co., Bulletin SP-188, Nov. (1967).

86. Reilley, C. R., Crawford, C. M.,
Anal. Chem., 27, 716 (1955).

87. Kawasaki, M., Yano, M., Imoto, T.,
22nd Meeting Chem. Soc. of Japan, 1969.

88. Yamada, S., Kitahara, S., Hattori, Y., Konakahara, Y.,
Kobunshi Kagaku, 24, 97 (1967).

89. Abdel-Alim, A. H., Hamielec, A. E.,
J. Appl. Polymer Sci., 16, 1093(1972).

90. Fox, T. G., Schnecko, H. W.,
Polymer (London), 3, 575 (1962).

91. Bovey, F. A.,
J. Polymer Sci., 46, 59 (1960).

92. Fox, T. G., Goode, W. E., Gratch, S., Huggett, C. M., Kincaid, J. F.,
Spell, A., Stroupe, J. D.,
J. Polymer Sci., 31, 173 (1958).

93. Smith, D. G.,
J. Appl. Chem., 17, 339 (1967).

94. Ito, K.,
J. Polymer Sci., A-1, 9, 577 (1971).

95. Ito, K., and Matsuda, T.,
J. Appl. Polymer Sci., 11, 311 (1970).

96. Ito, K.,
J. Polymer Sci., A-1, 8, 1823 (1970).

97. Ito, K.,
J. Polymer Sci., A-1, 7, 3387 (1969).

98. Ito, K.,
J. Polymer Sci., A-1, 7, 2707 (1969).

99. Ito, K.,
J. Polymer Sci., A-1, 7, 827 (1969).

100. Ito, K.,
J. Polymer Sci., A-1, 7, 2247 (1969).

101. Gee, G., Melville, H. W.,
Trans. Faraday Soc., 40, 240 (1944).

102. North, A. M.,
"The Kinetics of Free Radical Polymerization",
The International Encyclopedia of Physical Chemistry, Topic 17, 1,
Permagon Press, Oxford, (1966).

103. Allen, P. E. M., Patrick, C. R.,
Makromol. Chem., 47, 154 (1960).

104. Benson, S. W., North A. M.,
J. Am. Chem. Soc., 84, 935 (1962).

105. O'Driscoll, K. F., Dickson, J. R.,
J. Macromol. Sci. Chem., A2, 449 (1968).

106. Gordon, M., Roe, R. J.,
J. Polymer Sci., 21, 57 (1956).

107. Biesenberger, J. A., Capinpin, R.,
J. Appl. Polymer Sci., 16, 695 (1972).

108. Zeman, R. J.,
Keynote Address, Professional Development Course on
Polymer Reactors and Molecular Weight Distribution,
C.S.Ch.E. Meeting, Niagara Falls, October, (1967).

109. Abraham, W. H.,
I&EC Fund., 2, 221 (1963).

110. Chen, P. Y., Spencer, J. L.,
Preprint 31A, 63rd National Meeting, AIChE,
St. Louis, Missouri, Feb. 18-21, 1968.

111. Liu, S. L., Amundson, N. R.,
Rubber Chem. & Tech., 34, (1961).

112. Liu, S. L., Amundson, N. R.,
Chem. Eng. Sci., 17, 797 (1962).

113. Kowalik, J., Osborne, M. R.,
"Methods for Unconstrained Optimization Problems",
American Elsevier Publishing Co., New York, (1968).

114. Reilly, P. M.,
The Can. J. of Chem. Eng., 48, 168 (1970).

115. Elderton, W. P., Johnson, N. L.,
"Systems of Frequency Curves",
Cambridge at the University Press, New York, (1969).

116. Reilly, P. M., Private Communication,
University of Waterloo, Waterloo, Ontario (1971).

APPENDIX I-A

Stereospecificity in the AIBN Initiated Polymerization of Methyl Methacrylate

It is well established that two different propagation reactions may take place in this polymerization, giving different steric orientations of the monomer unit added. The monomer can add so that the triad (a polymer chain link along with its two neighbors on each side) is of units of the same configuration (ddd) or (lll) where "d" and "l" orientations are defined by:

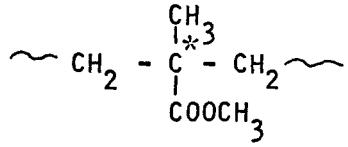

d form (I-28)

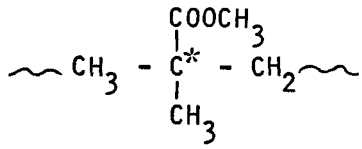

l form (I-29)

The middle link is in the isotatic configuration. If (dld) or (ldl) results the link is in the syndiotactic configuration. If (dll), (ldd) or (lld) result than the middle link is in the heterotactic configuration. The probability of the new link having the same configuration as the preceeding link is σ. Literature data[90-92] indicate that the isothermal free radical polymerization of MMA is characterized by a single value of σ and that σ is probably controlled by the configuration of the chain end unit. Then the probability of an isotactic configuration is σ^2, of a syndiotactic is $(1-\sigma)^2$ and of a heterotactic is $1-\sigma^2 - (1-\sigma)^2 = 2\sigma\ (1-\sigma)$. For

$\sigma = 0.5$ the polymer will be ideally random (atactic) with .25 isotactic triads, .25 syndiotactic and .50 heterotactic.

For PMMA polymerized using AIBN catalyst Fox et. al.[90] showed that the σ value was unaffected by degree of conversion, type of initiator or molecular weight. In polymerization, syndiotactic placement is preferred, but isotactic placement also occurs, so that the observed k_p is really the sum of two propagation constants.

$$k_p = k_{p\ isotactic} + k_{p\ syndiotactic} \qquad (I-30)$$

Fox et. al.[90] showed that the following Arrhenius equation fit experimental data over the polymerization temperature range -40 to 250°C.

$$\frac{\sigma}{1-\sigma} = \frac{k_{p\ isotactic}}{k_{p\ syndiotactic}} = 1.65 \exp(-1070/RT) \qquad (I-31)$$

The closeness of the ratio to unity (Equation (I-31)) results in there being no significant nonlinear effect on the usual Arrhenius plot of $\ln(k_p)$ versus $(1/T)$.[90]

Results of NMR analysis of selected samples from this study are shown in Table I-27 along with values calculated using (I-31). PMMA produced at these temperatures is not crystallisable.[90-92]

APPENDIX I-B

Development of the Kinetic Model

The derivation of equations from the kinetic model described in Section 3.1 is detailed in this appendix. Assumptions made are listed as they are introduced into the derivation. The polymerizing system is AIBN as initiator, methyl methacrylate as monomer and no added solvent.

Assumption 1: Only the following reactions are considered: (1) initiation, (2) propagation, (3) transfer to monomer, (4) termination by disproportionation and (5) termination by combination. The main reactions which have been considered negligible are: transfer to AIBN, transfer to polymer and terminal double bond polymerization.

The literature review (Section 2) suggested the validity of these assumptions. Their validity is further discussed in Section 3.4.5.2.

Assumption 2: All rate constants with the exception of k_t are independent of radical size. There are two main reasons for suspecting chain length dependence: (1) the initiator radical might influence future reactions of a chain by some inductive effect (this influence could only be expected to extend along the first few units of the chain), [93] and (2) diffusion controlled reactions can be chain length dependent particularly if translational diffusion of a chain influences the rate. [14]

The chain length dependence of the propagation reaction for the first mentioned reason can likely be adequately dealt with by use of the lumped unknown parameter I, (although this ignores monomer consumption) to include generation of R°_1 and hence the initial propagation

step. Chain length dependence of propagation as a result of diffusion control is not expected because of the monomer mobility.

The termination rate constant can become chain length dependent for both of the above reasons. In the literature, termination by primary free radicals is often studied as a separate topic in chain length dependence. Diffusion of the active end segment of the polymer chain just before termination has been shown by North, et.al.[33] to be the rate controlling step in termination, at least for dilute solutions. Ito,[81,94-100] in a theoretical development, has disputed chain length dependence while emphasizing primary radical termination (particularly at high conversions).

Various attempts have been made in the literature to introduce chain length dependence into a kinetic model.[14,19] Gee et. al.[101] and Bamford[3] used a factorization assumption (Equation (I-32)) with a proportionality assumption (Equation (I-33)).

$$k_{trs} = \lambda_r \lambda_s \tag{I-32}$$

$$\lambda_r = \zeta k_{pr} \tag{I-33}$$

Both North[102] and Patrick[103] have shown that these approaches are not correct for diffusion control and that a relation such as Equation (I-34) is required.

$$k_{trs} = \lambda_r + \lambda_s \tag{I-34}$$

Benson et. al.[104] present one approach to accomplish this but do not evaluate it. Duerksen[13] used the factorization assumption and replaced the proportionality assumption by empirical equations, with some success at fitting his data.

In the following derivation, chain length dependence of k_t is accounted for by assuming that only chains below a certain chain length N (a function of conversion) are mobile when diffusion control occurs. A similar idea was used by O'Driscoll et. al.[105] in a copolymerization study and by Gordon et. al.[106] in a cross linking MMA system.

Now the population balance equations of the model are:

(1) Free Radicals

$$\frac{dM^o}{dt} = k_{fm} M R^o - k_{pm} M M^o \tag{I-35}$$

when M^o is considered as R_1^o then:

$$\frac{dR_1^o}{dt} = I - k_p M R_1^o - k_{fm} M R_1^o - (k_{tc} + k_{td}) R_1^o R^o + k_{fm} M R^o \tag{I-36}$$

for $2 \leq r \leq N$

$$\frac{dR_r^o}{dt} = k_p M R_{r-1}^o - k_p M R_r^o - (k_{tc} + k_{td}) R_r^o R^o - k_{fm} M R_r^o \tag{I-37}$$

for $r > N$

$$\frac{dR_r^o}{dt} = k_p M R_{r-1}^o - k_p M R_r^o - (k_{tc} + k_{td}) R_r^o \sum_{r=1}^{N} R_r^o - k_{fm} M R_r^o \tag{I-38}$$

for the sum of all r

$$\frac{d \sum_{r=1}^{\infty} R_r^o}{dt} = \frac{dR^o}{dt} = I - (k_{tc} + k_{td}) R^o \sum_{r=1}^{N} R_r^o - (k_{tc} + k_{td}) \sum_{r=1}^{N} R_r^o \sum_{r=N+1}^{\infty} R_r^o \tag{I-39}$$

(2) Monomer

$$-\frac{dM}{dt} = k_p M R^o + k_{fm} M R^o + k_{pm} M M^o \tag{I-40}$$

(3) Dead Polymer

for $2 \leq r \leq N$

$$\frac{dP_r}{dt} = k_{fm}MR_r^o + k_{td}R_r^o R^o + \frac{k_{tc}}{2}\sum_{n=1}^{r-1} R_n^o R_{r-n}^o \qquad (I-41)$$

for $r > N$

$$\frac{dP_r}{dt} = k_{fm}MR_r^o + k_{td}R_r^o \sum_{r=1}^{N} R_r^o + \frac{k_{tc}}{2}\sum_{n=1}^{N-1} R_n^o R_{r-n}^o \qquad (I-42)$$

It is evident that for N=r Equation (I-42) reduces to Equation (I-41). Therefore, only Equation (I-41) need be solved. As will be seen, the solution for Equation (I-42) reduces to that for Equation (I-41) when N=r.

Assumption 3: Transfer reactions are negligible compared to propagation in consideration of monomer consumption. This is a common assumption and is certainly valid for long polymer chains.

Assumption 4: Transfer is non-degradative for methyl methacrylate polymerization (i.e. radicals produced by transfer are as reactive as other radicals present). This assumption is also likely valid.

Assumption 5: A stationary state for all free radical concentrations is established. As pointed out by Bamford, et.al.[3] this common assumption does not mean that the concentration of free radicals must remain constant throughout the polymerization but rather than the rate of change of their concentration must be much less than both their rate of production (through initiation) and their rate of depletion (through termination). Biesenberger, et.al.[107] have recently reviewed this assumption and has examined criteria for its validity by choosing rate constant values and numerical integration of the kinetic equations. At low conversions it has been

shown that this assumption is generally valid.[1-4] At higher conversions, its validity has been proven for styrene[82] and has been inconclusively questioned.[15-17] Mathematical techniques to avoid the assumption[50-52, 108-112] include Moment Generating Functions[112] and the Continuous Variable Method.[50-52] The mathematical simplicity gained by assuming a stationary state coupled with the need to avoid reliance on moments of the molecular weight distribution from GPC make this assumption very desirable.

The most clear manner of substantiating the assumption is to obtain rate constants from the model and the kinetic data and then to use these rate constants in the kinetic model without the assumption (i.e. using numerical integration) to see if the kinetic data can be reproduced. However, if groups of unknown parameters, rather than individual rate constant values are determined in the model, then this approach may not be possible if initiation and termination have been grouped together. Determination of upper and lower bounds for the validity of the assumption is then a possibility but these bounds depend in turn on the upper and lower bounds chosen for the unknown individual parameters (e.g. initiator efficiency). The attitude adopted here is that both the utility and the common validity of this assumption outweighs arguments against its use in this the initial study of new kinetic data.

The following parameters and dimensionless groups are defined to provide simplification of the model equations and to incorporate rate of polymerization into model parameters:

$$\alpha = \frac{k_{td}}{k_p^2} \frac{R_p}{M^2} \qquad (1\text{-}43)$$

$$\beta = \frac{k_{tc}}{k_p^2} \frac{R_p}{M^2} \tag{1-44}$$

$$C_m = \frac{k_{fm}}{k_p} \tag{1-45}$$

$$\tau = C_m + \alpha \tag{1-46}$$

$$R^o = \sum_{r=1}^{\infty} R_r^o = \sum_{r=1}^{N} R_r^o + \sum_{r=N+1}^{\infty} R_r^o \tag{1-47}$$

$$Z = \frac{\sum_{r=1}^{N} R_r^o}{\sum_{r=1}^{\infty} R_r^o} = \frac{\sum_{r=1}^{N} R_r^o}{R^o} \tag{1-48}$$

$$\phi_2 = R_1^o \tag{1-49}$$

Now from Equations (1-36) to (1-38).

$$\phi_2 = \frac{\frac{R_p}{k_p M} (Z(2-Z)\ \alpha + Z(2-Z)\ \beta + C_m)}{1 + \tau + \beta} \tag{1-50}$$

$$R_r^o = \frac{R_{r-1}^o}{1 + \alpha + \beta + C_m} \quad \text{for } 2 \le r \le N \tag{1-51}$$

$$= \phi_1 R_{r-1}$$

$$R_r^o = \frac{R_{r-1}^o}{1 + \beta Z + \alpha Z + C_m} \quad \text{for } r > N \tag{1-52}$$

$$= \phi_3^{r-N} R_N^o \tag{1-53}$$

The recurrence relationship for free radicals can thus be written as one equation:

$$R_r^o = \phi_3^{r-N}\ \phi_1^{N-1}\ \phi_2 \tag{1-54}$$

where N=r for calculation of free radical concentrations with chain length less than N and is a well known recurrence relationship.

From the dead polymer population balance for $r > N$

$$\frac{dP_r}{dt} = R_p \phi_3^{r-N} \phi_1^{N} (Z(2-Z)\alpha + Z(2-Z)\beta + C_m)(C_m + Z\alpha) + R_p \frac{\beta}{2} (Z(2-Z)\alpha + Z(2-Z)\beta + C_m)^2 (N-1) \phi_3^{r-2N} \phi_1^{2N} \quad (I-55)$$

since

$$W_r = \frac{drP_r}{d\sum_{r=1}^{\infty} P_r} = \frac{drP_r}{(-dM)} \quad (I-56)$$

multiply Equation (I-55) by r and use $R_p = -\frac{dM}{dt}$

$$W_r = r\phi_3^{r-N} \phi_1^{N} (Z(2-Z)\alpha + Z(2-Z)\beta + C_m)(C_m + Z\alpha) + \frac{\beta}{2} (Z(2-Z)\alpha + Z(2-Z)\beta + C_m)^2 r(N-1) \phi_1^{2N} \phi_3^{r-2N} \quad (I-57)$$

For $2 \leq r \leq N$

set N = r and z = 1 in Equation (I-57)

Then:

$$W_r = r\phi_1^{r} (\tau + \beta)\tau + \frac{\beta}{2} (\tau + \beta)^2 r^2 \phi_1^{r} \quad (I-58)$$

This is the classical expression for the chain length distribution.

Then:

$$Mn_i = M_o r_{N_i} = M_o(1/(\tau + \beta/2)) \quad (I-59)$$

$$Mw_i/Mn_i = 2\text{-}2\ (0.5\beta/(\tau + \beta))^2 \quad (I-60)$$

Assumption 6: There is no chain length dependence for any of the rate constants.

Then N = r and Equation (I-58) is used to calculate W_r.

The main reason that this commonly made assumption was introduced here was because although a relationship between "Z" and "N" can be derived via the free radical recurrence relationships the variation of N with conversion adds another unknown function to the model. At low conversion, as is evident from the above discussion, this assumption is likely valid. At higher conversions its validity is in doubt. However, as will become evident below, permitting variation of rate constants with conversion tends to eliminate this assumption.

Assumption 7: Disproportionation is the only significant termination mechanism. This is in agreement with much of the literature but was only made after some indication of its validity at low conversion was obtained through experimental data (ref. Section 3.4.4.2).

Setting β and C_m equal to zero gives

$$W_r = r\left(\frac{1}{1+\alpha}\right)^r \alpha^2 \simeq \alpha^2 r \exp(-\alpha r) \qquad (I-61)$$

Note that if chain length dependence were included

$$W_r = r\left(\frac{1}{1+Z\alpha}\right)^{r-N}\left(\frac{1}{1+\alpha}\right)^{NZ^2} \alpha^2 (2-Z) \qquad (I-62)$$

Let $\alpha^* = Z\alpha$

Then

$$W_r = r\left(\frac{1}{1+\alpha^*}\right)^r \left(\frac{1+\alpha^*}{1+\alpha}\right)^N (2-Z)\ \alpha^{*2} \qquad (I-63)$$

If Z is near unity (i.e. if most of the free radicals present are mobile) then a search for α^* is equivalent to a search for α. This is the situation at low conversion or at higher conversion when the existing free radicals are about equal in mobility.

Assumption 8: In calculating the cumulative W_r (the observed W_r) from summation of the instantaneous values it is assumed that shrinkage during polymerization is proportional to conversion. That is,

$$\frac{V-V_o}{V_o} = \epsilon X \qquad (I-64)$$

where V_o = initial volume of reactants

V = volume of reactants (monomer and polymer) at conversion X

ϵ = proportionality constant

X = weight of polymer/(weight of monomer + weight of polymer)

$$= \frac{M_o V_o - MV}{M_o V_o}$$

This assumption has been used before[82] although often shrinkage is ignored in polymerization studies.[I-4] Shrinkage in methyl methacrylate polymerization is about 25% at final conversion.[45]

APPENDIX I-C

Formulating the Search Objective Function

In this study, single and multivariable searches were used to obtain parameter estimates which allowed experimental chromatograms to be fit by the kinetic model. The objective function is the mathematical relation expressing the difference between the experimental and model-predicted chromatogram heights. The search seeks to minimize the objective function by successive guessing of the unknown parameters. This study used a Fibonacci Search for single parameter models and a Nelder Mead Simplex Search for two or three parameter models.[113] Unconstrained optimization was made possible by using the following transformation for the searched parameters:[113]

$$\theta_{N_i} = \frac{\exp(\bar{\theta}_i)}{\exp(\bar{\theta}_i) + \exp(-\bar{\theta}_i)} \tag{I-65}$$

$$\theta_i = \theta_{MIN_i} + (\theta_{MAX_i} - \theta_{MIN_i}) \cdot \theta_{N_i} \tag{I-66}$$

where $\bar{\theta}_i$ is searched $(-\infty \leq \theta_i \leq \infty)$

θ_{MAX_i} = maximum value of θ_i

θ_{MIN_i} = minimum value of θ_i

θ_{N_i} is the normalized parameter $(0 \leq \theta_{N_i} \leq 1)$

θ_i is the parameter value used in the objective function

Three major considerations are involved here in formulation of the objective function:

(1) Experimental Error in the Chromatogram Heights

One common way of introducing experimental error into the objective function is the Generalized Least Squares Method.[82,114] The method is based upon maximizing the Likelihood Function. If error covariances between heights are zero and the error standard deviation is proportional to the height than the following objective function is suitable:

$$O_1(\alpha) = \sum_{j=1}^{N_{CURVE}} \sum_{i=1}^{N_{HEIGHT}} \left\{ \frac{F_{N_j}(v_i) - F_{N_j}(v_i)_{MODEL}}{F_{N_j}(v_i)} \right\}^2 \quad (I\text{-}67)$$

where N_{CURVE} is the number of chromatograms to be simultaneously fit, and N_{HEIGHT} is the number of heights examined per curve.

Function $O_1(\alpha)$ was used throughout this study. Table I-26 shows its magnitude at the end of two and three variable searches. Some improvement is evident in the three variable search results. The two variable search always reduced the function by more than a factor of ten. Figures I-13 and II-6 justify the approximation that the standard deviation of the heights is proportional to the height. Attempts to introduce either experimental covariance or a Bayesian estimate[82] of covariance into the objective function met with no success because of the singularity of the resulting variance-covariance matrix. The most plausible reason found for this is that the heights are not independent because they are all interrelated as shown by the Tung Axial Dispersion equation (Equation (II-12)).

Elderton and Johnson[115] suggest the use of χ^2 to provide an estimate of best fit. This was also suggested in a private communication by Reilly.[116] The χ^2 objective function can be phrased as follows:

$$O_2(\alpha) = \sum_{j=1}^{N_{CURVE}} \sum_{i=1}^{N_{HEIGHT}} \frac{\left\{F_{N_j}(v_i)_{MODEL} - F_{N_j}(v_i)\right\}^2}{F_{N_j}(v_i)_{MODEL}} \qquad (I\text{-}68)$$

Given a series of chromatogram heights $F_N(v)$, the objective function is to decide whether or not the parameter estimates minimize the probability of obtaining deviations the same as or greater than that found by the search.

$O_2(\alpha)$ was used with the 70°C, 0.3% AIBN data for a two and three variable search. Chromatograms obtained were identical within experimental error to those obtained with $O_1(\alpha)$.

(2) The Effect of Axial Dispersion on the Chromatogram Heights

The effect is minimized by choosing heights near the points of inflection on the experimental chromatograms and by examining broad chromatograms.

(3) The Relative Importance of One Part of the Chromatogram with Respect to Another

For example, if a high molecular weight tail was important to fit by a kinetic model because of its effect on flow properties, then many heights could be taken from that area of the chromatogram for the objective function. In this study, heights were chosen across the chromatogram near the inflection points. Good overall fits were obtained. However, the sudden onset of the high molecular weight spike is not predicted well and, in addition, at 70°C, 0.3% AIBN Mw's are not fit well by either the two or the three variable searches, despite the fact that the objective function is well satisfied.

TABLE I-1

REPRODUCIBILITY STUDIES

CONVERSIONS BY GRAVIMETRIC METHOD

(1) PMMA PREPARED AT 50.0°C, 0.5 wt.% AIBN REACTION TIME = 300.0 MIN.

SAMPLE NO.	CONVERSION
9I	.8529
7F	.8453
7G	.8491
9O	.8509
9U	.8552
1E	.8694
6B	.8525
9X	.8522
8C	.8548
9Z	.8501
9H	.8485
9E	.8474
7E	.8465
9N	.8518
7H	.8504
7I	.8541
MEAN	.8519
SAMPLE ESTIMATE OF VARIANCE	3.00594E-05
.95 CONFIDENCE LIMITS	.0029
CONFIDENCE LIMITS AS PERCENT OF MEAN	.3428

(2) PMMA PREPARED AT 50.0°C, 0.5 wt.% AIBN, REACTION TIME = 240.0 MIN.

SAMPLE NO.	CONVERSION
9W	.6842
9Y	.6146
7C	.7161
10J	.6279
2N	.6179
8B	.6810
8D	.6828
9B	.5863
9G	.6739
9M	.6735
9V	.6843
9C	.5739
9D	.7070
7B	.7126

TABLE I-1 (CONTINUED)

MEAN	.6597
SAMPLE ESTIMATE OF VARIANCE	2.17988E-03
.95 CONFIDENCE LIMITS	.0270
CONFIDENCE LIMITS AS PERCENT OF MEAN	4.0856

(3) PMMA PREPARED AT 90.0°C, 0.5 wt.% AIBN, REACTION TIME = 14.0 MIN.

SAMPLE NO.	CONVERSION
26D	.4603
26E	.4571
26G	.4587
26H	.4569
26I	.4582

MEAN	.4582
SAMPLE ESTIMATE OF VARIANCE	1.84300E-06
.95 CONFIDENCE LIMITS	.0017
CONFIDENCE LIMITS AS PERCENT OF MEAN	.3678

TABLE I-2

REPRODUCIBILITY STUDIES

GPC MOLECULAR WEIGHT AVERAGES

(1) FIVE DIFFERENT AMPOULE EXPERIMENTS AT THE ONSET OF THE GEL EFFECT PREPARED AT 90.0°C, WITH 0.5 wt.% AIBN

REACTION TIME = 14.0 MIN., APPROXIMATE CONVERSION = 45%
(REFER TO TABLE I-10)

RUN	Mn (∞)	Mw (∞)	Mz (∞)	M(z+1) (∞)	Mw(∞)/Mn(∞)
602	5.96E+04	2.01E+05	1.24E+06	3.08E+06	3.37
603	5.72E+04	2.02E+05	1.49E+06	3.98E+06	3.52
604	5.73E+04	2.01E+05	1.78E+06	5.20E+06	3.51
605	5.52E+04	1.47E+05	1.04E+06	4.66E+06	2.66
606	6.16E+04	2.28E+05	1.68E+06	4.15E+06	3.70
MEAN	5.82E+04	1.96E+05	1.44E+06	4.21E+06	3.35
SAMPLE ESTIMATE OF VARIANCE	6.05E+06	8.85E+08	9.39E+10	6.29E+11	.164
.95 CONFIDENCE LIMITS	3.05E+03	3.69E+04	3.80E+05	9.85E+05	.504
CONFIDENCE LIMITS AS A PERCENT OF MEAN	5.25E+00	1.89E+01	2.64E+01	2.34E+01	15.2

(2) SIX DIFFERENT GPC INJECTIONS OF THE SAME PMMA SAMPLE PREPARED AT 70.0°C, 0.5 wt.% AIBN, LIMITING CONVERSION

RUN	Mn (∞)	Mw (∞)	Mz (∞)	M(z+1) (∞)	Mw(∞)/Mn(∞)
610	2.76E+05	1.40E+06	3.52E+06	5.59E+06	5.09
615	2.55E+05	1.38E+06	3.44E+06	5.38E+06	5.41
616	2.57E+05	1.39E+06	3.48E+06	5.49E+06	5.40
617	2.60E+05	1.36E+06	3.37E+06	5.20E+06	5.25
618	2.50E+05	1.35E+06	3.33E+06	5.11E+06	5.42
619	2.63E+05	1.39E+06	3.47E+06	5.43E+06	5.29
MEAN	2.60E+05	1.38E+06	3.44E+06	5.37E+06	5.31
SAMPLE ESTIMATE OF VARIANCE	7.84E+07	3.39E+08	4.88E+09	3.34E+10	.0162
.95 CONFIDENCE LIMITS	9.29E+03	1.93E+04	7.33E+04	1.92E+05	.134
CONFIDENCE LIMITS AS A PERCENT OF MEAN	3.57E+00	1.40E+00	2.13E+00	3.58E+00	2.52

TABLE I-3

GRAVIMETRICALLY DETERMINED AND PREDICTED CONVERSIONS

REACTION TEMPERATURE = 50.0°C
AIBN CONC = .3 wt.%
FIRST ORDER RATE CONSTANT = 1.070 E-03 (1./MIN)
SAWADA EQUATION CONSTANTS
a = .8704
b = .2020
k_k = 7.076 E-02
c_1^p = -1.994 E+01

SAMPLE NO.	AMPOULE TYPE,	TIME (min.)	X (experiment)	X (first order)	X (Sawada)	FREE VOLUME
11S	2	60.0	.0626	.0622		.172
11R	2	84.6	.0852	.0866		.168
11T	3	120.0	.1152	.1205		.164
11Q	3	160.0	.1585	.1574		.157
11P	3	200.0	.2023	.1927	.2157	.150
11B	5	220.0	.2493	.2098	.2361	.143
11F	3	240.0	.2795		.2832	.138
11C	5	250.0	.3273		.3234	.130
11G	3	260.0	.3831		.3776	.121
11H	3	272.0	.4628		.4599	.106
11D	3	280.0	.5147		.5222	.097
11U	3	290.0	.6807		.6000	.065
11O	5	300.0	.7721		.6716	.046
11V	1	300.0	.8002		.6716	.040
11N	3	320.0	.8297		.7761	.034
11M	3	340.0	.8411		.8303	.031
11K	3	371.3	.8522		.8609	.029
11L	3	460.0	.8647		.8703	.026
11J	3	187.3hrs.	.9240		.8704	.012

TABLE I-4

GRAVIMETRICALLY DETERMINED AND PREDICTED CONVERSION

REACTION TEMPERATURE = 50.0°C
AIBN CONC = .391 wt.%
FIRST ORDER RATE CONSTANT = 1.216 E-03 (1./MIN)
SAWADA EQUATION CONSTANTS
a = .8704
b = .2020
$k_p k$ = 8.104 E-02
c_1^p = -2.038 E+01

SAMPLE NO.	AMPOULE TYPE	TIME (min.)	X (experiment)	X (first order)	X (Sawada)	FREE VOLUME
12A	2	60.0	.0709	.0704		.171
4I	2	84.6	.1036	.0978		.166
12B	2	100.0	.1095	.1145		.165
4H	2	124.2	.1449	.1402		.159
12D	3	150.0	.1671	.1668		.156
12E	3	170.0	.1889	.1868	.2100	.153
4G	2	187.5	.2433	.2039	.2222	.144
12F	3	212.8	.2871		.2752	.137
12R	3	225.0	.3221		.3303	.131
12Q	5	240.4	.4127		.4384	.115
4D	2	254.4	.5642		.5624	.088
12K	3	260.0	.5985		.6116	.081
12H	3	272.0	.7232		.7046	.056
12L	3	280.0	.8079		.7528	.038
4C	2	302.4	.8413		.8305	.031
4B	2	371.3	.8601		.8694	.027
12I	3	460.0	.8662		.8704	.025
4F	2	266.3hrs.	.9170		.8704	.014

TABLE I-5

GRAVIMETRICALLY DETERMINED AND PREDICTED CONVERSIONS

REACTION TEMPERATURE = 50.0°C
AIBN CONC = .5 wt.%
FIRST ORDER RATE CONSTANT = 1.402 E-03 (1./MIN)
SAWADA EQUATION CONSTANTS
a = .8704
b = .2020
$k_p k$ = 6.513 E-02
c_1 = -1.556 E+01

SAMPLE NO.	AMPOULE TYPE,	TIME (min.)	X (experiment)	X (first order)	X (Sawada)	FREE VOLUME
2A	1	33.0	.0433	.0452		.175
1A	1	60.0	.0810	.0807		.169
2B	1	60.0	.0758	.0807		.170
10A	2	60.0	.0801	.0807		.169
10Z	2	84.6	.1096	.1119		.165
10K	2	84.6	.1117	.1119		.164
2K	2	90.0	.1128	.1186		.164
2C	1	105.0	.1300	.1369		.162
1B	1	120.0	.1518	.1549		.158
2L	2	120.0	.1461	.1549		.159
6A	3	120.0	.1568	.1549		.158
9F	3	120.0	.1481	.1550		.159
2M	2	135.0	.1663	.1725		.156
2D	1	150.0	.1922	.1897	.2157	.152
8A	2	150.0	.1913	.1897	.2157	.152
2E	1	165.5	.2174	.2071	.2283	.148
2F	1	180.0	.2463	.2231	.2498	.143
1C	1	180.0	.2473	.2231	.2498	.143
10P	3	186.4	.2612		.2638	.141
6H	3	186.4	.2727		.2638	.139
10L	2	186.4	.2703		.2638	.140
10M	2	210.0	.3571		.3500	.125
10I	3	210.0	.3492		.3500	.126
6C	3	212.2	.3404		.3611	.128
10Q	3	228.3	.4601		.4603	.107
10T	3	235.0	.5165		.5080	.097
9W	2	240.0	.6842		.5443	.064
9Y	3	240.0	.6146		.5443	.078
7C	3	240.0	.7161		.5443	.058
10J	3	240.0	.6279		.5443	.075
2N	2	240.0	.6179		.5443	.077
8B	2	240.0	.6810		.5443	.065
8D	2	240.0	.6828		.5443	.064
9B	3	240.0	.5863		.5443	.083
1D	1	240.0	.8562		.5443	.028
9G	2	240.0	.6739		.5443	.066

TABLE I-5 (CONTINUED)

SAMPLE NO.	AMPOULE TYPE	TIME (min.)	X (experiment)	X (first order)	X (Sawada)	FREE VOLUME
9M	3	240.0	.6735		.5443	.066
9V	2	240.0	.6843		.5443	.064
9C	3	240.0	.5739		.5445	.086
9D	2	240.0	.7070		.5445	.060
7B	3	240.0	.7126		.5449	.058
7M	3	240.6	.6836		.5493	.064
10W	3	245.0	.7043		.5804	.060
10O	2	245.0	.7790		.5804	.044
10V	3	245.0	.7129		.5804	.058
10H	3	252.0	.7996		.6291	.040
10N	2	254.4	.8270		.6449	.034
6F	3	262.5	.8263		.6959	.034
2G	1	270.0	.8451		.7333	.030
9K	2	270.0	.8330		.7333	.033
7J	3	270.0	.8403		.7333	.031
6G	3	278.3	.8415		.7686	.031
9I	2	300.0	.8529		.8267	.028
7F	3	300.0	.8453		.8267	.030
7G	3	300.0	.8491		.8267	.029
9O	3	300.0	.8509		.8267	.029
9U	3	300.0	.8552		.8267	.028
1E	1	300.0	.8694		.8267	.025
6B	3	300.0	.8525		.8267	.028
9X	2	300.0	.8522		.8267	.029
8C	2	300.0	.8548		.8267	.028
9Z	3	300.0	.8501		.8267	.029
9H	2	300.0	.8485		.8268	.029
9E	3	300.0	.8474		.8268	.030
7E	3	300.1	.8465		.8269	.030
9N	3	300.1	.8518		.8269	.029
7H	3	300.1	.8504		.8269	.029
7I	3	300.2	.8541		.8270	.028
2O	2	301.0	.8682		.8285	.025
2H	1	360.0	.8711		.8670	.024
1F	1	360.0	.8806		.8670	.022
10R	3	376.2	.8655		.8687	.026
1H	1	420.0	.8846		.8701	.021
2I	1	420.0	.8709		.8701	.024
1I	1	420.0	.8836		.8701	.022
1G	1	420.0	.8826		.8701	.022
2J	1	31.5hrs.	.9047		.8704	.017
10X	3	138.2	.9272		.8704	.012

TABLE I-6

GRAVIMETRICALLY DETERMINED AND PREDICTED CONVERSION

REACTION TEMPERATURE = 70.0°C
AIBN CONC = .3 wt.%
FIRST ORDER RATE CONSTANT = 6.215 E-03 (1./MIN)
SAWADA EQUATION CONSTANTS
a = .9189
b = .3163
$k_p k$ = 4.153 E-01
c_1^p = -2.856 E+01

SAMPLE NO.	AMPOULE TYPE	TIME (min.)	X (experiment)	X (first order)	X (Sawada)	FREE VOLUME
11W	2	10.0	.0588	.0603		.192
14A	3	15.0	.0896	.0892		.187
11X	2	20.0	.1157	.1170		.183
14B	3	35.0	.1905	.1955		.171
14D	3	50.0	.2841	.2671	.3217	.156
14E	3	60.1	.3785	.3118	.3784	.139
23C	6	65.0	.4857		.4857	.119
14F	3	70.0	.8317		.6643	.046
14G	3	80.0	.8854		.8848	.033
16F	3	85.0	.8977		.9087	.030
14H	3	90.0	.9030		.9159	.028
14I	3	100.0	.9051		.9187	.028
14C	3	105.0	.9100		.9188	.027
16G	3	114.6	.9123		.9189	.026
16D	3	120.0	.9133		.9189	.026
16B	3	130.0	.9123		.9189	.026
16C	3	140.0	.9218		.9189	.024
16A	3	150.0	.9201		.9189	.024
16I	3	170.0	.9201		.9189	.024
14J	3	217.9	.9221		.9189	.024
16H	3	46.5hrs.	.9551		.9189	.015

TABLE I-7

GRAVIMETRICALLY DETERMINED AND PREDICTED CONVERSION

REACTION TEMPERATURE = 70.0°C
AIBN CONC = .5 wt.%
FIRST ORDER RATE CONSTANT = 7.398 E-03 (1./MIN)
SAWADA EQUATION CONSTANTS
a = .9189
b = .3163
k_k = 5.483 E-01
c_1^P = -3.123 E+01

SAMPLE NO.	AMPOULE TYPE	TIME (min.)	X (experiment)	X (first order)	X (Sawada)	FREE VOLUME
19C	3	5.0	.0400	.0365		.195
19A	3	10.0	.0745	.0714		.190
10S	3	20.0	.1407	.1376		.179
19D	3	35.0	.2395	.2282	.3167	.163
15H	3	45.0	.3276	.2832	.3277	.148
15I	3	55.0	.5286		.5237	.111
19B	3	60.1	.7596		.7624	.062
15E	3	63.8	.8692		.8620	.037
18B	6	70.0	.8943		.9110	.031
18G	6	76.4	.9033		.9179	.028
18D	6	80.0	.9115		.9186	.026
18E	6	80.3	.9045		.9186	.028
18C	6	100.0	.9105		.9189	.027
18F	6	186.1	.9311		.9189	.021
18J	6	46.5hrs.	.9570		.9189	.015

TABLE I-8

GRAVIMETRICALLY DETERMINED AND PREDICTED CONVERSION

REACTION TEMPERATURE = 90.0°C
AIBN CONC = 0.0 wt.%
FIRST ORDER RATE CONSTANT = 2.136 E-04 (1./MIN)

SAMPLE NO.	AMPOULE TYPE	TIME (min.)	X (experiment)	X (first order)	FREE VOLUME
3L	2	81.7	.0251	.0173	.217
3H	2	88.5	.0196	.0187	.218
3J	2	127.8	.0355	.0269	.216
3I	2	127.8	.0350	.0269	.216
3K	2	171.9	.0420	.0360	.215
3E	2	196.9	.0486	.0412	.213
3M	2	203.5	.0497	.0425	.213
3N	2	254.4	.0602	.0529	.212
3B	2	256.4	.0567	.0533	.212
3A	2	302.6	.0681	.0626	.210
3C	2	321.8	.0760	.0664	.209
3D	2	379.6	.0863	.0779	.208
3G	2	895.8	.2576	.1741	.179

TABLE I-9

GRAVIMETRICALLY DETERMINED AND PREDICTED CONVERSION

REACTION TEMPERATURE = 90.0°C
AIBN CONC = .3 wt.%
FIRST ORDER RATE CONSTANT = 2.893 E-02 (1./MIN)
SAWADA EQUATION CONSTANTS
a = .9602
b = .4193
k_k = 1.705 E+00
c_1^p = -3.505 E+01

SAMPLE NO.	AMPOULE TYPE	TIME (min.)	X (experiment)	X (first order)	X (Sawada)	FREE VOLUME
23E	6	7.0	.1802	.1833		.192
25H	6	8.0	.2069	.2066		.188
23I	6	8.2	.2117	.2105		.187
25D	6	9.0	.2253	.2292		.184
23B	6	10.1	.2513	.2538		.180
25J	6	11.0	.2715	.2725		.176
23G	6	12.3	.3062	.3004		.170
25I	6	13.0	.3206	.3134		.167
25G	6	15.0	.3675	.3520	.4225	.159
23F	6	16.0	.4036	.3710	.4275	.152
25B	6	17.0	.4274		.4389	.147
25C	6	19.0	.5407		.5234	.125
23H	6	20.0	.6518		.6220	.101
25A	6	21.0	.7284		.7445	.083
25E	6	27.1	.9371		.9589	.031
25F	6	424.0	.9689		.9602	.022

TABLE I-10

GRAVIMETRICALLY DETERMINED AND PREDICTED CONVERSION

REACTION TEMPERATURE = 90.0°C
AIBN CONC = .5 wt.%
FIRST ORDER RATE CONSTANT = 3.595 E-02 (1./MIN)
SAWADA EQUATION CONSTANTS
a = .9602
b = .4193
$k_p k$ = 1.923 E+00
c_1^p = -3.169 E+01

SAMPLE NO.	AMPOULE TYPE	TIME (min.)	X (experiment)	X (first order)	X (Sawada)	FREE VOLUME
22C	3	6.0	.1911	.1946		.190
22E	3	7.1	.2265	.2244		.184
22D	3	8.0	.2532	.2505		.180
24F	6	10.0	.3083	.3017		.170
26C	6	10.0	.3040	.3020	.4199	.171
24C	6	12.0	.3746	.3509	.4245	.157
26A	6	13.0	.4077	.3733	.4334	.151
26D	6	14.0	.4603		.4574	.141
26E	6	14.0	.4571		.4574	.142
26G	6	14.0	.4587		.4574	.141
26H	6	14.0	.4569		.4574	.142
26I	6	14.0	.4582		.4574	.141
24A	6	15.0	.5389		.5147	.125
24E	6	16.0	.6331		.6260	.105
24G	6	17.0	.7335		.7609	.082
24B	6	18.1	.9007		.8724	.041
26B	6	19.0	.9193		.9235	.036
24D	6	20.1	.9283		.9483	.033
24J	6	27.1	.9407		.9602	.030
24H	6	60.0	.9515		.9602	.027
27A	3	122.0	.9586		.9602	.025
26F	6	400.0	.9663		.9602	.023

TABLE I-11

INFINITE RESOLUTION MOLECULAR WEIGHT AVERAGES

T = 50°C
AIBN = 0.3 wt.%

SAMPLE NO.	TIME (min.)	X	GPC #	COLUMN CODE	$M_n(\infty)$	$M_w(\infty)$	$M_z(\infty)$	$M_{z+1}(\infty)$	$P(\infty)$
11R	84.6	.0852	628	27	4.52 E+05	1.03 E+06	1.90 E+06	3.15 E+06	2.28
11R	84.6	.0852	640	28	3.89 E+05	1.02 E+06	1.93 E+06	3.31 E+06	2.63
11R	84.6	.0852	686MP*	28	4.37 E+05	1.01 E+06	1.76 E+06	2.68 E+06	2.31
11T	120.0	.1152	649	28	5.48 E+05	1.22 E+06	2.06 E+06	2.97 E+06	2.23
11P	200.0	.2023	642	28	4.92 E+05	1.26 E+06	2.42 E+06	3.97 E+06	2.56
11C	250.0	.3273	641	28	5.96 E+05	2.03 E+06	4.12 E+06	6.04 E+06	3.40

*MP indicates monomer polymer mixture rather than precipitated polymer

TABLE I-12

INFINITE RESOLUTION MOLECULAR WEIGHT AVERAGES

T = 50°C
AIBN = 0.391 wt.%

SAMPLE NO.	TIME (min.)	X	GPC #	COLUMN CODE	Mn (∞)	Mw (∞)	Mz (∞)	Mz+1 (∞)	P (∞)
4I	84.6	.1036	560MP*	25	3.67 E+05	1.22 E+06	3.75 E+06	9.78 E+06	3.32
4I	84.6	.1036	569MP	25	3.84 E+05	1.25 E+06	4.15 E+06	1.24 E+07	3.25
4I	84.6	.1036	626	27	3.91 E+05	9.85 E+05	2.17 E+06	4.44 E+06	2.52
4I	84.6	.1036	648	28	3.68 E+05	9.22 E+05	1.74 E+06	2.79 E+06	2.50
4H	124.2	.1449	559MP	25	3.54 E+05	1.02 E+06	2.26 E+06	4.37 E+06	2.88
4H	124.2	.1449	650	28	3.76 E+05	9.58 E+05	1.96 E+06	3.69 E+06	2.55
12D	150.0	.1671	700	28	3.69 E+05	9.34 E+05	1.75 E+06	2.84 E+06	2.52
4G	187.5	.2433	643	28	4.12 E+05	1.32 E+06	2.96 E+06	5.03 E+06	3.20

*MP indicates monomer polymer mixture rather than precipitated polymer

TABLE I-13

INFINITE RESOLUTION MOLECULAR WEIGHT AVERAGES

T = 50°C
AIBN = 0.5 wt.%

SAMPLE NO.	TIME (min.)	X	GPC #	COLUMN CODE	Mn(∞)	Mw(∞)	Mz(∞)	Mz+1(∞)	P(∞)
10A	60.0	.0801	627	27	3.38 E+05	7.19 E+05	1.21 E+06	1.77 E+06	2.12
10A	60.0	.0801	647	28	2.96 E+05	7.20 E+05	1.24 E+06	1.81 E+06	2.43
10A	60.0	.0801	685MP*	28	2.76 E+05	7.39 E+05	1.36 E+06	2.18 E+06	2.67
10K	84.6	.1117	644	28	3.24 E+05	8.04 E+05	1.48 E+06	2.39 E+06	2.48
9F	120.0	.1481	646	28	3.68 E+05	8.41 E+05	1.53 E+06	2.50 E+06	2.28
10I	210.0	.3492	645	28	4.96 E+05	1.81 E+06	4.63 E+06	9.85 E+06	3.65

*MP indicates monomer polymer mixture rather than precipitated polymer

TABLE I-14

INFINITE RESOLUTION MOLECULAR WEIGHT AVERAGES

T = 70°C
AIBN = 0.3 wt.%

SAMPLE NO.	TIME (min.)	X	GPC #	COLUMN CODE	Mn(∞)	Mw(∞)	Mz(∞)	Mz+1(∞)	P(∞)
11W	10.0	.0588	583	27	1.40 E+05	3.09 E+05	5.28 E+05	7.79 E+05	2.20
11W	10.0	.0588	612	27	1.43 E+05	3.14 E+05	5.41 E+05	8.05 E+05	2.19
11W	10.0	.0588	634	28	1.52 E+05	3.31 E+05	5.90 E+05	9.19 E+05	2.18
14A	15.0	.0896	593	27	1.44 E+05	3.06 E+05	5.18 E+05	7.57 E+05	2.13
14A	15.0	.0896	613	27	1.41 E+05	3.17 E+05	5.87 E+05	9.96 E+05	2.25
14A	15.0	.0896	670MP*	28	1.44 E+05	3.19 E+05	5.77 E+05	9.42 E+05	2.22
11X	20.0	.1157	584	27	1.39 E+05	2.98 E+05	4.98 E+05	7.15 E+05	2.14
14E	60.1	.3785	588	27	1.66 E+05	6.75 E+05	3.10 E+06	6.69 E+06	4.07
14E	60.1	.3785	637	28	1.61 E+05	7.39 E+05	3.45 E+06	7.38 E+06	4.58
14E	60.1	.3785	669MP	28	1.58 E+05	6.61 E+05	2.79 E+06	6.21 E+06	4.18
23C	65.0	.4857	589	27	2.05 E+05	1.02 E+06	3.73 E+06	6.54 E+06	5.00
14F	70.0	.8317	595	27	3.02 E+05	1.61 E+06	3.88 E+06	5.81 E+06	5.31
14H	90.0	.9030	586	27	3.52 E+05	1.81 E+06	4.06 E+06	5.84 E+06	5.12
16H	46.5hrs.	.9551	598	27	3.73 E+05	1.82 E+06	4.09 E+06	5.92 E+06	4.88

*MP indicates monomer polymer mixture rather than precipitated polymer

TABLE I-15

INFINITE RESOLUTION MOLECULAR WEIGHT AVERAGES

T = 70°C
AIBN = 0.5 wt.%

SAMPLE NO.	TIME (min.)	X	GPC #	COLUMN CODE	Mn (∞)	Mw(∞)	Mz (∞)	Mz+1 (∞)	P (∞)
19C	5.0	.0400	600	27	1.23 E+05	2.57 E+05	4.34 E+05	6.29 E+05	2.09
19C	5.0	.0400	622	27	1.11 E+05	2.79 E+05	6.29 E+05	1.50 E+06	2.51
19A	10.0	.0745	599	27	1.14 E+05	2.45 E+05	4.23 E+05	6.44 E+05	2.14
19A	10.0	.0745	620	27	1.05 E+05	2.74 E+05	7.09 E+05	1.98 E+06	2.60
19A	10.0	.0745	671MP*	28	1.09 E+05	2.34 E+05	3.82 E+05	5.28 E+05	2.14
10S	20.0	.1407	585	27	1.11 E+05	2.88 E+05	9.70 E+05	3.01 E+06	2.59
10S	20.0	.1407	611	27	1.17 E+05	2.84 E+05	9.86 E+05	3.33 E+06	2.44
10S	20.0	.1407	636	28	1.12 E+05	2.39 E+05	4.04 E+05	5.83 E+05	2.14
15H	45.0	.3276	587	27	1.24 E+05	4.01 E+05	2.47 E+06	6.88 E+06	3.24
15H	45.0	.3276	635	28	1.21 E+05	3.81 E+05	1.94 E+06	5.45 E+06	3.16
15I	55.0	.5286	576	27	1.85 E+05	9.44 E+05	3.85 E+06	6.92 E+06	5.10
15I	55.0	.5286	581	27	1.68 E+05	8.52 E+05	3.31 E+06	5.83 E+06	5.06
19B	60.1	.7596	573	27	2.23 E+05	1.18 E+06	3.14 E+06	4.92 E+06	5.30
19B	60.1	.7596	582 (1)	27	2.26 E+05	1.17 E+06	3.19 E+06	5.14 E+06	5.15
18B	70.0	.8943	673MP (1)	28	2.81 E+05	1.52 E+06	3.69 E+06	5.70 E+06	5.40
18B	70.0	.8943	678MP (1)	28	2.71 E+05	1.47 E+06	3.51 E+06	5.28 E+06	5.42
18B	70.0	.8943	672MP (2)	28	2.64 E+05	1.44 E+06	3.39 E+06	5.07 E+06	5.45
18B	70.0	.8943	677MP (2)	28	2.59 E+05	1.37 E+06	3.20 E+06	4.73 E+06	5.29
18E	80.3	.9045	570	27	2.82 E+05	1.40 E+06	3.36 E+06	5.11 E+06	4.98
18J	46.5HRS	.9570	610	27	2.76 E+05	1.40 E+06	3.52 E+06	5.60 E+06	5.09
18J	46.5HRS	.9570	615	27	2.55 E+05	1.38 E+06	3.44 E+06	5.37 E+06	5.41
18J	46.5HRS	.9570	616	27	2.57 E+05	1.39 E+06	3.48 E+06	5.49 E+06	5.40
18J	46.5HRS	.9570	617	27	2.60 E+05	1.36 E+06	3.37 E+06	5.20 E+06	5.25
18J	46.5HRS	.9570	618	27	2.50 E+05	1.35 E+06	3.33 E+06	5.11 E+06	5.42
18J	46.5HRS	.9570	619	27	2.63 E+05	1.39 E+06	3.47 E+06	5.43 E+06	5.29
18J	46.5HRS	.9570	631 (3)	28	2.57 E+05	1.44 E+06	3.45 E+06	5.20 E+06	5.61
18J	46.5HRS	.9570	717 (3)	28	2.76 E+05	1.42 E+06	3.40 E+06	5.15 E+06	5.16
18J	46.5HRS	.9570	668MP	28	2.72 E+05	1.46 E+06	3.53 E+06	5.32 E+06	5.37

(1) 3mm O.D. Ampoule Section
(2) 2mm O.D. Ampoule Section
(3) Heated previous to injection

*MP indicates monomer polymer mixture rather than precipitated polymer

TABLE I-16

INFINITE RESOLUTION MOLECULAR WEIGHT AVERAGES

T = 90°C
AIBN = 0.3 wt.%

SAMPLE NO.	TIME (min.)	X	GPC #	COLUMN CODE	Mn (∞)	Mw (∞)	Mz (∞)	Mz+1 (∞)	P (∞)
23E	7.0	.1802	579	27	6.03 E+04	1.14 E+05	1.82 E+05	2.55 E+05	1.90
23E	7.0	.1802	638	28	6.05 E+04	1.17 E+05	1.90 E+05	2.72 E+05	1.94
23E	7.0	.1802	681MP*	28	4.96 E+04	1.11 E+05	1.83 E+05	2.61 E+05	2.24
23I	8.2	.2117	601	27	6.06 E+04	1.17 E+05	1.89 E+05	2.69 E+05	1.92
23I	8.2	.2117	639	28	6.07 E+04	1.19 E+05	1.99 E+05	3.01 E+05	1.97
23I	8.2	.2117	682MP	28	4.92 E+04	1.14 E+05	1.92 E+05	2.79 E+05	2.31
23B	10.1	.2513	590	27	6.28 E+04	1.20 E+05	1.99 E+05	3.01 E+05	1.92
23F	16.0	.4036	575	27	6.54 E+04	1.30 E+05	2.08 E+05	2.85 E+05	1.99
25C	19.0	.5407	713	28	7.86 E+04	3.46 E+05	2.17 E+06	5.14 E+06	4.40
23H	20.0	.6518	580	27	9.94 E+04	5.41 E+05	2.67 E+06	5.76 E+06	5.44
23H	20.0	.6518	712	28	9.45 E+04	4.67 E+05	1.97 E+06	3.83 E+06	4.94
25A	21.0	.7284	578	27	1.02 E+05	4.02 E+05	1.19 E+06	2.21 E+06	3.94
25E	27.0	.9371	608	27	1.31 E+05	5.65 E+05	1.48 E+06	2.69 E+06	4.33
25F	424.0	.9689	607	27	1.27 E+05	5.45 E+05	1.35 E+06	2.25 E+06	4.28
25F	424.0	.9689	714	28	1.18 E+05	5.64 E+05	1.45 E+06	2.44 E+06	4.77

*MP indicates monomer polymer mixture rather than precipitated polymer

TABLE I-17

INFINITE RESOLUTION MOLECULAR WEIGHT AVERAGES

T = 90°C
AIBN = 0.5%

SAMPLE NO.	TIME (min.)	X	GPC #	COLUMN	Mn (∞)	Mw (∞)	Mz (∞)	Mz+1 (∞)	P (∞)
22C	6.0	.1911	592	27	4.87 E+04	9.35 E+04	1.52 E+05	2.21 E+05	1.92
22C	6.0	.1911	632	28	4.87 E+04	9.49 E+04	1.62 E+05	2.58 E+05	1.95
22C	6.0	.1911	666MP*	28	3.28 E+04	8.70 E+04	1.52 E+05	2.37 E+05	2.65
22E	7.1	.2265	574	27	5.13 E+04	9.15 E+04	1.44 E+05	2.03 E+05	1.78
22E	7.1	.2265	667MP	28	3.42 E+04	8.60 E+04	1.47 E+05	2.20 E+05	2.52
22D	8.0	.2532	596	27	4.91 E+04	9.18 E+04	1.48 E+05	2.18 E+05	1.87
22D	8.0	.2532	597	27	4.85 E+04	9.17 E+04	1.48 E+05	2.13 E+05	1.89
22D	8.0	.2532	630	28	4.85 E+04	9.28 E+04	1.51 E+05	2.19 E+05	1.91
22D	8.0	.2532	683MP	28	3.93 E+04	8.69 E+04	1.45 E+05	2.09 E+05	2.20
26C	10.0	.3040	716	28	4.79 E+04	9.35 E+04	1.53 E+04	2.20 E+05	1.95
26D	14.0	.4603	602	27	5.96 E+04	2.01 E+05	1.24 E+06	3.08 E+06	3.37
26D	14.0	.4603	633	28	5.37 E+04	1.92 E+05	1.28 E+06	3.30 E+06	3.58
26D	14.0	.4603	680MP	28	4.05 E+04	2.25 E+05	2.67 E+06	7.99 E+06	5.54
26E	14.0	.4571	603	27	5.72 E+04	2.02 E+05	1.49 E+06	3.98 E+06	3.52
26E	14.0	.4571	655MP (1)	27	4.66 E+04	1.84 E+05	1.31 E+06	3.72 E+06	3.94
26E	14.0	.4571	656MP (2)	27	4.74 E+04	2.18 E+05	1.78 E+06	4.22 E+06	4.61
26G	14.0	.4587	604	27	5.73 E+04	2.01 E+05	1.78 E+06	5.20 E+06	3.51
26H	14.0	.4569	605	27	5.52 E+04	1.47 E+05	1.03 E+06	4.65 E+06	2.66
26I	14.0	.4582	606	27	6.16 E+04	2.28 E+05	1.68 E+06	4.15 E+06	3.70
26I	14.0	.4582	614	27	5.80 E+04	1.94 E+05	1.38 E+06	3.61 E+06	3.35
24A	15.0	.5389	594	27	6.25 E+04	2.47 E+05	1.39 E+06	3.13 E+06	3.95
24E	16.0	.6331	572	27	7.27 E+04	3.43 E+05	1.64 E+06	3.40 E+06	4.72
24G	17.0	.7335	591	27	8.09 E+04	2.97 E+05	8.51 E+05	1.52 E+06	3.67
24D	20.1	.9283	571	27	9.47 E+04	3.89 E+05	1.00 E+06	1.77 E+06	4.10
24D	20.1	.9283	651MP (1)	27	7.71 E+04	3.73 E+05	9.97 E+05	1.87 E+06	4.84
24D	20.1	.9283	665MP (1)	27	7.96 E+04	3.76 E+05	9.54 E+05	1.58 E+06	4.72
24D	20.1	.9283	652MP (2)	27	7.78 E+04	3.74 E+05	9.29 E+05	1.50 E+06	4.81
26F	400.0	.9663	609	27	1.04 E+05	3.98 E+05	9.70 E+05	1.61 E+06	3.84

(1) 3mm O.D. Ampoule Section
(2) 2mm O.D. Ampoule Section
*MP indicates monomer polymer mixture rather than precipitated polymer

TABLE I-18

α_1 BY THE METHOD OF CHROMATOGRAM HEIGHTS

T = 50°C
AIBN = 0.3 wt.%

SAMPLE NO.	TIME (min.)	X	GPC #	COLUMN CODE	Mn(∞)	Mn Model	Mw(∞)	Mw Model	α_1
11R	84.6	.0852	628	27	4.52 E+05	5.04 E+05	1.03 E+06	1.01 E+06	1.837 E-04
11R	84.6	.0852	640	28	3.89 E+05	5.13 E+05	1.02 E+06	1.03 E+06	1.805 E-04
11R	84.6	.0852	686MP*	28	4.37 E+05	5.30 E+05	1.01 E+06	1.06 E+06	1.747 E-04
11T	120.0	.1152	649	28	5.48 E+05	5.90 E+05	1.22 E+06	1.19 E+06	1.522 E-04
11P	200.0	.2023	642	28	4.92 E+05	6.12 E+05	1.26 E+06	1.24 E+06	1.341 E-04

*MP indicates monomer polymer mixture rather than precipitated polymer

TABLE I-19

α_1 BY THE METHOD OF CHROMATOGRAM HEIGHTS

T = 50°C
AIBN = 0.391 wt.%

SAMPLE NO.	TIME (min.)	X	GPC #	COLUMN CODE	Mn(∞)	Mn Model	Mw(∞)	Mw Model	α_1
4I	84.6	.1036	560MP*	25	3.67 E+05	5.03 E+05	1.22 E+06	1.01 E+06	1.806 E-04
4I	84.6	.1036	569MP	25	3.84 E+05	5.15 E+05	1.25 E+06	1.03 E+06	1.764 E-04
4I	84.6	.1036	626	27	3.91 E+05	4.32 E+05	9.85 E+05	8.67 E+05	2.103 E-04
4I	84.6	.1036	648	28	3.68 E+05	4.47 E+05	9.22 E+05	8.98 E+05	2.032 E-04
4H	124.2	.1449	559MP	25	3.54 E+05	4.80 E+05	1.02 E+06	9.66 E+05	1.816 E-04
4H	124.2	.1449	650	28	3.76 E+05	4.48 E+05	9.58 E+05	9.02 E+05	1.946 E-04
12D	150.0	.1671	700	28	3.69 E+05	4.51 E+05	9.34 E+05	9.10 E+05	1.888 E-04
4G	187.5	.2433	643	28	4.12 E+05	5.53 E+05	1.32 E+06	1.13 E+06	1.416 E-04

*MP indicates monomer polymer mixture rather than precipitated polymer

TABLE I-20

α_1 BY THE METHOD OF CHROMATOGRAM HEIGHTS

T = 50°C
AIBN = 0.5 wt.%

SAMPLE NO.	TIME (min.)	X	GPC #	COLUMN CODE	Mn(∞)	Mn Model	Mw(∞)	Mw Model	α_1
10A	60.0	.0801	627	27	3.38 E+05	3.40 E+05	7.19 E+05	6.81 E+05	2.735 E-04
10A	60.0	.0801	647	28	2.96 E+05	3.65 E+05	7.20 E+05	7.32 E+05	2.547 E-04
10A	60.0	.0801	685MP*	28	2.76 E+05	3.62 E+05	7.39 E+05	7.26 E+05	2.566 E-04
10K	84.6	.1117	644	28	3.24 E+05	3.81 E+05	8.04 E+05	7.65 E+05	2.365 E-04
9F	120.0	.1481	646	28	3.68 E+05	4.08 E+05	8.40 E+05	8.22 E+05	2.129 E-04

*MP indicates monomer polymer mixture rather than precipitated polymer

TABLE I-21

α_1 BY THE METHOD OF CHROMATOGRAM HEIGHTS

T = 70°C
AIBN = 0.3 wt.%

SAMPLE NO.	TIME (min.)	X	GPC #	COLUMN CODE	Mn (∞)	Mn Model	Mw (∞)	Mw Model	α_1
11W	10.0	.0588	583	27	1.40 E+05	1.45 E+05	3.09 E+05	2.90 E+05	6.549 E-04
11W	10.0	.0588	612	27	1.43 E+05	1.47 E+05	3.14 E+05	2.94 E+05	6.463 E-04
11W	10.0	.0588	634	28	1.52 E+05	1.48 E+05	3.32 E+05	2.96 E+05	6.429 E-04
14A	15.0	.0896	593	27	1.44 E+05	1.40 E+05	3.06 E+05	2.81 E+05	6.587 E-04
14A	15.0	.0896	613	27	1.41 E+05	1.43 E+05	3.17 E+05	2.87 E+05	6.444 E-04
14A	15.0	.0896	670MP*	28	1.44 E+05	1.43 E+05	3.19 E+05	2.87 E+05	6.436 E-04
11X	20.0	.1157	584	27	1.39 E+05	1.43 E+05	2.98 E+05	2.86 E+05	6.305 E-04

*MP indicates monomer polymer mixture rather than precipitated polymer

TABLE I-22

α_1 BY THE METHOD OF CHROMATOGRAM HEIGHTS

T = 70°C
AIBN = 0.5 wt.%

SAMPLE NO.	TIME (min.)	X	GPC #	COLUMN CODE	Mn (∞)	Mn Model	Mw (∞)	Mw Model	α_1
19C	5.0	.0400	600	27	1.23 E+05	1.27 E+05	2.57 E+05	2.54 E+05	7.612 E-04
19C	5.0	.0400	622	27	1.11 E+05	1.25 E+05	2.79 E+05	2.50 E+05	7.739 E-04
19A	10.0	.0745	599	27	1.14 E+05	1.14 E+05	2.45 E+05	2.29 E+05	8.198 E-04
19A	10.0	.0745	620	27	1.05 E+05	1.18 E+05	2.73 E+05	2.36 E+05	7.930 E-04
19A	10.0	.0745	671MP*	28	1.09 E+05	1.14 E+05	2.34 E+05	2.28 E+05	8.227 E-04

*MP indicates monomer polymer mixture rather than precipitated polymer

TABLE I-23

α_1 BY THE METHOD OF CHROMATOGRAM HEIGHTS

T = 90°C
AIBN = 0.3 wt.%

SAMPLE NO.	TIME (min.)	X	GPC #	COLUMN CODE	Mn(∞)	Mn Model	Mw(∞)	Mw Model	α_1
23E	7.0	.1802	579	27	6.03 E+04	5.38 E+04	1.14 E+05	1.08 E+05	1.570 E-03
23E	7.0	.1802	638	28	6.05 E+04	5.56 E+04	1.17 E+05	1.12 E+05	1.519 E-03
23E	7.0	.1802	681MP*	28	4.96 E+04	5.37 E+04	1.11 E+05	1.08 E+05	1.572 E-03
23I	8.17	.2117	601	27	6.06 E+04	5.52 E+04	1.17 E+05	1.12 E+05	1.480 E-03
23I	8.17	.2117	639	28	6.07 E+04	5.65 E+04	1.19 E+05	1.15 E+05	1.444 E-03
23I	8.17	.2117	682MP	28	4.92 E+04	5.54 E+04	1.14 E+05	1.12 E+05	1.473 E-03
23B	10.12	.2513	590	27	6.28 E+04	5.60 E+04	1.20 E+05	1.14 E+05	1.394 E-03

*MP indicates monomer polymer mixture rather than precipitated polymer

TABLE I-24

α_1 BY THE METHOD OF CHROMATOGRAM HEIGHTS

T = 90°C
AIBN = 0.5 wt.%

SAMPLE NO.	TIME (min.)	X	GPC #	COLUMN CODE	Mn(∞)	Mn Model	Mw(∞)	Mw Model	α_1
22C	6.02	.1911	592	27	4.87 E+04	4.37 E+04	9.35 E+04	8.85 E+04	1.908 E-03
22C	6.02	.1911	632	28	4.87 E+04	4.43 E+04	9.49 E+04	8.97 E+04	1.882 E-03
22C	6.02	.1911	666MP*	28	3.28 E+04	4.25 E+04	8.70 E+04	8.60 E+04	1.963 E-03
22E	7.07	.2265	574	27	5.13 E+04	4.29 E+04	9.15 E+04	8.72 E+04	1.872 E-03
22E	7.07	.2265	667MP	28	3.42 E+04	4.10 E+04	8.60 E+04	8.34 E+04	1.958 E-03
22D	8.02	.2532	596	27	4.91 E+04	4.32 E+04	9.17 E+04	8.83 E+04	1.803 E-03
22D	8.02	.2532	597	27	4.86 E+04	4.34 E+04	9.17 E+04	8.87 E+04	1.794 E-03
22D	8.02	.2532	630	28	4.85 E+04	4.41 E+04	9.28 E+04	9.00 E+04	1.769 E-03
22D	8.02	.2532	683MP	28	3.93 E+04	4.08 E+04	8.69 E+04	8.33 E+04	1.912 E-03
26C	10.00	.3040	697	28	4.79 E+04	4.48 E+04	9.35 E+04	9.26 E+04	1.638 E-03

*MP indicates monomer polymer mixture rather than precipitated polymer

TABLE I-25

SHRINKAGE IN MMA POLYMERIZATION

Temperature (^{o}C)	ϵ (Dilatometer Runs-This Study)	$\frac{\rho_{monomer}}{\rho_{polymer}} - 1$* ϵ
50	-.244	-.228
70	-.265	-.246
90	-.295	-.264

* Density data from: Barrett, K. J., Thomas, H.R., J. Polymer Sci., A-1, 7, 2621 (1969)

TABLE I-26

α_1 AS A FUNCTION OF CONVERSION

$\alpha_1 = EXP(A + BX + CX^2 + DX^3)$

ORIGIN OF FUNCTION	TEMP °C	(wt.%) AIBN	A	B	C	D	$0_1(\alpha_1)$
FIT #1 OF α_1 FROM METHOD OF DIFFERENTIAL CHROMATOGRAMS	70	0.3	-7.113	-4.39	-3.50	0	-
		0.5	-6.982	-3.44	-4.24	0	-
	90	0.3	-6.330	-2.23	-5.06	0	-
		0.5	-6.108	-1.49	-6.07	0	-
FIT #2 OF α_1 FROM METHOD OF DIFFERENTIAL CHROMATOGRAMS	70	0.3	-7.214	-2.25	-10.23	5.17	-
		0.5	-7.125	-0.130	-15.13	8.73	-
	90	0.3	-6.434	0.180	-13.30	6.82	-
		0.5	-6.245	2.49	-18.91	10.20	-
SEARCH FOR B AND C METHOD OF CHROMATOGRAM HEIGHTS	70	0.3	-7.113	-4.35	-3.14	0	9.651
		0.5	-6.982	-2.98	-5.27	0	10.387
	90	0.3	-6.330	-1.75	-6.66	0	5.523
		0.5	-6.108	-1.63	-6.36	0	8.308
SEARCH FOR B, C, AND D METHOD OF CHROMATOGRAM HEIGHTS	70	0.3	-7.214	-1.77	-13.42	9.30	9.015
		0.5	-7.125	1.48	-22.67	15.32	8.351
	90	0.3	-6.434	-0.42	-10.34	2.69	5.265
		0.5	-6.245	2.13	-19.66	11.04	7.633

TABLE I-27

RESULTS OF NMR ANALYSES

KINETIC SAMPLE NO.	REACTION TEMP (^{o}C)	Wt.% AIBN	CONVERSION	i %	h %	s %	σ	σ EQN. I-31
704H	50	0.391	.1449	3.0	29.9	67.0	.221	.238
704C	50	0.391	.8413	2.4	32.8	64.7	.244	.238
704B	50	0.391	.8601	2.1	32.2	67.2	.220	.238
718J	70	0.5	.9570	3.4	34.6	62.0	.271	.256
722D	90	0.5	.2531	3.0	34.8	62.0	.271	.272
726D	90	0.5	.4602	2.2	34.2	63.5	.255	.272
726F	90	0.5	.9663	3.3	37.2	59.5	.297	.272

TABLE I-28

CONVERSION BY GPC

SAMPLE NO.	X EXP.	GPC NO.	TOTAL MG INJECTED (PMMA+MMA)	CHROMATOGRAM AREA X 10^{-3}	CHROMATOGRAM† AREA ÷ MG PURE PMMA	X* GPC
4I	.1036	560	12.26	.514	392.55	.1069
4I	.1036	569	12.26	.510	392.55	.1059
4H	.1449	559	13.09	.752	392.55	.1464
24D	.9283,	651	3.83	1.919	517.09	.9690
24D	.9283	665	3.83	1.840	517.09	.9291
24D	.9283	652	3.82	1.908	517.09	.9659
18B	.8943	673	3.97	1.945	517.09	.9475
18B	.8943	678	3.97	1.861	517.09	.9065
18B	.8943	672	3.97	1.859	517.09	.9056
18B	.8943	677	3.97	1.796	517.09	.8749
18J	.9570	668	3.75	1.864	517.09	.9613

$$* \; X_{GPC} = \frac{\text{MG PMMA}}{\text{MG PMMA + MMA}} = \frac{\text{CHROMATOGRAM AREA}}{\frac{\text{AREA}}{\text{MG PURE PMMA}}} \cdot \text{TOTAL MG INJECTED}$$

†These values were obtained from area under the chromatograms of pure PMMA (no monomer present).

TABLE I-29 : EXPERIMENTAL AND MODEL PREDICTED CHROMATOGRAMS

GPC	PREDICTED BY MODEL	AREA UNDER CURVE
(1) CHROMATOGRAM ($F(v)$) $F(v)$ = conventional raw chromatogram heights as a function of retention volume	$(F(v)_{MODEL})$ $F(v)_{MODEL} = W_{r\ CUM} \frac{dr}{dv} \int_{-\infty}^{\infty} F(v)dv$ where $W_{r\ CUM} = (\int_{o}^{X} W_r dX)/X$	PROPORTIONAL TO WEIGHT OF POLYMER INJECTED INTO THE GPC
(2) NORMALIZED CHROMATOGRAM ($F_N(v)$) $F_N(v) = \frac{F(v)}{\int_{-\infty}^{\infty} F(v)dv}$	$(F_N(v)_{MODEL})$ $F_N(v)_{MODEL} = W_{r\ CUM} \frac{dr}{dv}$	UNITY
(3) CUMULATIVE CHROMATOGRAM ($F_c(v)$) $F_c(v) = F_N(v) \cdot X$	$(F_c(v)_{MODEL})$ $F_c(v)_{MODEL} = F_N(v)_{MODEL} \cdot X$	X
(4) DIFFERENTIAL CHROMATOGRAM ($\Delta F(v)$) $\Delta F(v) = F_c(v)_{X=X_2} - F_c(v)_{X=X_1}$	$(\Delta F(v)_{MODEL})$ $\Delta F(v)_{MODEL} = F_c(v)_{MODEL,\ X=X_2} - F_c(v)_{MODEL,\ X=X_1}$	$X_2 - X_1$
(5) NORMALIZED DIFFERENTIAL CHROMATOGRAM ($\Delta F_N(v)$) $\Delta F_N(v) = \frac{\Delta F(v)}{X_2 - X_1}$	$(\Delta F_N(v)_{MODEL})$ $\Delta F_N(v)_{MODEL} = \frac{\Delta F(v)_{MODEL}}{X_2 - X_1} = \frac{\int_{X_1}^{X_2} W_r dX \frac{dr}{dv}}{X_2 - X_1}$	UNITY

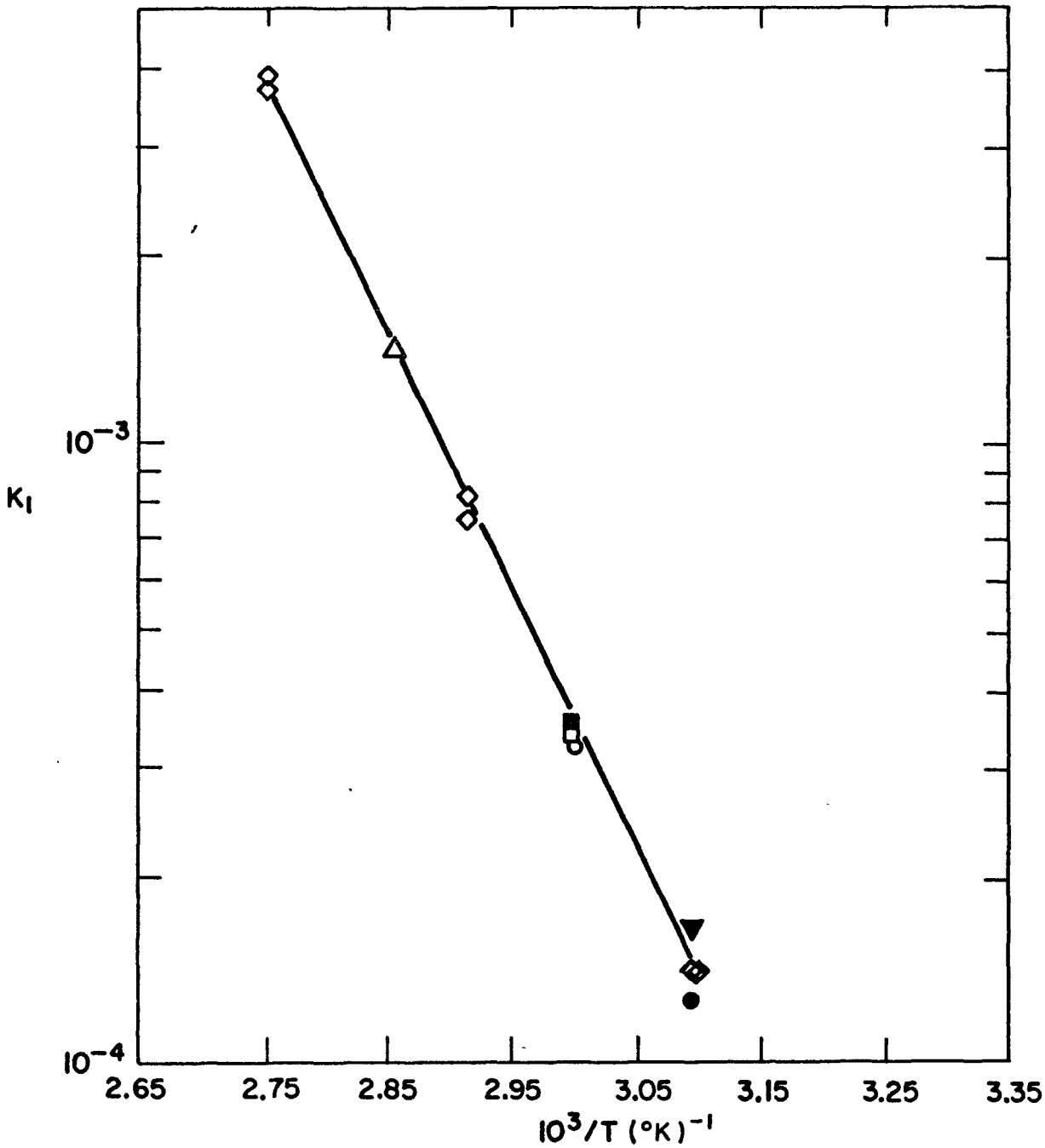

FIGURE I-1 : $K_I (= \sqrt{2f\ k_d/k_t}\ k_p)$ vs. $10^3/T$

Symbols and reference sources

◇ this study □ 63 ○ 69

△ 99 in 2 ■ 64

● 62 ▼ 105 in 2

FIGURE I-2 : A' (= $(.5(1.+\lambda)\ k_{td}/k_p^2)$ vs. $10^3/T$

Symbols and reference sources:

◇ this study	⬡ 69	□ 67	○ 65
△ 99 in 2	⬙ 70	◧ 63	⚲ 68
▲ 62	⬬ 104 in 2	◨ 64	○–72
◭ 94 in 2	▽ 71		◒ 66

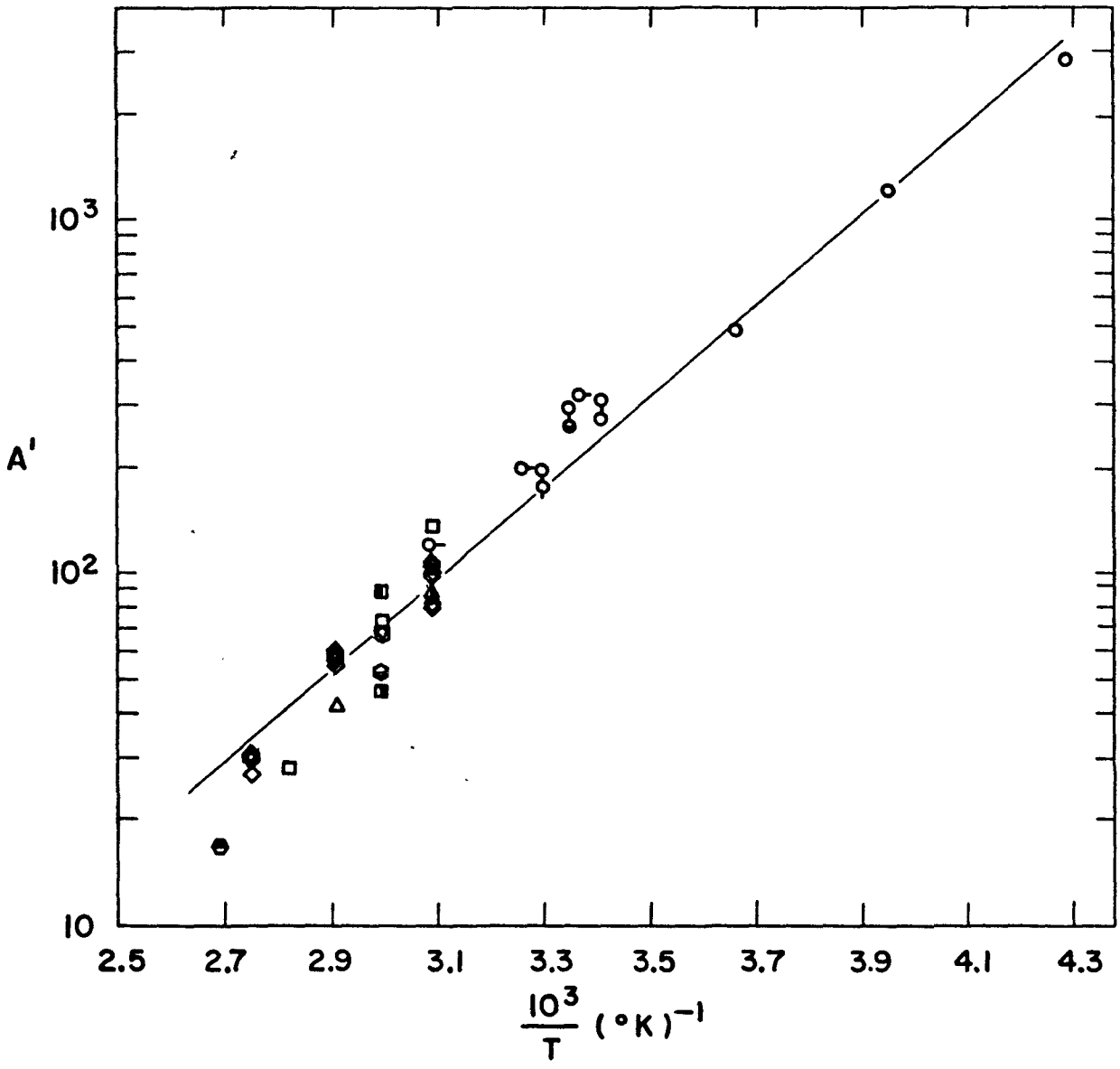
A'
10^3
10^2
10
2.5
2.7
2.9
3.1
3.3
3.5
3.7
3.9
4.1
4.3
$\frac{10^3}{T}$ (°K)$^{-1}$

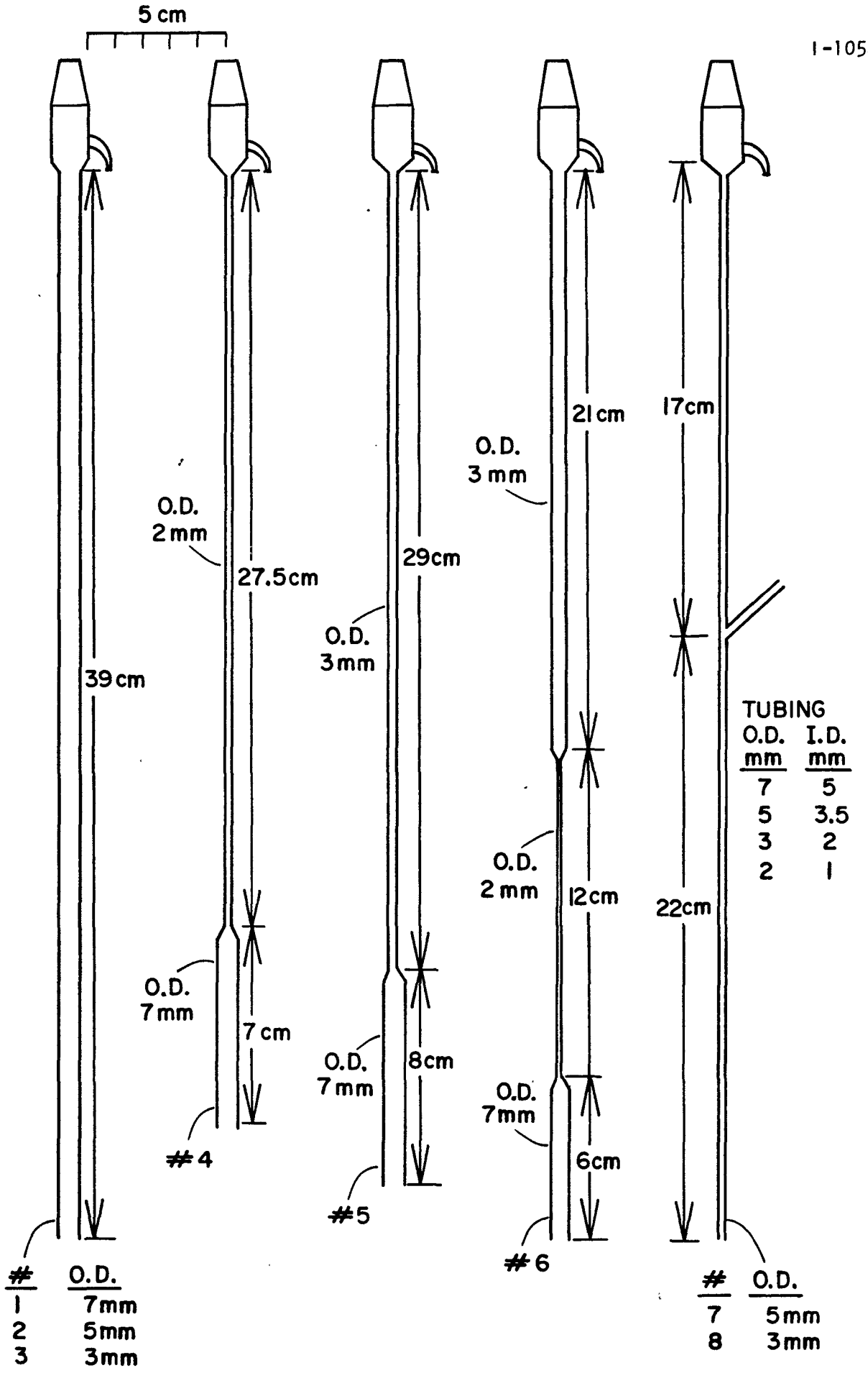

FIGURE I-3 : Ampoule Reactors

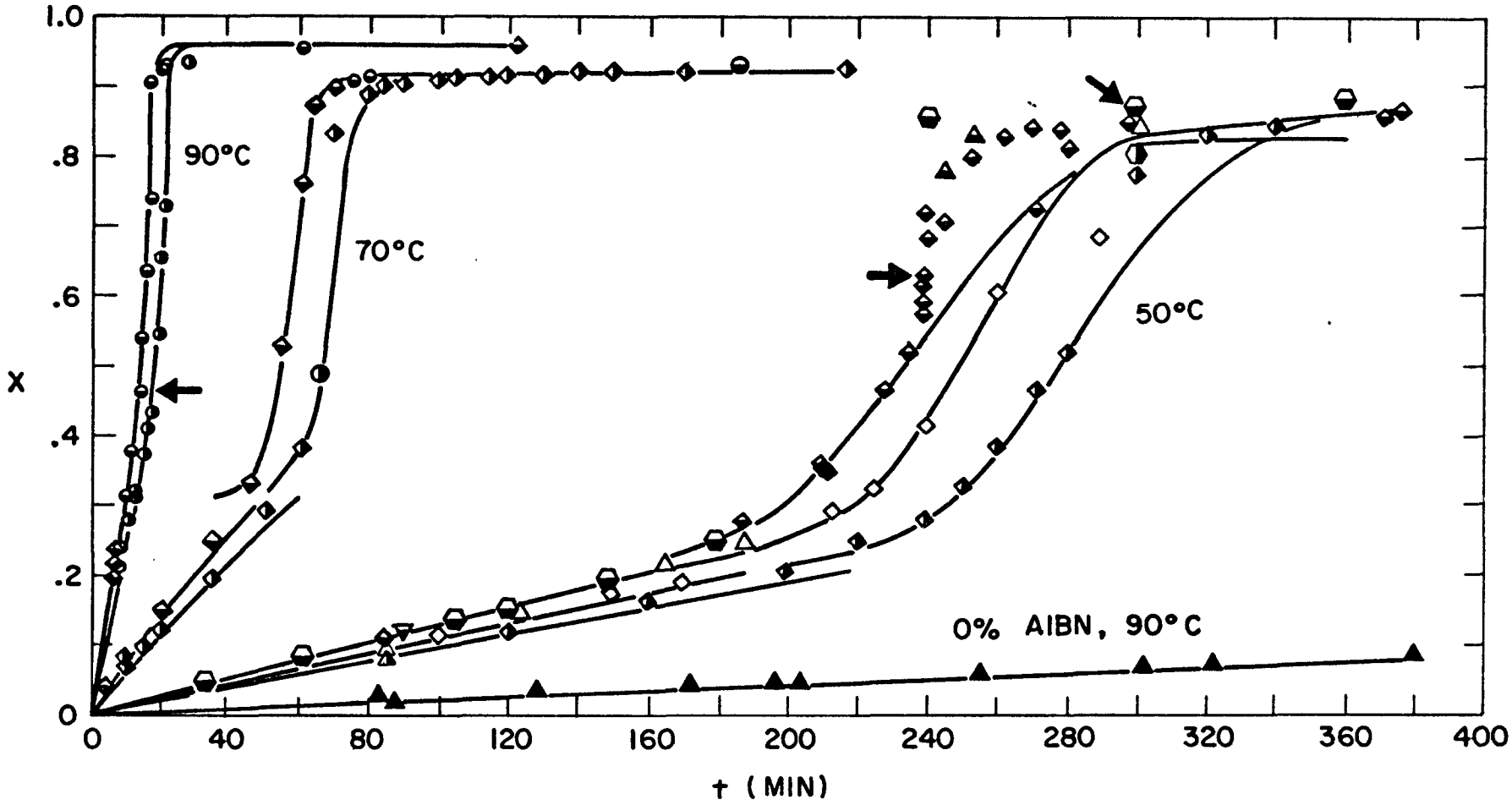

FIGURE I-4 : Conversion vs. Time at 50, 70 and 90°C

Ampoule Type 1* .5% AIBN
Ampoule Type 2* .4% AIBN
Ampoule Type 2 .3% AIBN
Ampoule Type 3 0% AIBN
Ampoule Type 6

Site of Main Replicates

Model Fit (first order at low conversion, Sawada equation at high conversion)

* 10 ppm MEHQ present as inhibitor

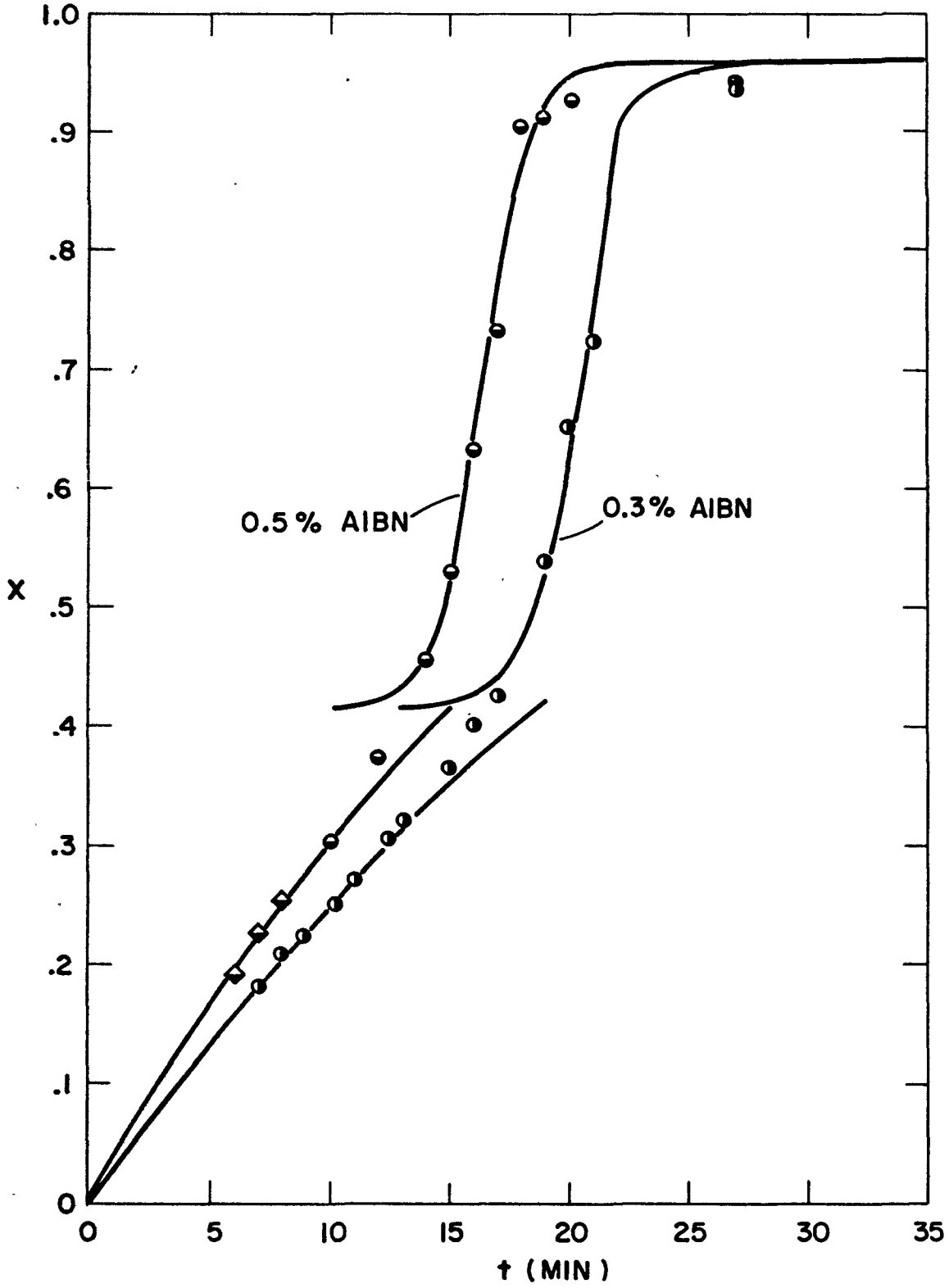

FIGURE I-5 : Conversion vs. Time at 90°C

◆ Ampoule Type 3 ◆ ● 0.5% AIBN

◑ ● Ampoule Type 6 ◑ 0.3% AIBN

— Model Fit

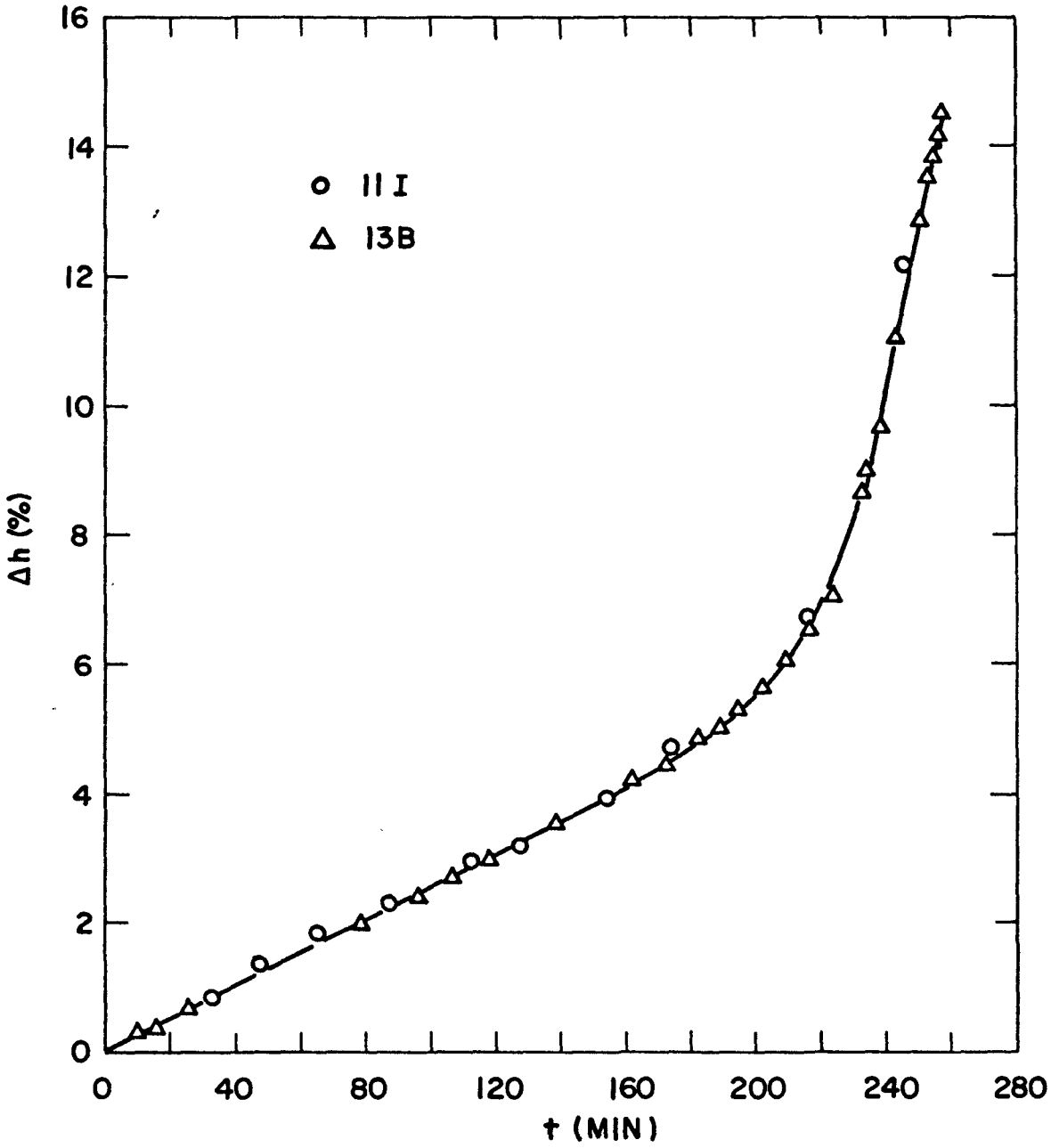

FIGURE I-6 : Percent Contraction vs. Time, 50°C, 0.3% AIBN

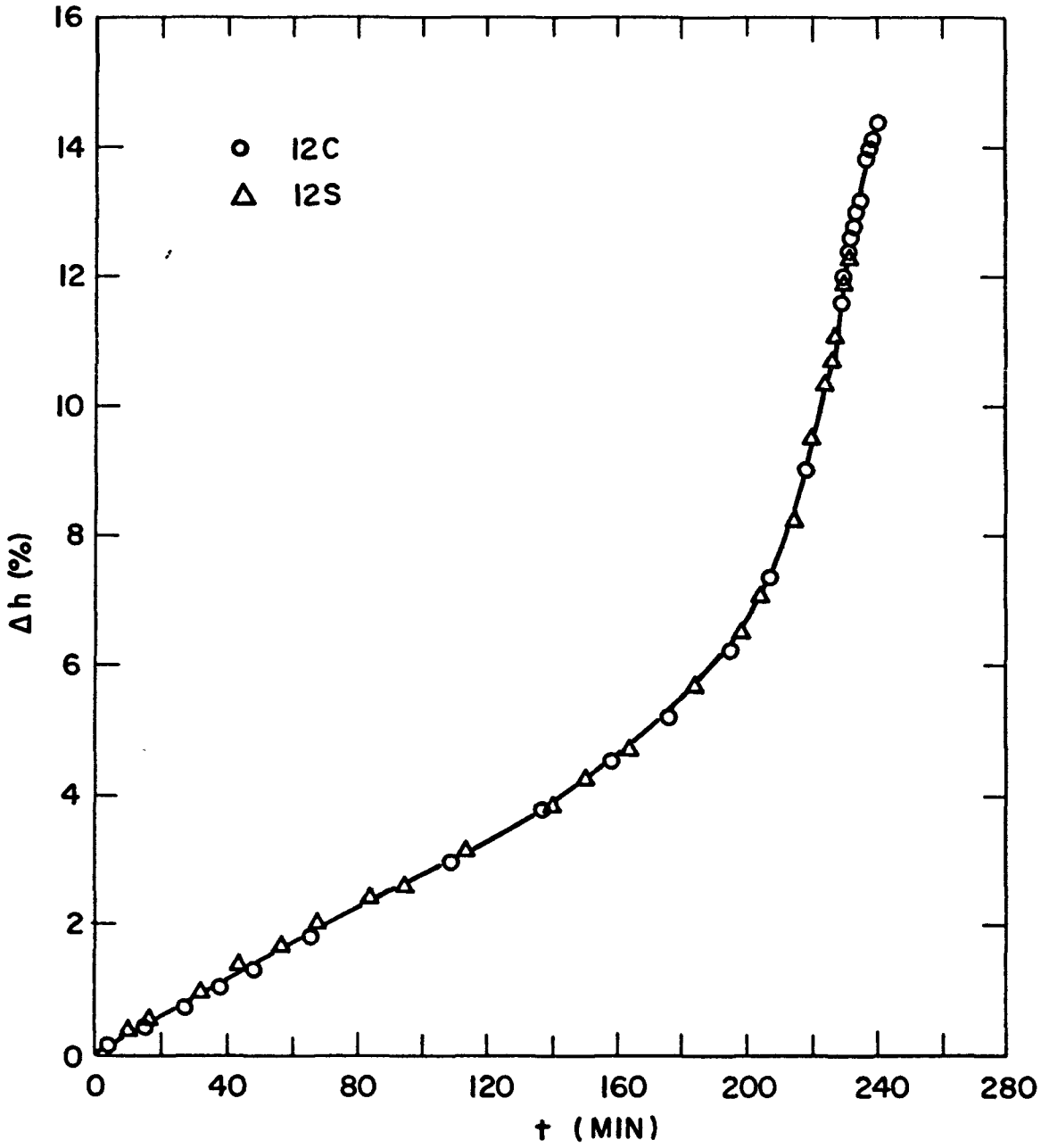

FIGURE I-7 : Percent Contraction vs. Time, 50°C, 0.391% AIBN

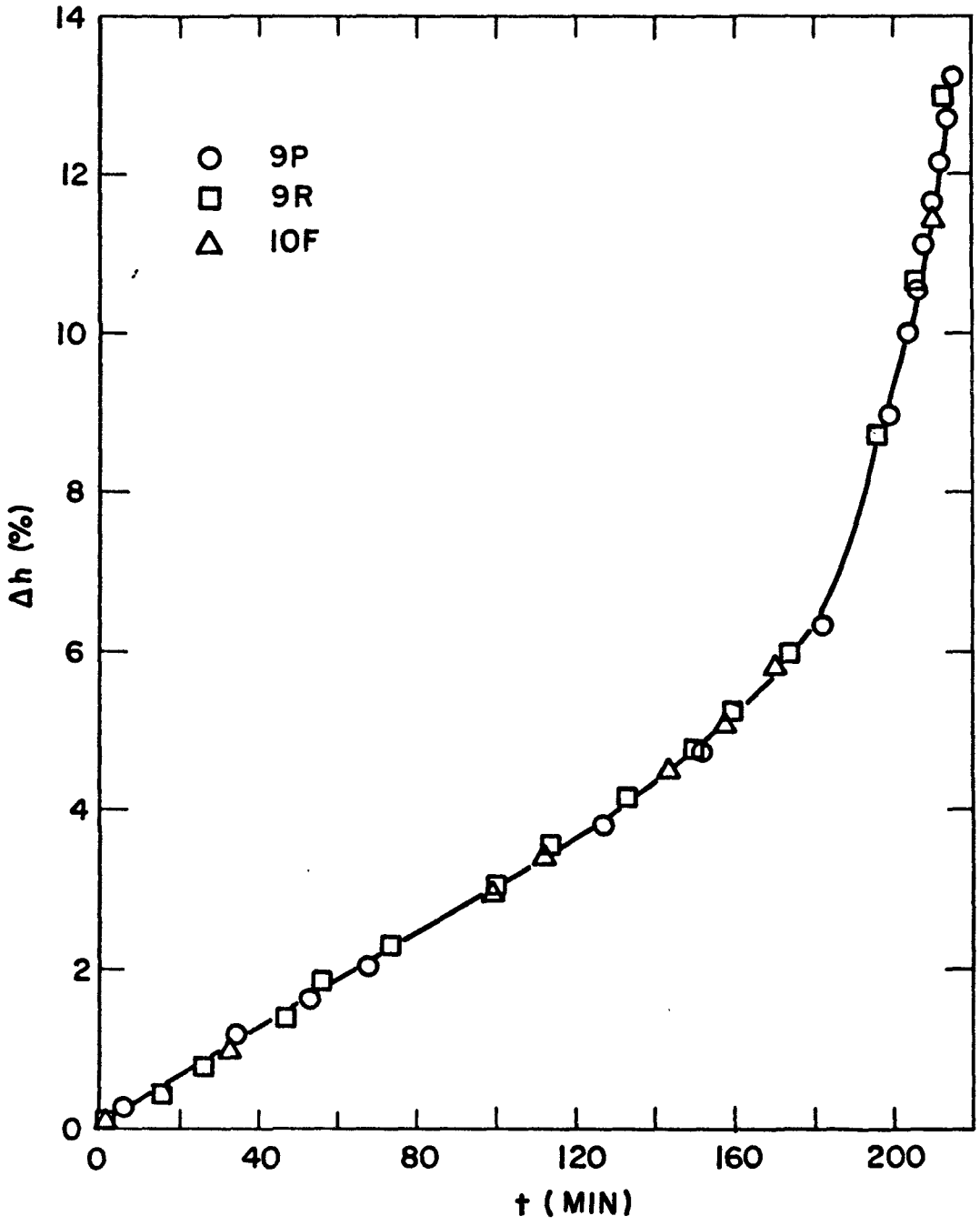

FIGURE I-8 : Percent Contraction vs. Time, 50°C, 0.5% AIBN

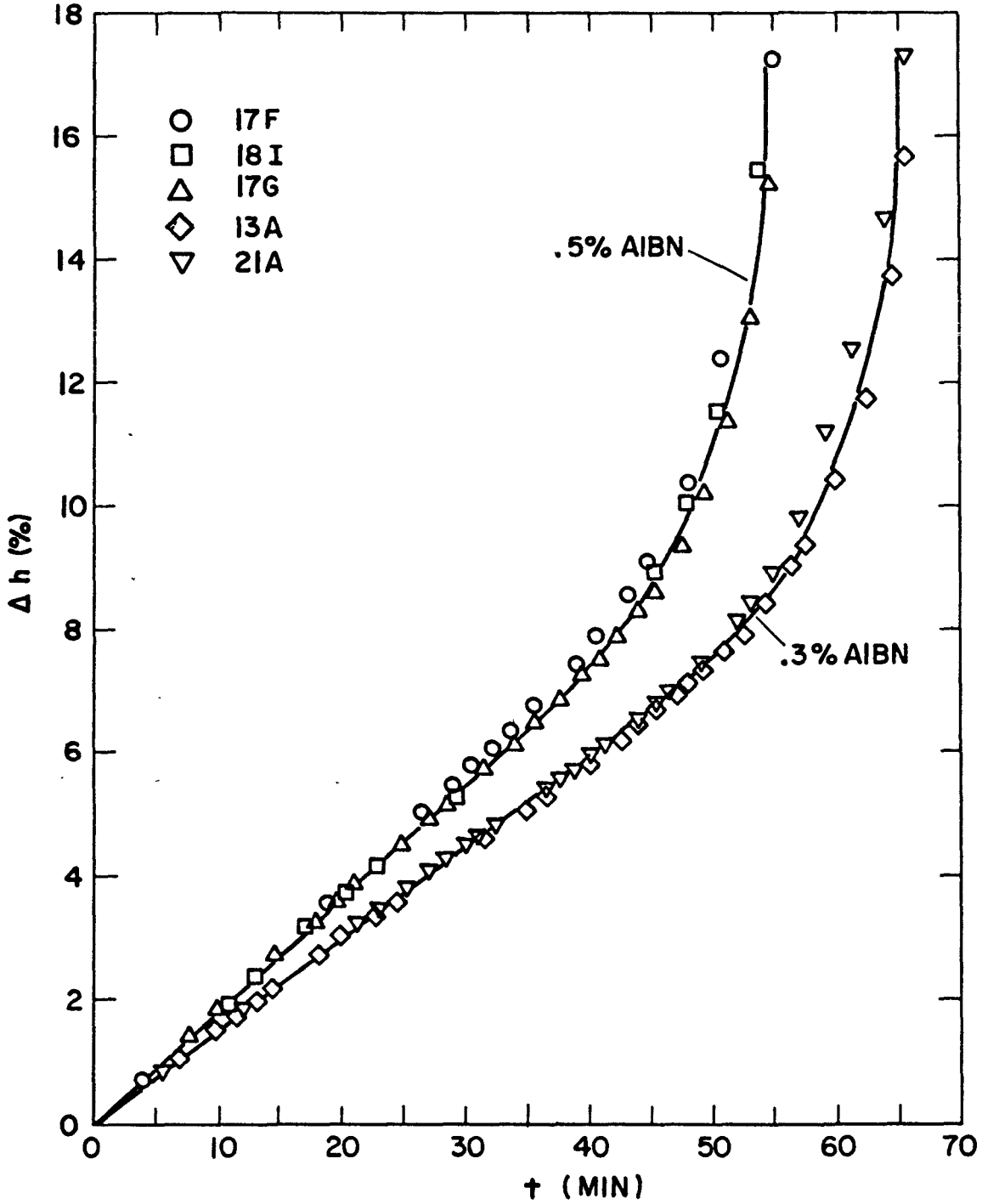

FIGURE I-9 : Percent Contraction vs. Time, 70°C, 0.3 and 0.5% AIBN

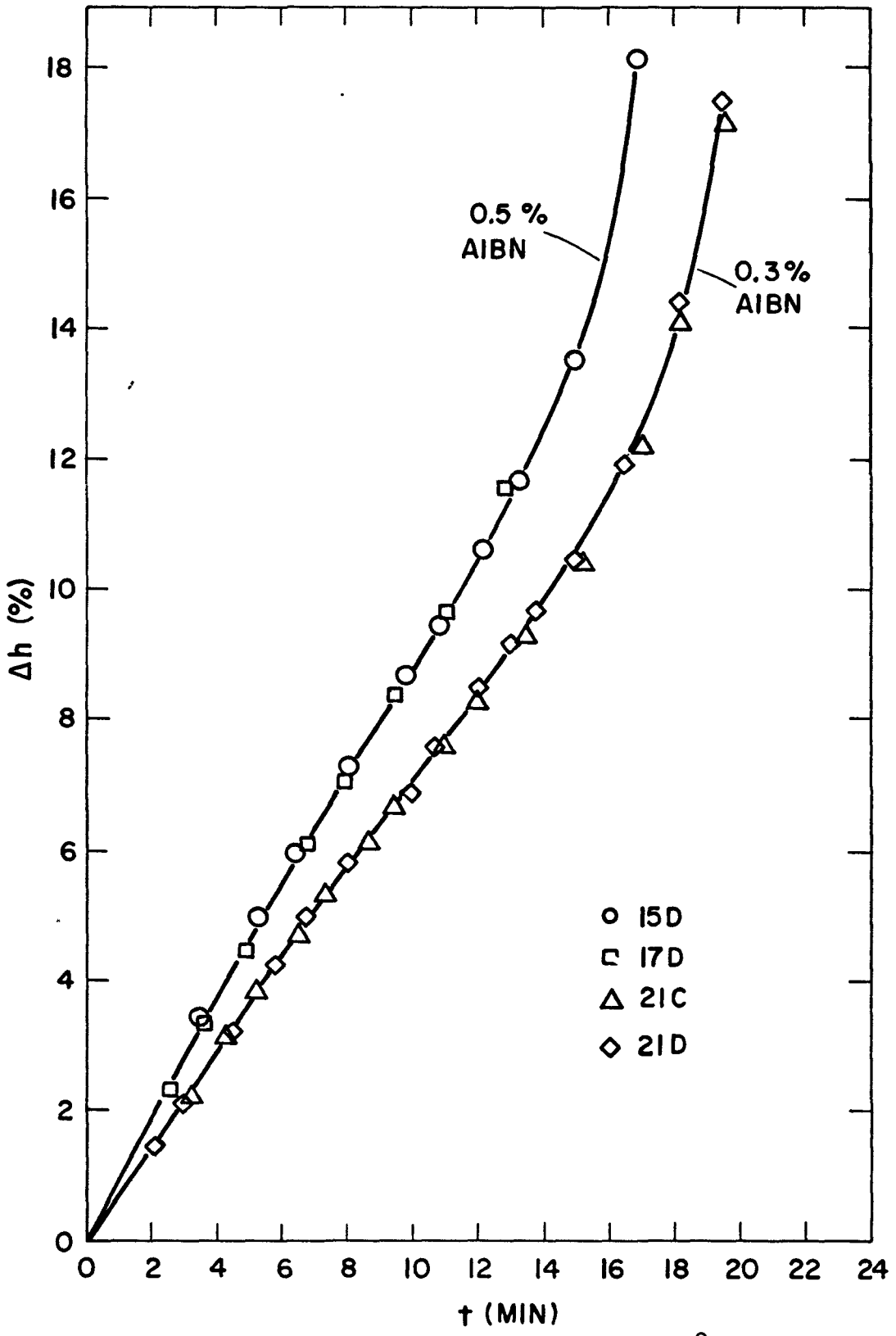

FIGURE I-10 : Percent Contraction vs. Time, 90°C, 0.3 and 0.5% AIBN

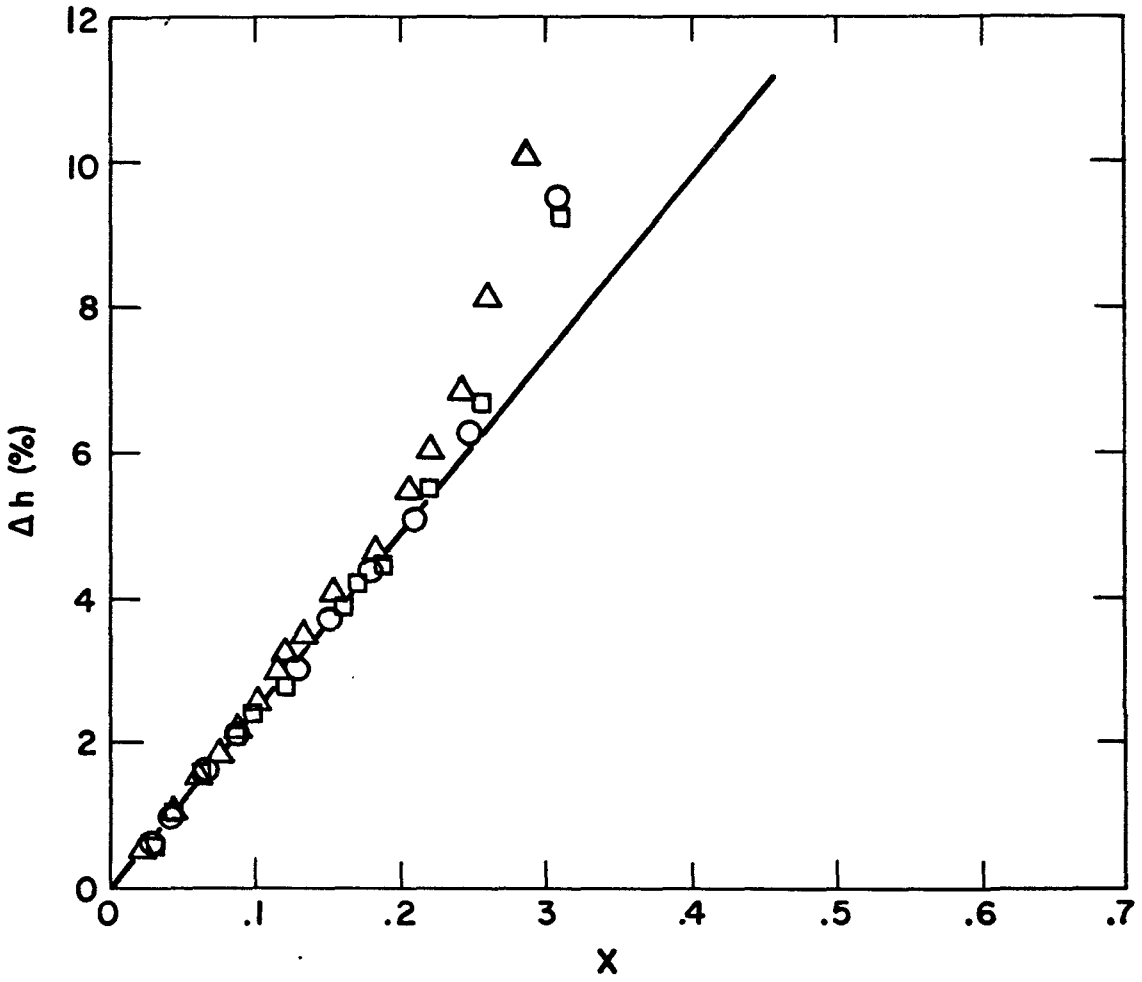

FIGURE I-11 : Percent Contraction vs. Conversion, 50°C

△ 0.3% AIBN

□ 0.391% AIBN

○ 0.5% AIBN

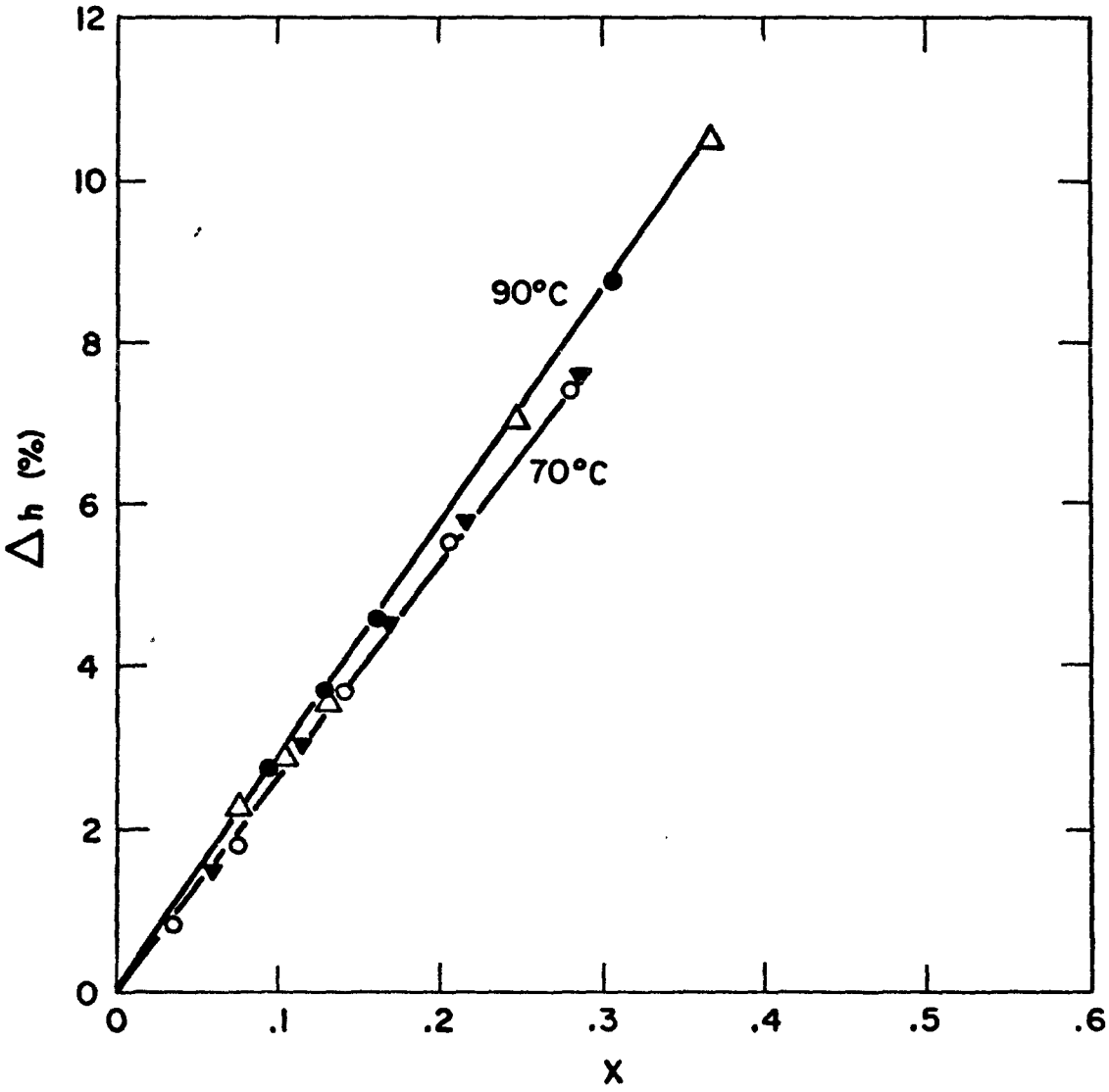

FIGURE I-12 : Percent Contraction vs. Conversion, 70°C and 90°C

▼ △ .3% AIBN

○ ● .5% AIBN

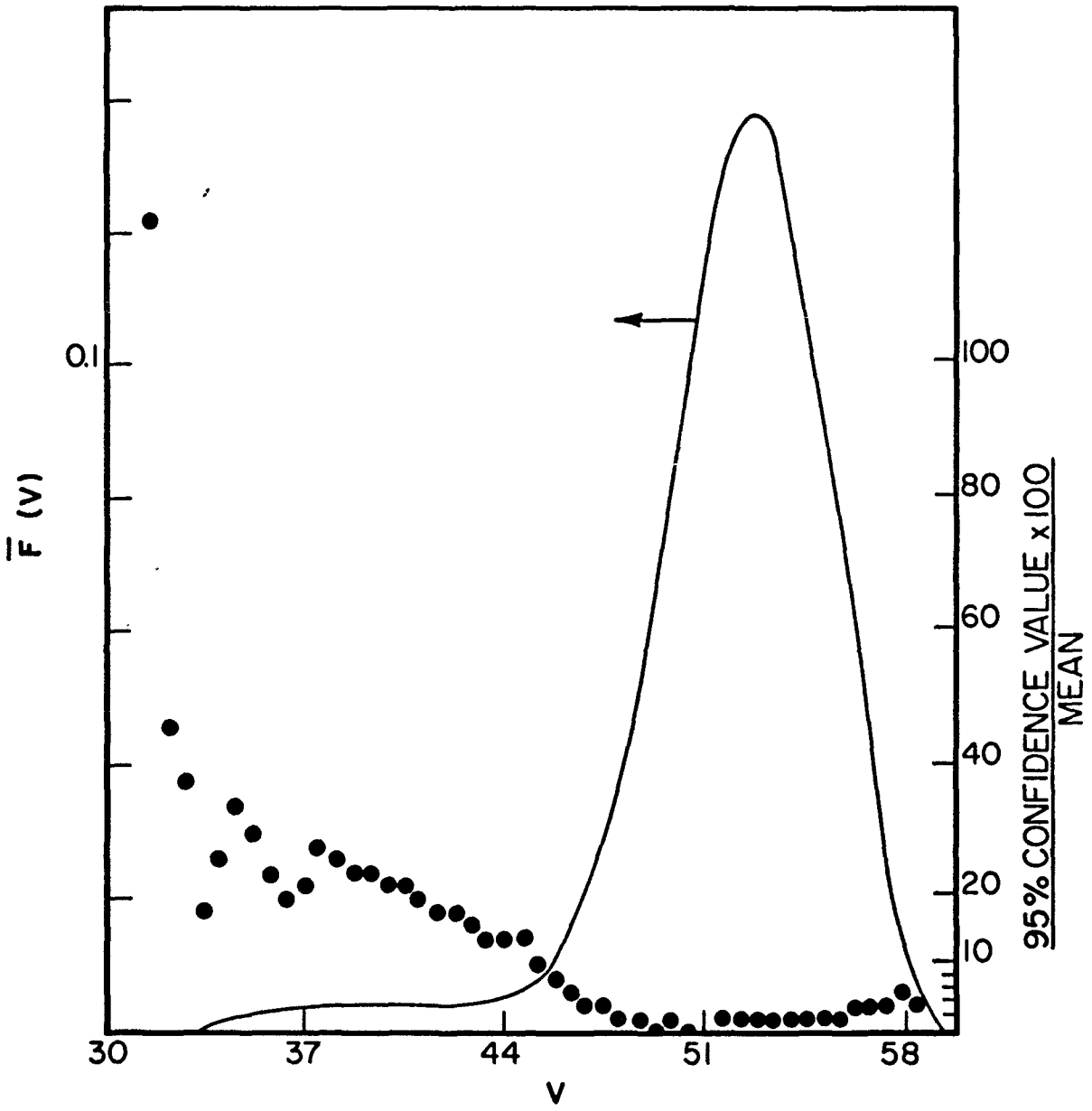

FIGURE I-13 : Mean Height Values of Chromatograms of Five Ampoule Prepared PMMA Samples (Nos. 26-D,E,G,H,I; GPC Nos. 602-606) and Confidence Value as a Percent of Mean vs. Retention Volume

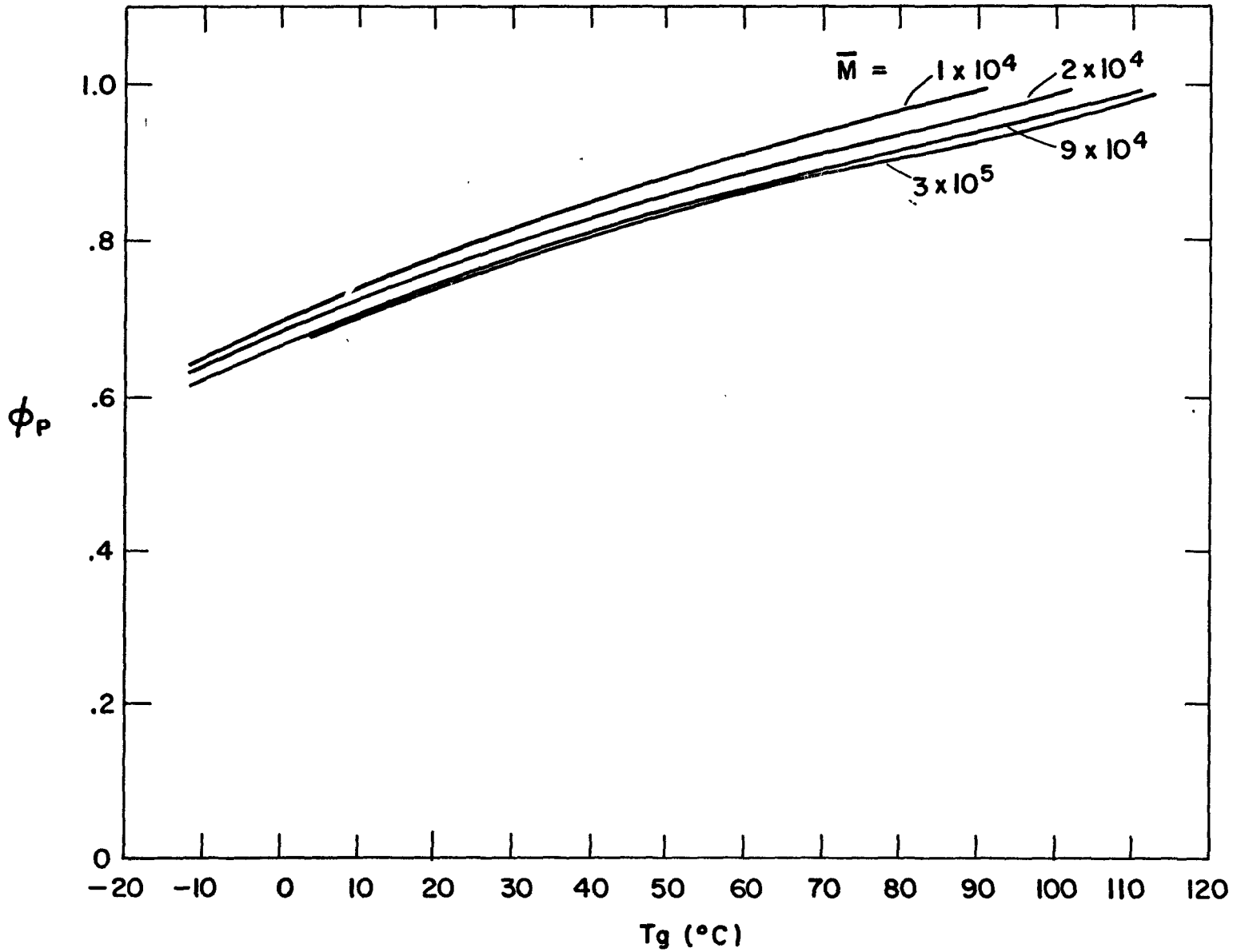

FIGURE I-14 : Volume Fraction of Polymer vs. Glass Transition Temperature and Molecular Weight

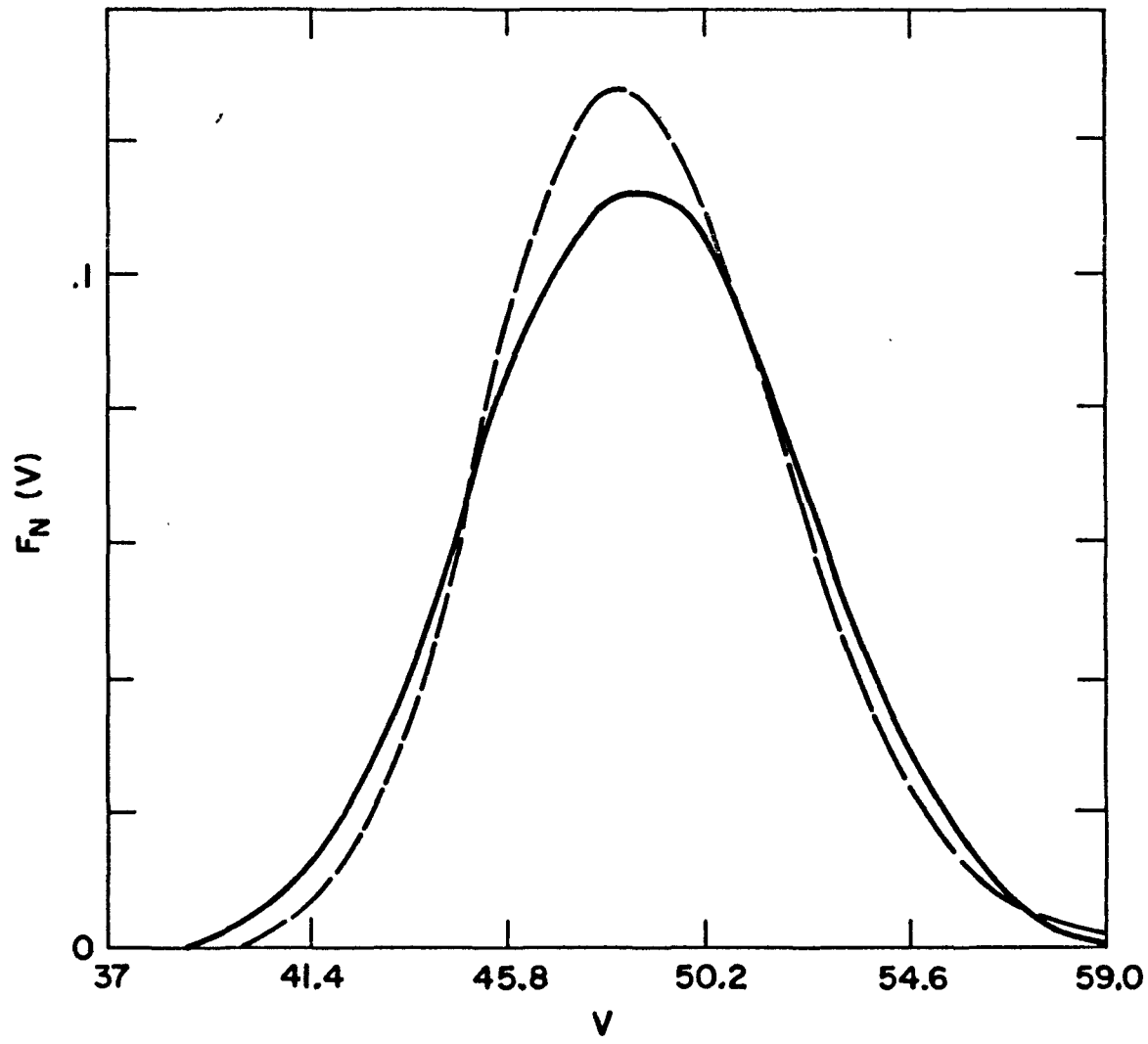

FIGURE I-15 : Result of a Single Variable Search for α_1 Using the Method of Chromatogram Heights

——— Chromatogram of Sample No. 11X (GPC No. 584)

— — — Chromatogram from α_1 Search

FIGURE I-16 : Experimental and Model Mn and Mw, 70°C, 0.3% AIBN

Mw		Mn	
○	Mw(∞), Code * 27	△	Mn(∞), Code * 27
□	Mw(∞), Code * 28	▽	Mn(∞), Code * 28
◑	Mw(∞), Code ** 27	◭	Mn(∞), Code ** 27
◨	Mw(∞), Code ** 28	▼	Mn(∞), Code ** 28

α_1 from:

-·—·— Fit #1 Method of Differential Chromatograms

····· Fit #2

— — — — 2 Variable Search Method of Chromatogram Heights

——— 3 Variable Search

— — Conventional Kinetics (constant k_{td})

α_1 from:

——— { Fit #1, #2 / 2 Variable Search / 3 Variable Search

— — Conventional Kinetics (constant k_{td})

* Precipitated Polymer

** Monomer Polymer Mixture

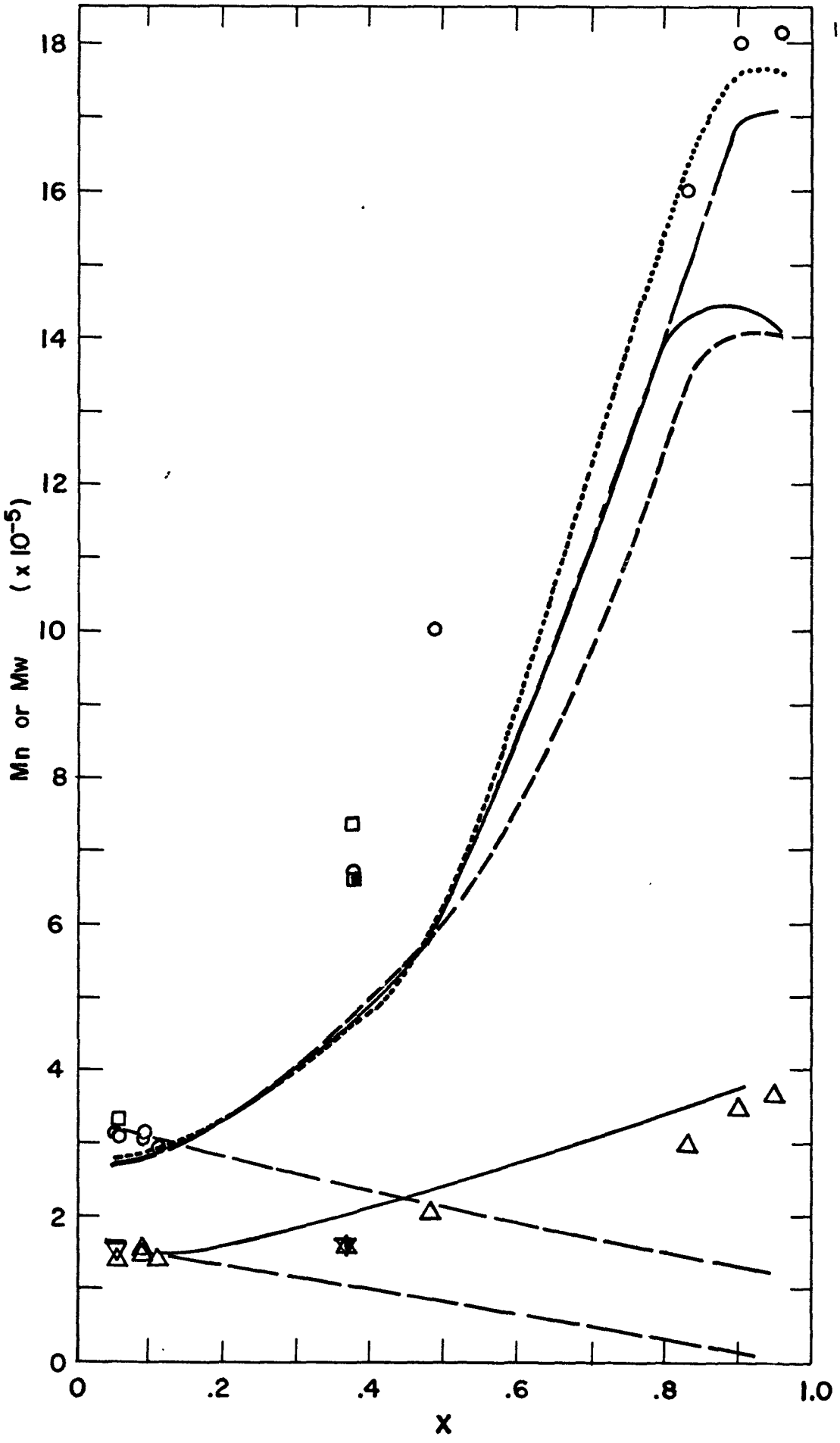
Mn or Mw (x 10⁻⁵)
X
0
2
4
6
8
10
12
14
16
18
.2
.4
.6
.8
1.0

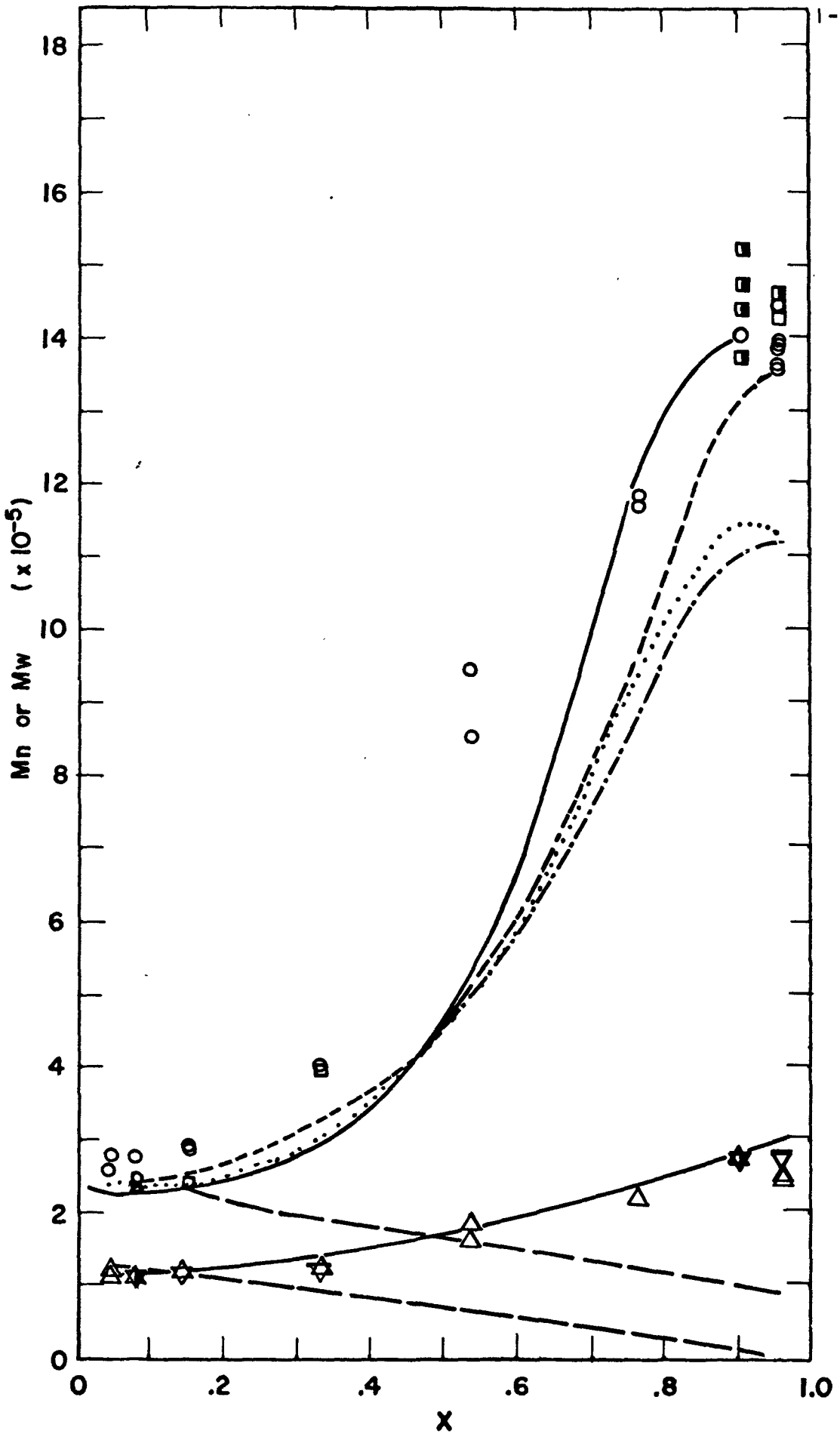

FIGURE I-17 : Experimental and Model Mn and Mw, 70°C, 0.5% AIBN
(Ref. Figure I-16 for index)

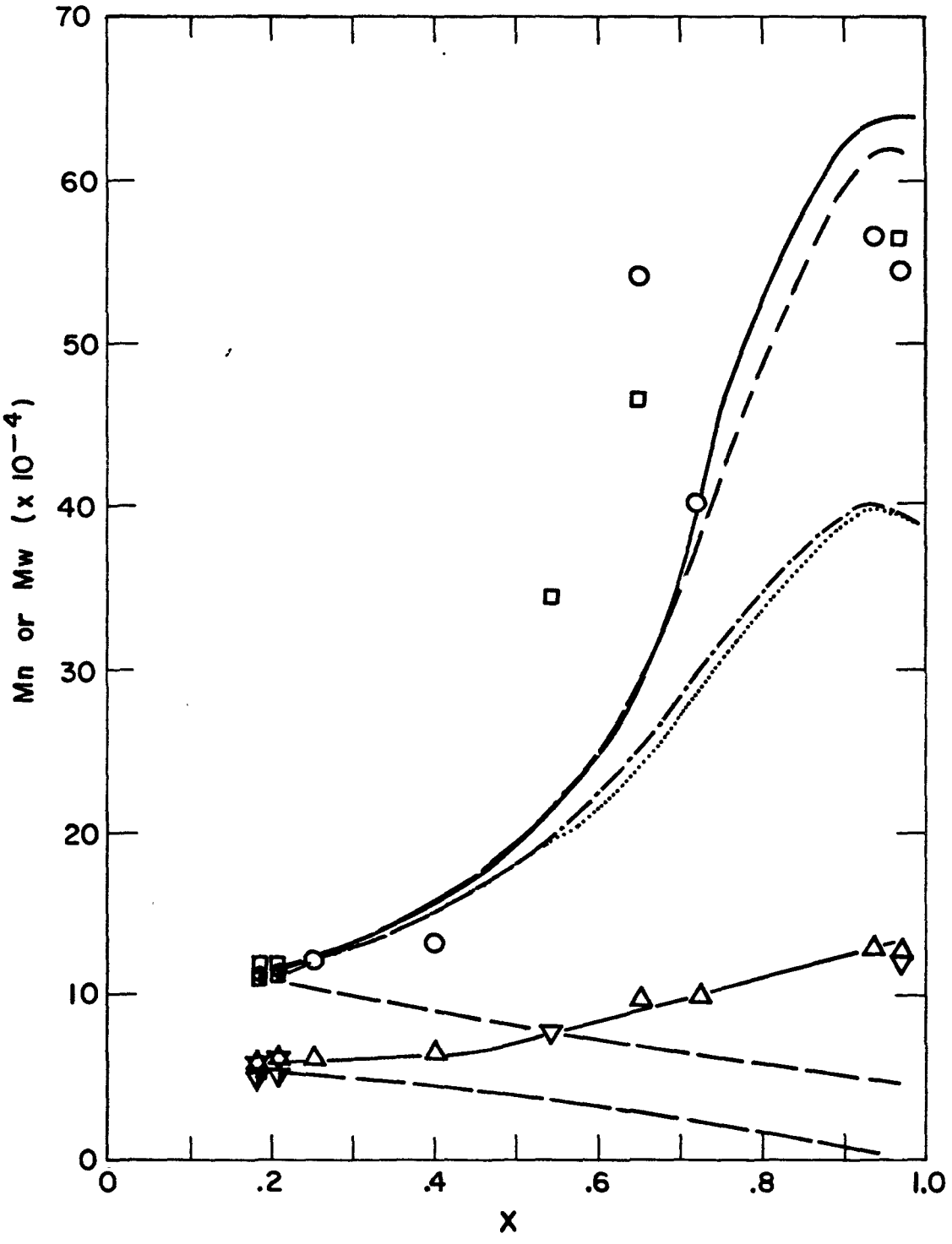

FIGURE I-18 : Experimental and Model Mn and Mw, 90°C, 0.3% AIBN
(Ref. Figure I-16 for Index)

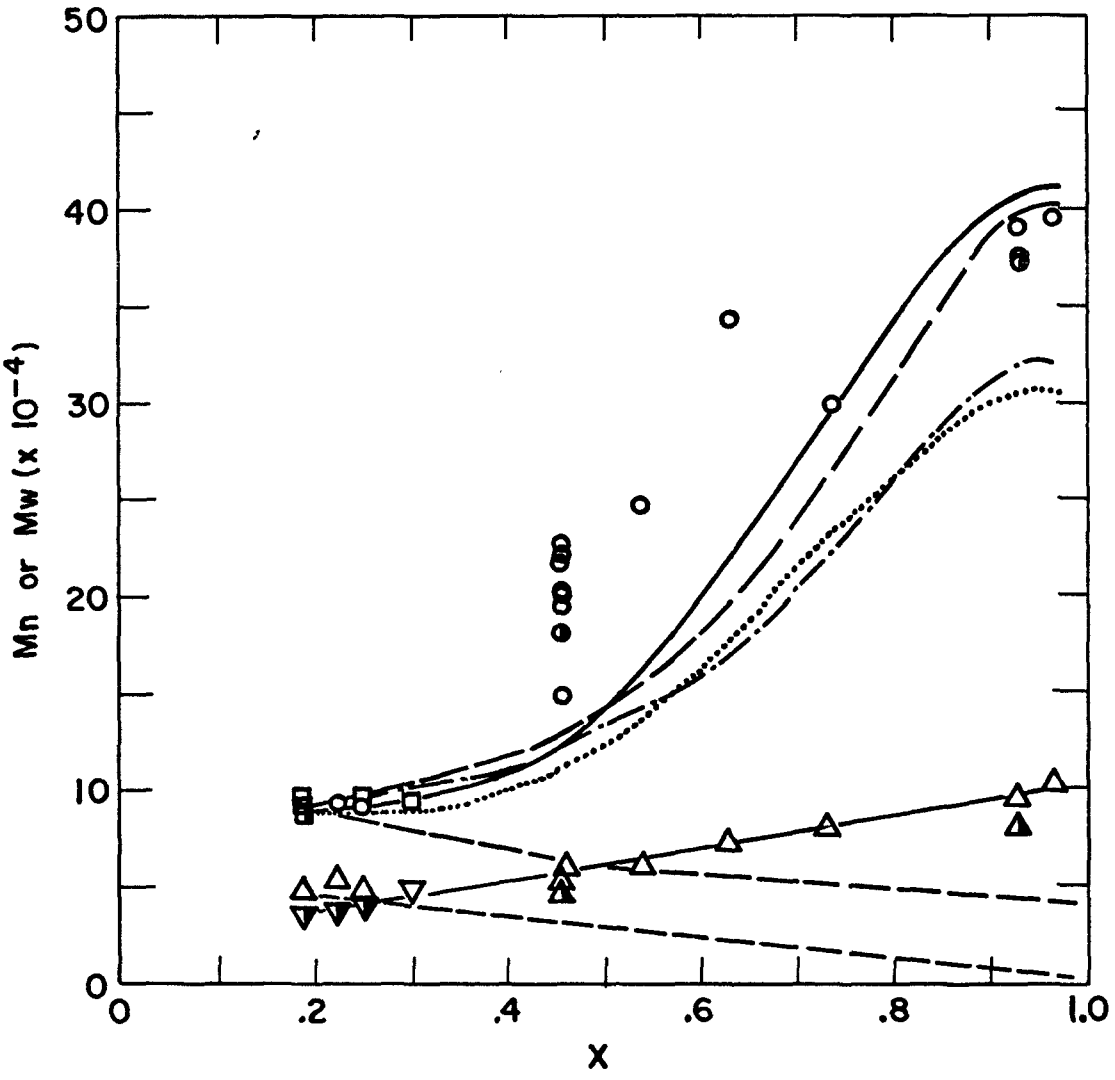

FIGURE I-19 : Experimental and Model Mn and Mw, 90°C, 0.5% AIBN
(Ref. Figure I-16 for Index)

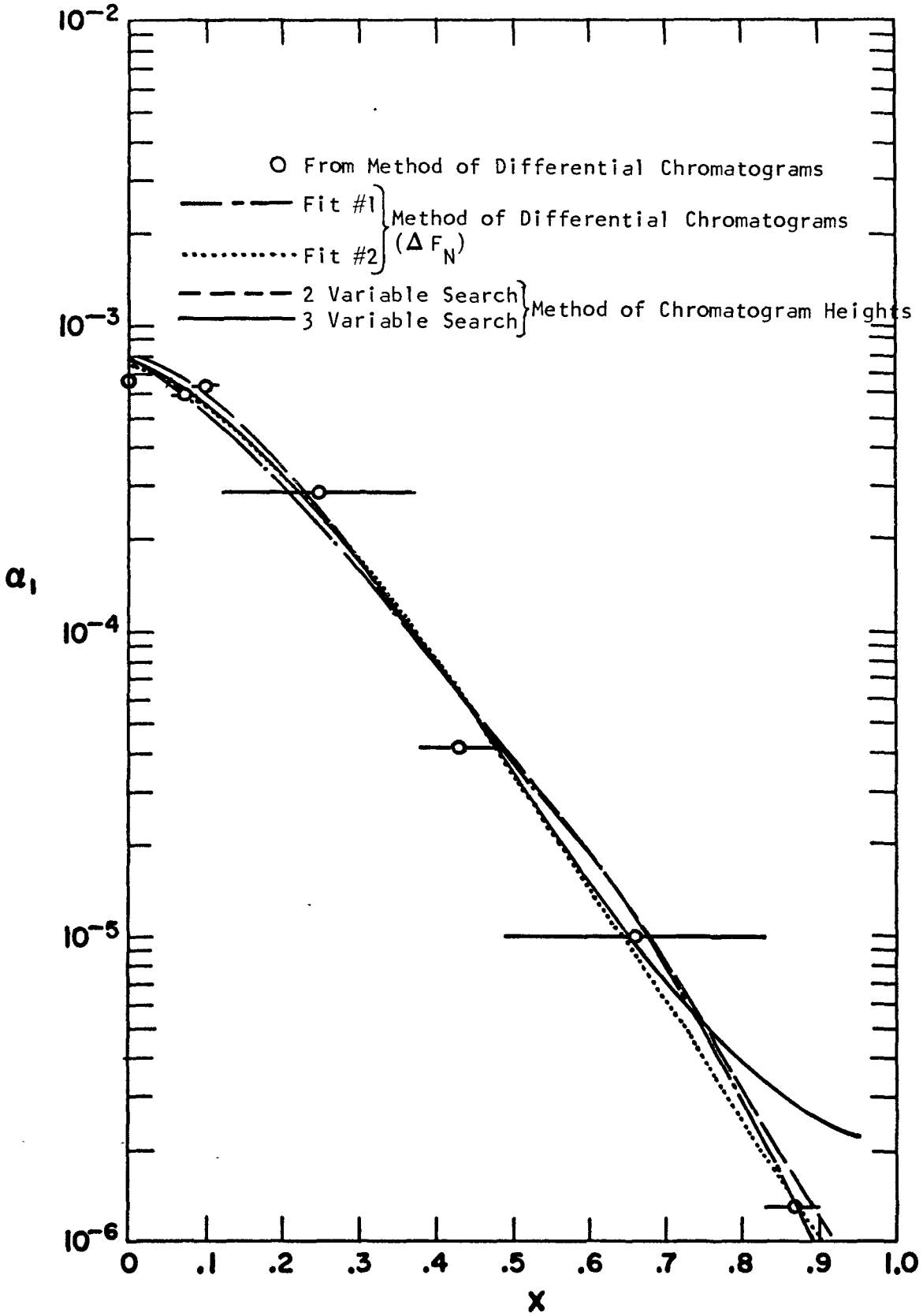

FIGURE I-20 : α_1 vs. X, 70°C, 0.3% AIBN

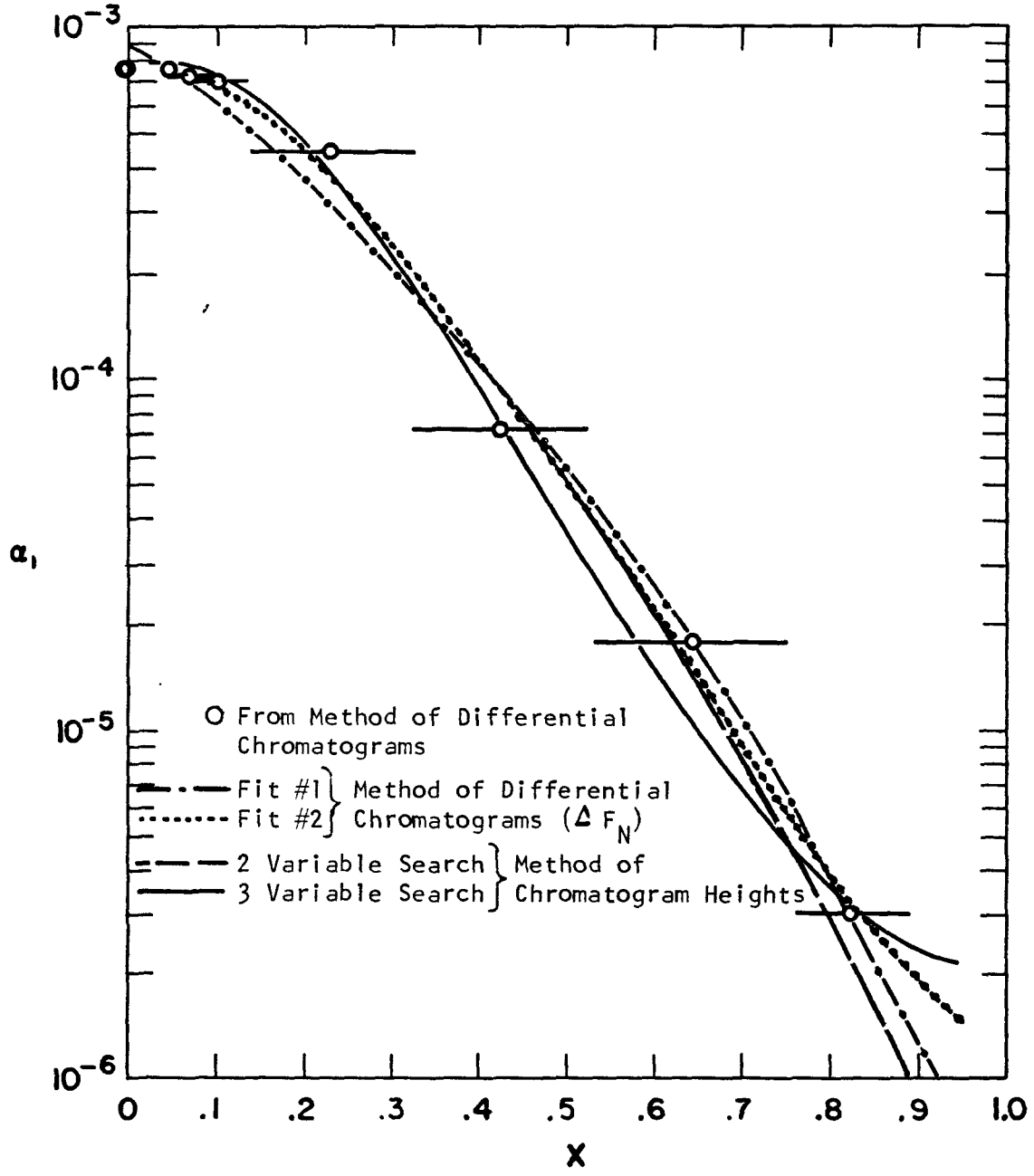

FIGURE I-21 : α_1 vs. X, 70°C, 0.5% AIBN

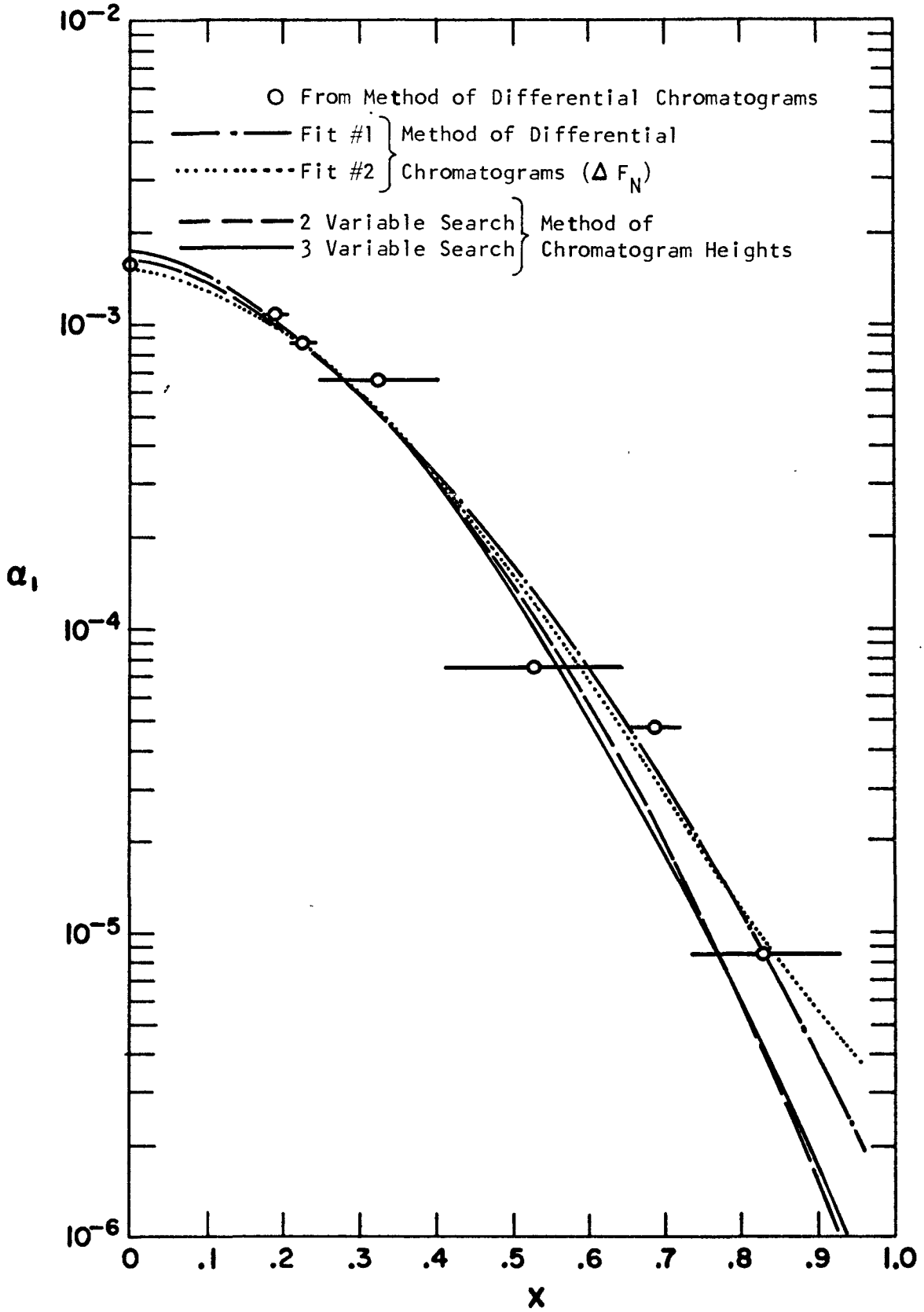

FIGURE I-22 : α_1 vs. X, 90°C, 0.3% AIBN

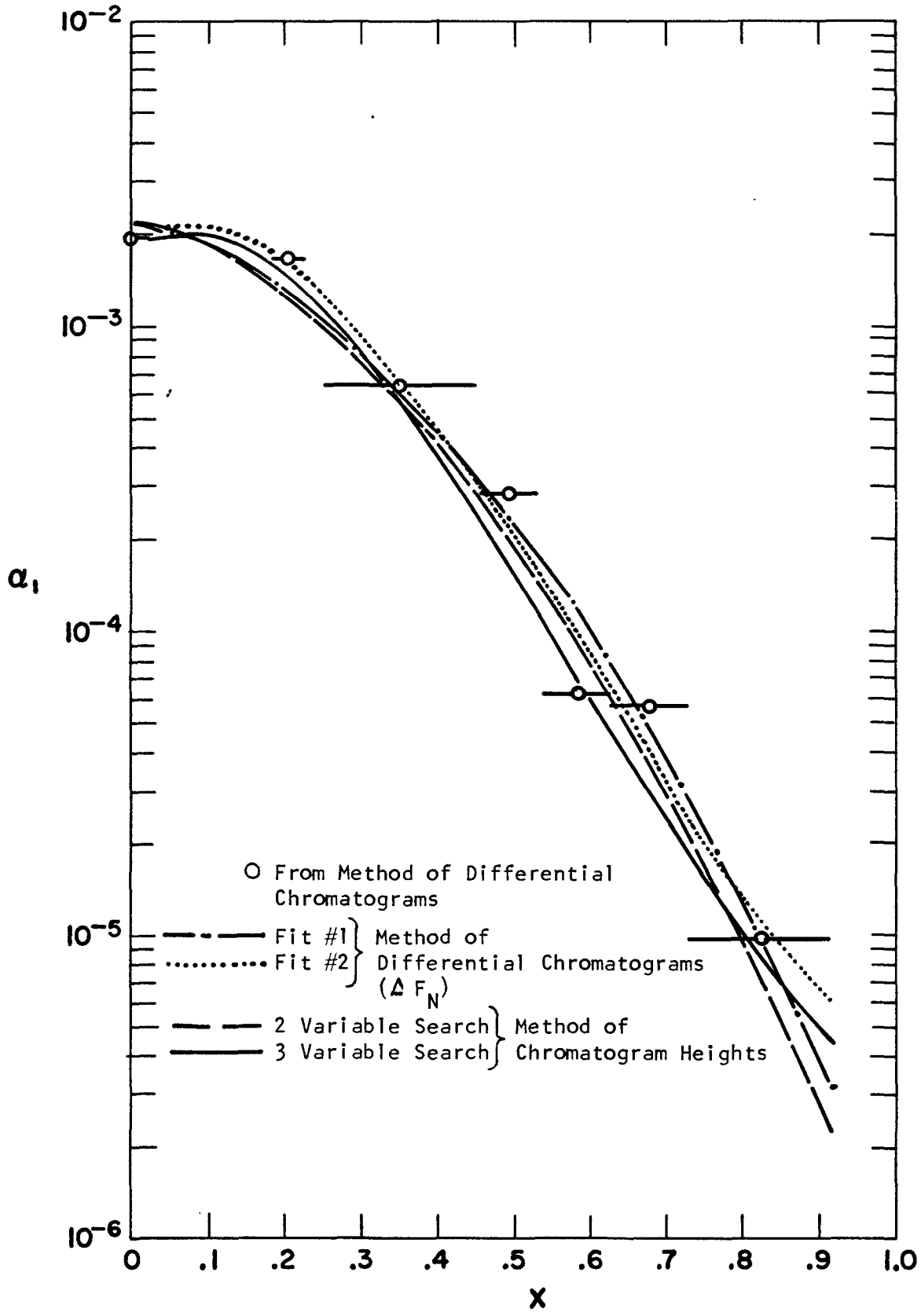

FIGURE I-23 : α_1 vs. X, 90°C, 0.5% AIBN

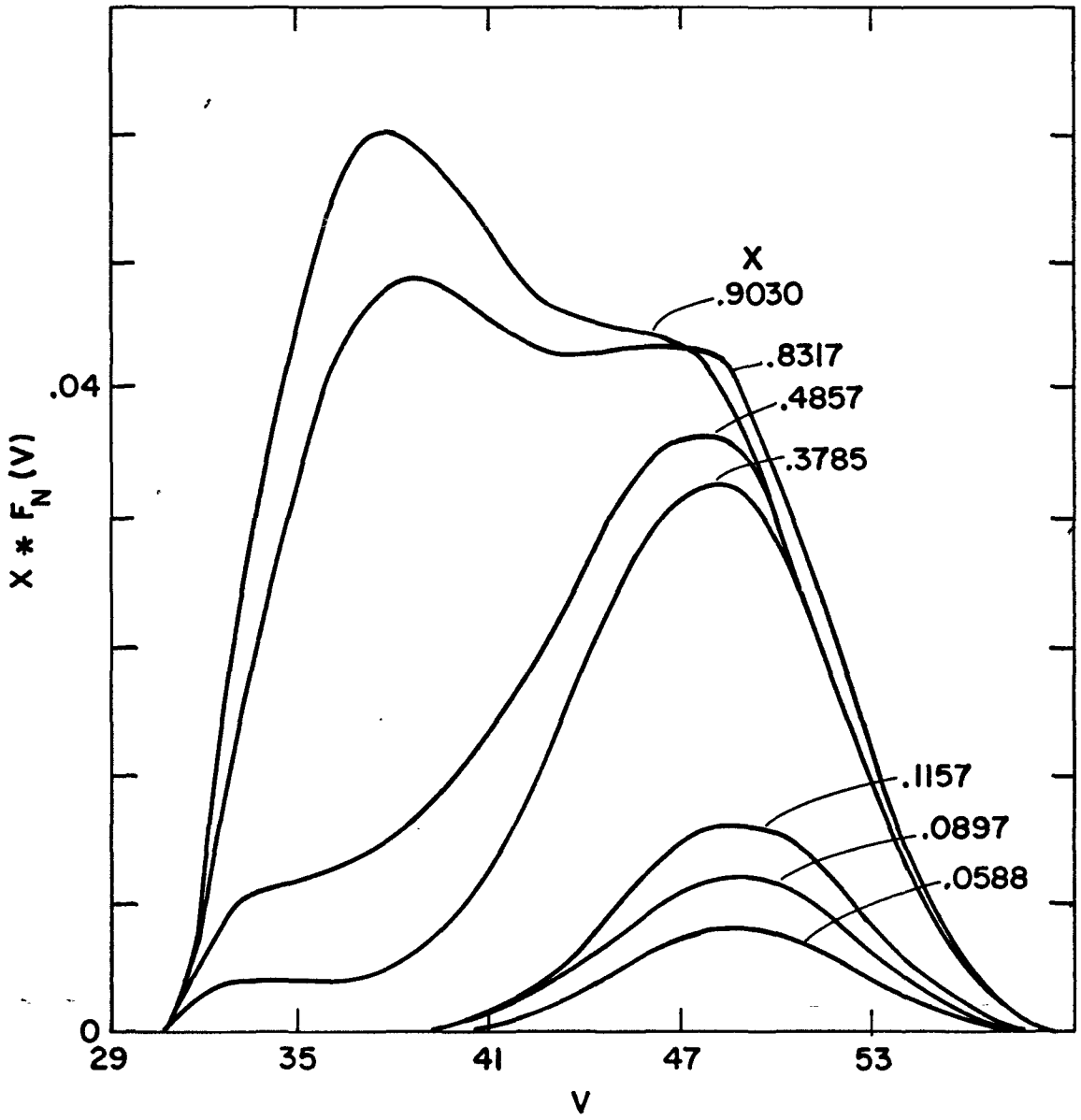

FIGURE I-24 : Cumulative Chromatograms at Different Conversions, 70°C, 0.3% AIBN

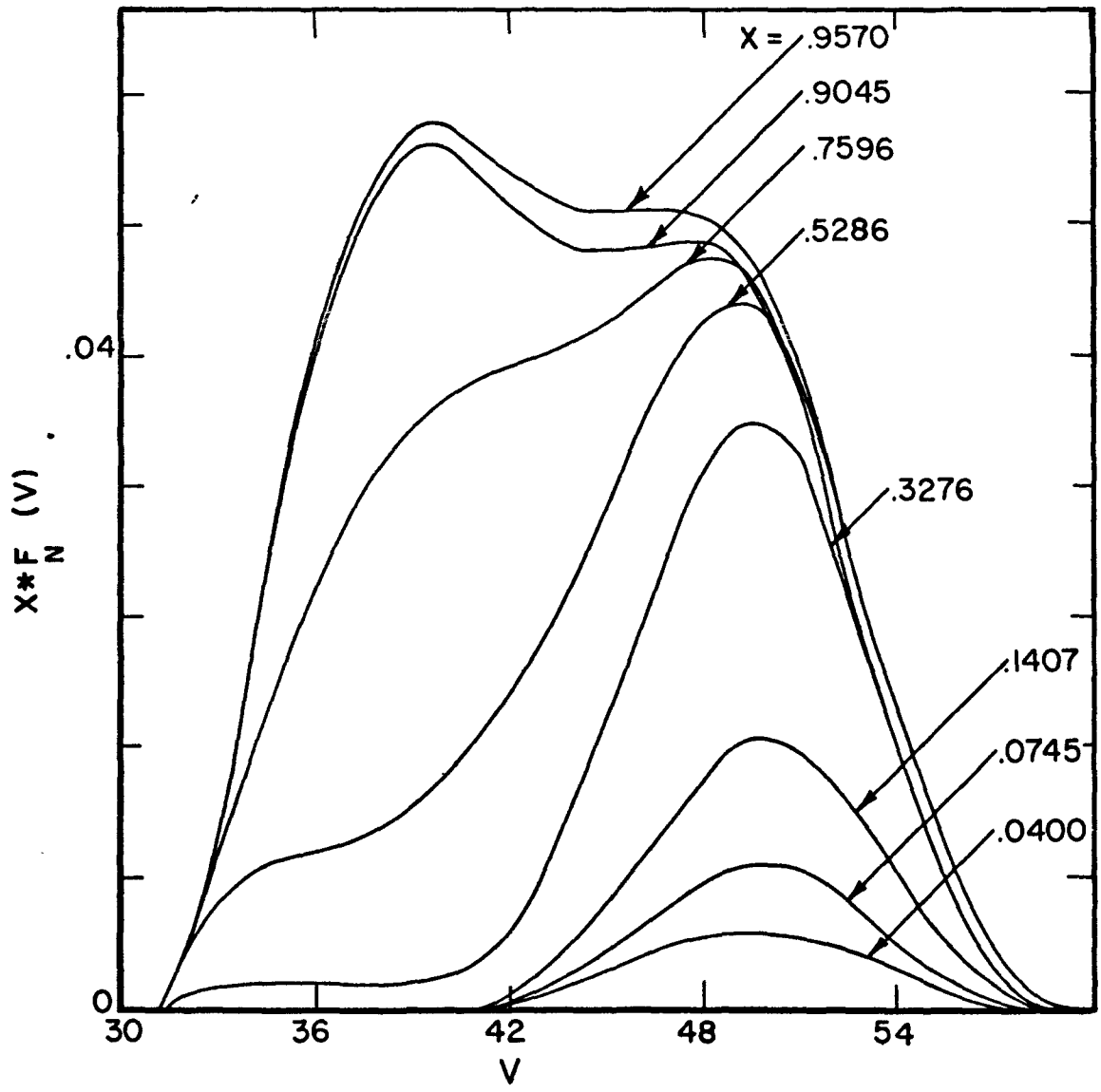

FIGURE I-25 : Cumulative Chromatograms at Different Conversions, 70°C, 0.5% AIBN

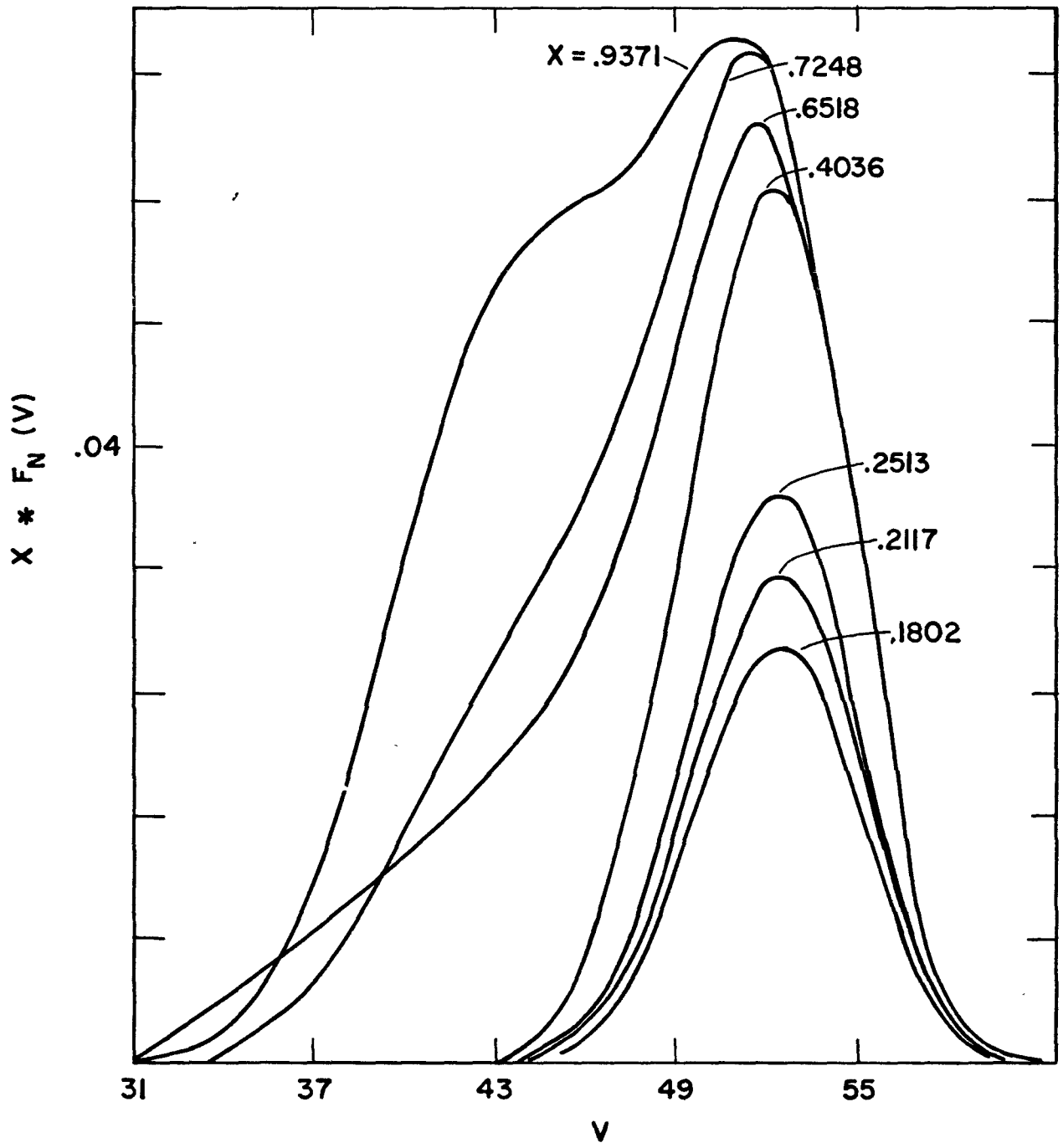

FIGURE I-26 : Cumulative Chromatograms at Different Conversions, 90°C, 0.3% AIBN

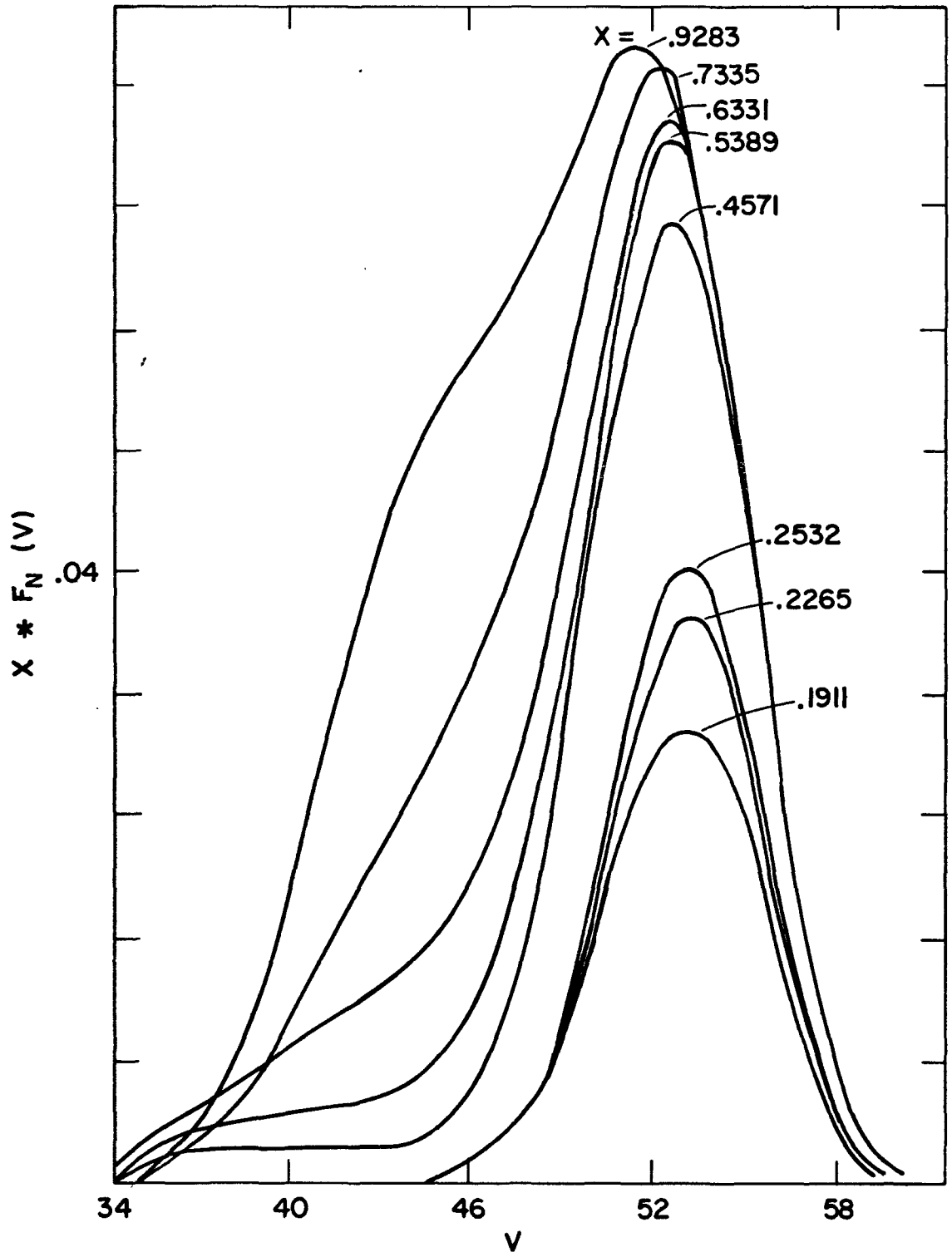

FIGURE I-27 : Cumulative Chromatograms at Different Conversions, 90°C, 0.5% AIBN

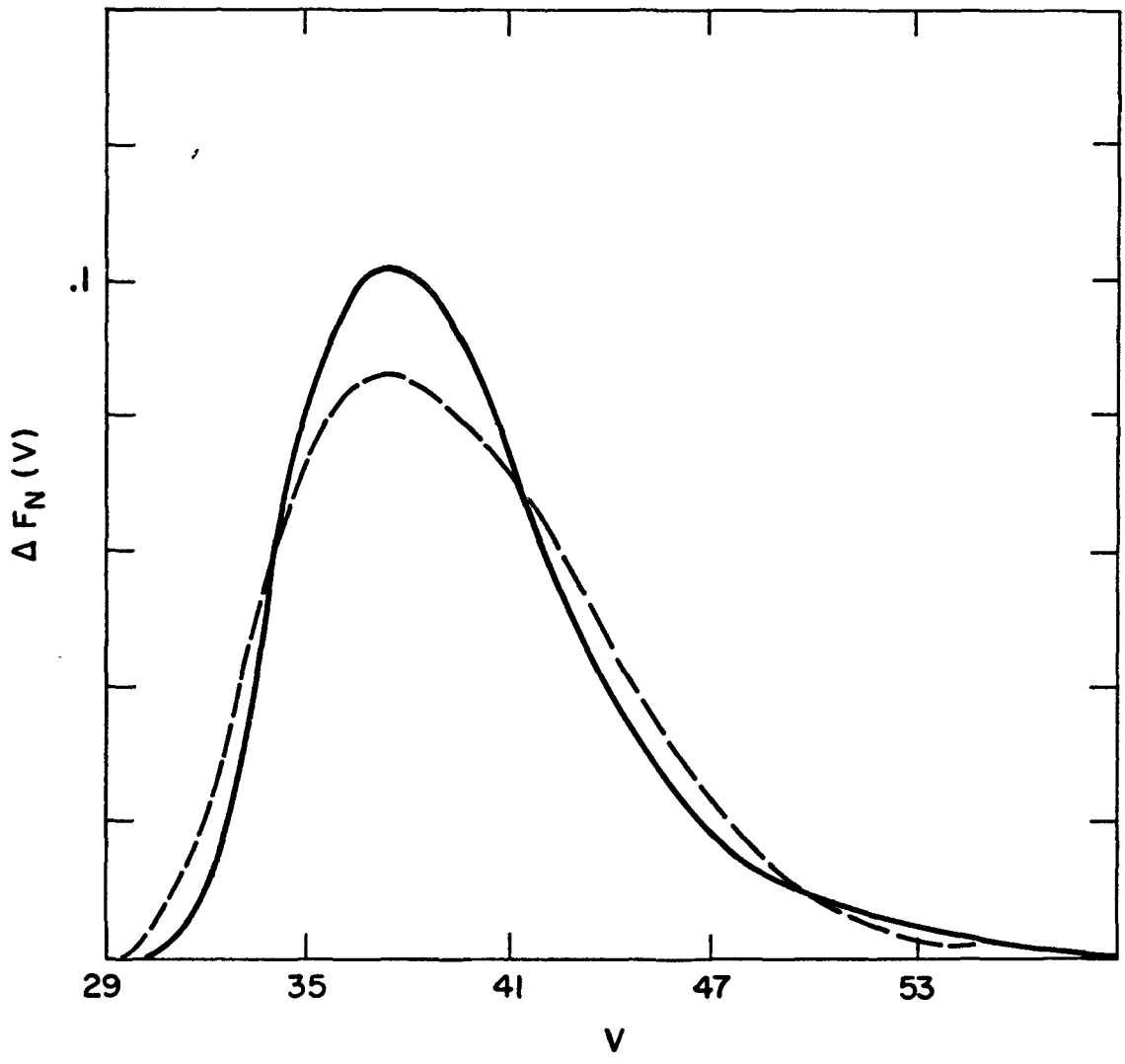

FIGURE I-28 : Results of a Single Variable Search for α_1 Using the Method of Differential Chromatograms

——— Differential Chromatogram from GPC Nos. 589 and 595 (X = .4857 to .8317)

— — — Chromatogram from α_1 Search

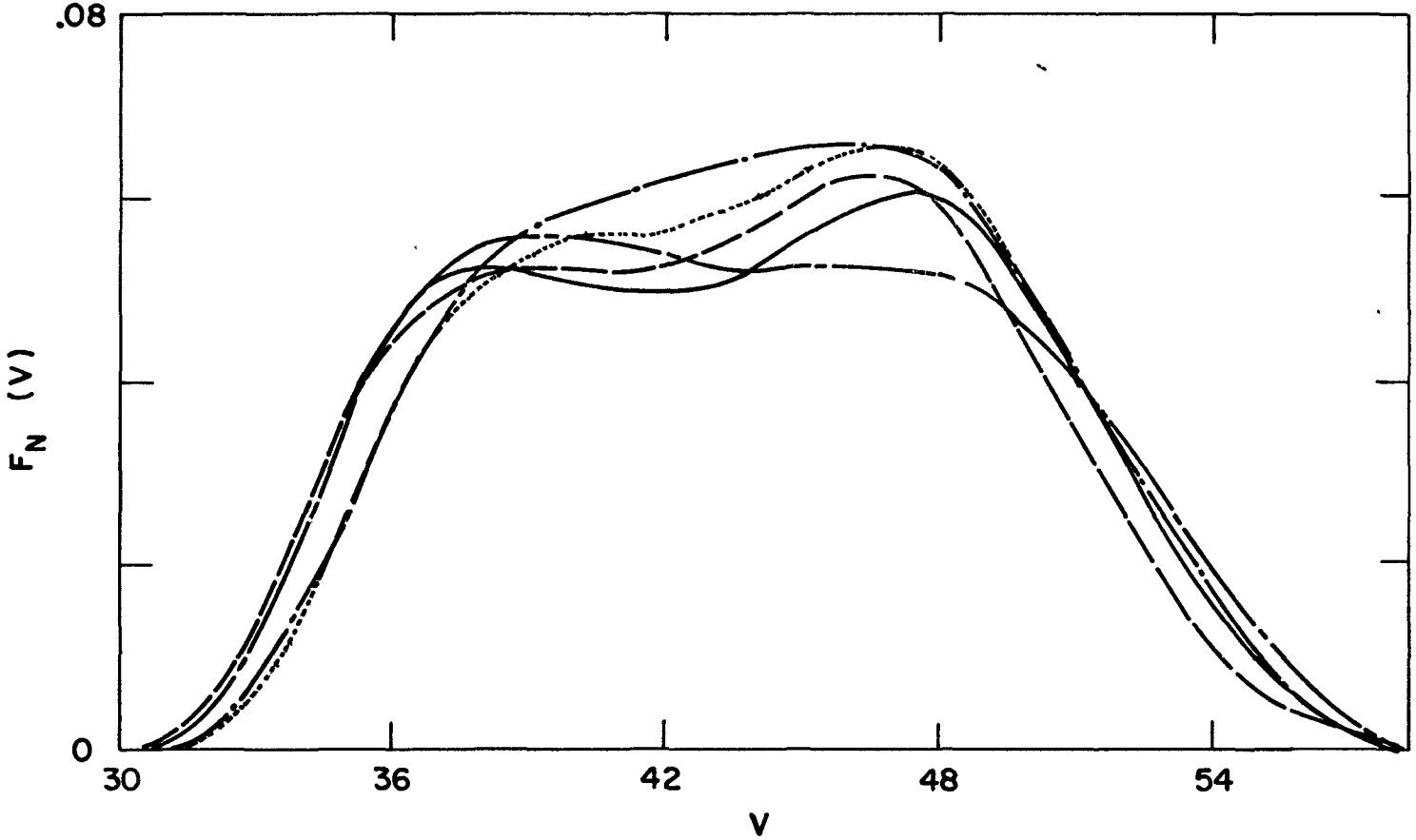

FIGURE I-29 : Results of Method of Chromatogram Heights on High Conversion Sample (GPC No. 615)(X = .9570)

——— Experimental Chromatogram
——·—— Chromatogram Using α_1 from Fit #1
- - - - - Chromatogram Using α_1' from Fit #2
——— ——. Chromatogram Using α_1' from 2 Variable Search
——— Chromatogram Using α_1' from 3 Variable Search

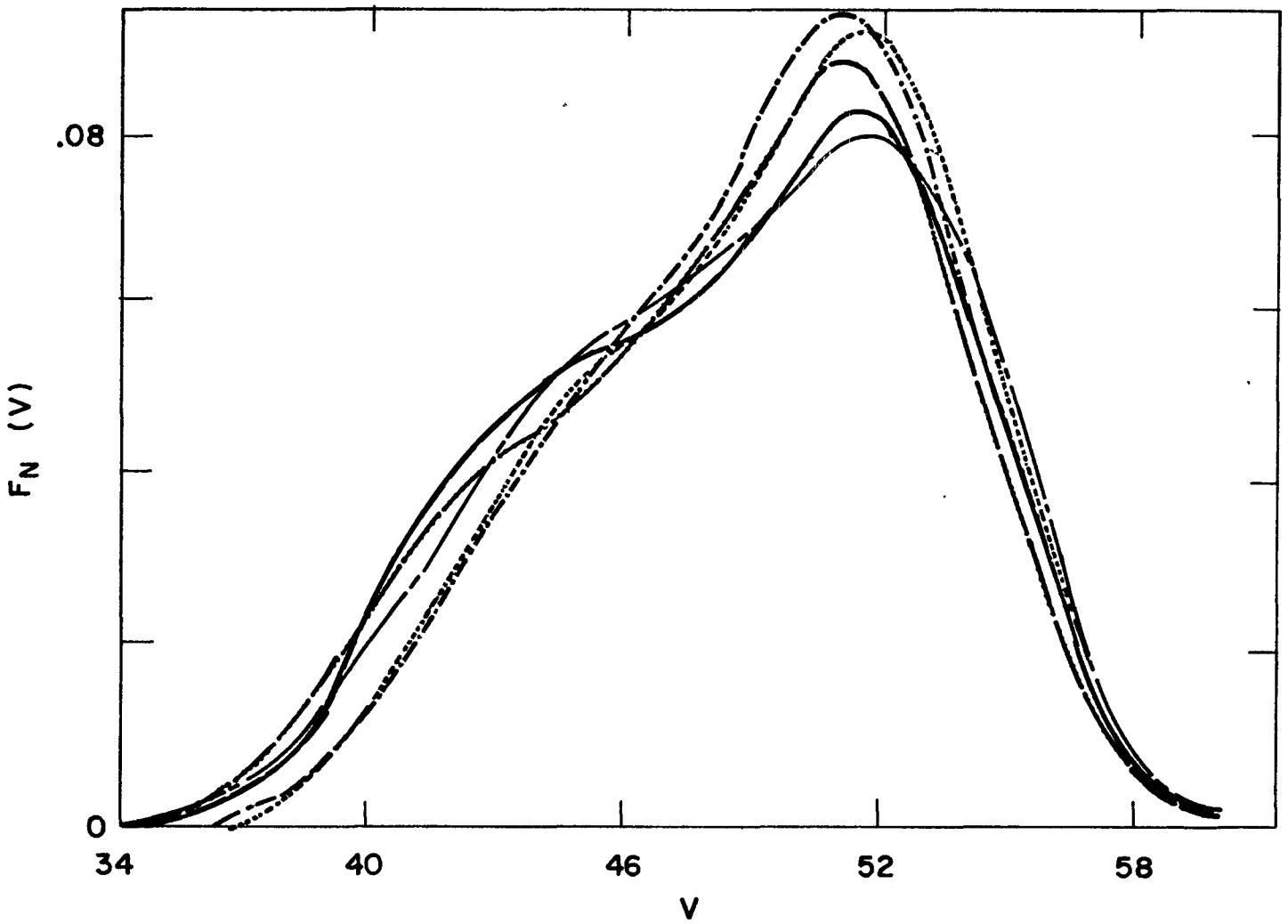

FIGURE I-30 : Results of Method of Chromatogram Heights on High Conversion Sample (GPC No. 571)(X = .9283)

——— Experimental Chromatogram
——·—— Chromatogram Using α_1 from Fit #1
····· Chromatogram Using α_1 from Fit #2
—— —— Chromatogram Using α_1 from 2 Variable Search
——— Chromatogram Using α_1 from 3 Variable Search

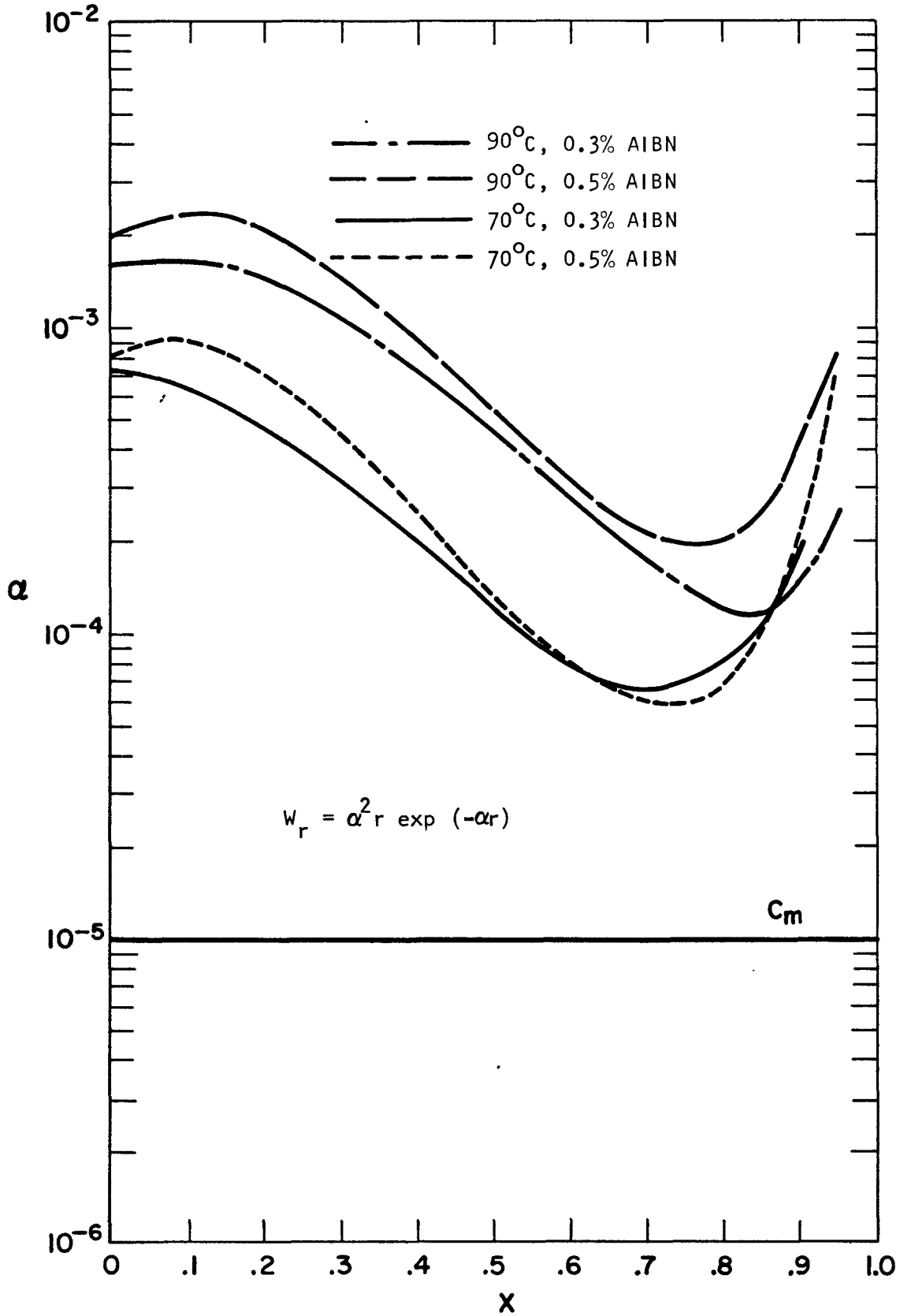

FIGURE I-31 : $\alpha \left(= \alpha_1 \frac{(1+eX)}{(1-X)^2}\right)$ vs. X

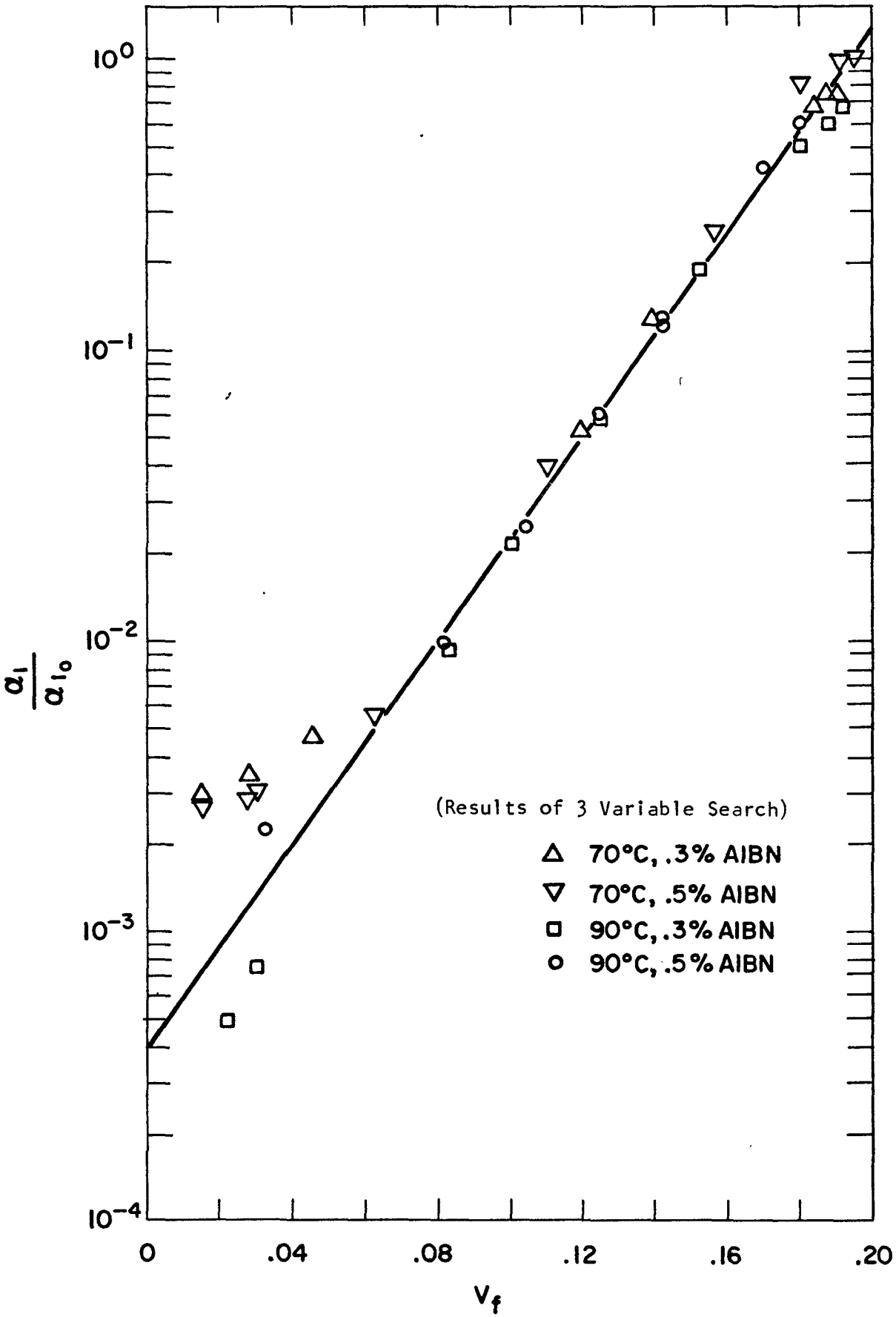

FIGURE I-32 : $\frac{\alpha_1}{\alpha_{1_o}}$ vs. Free Volume for 70° and 90°C

PART II

DEVELOPMENT OF GEL PERMEATION CHROMATOGRAPHY (GPC) INTERPRETATION

1. Introduction

Polymers are difficult to analyze. They are multi-component materials in the extreme with even a linear homopolymer (the concern of this work) having as many as ten thousand different molecular weight species (each consisting of a repeated chemical group--a mer--all identical for a homopolymer except perhaps the first and last in a chain) and all having various concentrations. This usually results in a broad molecular weight distribution. Copolymers and terpolymers (two and three different monomer types) are today also in common industrial use. Since the monomer units can appear in different amounts and combinations per chain, these non-homopolymers require other descriptions, such as composition distribution, as well as molecular weight distribution. Polymers may be branched and the branching might be "comb" or "star" "long chain" or "short chain" and is distributed in some manner among the various molecular sizes present. Stereoregularity and crystallinity of polymers are variable. Also, polymers are sometimes completely or partially crosslinked. Furthermore, they may be combined with various other materials (e.g. plasticizers) or may contain varying amounts of monomer.

All of the above variables can be highly significant to the desired physical properties, and generally they unite to make analysis of a polymer an imposing problem. A knowledge of the processing history of the polymer,

combined with one or more analytical techniques, has been the classical solution. However, until recently, this has usually involved long and tedious procedures, which, in the end, gave an uncertain and a very partial description of the polymer. Lately, new instruments, combined with high speed computer interpretation are greatly improving the situation. The GPC is one such new instrument and is principally used to measure the molecular weight distribution.

GPC permits a rapid and reproducible measure of the molecular size distribution. However, molecular weight calibration has been limited by a lack of standards for a wide variety of polymers. In addition, branching and copolymer composition distributions have made calibration for many industrial polymers almost impossible. Furthermore, mathematical methods of correcting for axial dispersion in GPC are complex, difficult to apply and generally inadequate.

The objectives of this study are to review the state of the art of GPC interpretation, to evaluate proposed methods of interpretation and to develop new and practical ways of interpreting chromatograms.

This study had two definite phases. The first was in 1968 and involved exploring limitations in both instrument operation and chromatogram interpretation. This led to a new method of interpretation, "The Method of Molecular Weight Averages". The results were published and, as will be described in Section 3.2.3.4, led to considerable further development of GPC interpretation in the literature. The second phase was in 1970, when the kinetic study described in Part I of this thesis was nearing completion. Its main objective was to determine the best way of interpreting chromatograms resulting from a polymerization kinetic mechanism

which yielded broad and sometimes bimodal chromatograms. This led to the development of two new methods of chromatogram interpretation, "The Method of Chromatogram Heights" and "The Method of Differential Chromatograms".

2. Literature Review--GPC Interpretation

2.1 General

2.1.1 Description of the Instrument

The GPC is an instrument which fractionates a polymer sample according to the distribution of molecular sizes in the carrier solvent. This molecular size distribution is interpreted to give a molecular weight distribution. Operation of the GPC involves dissolving the sample and injecting it as a pulse into a carrier solvent which transports it through a series of columns containing a porous packing. Because of the distribution of pore sizes, the smaller molecules enter the packing more often than the larger ones and hence they exit last from the columns. Concentration of polymer in the eluent is continuously monitored by a detector. The commercial version of the GPC was introduced in 1964. It employed a cross linked polystyrene gel and a differential refractometer detector. Various porous glass bead packings[1,2] and u.v. detectors as well as I.R. detectors have been used. Several reviews have been published.[3-7]

2.1.2 GPC Interpretation--Resolution of the Instrument

The main object in interpretation of a GPC chromatogram is to obtain molecular weight distribution information about the sample. This inherently depends on how well the instrument can actually separate the molecular weights present in the sample (i.e. its resolution).

In chromatography, resolution is generally defined by Equation (II-1), where V_1, V_2 and W_1, W_2 are the peak retention volumes and peak widths for molecular weight species 1 and 2 respectively.[8,9] For complete separation $R_s \geq 1$.

$$R_s = \frac{2(V_2 - V_1)}{W_1 + W_2} \qquad (II-1)$$

This definition shows that the peak retention time of each species (V_1, V_2) and the spreading of each by the axial dispersion process (W_1, W_2) determine resolution. Retention time of each species is determined by calibration. Curve spreading is accounted for by a variety of methods. Both of these topics will be considered in detail below.

2.2 Calibration of GPC

2.2.1 Conventional Calibration

A conventional calibration curve is a plot of ℓn (molecular weight) versus retention volume. This plot is generally nearly linear in the central region, but tails up at low retention volumes and down at high retention volumes. Considerable research has attempted to elucidate the separation mechanism of GPC with prediction of the calibration curve as a test of the mechanism proposed. These attempts have usually emphasized either a steric exclusion or a nonequilibrium diffusion mechanism.[10,11] It is expected that both of these mechanisms, as well as several factors, such as: adsorption, deformation of the gel by swelling and pressure, deformation of the macromolecular shapes by shear, viscosity effects, eddy diffusion, gel structure, and column packing may all be influential. Research in this area usually results in expressions which can be made to fit some GPC

calibration curves by adjusting variable parameters. Yau[12] combined steric exclusion and nonequilibrium diffusion in one unified approach with some success. The calibration curve form that he proposed was shown to be of practical use by Rosen and Provder.[13] At present,[10,11] the main GPC separation mechanism is considered to be due to equilibrium distribution of polymer between the carrier solvent and the solvent within the pores, as the polydisperse sample is carried through the columns, although this complex topic is still in considerable dispute. Because of the state of these theories, GPC calibration is carried out in a purely empirical manner by injecting polymers whose molecular weight characterization has been done by some other instruments. Such methods are now available for calibration with either monodisperse or polydisperse standards.

2.2.1.1 Use of Monodisperse Standards

A monodisperse standard is a polymer sample which contains a relatively small number of polymer species (the polydispersity $Mw/Mn \cong 1$). Standards termed "monodisperse" are produced by anionic polymerization and are now available for several polymers. Calibration of the GPC using these standards involves injecting those which are the same polymer as the unknown and plotting their molecular weight versus their peak retention volume. Monodisperse samples of different polymers give different calibration curves for the same GPC operating conditions.

After the calibration curve is fit with an empirical or semiempirical equation, the molecular weight averages and molecular weight distribution can then be calculated if GPC imperfect resolution is neglected.

The calculation of molecular weight distributions is discussed in Appendix II-A. Although the GPC chromatogram F(v) normalized ($F_N(v)$) is likely the best way of presenting a molecular weight distribution from GPC, an often used way is to plot weight fraction of each chain length, $W(r)_{CUM}$, versus chain length r.

If perfect resolution is assumed:

$$W(v) = F(v)$$

then

$$W(r)_{CUM} = F(v) \frac{dv}{dr} \frac{1}{\int_{-\infty}^{\infty} F(v)dv} \tag{II-2}$$

The molecular weight averages are calculated as follows

$$M_k = M_o \bar{r}_k = M_o \frac{Q_k}{Q_{k-1}} \tag{II-3}$$

$$= M_o \frac{\sum_{r=1}^{\infty} r^k P_r}{\sum_{r=1}^{\infty} r^{k-1} P_r}$$

$$= \frac{\int_{-\infty}^{\infty} M(v)^{k-1} F(v)dv}{\int_{-\infty}^{\infty} M(v)^{k-2} F(v)dv} \tag{II-4}$$

where M_k is M_n with k=1, M_w with k=2, etc.

M_o is the monomer molecular weight

$\bar{r}_k$ is the kth average chain length

Q_k is the kth moment of P_r versus r and

P_r is concentration (moles/l) of polymer of chain length r

M(v) is molecular weight as a function of retention volume (the conventional GPC calibration curve)

For k=1

$$M_1 = Mn(t) = \frac{\dot{M}_o Q_1}{Q_o} = \frac{\int_{-\infty}^{\infty} F(v)\,dv}{\int_{-\infty}^{\infty} \frac{F(v)}{M(v)}\,dv} \qquad (II\text{-}5)$$

For k=2

$$M_2 = M_w(t) = \frac{M_o Q_2}{Q_1} = \frac{\int_{-\infty}^{\infty} F(v)M(v)\,dv}{\int_{-\infty}^{\infty} F(v)\,dv} \qquad (II\text{-}6)$$

2.2.1.2 Use of Polydisperse Standards

Cantow et.al.[14] showed that if a polydisperse sample with known cumulative molecular weight distribution and of the same type of polymer as the unknown is obtained, then, analysis of this chromatogram from the same GPC operating conditions as used for the unknown can yield a calibration curve, if the effect of imperfect resolution is assumed negligible. This involves determining the weight fraction of the sample eluted over a fractional retention volume from the chromatogram, determining the molecular weight that this corresponds to by reference to the known cumulative molecular weight distribution, and plotting the log of this molecular weight versus its retention volume. When this procedure is repeated for successive retention volume fractions, a calibration curve results.

Weiss et.al.[15] added to the above approach by assuming that the true molecular weight distribution of a polydisperse standard could be fit by a two parameter Schulz-Zimm distribution. If only two averages of a polydisperse standard were known, the two parameters could be evaluated and the cumulative molecular weight distribution was then calculated for calibration by the above mentioned method. Weiss so evaluated and supplied a "composite" polydisperse PMMA standard used in this study.

The calibration curve may also be determined from a polydisperse standard by using optimization techniques to find the parameter values necessary in the assumed form of the calibration curve in order to obtain the known molecular weight averages of the sample from its GPC chromatogram.[16,17] The calibration curve obtained is an "effective" one in that it combines correction for peak broadening with molecular weight calibration.

2.2.2 Universal Calibration

Benoit et.al.[18] showed that, in general, separation accomplished by GPC is not directly on the basis of molecular weight, but rather according to the hydrodynamic volume of the polymer molecules in solution (the larger volumes exit first, followed by the smaller, regardless of polymer type). A universal calibration curve is then a plot of ℓn (hydrodynamic volume) versus peak retention volume (v). Once established for the GPC operating conditions by using only one type of polymer, the hydrodynamic volume distribution of any polymer sample injected may then be determined. This approach has now been applied to a variety of polymers, and although there have been some exceptions and some other bases for calibration proposed, the hydrodynamic volume concept has been widely successful and flexible.[19,20]

The molecular weight, rather than the hydrodynamic volume, is the generally known quantity for monodisperse standards and the molecular weight distribution (or the molecular weight averages) are desired for polymer unknowns rather than the hydrodynamic volume distribution. Hence, some relation between the molecular weight and hydrodynamic volume must be used.

Based on the Einstein viscosity law, the hydrodynamic volume (V') is proportional to the product of intrinsic viscosity ((η)) and molecular weight (M) for a monodisperse sample.

$$(\eta)M = 2.5\ N_o V' \epsilon_o = V \qquad (II-7)$$

In Equation (II-7) N_o is Avogadro's number and ϵ_o is an effective volume factor to allow for swelling of the polymer molecule by solvent.[21] When "hydrodynamic volume" is discussed with regards to GPC calibration it is actually "effective hydrodynamic volume" V that is meant.

The intrinsic viscosity can be measured experimentally or, if the polymer obeys the Mark Houwink Equation (i.e. it is linear and of homogeneous unbranched composition):

$$(\eta) = KM^a \qquad (II-8)$$

where K and a are constants, then the intrinsic viscosity can be calculated. Calibration is thus carried out by so determining the hydrodynamic volume of any available monodisperse standards and plotting $\ell n V$ versus retention volume. Then, when the conventional calibration curve for any polymer is desired, and the relationship between molecular weight and intrinsic viscosity known for the polymer, the conventional curve can be generated as follows:

1. The universal calibration curve is fit by an equation. For example, it may be fit by a cubic polynomial using a computer library subroutine for least squares fitting.

   Then:

$$\ell n\ (V) = \ell n((\eta)M) = B_1 + B_2 v + B_3 v^2 + B_4 v^3 \qquad (II-9)$$

2. The relation for intrinsic viscosity is used to change Equation II-9 to a fit of the conventional calibration curve. For example, if the polymer obeys the Mark Houwink Equation and the constants "K" and "a" are known then

$$M = \left\{ \frac{EXP(B_1 + B_2 v + B_3 v^2 + B_4 v^3)}{K} \right\}^{\frac{1}{a+1}} \qquad (II-10)$$

Equation (II-10) is the conventional calibration curve for the polymer.

2.2.3 Influential Variables

The calibration curve is affected most by the number and type of GPC columns used. For example, if columns with packing of large diameter porosity are used, then separation of large molecules will improve and the slope of the calibration curve in that region will decrease. The greater the number of columns the better the separation. The order of columns in the direction of carrier solvent flow rate and the pore size distribution in each is always determined empirically. Conventionally, large pore size columns are first followed by smaller, although Osterhout et.al.[22] has recommended that having all columns with identical high average pore size is preferred for high molecular weight polydisperse samples.

Increased temperature of operation shifts the calibration curve to lower retention volumes. Increased expansion of the hydrodynamic volume of the molecules[23] along with factors such as less adsorption of very small molecules, greater polymer diffusivity, decreased solvent viscosity, gel swelling, and lowered pressure drop all might be influential.

Increased weight of polymer injected causes poorer separation by decreasing the effective pore volume available per molecule and encourag-

ing viscosity effects.[24] Phenomena such as secondary exclusion[25] (exclusion of large molecules from pores by the action of small molecules) are also possible. The minimum value of concentration permitted depends on the sensitivity of the detector for the polymer used. Variation of peak retention volume with concentration was reviewed by Duerksen.[6] Often a shift to higher peak retention volumes results, particularly for high molecular weights. Increased concentration decreases the effective hydrodynamic volume of a macromolecule. Very recently, Rudin et.al.[21] have suggested correcting for this effect on peak retention volume of monodisperse standards. They show that such correction is useful for high molecular weights and highly solvated molecules.

In GPC calibration, it is usually assumed that refractive index is independent of molecular weight and proportional to concentration. If this is not the case for a particular polymer solvent combination, then correction must be made in calculating concentration (Equations (II-2 to 6)) although the peak retention volume would likely be unchanged for "monodisperse" samples. Such correction has been shown to be unnecessary for molecular weights which are above 5000 for polystyrene in THF.[26] PMMA in THF has been analyzed successfully at such intermediate molecular weights.[27] The ratio of area under the chromatogram to the product of the amount injected and sensitivity indicates the validity of the assumption, although this is also a test of linearity of the GPC electronics, sample preparation procedures, and of error introduced by baseline drift. Furthermore, any adjustment or drift with time (due to vibration for example) of the refractometer optics affect this ratio. The few literature studies which include

this quantity estimate its reproducibility to be about 10%.[28,29] The ratio (termed the specific area) is usually not calculated because molecular weight averages are calculated from normalized GPC chromatograms.

The closeness of the polydispersity to unity of monodisperse polystyrene standards also affects the accuracy of the calibration. Low molecular weight tails on such standards can be present due to transfer reactions in anionic polymerization. As has been recently shown[30] the higher molecular weight standards are particularly poor.

Flow rate has little effect on the curve if correct retention volume measurements are made by allowing for the change in volume per count of the instrument siphon bottle. After the initial work here at high flow rates (to 8.4 ml/min)(Phase I of this study) high flow rate studies began to appear in the literature. An observed shift to lower elution volume was observed by Yau[12] and interpreted to be the result of nonequilibrium diffusion. Subsequent studies have not shown such a shift.[31]

Other effects which influence calibration include polymer-gel compatibility (e.g. adsorption), effects of solvent,[32] and validity of the Universal Calibration Curve concept for low molecular weights (random coil statistics fail at molecular weights less than about 5000 for polystyrene).[33]

2.3 Chromatogram Broadening in GPC

2.3.1 Imperfect Resolution and its Effect on Chromatogram Interpretation

Imperfect resolution results in the observed chromatogram of a polydisperse sample being made up of a series of overlapping, unseen chroma-

tograms, one for each molecular size present in the sample. The reason for this situation is axial dispersion (i.e. undesirable mixing and concentration effects) of the sample in the GPC tubing, detector, and columns. The result is that the observed height of the chromatogram at each retention volume contains a contribution from the molecular size that is expected at that volume (according to the calibration curve), along with a contribution from molecular sizes which should all be exiting at neighboring elution volumes, but which have spread out in passage through the instrument. Thus, the observed chromatogram is wider than it should be, and the tails of the chromatogram do not really represent molecular sizes present in the sample.

Elucidation of the degree of seriousness of this effect in chromatogram interpretation has been slowed by several factors. In particular, the polydispersity of both the unknown sample, and even of many "monodisperse standards", coupled with the uncertain nature of the desirable molecular size separation mechanism in GPC, has been a hinderance.

In the chromatography field, the Height Equivalent to a Theoretical Plate[8] has been used to describe curve spreading:

$$H = L \left(\frac{W}{4V}\right)^2 \qquad (II\text{-}11)$$

Giddings et.al.[8,34] have expressed H in a very general form and applied it to GPC.[34] It includes the effect of longitudinal molecular diffusion, nonequilibrium and mass transfer effects in the stationary phase, and the coupling of flow pattern and nonequilibrium effects in the mobile phase. It involves eight geometrical factors in the coupling term which are difficult to estimate.

Billmeyer et.al.[35-37] have used a different approach. They solved the coupled component mass balance equations for the mobile phase and the stationary phase simultaneously using Laplace Transforms. The result was an expression for H in terms of a longitudinal dispersion coefficient, flow rate and mass transfer into pores. The longitudinal dispersion coefficient included a velocity profile term which was inversely proportional to a radial diffusivity coefficient D_r. In experimental testing of the theory,[36] H for the nonpermeating solute was found much higher than for the permeating solute. One possible reason for this was a higher D_r of the latter which outweighed the contribution of permation to H. Further evidence was obtained[37] by using nonporous glass beads as packing. Both of the above theories incorporate the coupling of molecular and eddy diffusion, and so predict that plate height is concave downwards at low flow velocities and linearly increases at higher velocities. Experimental results are in qualitative agreement,[38] but polydispersity effects and the fact that the theories have not yet included concentration effects discourages their use in practical interpretation. Because of the permeation contribution to peak spreading, it is evident that theoretical development in this area is linked to improved understanding of the mechanism of separation in GPC.

2.3.2 Methods of Chromatogram Interpretation Correcting for Imperfect Resolution

The underdeveloped state of theories on the mechanism of GPC resolution has led to the use of empirical methods of resolution correction in GPC practice. Because of the high polydispersity of the samples usually examined, this has involved development of computer techniques for correct-

ing the data. Most methods[39-47] have assumed that the GPC calibration curve adequately accounts for species retention times and have concentrated on correcting the raw GPC chromatogram for curve spreading by axial dispersion. The calibration curve is applied to the corrected chromatogram in order to obtain the molecular weight distribution. These methods all basically follow the approach of Tung.[39-42]

Tung[39] stated that the observed raw chromatogram could be considered as the summation of a series of individual, overlapping, unseen curves (one for each molecular weight present). This is the basis for the Tung Integral Dispersion Equation. (Equation (II-12)).

$$F(v) = \int_{-\infty}^{\infty} W(y)G(v,y)dy \qquad (II-12)$$

where $F(v)$ is the function giving the observed chromatogram heights,

$W(y)$ is the function giving the heights of the chromatogram after correction for axial dispersion,

$G(v,y)$ is the "shape function" the function giving the heights of each normalized monodisperse chromatogram present in the overall chromatogram $F(v)$.

The problem is to solve this equation for the corrected heights $W(y)$. The shape function is unknown and very difficult to determine, since it is likely a function of both molecular weight and concentration in the polydisperse sample. If it is assumed that the variation with molecular weight factors is negligible, then Equation (II-12) can be written:

$$F(v) = \int_{-\infty}^{\infty} W(y)G(v-y)dy \qquad (II-13)$$

In addition, if the assumption is made that the shape function is Gaussian (symmetrical axial dispersion) then

$$G(v-y) = \sqrt{\frac{h}{\pi}} \exp\ (-h(v-y)^2) \qquad (II-14)$$

where $h = \frac{1}{2 \times (\text{variance of a truly monodisperse sample})}$

Both of the above mentioned assumptions are generally made in methods of correcting for imperfect resolution.

In an evaluation by Duerksen[6] of four methods[39,43-45] of solving the equation for W(y), all were shown to often give artificial oscillations in the corrected chromatogram heights which made the modality of the resulting molecular weight distribution uncertain. Also molecular weight averages often did not agree with values obtained by absolute methods even when no oscillations were present. These deficiencies were particularly evident at molecular weights greater than 50,000 and in the best of the four methods (Tung's Polynomial Method)[39] were attributed to inadequacy of the assumed Gaussian shape, although the reason was not certain. Furthermore, of the two evaluated methods for obtaining the resolution factor h[41] (namely a reverse flow technique and a once through technique assuming monodispersity) neither was satisfactory.

As already mentioned, an alternative to correcting for imperfect resolution by interpreting curve spreading is to change the actual retention time to an effective value by altering the calibration curve. The only published attempt to do this previous to this study was that of May et.al.[48] In a kinetic study, they obtained reasonable results using this procedure.

Within the last three years, several new methods of solving the Tung Axial Dispersion Equation for W(y) have been developed.[49-52] Two of these have been by Tung[52] (an 8 Term Polynomial Method and a Fourier Transform Method). He generally encourages use of only a Gaussian Shape Function. Provder and Rosen[51] have used singular value decomposition to solve the equation without numerical instabilities with some success. They[13] also evaluated Tung's Fourier Transform Method and found it difficult to apply to experimental chromatograms because of numerical instabilities. Smit et.al.[49] developed an iterative method of solving Tung's Equation with a variable h factor, but they admit some problems with numerical instabilities.

Ishige, Lee and Hamielec[53] published three iterative solution methods. The second of these is very general (any shape function can be used and the function can vary with retention volume) and is simple to program.

Recently, the Chang et.al.[47] smoothing routine was added to the latter methods to reduce the possibility of numerical oscillations due to height inaccuracy. May[54] used a calibration curve change combined with the Method of Smith for resolution correction and the Chang et.al.[47] smoothing routine. He notes that smoothing is necessary to eliminate oscillations, but it may destroy essential chromatogram details. He concludes that simple comparison of chromatograms, run consecutively on the same set of operating conditions, is often the most desirable route, although he dismisses the possibility of comparing chromatograms from different GPC operating conditions.

Unfortunately, all of the above mentioned correction methods retain the old common deficiency of at least occasional oscillations in the resulting solution as well as an uncertainty as to the validity of the solution. The reasons for this situation are: the sensitivity of the solution to experimental error (this is similar to the problems involved in attempting to numerically invert a Laplace Transform), poor polynomial fits and, inability of the assumed shape function to describe the real shape of the chromatogram of a truly monodisperse sample. The last mentioned factor is the remaining source of greatest difficulty for these methods because the real shape and its variation with retention volume is unknown.

It may be possible to improve experimental resolution to such a degree that the desirable peak separation overcomes the undesirable peak spreading. Screaton[30] matched Mn and Mw of polydisperse standards by adding columns and reducing carrier solvent flow rate. Operation of the GPC in a recycle mode is currently being examined.[55]

Lack of well characterized polymer standards (standards of accurately known molecular weight distribution) is the source of the problem of accounting for GPC imperfect resolution. At present, without better standards the shape function for resolution correction cannot be obtained with any certainty and even the degree of experimental resolution available cannot be accurately ascertained. However, molecular weight distributions by other methods (e.g. fractionation or ultracentrifuge) are likely not accurate enough for the purpose even if they were available.

Because of this situation, the problem of resolution correction is ignored by most GPC users. Direct comparison of chromatograms is common, but difficulties ensue when operating conditions must be changed. Use of

high carrier solvent flow rates (low analysis times) is therefore not widespread, despite the fact that the cost in resolution is low, because chromatogram shapes would change. Additional GPC's are purchased instead. Polymerization kinetic studies which employed GPC for quantitative information are few (ref. Section 2.4).

2.3.3 Influential Variables

Because of the state of understanding of chromatogram spreading in GPC, knowledge of the influence of the various factors on imperfect resolution is based mainly on previous experience with older types of chromatography. It is thus expected that resolution should be increased by higher residence times and longer column path length.[8] Also, factors which are known to affect the GPC calibration curve, such as concentration of injected sample, likely have even more effect on chromatogram spreading because the shape of the monodisperse sample chromatogram can vary considerably while at the same time its peak position is almost unaffected.

2.4 The Use of GPC in Polymerization Kinetic Studies

Polymerization kinetic models contain one or more unknown parameters that can be evaluated by fitting the experimental data available. May[56] fitted the actual molecular weight distribution obtained by GPC by assuming infinite resolution and using a graphical method. Duerksen[6] and Hui[5] derived rate parameters from the molecular weight averages obtained from chromatograms corrected for axial dispersion using Tung's Hermite Polynomial Method. The problem of imperfect resolution and its mainly unknown effects on interpretation caused difficulties in both of these approaches.

3. Phase I -- Evaluation of GPC Data Interpretation Methods and Development of a New Method

3.1 Experimental

To study GPC chromatograms over a range of conditions, polystyrene standards and polystyrene samples produced by free radical polymerization ranging as high as one million in molecular weight were analyzed with three different column combinations and five different flow rates as described in Table II-1. The data used for column codes 8,5 and 12 as well as the reverse flow results have been previously obtained for other studies by Duerksen and Hamielec.[6] The polystyrene standards used have been summarized by Duerksen.[6]

The GPC was the standard Waters Model 100. The solvent was tetrahydrofuran (THF) and the operating temperature was 24 ± 2°C. One ml. of solution was contained in the injection sample loop. For column codes 5,8 and 12 the concentration was 0.1%. For the other codes the concentration was generally 0.05%. The lower concentrations were made possible by the installation of the Waters R-4 conversion kit. The Waters digital translator was also installed. At flow rates above 2 ml/min reading of the chromatograms was accomplished with the aid of a combined linear and quadratic interpolation program since the minimum time increment for height read out on the digital translator was once every 20 seconds.

The maximum pressure obtained was 600 psi with code 15. No compression of the crosslinked polystyrene gel was evident, either in successive chromatograms obtained or in any deviation of pressure variation with increasing flow rate. No leaks in the system resulted from the high pressure.

3.2 Results and Discussion

3.2.1 Reproducibility

It has already been shown by Duerksen[6] and others that GPC data is highly reproducible (< 5%) for polystyrene, at least for Mn, Mw, and peak retention volume and for flow rates up to 3 ml per minute. Since in this Phase I study, only polystyrene was examined and the emphasis was on a wide range of operating conditions, tests of reproducibility consisted of duplicates or triplicates throughout the study. Examination of Table II-2 as well as the tables and figures in the publication[16] shows that accuracy of the above chromatogram characteristics, even at extreme conditions of operation, are better than 10% in reproducibility.

3.2.2 Molecular Weight Calibration

Since monodisperse standards were available for polystyrene, the only polymer used in this phase, only conventional calibration was carried out. A typical calibration curve is shown in Figure II-1 (the others are in[16]). The curves were considered linear over the range of interest. The change in retention volume per count with flow rate[16] has been taken into account.

3.2.3 Resolution Correction

As expected, because of axial dispersion, molecular weight averages calculated from the GPC chromatogram assuming perfect resolution did not agree with the averages known for the samples through other methods (e.g. light scattering). Resolution correction was necessary.

3.2.3.1 The Method of Pierce and Armonas[46]

This method is based on a Fourier Transform solution of Tung's Integral Dispersion Equation for the corrected chromatogram W(y). It attempts to solve the equation for W(y) using the given experimental chromatogram (F(v)) and a Gaussian function for G(v-y). The two problems of determining the unknown h factors and implementing the method without oscillations in the solution are thus involved. One computer program was developed to implement the method and two others to calculate h in the integral equation by using the known molecular weight averages of standards along with the F(v). In the latter cases, a resolution factor h or coefficients in a polynomial expressing h as a function of retention volume are guessed by a computer optimization method, the W(y) is calculated using the Method of Pierce and Armonas, the molecular weight averages are calculated from the moments of this corrected chromatogram and their deviation from the known true averages is used to guide the optimization program in its next guess. The process is continued until the molecular weight averages are matched.

This evaluation showed that none of these ways of using the Method of Pierce and Armonas were practical because artificial oscillations very easily resulted in the W(y) obtained due primarily to numerical instability.

However, an important result of this evaluation was that a definite trend in the change of molecular weight averages with such symmetrical (Gaussian) axial dispersion became evident. The results of successful solutions of the Tung Equation are shown in Figure II-2. The symmetry of this plot was observed to also be present in some similar data of Duerksen. This rapidly led to a new method of resolution correction, later called by Provder and Rosen "The Method of Molecular Weight Averages".

3.2.3.2 The Method of Molecular Weight Averages

3.2.3.2.1 The Molecular Weight Averages Corrected for Axial Dispersion

Correct molecular weight averages from GPC are desired for two main reasons: (1) Averages are obtainable from many other instruments and have been used as a basis for correlation of many polymer properties. (2) The Method of Moments applied to kinetic mechanisms is an extremely powerful technique. It avoids the use of the pseudo stationary state assumption and provides expressions for the molecular weight averages which contain unknown model parameters. Thus, if experimental molecular weight averages are known, the parameters can be evaluated.

The change of GPC molecular weight averages, upon symmetrical axial dispersion correction, suggested the following two equations for this type of correction:

for Mn

$$\frac{Mn(h)}{Mn(\infty)} = 1 + \frac{A}{h} \qquad (II\text{-}15)$$

where Mn(h) is the Mn calculated from F(v) after correction for symmetrical axial dispersion

Mn(∞) is the Mn calculated from F(v) before any correction

A is an empirical constant

For Mw

$$\frac{Mw(h)}{Mw(\infty)} = 1 - \frac{A}{h} \qquad (II\text{-}16)$$

In fact a value of A = .07 was found to enable a fit of the data in Figure II-2.

An analytical solution by Hamielec and Ray[57] using the Bilateral Laplace Transformation then followed. Since it provided an analytical basis for the whole method, the solution is briefly outlined below.

The solution contains two main assumptions:

(1) The calibration is linear (i.e. of the form)

$$M(v) = D_1 \exp(-D_2 * v) \tag{II-17}$$

where M(v) is molecular weight, D_1 and D_2 are empirical constants.

(2) The shape function, G(v), is unchanged over the elution range of the sample chromatogram.

With these assumptions the Tung Integral Dispersion Equation can be considered as the convolution integral of the Bilateral Laplace Transform.

The transform is defined by:

$$L(s) = \int_{-\infty}^{\infty} L(v) e^{-sv} dv \tag{II-18}$$

Application of this transform to Equation (II-13) yields:

$$F(s) = W(s)\ G(s) \tag{II-19}$$

If both sides of the equation are multiplied by D_1 and s is considered as a function of D_2, then the resulting transforms of F(v) and W(y) are one of the moments Q_k used in calculating a molecular weight average. That is, D_1 F(s) is an uncorrected moment and D_1 W(s) is a moment corrected for axial dispersion when the shape G(v-y) is assumed.

If G(v-y) is assumed Gaussian the solution for the kth molecular weight average is

$$\frac{M_k(h)}{M_k(\infty)} = \exp\left\{ (3-2k) \frac{D_2^2}{4h} \right\}_{k=1,2\ldots} \tag{II-20}$$

For Mn, k=1 and

$$\frac{Mn(h)}{Mn(\infty)} = \exp\left\{\frac{D_2^2}{4h}\right\} \qquad (II\text{-}21)$$

$$\simeq 1 + \frac{D_2^2}{4h} \text{ by Taylor Series Expansion}$$

For Mw, K=2 and

$$\frac{Mw(h)}{Mw(\infty)} = \exp\left\{\frac{-D_2^2}{4h}\right\} \qquad (II\text{-}22)$$

$$\simeq 1 - \frac{D_2^2}{4h} \text{ by Taylor Series Expansion}$$

Thus the empirically derived relations (Equations (II-15, II-16)) were explained. Furthermore, it was then evident that symmetrical axial dispersion correction would never be sufficient to correct the experimentally obtained GPC molecular weight averages since some of the Mw values were already too low and such correction would lower them still further. This problem was overcome by introducing an empirical skewing factor (SK).

By addition of Equations (II-21) and (II-22):

$$\frac{Mn(h)}{Mn(\infty)} + \frac{Mw(h)}{Mw(\infty)} = \exp\ (D_2^2/4h) + \exp\ (-D_2^2/4h) \simeq 2 \qquad (II\text{-}23)$$

The skewing factor was defined by

$$SK = \frac{Mn(t)}{Mn(\infty)} + \frac{Mw(t)}{Mw(\infty)} - (\exp(D_2^2/4h) + \exp\ (-D_2^2/4h)) \qquad (II\text{-}24)$$

The purpose of this factor was to provide a correction to the molecular weight averages in addition to that provided by symmetrical axial dispersion correction. From its definition, if symmetrical axial dispersion correction was sufficient then SK would be zero.

By assuming that any non-symmetrical axial dispersion could be accounted for once the symmetrical correction had been applied through a shift of the calibration curve (i.e. a change of D_1), then the skewing correction to Mn and to Mw would be by the same factor.

Thus, the full correction equations are:

$$Mn(t) = Mn(\infty)(1 + \tfrac{1}{2}\,SK)\,\exp\,(D_2^2/4h) \qquad (II\text{-}25)$$

$$Mw(t) = Mw(\infty)(1 + \tfrac{1}{2}\,SK)\,\exp\,(-D_2^2/4h) \qquad (II\text{-}26)$$

Use of these equations to correct the molecular weight averages for imperfect resolution proceeded in two main steps:

(1) Determining the h and SK versus v plots for GPC Operating Conditions

(a) From injections of broad or narrow standards (preferably broad to avoid errors in polydispersity) calculate Mn(∞) and Mw(∞) using the true calibration curve. Avoid concentration variations between samples wherever possible.

(b) Using the known Mn(t) and Mw(t) employ Equations (II-25,26) to obtain SK and h.

(c) Plot results for both broad and narrow standards together against v . (Typical plots[16] are shown in Figures II-3,4).

(2) Determining the Corrected Molecular Weight Averages for an Unknown

(a) Determine SK and h from v by reading these values on the previously found SK versus v and h versus v plots for the particular GPC operating conditions.

(b) Calculate Mn(t) and Mw(t) from Equations (II-25,26).

3.2.3.2.2 The Molecular Weight Distribution Corrected for Axial Dispersion

Once the averages corrected for imperfect resolution have been obtained, the problem remains of how to obtain the molecular weight distribution corresponding to these averages. This is the same as the problem of generating a distribution given the moments of the distribution--a problem often solved in statistics by assuming some function (a Hermite Polynomial for example) and determining the value of its coefficients via the Method of Moments. However, this approach could certainly give oscillations in the solution when the polynomial fit was inexact.

The method developed[16,17] was to alter the calibration curve and calculate the molecular weight averages from the experimental GPC chromatogram until the known corrected averages were obtained. The whole molecular weight distribution was then calculated with this altered (or "effective") calibration curve by using Equation (II-2). That is, correction for imperfect resolution was obtained for the distribution by correcting the retention times of the molecular weights rather than by correcting the curve spreading contribution to the imperfect resolution. Although initially this was done by using a two variable search to find the required constants C_1 and C_2 in the effective calibration curve

$$V = C_1 + C_2 \log_{10} M(v) \qquad (II\text{-}27)$$

it was found that by using Equation (II-17) and matching the polydispersity rather than the averages, the search was reduced to a single variable search for D_2 and results were identical to the previous.

3.2.3.3 Advantages and Limitations of the Method of Molecular Weight Averages

The two main advantages of the method are: (1) the correction factors h and SK could be calculated directly from the chromatograms of standards (Equations (II-25, 26)). (Previous methods of obtaining h, such as reverse flow procedures, were difficult) and, (2) corrections were simple and direct (no mathematical instabilities could result). Also, using the data of Cantow et al.[58] SK was shown to be a linear function of mg. of polymer injected (Figure II-5). An advantage and the inherent disadvantage of the approach was the empirical nature of SK. No skewed shape of chromatogram was assumed so that presence of any skewness could definitely be indicated by SK but both the effect of the shape and its variation with retention volume on the GPC molecular weight averages were lumped into this one parameter for both broad and narrow chromatograms.

Thus, the main disadvantages of the method are: (1) correlation of correction factors SK and h against v often obtained mostly from narrow standards can be difficult to use for broad unknowns if the variation of the shape function with retention volume (i.e. the variation of the correction factors with v) is significant, (2) the assumption of a linear calibration curve over the range of elution of the sample was often violated for a broad chromatogram (this problem can be avoided by expressing the calibration curve as a Dirchlet Series (the sum of exponentials); the fit can be accomplished for most curves by segmenting the curve and piecewise fitting of the each linear segment in turn along with residuals), (3) the reproducibility of ratios of molecular weight averages, regardless of their source, is only about 10%, (as a result this always results in scatter when SK or h is plotted against v) and (4) the resolution correction on a bimodal distribution by a linear calibration curve search was obviously of limited accuracy.

3.2.3.4 Development of the Method of Molecular Weight Averages in the Literature

Publication of the above mentioned method[16] focussed more attention on the need for unsymmetrical axial dispersion correction, as well as the problem of artificial oscillations in the other methods of GPC interpretation. The desirability of a successful method of resolution correction was emphasized by the fact that the study showed that GPC could be used to obtain molecular weight distributions at extremely low analysis times.

Hui[5] used the method in a kinetic study of styrene polymerization with the Method of Moments. Chan[59,60] used it to determine the unperturbed dimensions of PVC. Both studies were successful, but in both cases the authors desired better reproducibility from the method (as already mentioned, the parameters h and SK involve ratios of molecular weight averages, and hence cannot easily be determined with a reproducibility greater than 10%). Perrault et.al.[61] used the method to demonstrate lack of skewing in a polybutadiene study.

Using the analytical solution, Hamielec[62] developed a specific resolution factor which showed the basis of Bly's[9] empirical factor. He also showed that if skewing was negligible, recycle could result in perfect resolution.

The method compared very favorably with other methods in a recent evaluation by Duerksen.[63] Smit[49] obtained near perfect Gaussian chromatograms in reverse flow experiments, so he dismissed the presence of skewing in shape factors as unimportant. Tung[52] has shown that the reverse flow chromatogram is symmetrical, although the shape function may be skewed, but he and others maintained that assumption of a symmetrical shape function

was the most practical course. Tung admits the presence of skewing at high flow rates or high molecular weights, but states that the monodisperse chromatograms cannot yield information on skewing because they have a true low molecular weight tail. It should be noted that the skewing factor includes the true Mn in its definition. If this Mn value is valid (e.g. if vapor phase osmometry is used for low molecular weights which would permeate the membrane of a membrane osmometer) then this factor includes only the axial dispersion skewing and is unaffected by the presence of a true low molecular weight tail.

The method provided a very rapid way of evaluating h from the known molecular weight averages of standards. Tung[52] criticized the method for its assumption of a linear calibration curve and proposed another method of evaluating h by fitting the front half of a monodisperse standard (to avoid the skewing problem). A linear calibration curve is often used in the literature.[9]

Provder and Rosen[64] introduced the "General Normalized Statistical Shape Function" (the Gram Charlier or Edgeworth Series) and baptized the method. The "General Shape Function" is given by:

$$G(v-y) = \phi(v-y) + \sum_{n=3}^{\infty} (-1)^n \frac{A_n}{n!} \frac{\partial \phi^n (v-y)}{\partial (v-y)} \frac{}{(\sqrt{2h})^n} \qquad (11\text{-}28)$$

$\phi(v-y)$ is the Gaussian Shape Function (Equation (11-14))

$$A_3 = \frac{\mu_3}{\mu_2^{3/2}}$$

$$A_4 = \left(\frac{\mu_4}{\mu_2^2} - 3\right)$$

where μ_i are the ith order moments about the mean elution volume

$$\mu_2 = \frac{1}{2h}$$

When used for G(v-y) in Equation (II-13) the resulting G(s) yields correction factors in addition to h which permitted skewed shapes to be included. In fact, they showed that under certain limiting conditions their equations could reduce to the original h-SK equations (Equations (II-25, 26).

Novikov et.al.[65] showed ways of avoiding both the assumption of a constant shape function and that of a linear calibration curve, but without any attempt at evaluation. Provder and Rosen[13] also expanded the calibration curve search part of the method by introducing the universal calibration curve instead of the conventional calibration curve and later the nonlinear calibration curve equation of Yau and Malone[12] instead of the linear form (Equation (II-17)) originally used. Hamielec[66] showed that the linear calibration curve search could be proven correct when the experimental chromatogram is Gaussian (i.e. a Gaussian F(v)). He[62] corrected errors in the equations of the initial publication of Provder and Rosen and made the important point that truncation of the series prematurely could result in physically impossible corrections to the molecular weight averages. Provder et.al.[67] replied but confused Hamielec's reference to a truly monodisperse standard with reference to available (not truly) monodisperse standards. They defended the General Shape Function by offering guidelines[68] to its truncation, but concluded that it was ineffective in one main advantage over SK, its ability to supply corrections to higher molecular weight averages (e.g. M_z, M_{z+1}, etc.).

4. Phase II--Using GPC in Polymerization Kinetic Studies

4.1 General

The objective of this second phase of the work was to use GPC to analyze polymethyl methacrylate (PMMA) samples produced in the kinetic study described in Part I of this thesis. Analyzing of these samples was an order of magnitude more difficult than the analysis of polystyrene standards carried out in Phase I, and is one of the main reasons why so little success had been previously published in the literature regarding modeling the polymerization to complete conversion.[27] It is interesting to note that the polymer (plexiglas) has been produced industrially since the 1920's. No monodisperse standards are available for PMMA. Broad, possibly multimodal chromatograms of very high molecular weight were expected in the kinetic study. The polymer has been successfully used in GPC before, but quantitatively for only low conversion and low molecular weight samples.[27,56] High conversion PMMA has only been qualitatively examined.[56] Yamada et.al.[69] mentioned possible negative adsorption for PMMA in the packings that he used. Variations is stereoregularity might cause significant variations in dilute solution properties.

4.2 Experimental

The same instrument as in Phase I was used, a Waters Model 100 GPC. However, because chromatograms were broad and sometimes had low height tails, modifications to operation were made to minimize baseline drift. The refractometer was heavily insulated and a proportional controller maintained the temperature to better than $\pm$ 0.01^{o}C. The temperature of the small air conditioned room containing the instrument was controlled to about

$\pm$ .5°C by using five 100 Watt lights as heaters connected to a thermistor probe and an on-off controller.

Experimentally, high resolution (reducing dependence on mathematical resolution correction methods) was emphasized by using up to nine columns in series (Table II-3 shows the column codes used). Flow rate was maintained at 2.40 ml per minute and automatically checked via the elution counts in the computer program which processed the digital translator output. Several columns were repacked with porous glass instead of styragel because high angstrom styragel proved too fragile. (Table II-3 lists column combinations used). Polyvinyl chloride and polybutadiene as well as two polydisperse PMMA standards were injected for calibration purposes along with polystyrene. (Table II-4 lists specifications on standards). Preparation and injection of samples was more carefully carried out than previously. To a weighed quantity of polymer was added the correct amount of THF by burette, the sample stood overnight to dissolve and the whole sample loop (2cc) was injected. Concentrations injected varied from .1 to .3 wt. percent and are shown in Tables II-5 to 8. As before, variation of retention volume per count was accounted for in interpretation, and in addition, an anti-evaporation device (a tube connected to a bottle saturated with THF vapor) was attached to the siphon top.[70] Heights were corrected by interpolation for voltage superposition in the digital translator.[71]

A reproducibility study on a high molecular weight PMMA sample was done by injecting the same sample six times into the instrument using one column combination (Table I-2(2) and Figure II-6). Many duplicates or replicates were made throughout analysis of the kinetic samples (Table I-2, I-11 to 17, II-5 to 8).

GPC sample numbers were allocated for identification purposes only and do not indicate chronological order of injection. Replicates were adequately randomized.

4.3 Results and Discussion

4.3.1 Reproducibility

The reproducibility of molecular weight averages, even the z+1 average, was less than ± 5% as long as most chromatogram heights were reasonably high (Table I-2). Reproducibility of central heights was excellent but of tail heights was poor. These results are shown in Table I-2 and Figures I-13 and II-6 and also from the results of duplicates and replicates over all conditions (Table II-11 to 14, I-11 to 17).

From Tables II-5 to 8 peak retention volume (PRV) was very reproducible but was affected by concentration at very high molecular weights.

4.3.2 Molecular Weight Calibration

Calibration for PMMA was carried out in two different ways for all three column combination codes--Universal Calibration and, use of a polydisperse sample of PMMA of known cumulative molecular weight distribution.

The conventional calibration curves for the monodisperse standards available are shown in Tables II-5 to 8 and Figures II-7 and 8. Using the Mark Houwink constants listed in Table II-9, a typical universal calibration curve obtained is shown in Figure II-9. (Note that the polybutadiene monodisperse standards could not be used for universal calibration because the Mark Houwink constants in THF were not available). The equations used to fit the Universal Calibration Curves are shown in Table II-10. (They are the result of a least squares fit on the data of the same concentration

as the majority of the unknowns injected with one fictitious point added in each case at extremely high molecular weight to insure a reasonable extrapolation of the calibration beyond the range of the highest standard). Conventional calibration curves for PMMA (and for other types of polymers as well) were then obtained by using the constants listed in Table II-9 along with the equations of II-10. The conventional calibration curves obtained for PMMA are shown in Figure II-10 to 12.

The calibration curves obtained by using the polydisperse PMMA standard are also shown in Figures II-10 to 12.

Disparities between the results of the two methods are small and can be attributed to concentration effects, imperfect resolution (in the case of the polydisperse sample method, it is notable that little effect is noted), the error in the tail chromatogram heights of the polydisperse sample and the fact that the high molecular weight standards and the PVC standards were far from being monodisperse.

4.3.3 Accounting for Imperfect Resolution

4.3.3.1 Evaluation of Existing Methods

Methods of solving Tung's equation for W(y) required a shape function G(v,y) and a known variation of the shape function parameters with retention volume (established by injecting a series of polymer standards). Although there was some indication that the shape function could be considered universal (i.e. could be established for PMMA by injection of polystyrene standards), the fact that these mathematical methods regularly produced oscillations in W(y), combined with the observed bimodality of the broad high conversion PMMA chromatograms, definitely discouraged their use.

The use of the Method of Molecular Weight Averages was another possibility. However, the PMMA calibration curves were all nonlinear, the chromatograms were broad and sometimes bimodal and only two (polydisperse) standards were available. The above factors effectively prevented the use of the method. However, the method indicated that a plot of the ratio of the corrected to uncorrected molecular weight averages versus v might provide a correlation for the correction of the molecular weight averages obtained from the PMMA chromatograms assuming perfect resolution. Instead of plotting the ratios against v, a plot against Mn(t) and Mw(t) was made for polystyrene for each respective ratio (Figures II-13, 14) to enable comparison of the resolution of the four new column combinations (codes 25 to 28). These figures show several main results: (1) the resolution of all column sets is nearly identical (this is likely because the extra resolution gained by codes 26, 27 and 28 over 25 is at the low molecular weight end and the increased resolution is hidden by impurity peak interference in calculation of $Mn(\infty)$ and $Mw(\infty)$, (2) the ratios required for correction of $Mn(\infty)$ and $Mw(\infty)$ of PMMA and PVC are not the same as for polystyrene, (3) concentration affects resolution only at the high molecular weight end and (4) operating the GPC with large porosity columns last may be advantageous for high molecular weight resolution.

4.3.3.2 Development of New Methods

4.3.3.2.1 Preliminary Investigation

Because of the inadequacy of all existing methods of resolution correction for the PMMA samples, it was decided to develop new methods using the knowledge of the polymerization kinetic mechanism as a substitute for the lack of well characterized PMMA standards.

The first attempt was to use the Tung Equation as a foundation for the method. W(y) was derived directly from $W(r)_{CUM}$ calculated by the polymerization kinetic model, and at low conversions contained only one unknown parameter. G(v,y) was taken to be the General Shape Function and could contain any number of unknown parameters. The problem then became that of determining the unknown parameters in W(y) and G(v,y) required in the Tung Equation in order to obtain the observed F(v).

It was almost immediately observed that the General Shape Function was too unreliable for use. If the terms chosen included the first four moments (of the chromatogram of a truly monodisperse sample) the positive definite unimodal region of the shapes obtained have been derived,[68] but as found before (Section 3.2.3.4), were too limited for experimental GPC chromatograms. Use of more terms of the series lead both to more unknown parameters in the search and to rather complex shapes for single species. Use of fewer terms in the series drastically restricts the shapes obtainable in the positive definite region. The statistical literature[72] showed that the SU system was likely the best choice of function, although Pearson Curves also look promising. However, two other factors also became apparent: (1) the computer time required to accomplish the solution was long (mainly for the integration of the Tung Equation) and (2) chromatogram heights were not very sensitive to the shape function. Thus the possibility of multi solutions to the problem as posed was prevalent. However, the stability of chromatogram heights to axial dispersion correction became the key to the problem.

In development of the Method of Molecular Weight Averages it was shown that, within the assumptions of the method, the averages were affected by imperfect resolution independent of polydispersity (i.e. breadth) of the chromatogram. To accomplish the same change in molecular weight averages with a given shape function, the heights of a narrow experimental chromatogram would generally require a much greater correction than the heights of a broad chromatogram because the averages are integrals over the whole chromatogram.

To demonstrate the degree of change to be expected in the PMMA chromatograms two exercises were carried out: (1) PMMA chromatograms from different column combinations were translated to the same scale through use of the calibration curves and plotted in Figure II-15, and (2) Method 2[53] with Chang et.al.[47] smoothing routine was applied to PMMA chromatograms using a Gaussian Shape Function with various h values and the results plotted in Figure II-16. The results indicated that, as expected from literature chromatograms, the side heights near the inflection point of the broad chromatograms were little affected by axial dispersion. Tail heights and molecular weight averages were the most affected. These observations led to two new and practical methods of GPC interpretation: The Method of Chromatogram Heights and The Method of Differential Chromatograms.

4.3.3.2.2 The Method of Chromatogram Heights

This method proceeds as follows:

(1) The equation for the distribution of chain lengths ($W(r)_{CUM}$ versus r) is derived from the kinetic model. There are a variety of ways of accomplishing this depending on the model and the assumptions

employed. The equation expresses $W(r)_{CUM}$ as a function of unknown model parameters (e.g. rate constants) and known experimental values (e.g. conversion).

(2) Values of the unknown parameters are guessed by an optimization routine and $W(r)_{CUM}$ is calculated at r values corresponding to any desired number of retention volumes.

(3) Using Equation (II-2), the GPC chromatogram height ($F_N(v)_{MODEL}$, ref. Table I-29) at each retention volume is calculated from the $W(r)_{CUM}$ and the GPC calibration curve.

(4) The experimental chromatogram heights and those calculated in (3) are compared in an "objective function".

(5) Steps (2) through (4) are repeated until the experimental heights are matched.

The questions pertaining to how many heights to choose and how to phrase the objective function are discussed in Appendix I-C. One or more chromatograms can be used at each iteration depending on the complexity of the model.

4.3.3.2.3 The Method of Differential Chromatograms

This method is similar to that described in Section 4.3.3.2.2 except that a differential chromatogram ($\Delta F_N(v)$, ref. Table I-29) rather than the directly observed chromatogram is used. A differential chromatogram is defined as the chromatogram which characterizes the polymer produced during any small time (or conversion) increment in a polymer reaction. It is calculated from two experimental chromatograms observed at neighboring conversions. If chromatogram $F_1(v)$ is observed at conversion X_1 and chromatogram

$F_2(v)$ at conversion X_2 then the differential chromatogram is:

$$\Delta F_N(v) = \frac{\Delta F(v)}{(X_2-X_1)} = \left(\frac{X_2 F_2(v)}{\int_{-\infty}^{\infty} F_2(v)dv} - \frac{X_1 F_1(v)}{\int_{-\infty}^{\infty} F_1(v)dv}\right) \frac{1}{(X_2-X_1)} \quad (II-29)$$

The width of the time (or conversion) increment cannot be too small or inaccuracy in height determination will invalidate the result. If the increment is too large the values found will not be a reasonable approximation of the instantaneous distribution. A check on this is obtained by graphing $\Delta F_N(v)$ and by numerical integration of the areas under the various chromatograms.

The method proved extremely useful in giving a good first approximation to the change of rate constants with conversion. The differential chromatograms ($\Delta F_N(v)$, Table I-29) and the chromatograms from which they were calculated ($F_c(v)$ for example) provided a graphic insight into the polymerization mechanism (refer to Part I of this thesis).

5. Summary

The current state of GPC interpretation was reviewed. Methods of interpretation were evaluated and three new and useful methods were developed. The Method of Molecular Weight Averages aims at obtaining molecular weight averages from a GPC chromatogram which corresponds to those obtained from absolute instruments. The Method of Chromatogram Heights and the Method of Differential Chromatograms aim at analysis of broad chromatograms--a common problem in industry. These developments have also considerably clarified the effect of imperfect resolution in GPC interpretation as well as providing direct solutions to the problem. The GPC was successfully

run at conditions of poor resolution (short column path lengths) and very good resolution (long column path lengths). Polystyrene, polyvinyl chloride, polybutadiene and polymethyl methacrylate standards were analyzed on different column packings. Calibration for PMMA by two different methods which did not require monodisperse PMMA standards was accomplished. Experimental techniques were developed which permitted highly reproducible results even at very high molecular weights. The reproducibility and accuracy of chromatogram heights was shown to be an important fundamental property of GPC analysis.

6. Conclusions

(1) The three new methods of GPC interpretation proposed are evaluated and proven practical. Further development and refinement of these methods is expected and has already begun in the literature.

(2) The GPC is capable of providing molecular weight distribution information at extremely low analysis times (this too has now been further undertaken in the literature).

(3) Methods of GPC interpretation should be applied to real experimental chromatograms in evaluations. Any artificial oscillations resulting from such methods severely limits their practicality.

(4) The GPC can be reliably used for PMMA in THF carrier solvent with columns of either styragel, Corning glass or Bioglas (unsilanized).

7. Recommendations

The main recommendations here originate from the idea that knowledge of polymerization mechanism for the polymer standard used should help to elucidate the imperfect resolution in GPC by providing detailed molecular weight distribution information on the standard.

(1) Calibration without monodisperse standards can be carried out in a manner analogous to that proposed by Weiss but using an expression for the molecular weight distribution based on a knowledge of low conversion kinetics of the standard rather than the Schulz-Zimm type distribution.

(2) Determination of the shape function G(v,y) characteristic of GPC axial dispersion can be obtained by using the $W(r)_{CUM}$ known from the polymerization mechanism combined with a realistic shape function (e.g. the SU curve) containing unknown parameters, in the Tung Equation to match infinite resolution molecular weight averages by estimating the correct value of these unknown parameters through optimization routines.

(3) The accuracy and reproducibility of chromatogram heights should be stressed in GPC interpretation. Their accuracy may enable elucidation of chain length dependence in polymerization kinetics if this should be important. Their reproducibility may enable elucidation of the shape function via their interdependence.

8. Nomenclature

a	Mark Houwink constant (Eqn. II-8)
A	empirical constant (Eqn. II-15)
A_n	constants in General Shape Function (Eqn. II-28)
B_1, B_2, B_3, B_4	coefficients of polynomial fit to Universal Calibration Curve (Eqn. II-9)
C_1, C_2	constants in linear calibration curve (Eqn. II-27)
CMWD	MWD cumulative with respect to M
D_1, D_2	constants in linear calibration curve (Eqn. II-17)
D_r	radial diffusion coefficient
DMWD	MWD differential with respect to M
F(s)	Bilateral Laplace Transform of F(v)
F(v)	GPC chromatogram
$F_c(v)$	cumulative GPC chromatogram
$F_N(v)$	normalized GPC chromatogram
G(v,y)	shape function
G(s)	bilateral Laplace Transform of shape function
H	height equivalent to a theoretical plate

h	resolution factor Eqn. (II-14)
K'	proportionality constant in Eqn. (II-7)
K	Mark Houwink constant
k	GPC detector proportionality constant
L	column length
L(s)	bilateral Laplace Transform of L(v)
L(v)	some function of v
M	molecular weight of a truly monodisperse sample
M_{RMS}	root mean square average molecular weight
M_o	monomer molecular weight (g/mole)
M(v)	molecular weight as a function of retention volume
M_k	the k'th molecular weight average (M_1 = Mn, M_2 = Mw, etc.)
$M_k(t)$	true molecular weight average
$M_k(\infty)$	GPC molecular weight average calculated assuming infinite resolution
$M_k(h)$	GPC molecular weight average after correction for symmetrical axial dispersion has been applied
MWD	molecular weight distribution

N_o	Avogadro's Number $(g\ mole)^{-1}$
P_r	concentration of polymer molecules of chain length r (moles/ℓ)
PRV	peak retention volume (counts)
PS	polystyrene
PBD	polybutadiene
PVC	polyvinylchloride
PMMA	poly methylmethacrylate
Q_k	kth moment of P_r versus r
R_s	resolution index
r	chain length
s	Laplace Transform parameter
SK	skewing factor
v or y	retention volume (or peak retention volume of a monodisperse standard) (counts) (note: 1 count $\approx$ 5 ml)
V	(effective) hydrodynamic volume
V'	hydrodynamic volume
V_1, V_2	peak retention volumes of adjoining monodisperse standards

W, W_1, W_2	width of base of the chromatogram of monodisperse standard
W_c	weight fraction in a CMWD
$W(M)_{CUM}dM$, $W_N(M)_{CUM}dM$	weight fraction in a DMWD
$W(\log M)_{CUM}d\log M$, $W_N(\log M)_{CUM}d\log M$	weight fraction in a DMWD where logM is plotted as abscissa
$W(r)_{CUM}dr$, $W_N(r)_{CUM}dr$	weight fraction in a DMWD where r is plotted as abscissa
$W(s)$	bilateral Laplace Transform of W(v)
$W(v)$	GPC chromatogram corrected for axial dispersion
$W_N(v)$	normalized W(v)

Greek Symbols

$\Delta F(v)$	differential GPC chromatogram
$\Delta F_N(v)$	normalized differential GPC chromatogram
ε_o	effective volume factor
(η)	intrinsic viscosity (deciliters/g)
μ_i	ith order moments about mean retention volume
$\phi(v-y)$	Gaussian Shape Function

9. References

1. Cooper, A. R., Bruzzone, A. R., Cain, J. R., Barrall II, E. M., J. Appl. Polymer Sci., 15, 571 (1971).

2. Harmon, D. J., Sep. Sci., 5, 403 (1970).

3. Barall II, E. M., Johnson, J. F., Sep. Sci., 5, 415 (1970).

4. Zweig, G., Sherma, J., Anal. Chem., 44, 42R (1972).

5. Hui, A. W. T., "Kinetics of Free Radical Polymerization of Styrene to Complete Conversion", Ph.D. Thesis, McMaster University, Hamilton, Ontario, (1970).

6. Duerksen, J. H., "Free Radical Polymerization of Styrene in Continuous Stirred Tank Reactors", Ph.D. Thesis, McMaster University, Hamilton, Ontario, (1968).

7. Johnson, J. F., Porter, R. S., Cantow, M. J. R., Rev. in Macromol. Chem., 1, (2), 393 (1966).

8. Giddings, J. C., "Dynamics of Chromatography, Part I, Principles and Theory", Marcel Dekker, Inc., New York, (1965).

9. Bly, D. D., J. Polymer Sci., C(21), 13 (1968).

10. Yau, W. W., Malone, C. P., Suchan, H. L., Sep. Sci., 5, 259 (1970).

11. Casassa, E. F., Sept. Sci., 6, (2), 305 (1971).

12. Yau, W. W., J. Polymer Sci., A2 7, 483 (1969).

13. Rosen, E. M., Provder, T., Sep. Sci., 5, (4), 485 (1970).

14. Cantow, J. R., Porter, R. S., Johnson, J. F., J. Polymer Sci., A-1, 5, 1391 (1967).

15. Weiss, A. R., Cohn-Ginsberg, E.,
J. Polymer Sci., A-2, 8, 148 (1970).

16. Balke, S. T., Hamielec, A. E.,
J. Appl. Polymer Sci., 13, 1381 (1969).

17. Balke, S. T., Hamielec, A. E., LeClair, B. P., Pearce, S. L.,
I.&E.C. Prod. Res. & Dev., 8, 54 (1969).

18. Grubisic, Z., Rempp, P., Benoit, H.,
J. Polymer Sci., B5, 753 (1967).

19. Coll, H.,
Sep. Sci., 5, 273 (1970).

20. Coll, H., Gilding, D. K.,
J. Polymer Sci., A-2, 8, 89 (1970).

21. Rudin, A., Hoegy, H. L. W.,
J. Polymer Sci., A-1, 10, 217 (1972).

22. Osterhout, H. W., Ray, L. N.,
J. Polymer Sci., A-2, 5, 569 (1967).

23. Little, J. N., Pauplis, W. J.,
J. Chrom., 55, 211 (1971).

24. Moore, J. C.,
Sep. Sci., 5, 723 (1970).

25. Altgelt, K. H.,
Sep. Sci., 5, 777 (1970).

26. Barall, E. M., Cantow, M. J. R., Johnson, J. F.,
J. Appl. Polymer Sci., 12, 1373 (1968).

27. Berger, K. C., Schulz, G. V.,
Sep. Sci., 6, (2), 297 (1971).

28. Pickett, H. E., Cantow, M. J. R., Johnson, J. F.,
J. Appl. Polymer Sci., 10, 917 (1966).

29. Provder, T., Clark, J. H., Drott, E. E.,
ACS Polymer Preprints, Vol. 12, #2, Sep. 1971.

30. Screaton, R. M.,
Abstracts, 15th Can. High Polymer Forum, Kingston, Ontario, (1969).

31. Little, J. N., Waters, J. L., Bombaugh, K. J.,
Sep. Sci., 5, 765 (1970).

32. Bergmann, J. G., Duffy, L. J., Stevenson, R. B.,
Anal. Chem., 43, 131 (1971).

33. Zinbo, M., Parsons, J. L.,
J. Chrom., 55, 55 (1971).

34. Giddings, J. C., Malik, K. L.,
Anal. Chem. 38, 997 (1966).

35. Billmeyer, F. W., Johnson, G. W., Kelley, R. N.,
J. Chrom., 34, 316 (1968).

36. Billmeyer, F. W., Kelley, R. N.,
J. Chrom., 34, 322 (1968).

37. Billmeyer, F. W., Kelley, R. N.,
Proceedings, 6th International GPC Seminar, Miami Beach, (1968).

38. Kelley, R. N., Billmeyer, Jr., F. W.,
Sep. Sci., 5, (3), 291 (1970).

39. Tung, L. H.,
J. Appl. Polymer Sci., 10, 375 (1966).

40. Tung, L. H.,
J. Appl. Polymer Sci., 10, 1271 (1966).

41. Tung, L. H., Moore, J. C., Knight, G. W.,
J. Appl. Polymer Sci., 10, 1261 (1966).

42. Tung, L. H.,
J. Appl. Polymer Sci., 13, 775 (1969).

43. Hess, M., Kratz, R. F.,
J. Polymer Sci., A-2, 4, 731 (1966).

44. Smith, W. N.,
J. Appl. Polymer Sci., 11, 639 (1967).

45. Pickett, H. E., Cantow, M. J. R., Johnson, J. F.,
J. Polymer Sci.,

46. Pierce, P. E., Armonas,
J. Polymer Sci., C, No. 21, 23 (1968).

47. Chang, K. S., Huang, R. Y. M.,
J. Appl. Polymer Sci., 13, 1459 (1969).

48. May, J. A., Smith, W. B.,
J. Phys. Chem., 72, 216 (1968).

49. Smit, J. A. M., Hooger vorst,
J. Appl. Polymer Sci.,. 15, 1479 (1971).

50. Vladimiroff, T.,
J. Chrom., 55, 175 (1971).

51. Rosen, E. M., Provder, T.,
J. Appl. Polymer Sci., 15, 1687 (1971).

52. Tung, L. H., Runyon, J. R.,
J. Appl. Polymer Sci., 13, 2397 (1969).

53. Ishige, T., Lee, S. I., Hamielec, A. E.,
J. Appl. Polymer. Sci., 15, 1607 (1971).

54. May, Jr., J. A., Knight, G. W.,
J. Chrom., 55, 111 (1971).

55. Bombaugh, K. J., Levangie, R. F.,
Sep. Sci., 5, 751 (1970).

56. May, J. A.,
'Polymer Studies by Gel Permeation Chromatography''
Ph.D. Thesis, Texas Christian University, Fort Worth, Texas, (1968).

57. Hamielec, A. E., Ray, J.,
J. Appl. Polymer Sci., 13, 1319 (1969).

58. Cantow, M. J. R., Porter, R. S., Johnson, J. F.,
J. Polymer Sci., B, 4, 707 (1966).

59. Chan, R. K. S.,
Polymer Eng. & Sci., 11, 187 (1971).

60. Chan, R. K. S.,
Polymer Eng. & Sci., 11, 152 (1971).

61. Perrault, G., Tremblay, M., Lavertu, R., Tremblay, R.,
J. Chrom., 55, 121 (1971).

62. Hamielec, A. E.,
J. Appl. Polymer Sci., 14, 1519 (1970).

63. Duerksen, J. H.,
Sep. Sci., 5, (3), 317 (1970).

64. Provder, T., Rosen, E. M.,
Sep. Sci., 5, (4) 437 (1970).

65. Novikov, D. D., Taganov, N. G., Korovina, G. V., Entilo, S. G., J. Chrom., 53, 117 (1970).

66. Hamielec, A. E., "Interpretation of GPC for Linear Homopolymers", A 2½ Day Continuing Education Course in Chemical Instrumentation, Washington University, St. Louis, Mo., April, 1969.

67. Provder, T., Rosen, E. M., J. Appl. Polymer Sci., 15, 247 (1971).

68. Barton, D. E., Dennis, K. E., Biometriks, 39, 28

69. Yamada, S., Kitahara, S., Hattori, Y., Konakahara, Y., Kobunski Kagaku, 24, 97 (1967).

70. Hudson, Jr., B. B., J. Chrom., 55, 185 (1971).

71. Brussau, R. J., J. Chrom. Sci., 9, 1 (1971).

72. Elderton, W. P., Johnson, N. L., "Systems of Frequency Curves", Cambridge at the University Press, New York (1969).

APPENDIX II-A

Presentation of the Molecular Weight Distribution

The GPC chromatogram is a reflection of a differential molecular weight distribution (DMWD). The many ways of presenting this information will be clarified and reviewed in the following paragraphs. It should be initially mentioned that a normalized curve is one in which each height has been divided by the total area under the curve.

Polymer concentration is a function of both molecular weight (or chain length) and conversion. A distribution, cumulative with respect to molecular weight (a CMWD) is a plot of total weight fraction (W_c) present in the sample up to molecular weight M versus M. If this curve is differentiated with respect to M and the differential dW_c/dM plotted against M a DMWD results.

Since the sample is generally cumulative with respect to conversion, in that it contains polymer of all conversions up to the conversion at which it was taken, the ordinate of the DMWD, dW_c/dM is symbolized by $W(M)_{CUM}$. $W(M)dM_{CUM}$ is then the weight fraction of polymer in the sample between molecular weights M and M + dM. If log(M) is plotted as the abscissa then $W(\log M)_{CUM}d\log M$ must be the weight fraction of the sample between logM and logM + dlogM. Although correct mathematically the distribution appears rather distorted because of the nonlinear abscissa. With a GPC chromatogram, retention volume (v) is the abscissa and an area increment, $F_N(v)dv$, where $F_N(v)$ is the normalized chromatogram height, is directly proportional to $W(M)_{CUM}dM$. If perfect resolution is assumed, or if imperfect resolution

has been accounted for, then $F_N(v)dv$ is replaced by $W_N(v)dv$. W(v) indicates that each retention volume corresponds to a unique molecular hydrodynamic volume (or, for linear homopolymers, a unique molecular weight). The relation between the retention volume and the molecular weight is given by the conventional calibration curve.

As already mentioned, because the total area under the unnormalized chromatogram (corrected or uncorrected for axial dispersion, must be proportional to the weight of the sample injected) then

$$\int_{-\infty}^{\infty} F(v)dv = \int_{-\infty}^{\infty} W(v)dv \qquad (II\text{-}30)$$

In addition

$$kW(v)dv = W(M)dM_{CUM} = W(r)dr_{CUM} = W(\log M)d(\log M)_{CUM} \qquad (II\text{-}31)$$

or

$$W_N(v)dv = W_N(M)dM_{CUM} = W_N(r)dr_{CUM} = W_N(\log M)d(\log M)_{CUM} \qquad (II\text{-}32)$$

where k is a proportionality constant. In general, because of axial dispersion:

$$F(v)dv \neq W(v)dv \qquad (II\text{-}33)$$

Another plot which can be made, although it cannot properly be called a DMWD because it does not obey Equation (II-31) and therefore, distorts the shape of regions of the curve, is a plot of $W_N(r)_{CUM}$ versus log r.

In polymerization kinetics, molecular weight distributions are often presented as plots of P_r versus r where P_r is concentration of polymer (moles per liter) of chain length r. As is seen from Equation (II-3) the moments of this curve were used to define the molecular weight averages.

Each of the above ways of presenting a molecular weight distribution has its advantages and disadvantages. DMWD are more sensitive pictures of the molecular weight distribution than are CMWD and are given more directly by the GPC data. However, comparison with fractionation data (obtained as a CMWD) may require calculation of a CMWD from GPC. Plots of $W_N(M)_{CUM}$ versus M or $W_N(r)_{CUM}$ versus r as well as P(r) versus r hide variations (such as shoulders or even bimodality) evident in the GPC chromatogram. Use of log(M) abscissae are closer to the actual raw chromatogram provided by the GPC but as already pointed out, present distorted views of the distribution.

The course taken in this work was to present mainly $F_N(v)$ versus v plots. The relationship between the molecular weight and the retention volume is then not immediately obvious from the plot but the calibration curves and molecular weight averages have been supplied to help overcome this disadvantage. The main reason for this course is that the chromatogram is the basic raw data obtained. Its accuracy and reproducibility are the subject of much of this thesis. Furthermore, in industry today and in the GPC literature, it is the raw chromatogram which is most readily available and most often examined. This is understandable when the fact that it is the easiest data to obtain is combined with the known disadvantages of presenting the data in other ways.

The equation necessary to convert a chain length distribution ($W_N(r)_{CUM}$ versus r---- the result of a kinetic model perhaps) to a GPC chromatogram is:

$$W_N(v) = W_N(r)_{CUM} \frac{dr}{dv} \qquad (II-34)$$

where $\frac{dr}{dv}$ is obtained from the conventional calibration curve

As pointed out in Section 4.3.3.2.2 if axial dispersion is small, then this is directly comparable to the experimental chromatogram ($F_N(v)$).

However, since the molecular weight averages are integrals, then most often, molecular weight averages calculated from the experimental chromatogram ($F'_N(v)$) cannot be expected to compare well to those of $W_N(r)_{CUM}$. Central averages (Mn, Mv, Mw) or other central distribution characteristics ((η), or F(s) with low values of s) are better in this respect than higher averages (Mz, Mz+1) because the central heights are often less affected by axial dispersion than are the tails.

To translate a chromatogram from that observed on one set of GPC operating conditions (retention volume v') to that observed at another (retention volume v'') proceeds as follows (assuming heights are not significantly affected by axial dispersion - i.e. that $F_N(v) = W_N(v)$)

(1) Calculate r_i corresponding to v_i' from the calibration curve at the first set of GPC operating conditions. $r_i = f(v_i')$

(2) Calculate $W_N(r_i)_{CUM}$ from $F(v_i')$ using the same calibration curve as in (1) in:

$$W_N(r_i)_{CUM} = F_N(v_i') \left.\frac{dv'}{dr}\right]_{v' = v_i'} \qquad (11\text{-}35)$$

(3) Calculate v_i'' corresponding to each r_i in (1) and (2) from the second calibration curve: $v'' = f(r_i)$

(4) Calculate $F_N(v'')$ from $W_N(r)_{CUM}$ using the same calibration curve as in (3)

$$F_N(v_i'') = W_N(r_i)_{CUM} \left.\frac{dr}{dv''}\right]_{v'' = v_i''} \qquad (11\text{-}36)$$

TABLE II-1

DESCRIPTION OF GPC COLUMN COMBINATIONS*-- PHASE I

COLUMN COMBINATION CODE NO.	NO. OF COLUMNS IN SERIES	MAXIMUM RATED POROSITIES, STRAIGHT CHAIN ANGSTROMS					THF FLOW RATE ML/MIN	COMBINATION PLATES/ (ODCB)
		COLUMN 1	COLUMN 2	COLUMN 3	COLUMN 4	COLUMN 5		
8	2	10^5	800	-	-	-	2.0	470
5	3	10^5	10^4	800	-	-	1.0	615
13	3	10^5	10^4	800	-	-	3.0	467
14	3	10^5	10^4	800	-	-	6.0	-
15	3	10^5	10^4	800	-	-	8.4	-
12	5	7×10^6	10^6	10^5	10^4	800	2.0	-
16	5	7×10^6	10^6	10^5	10^4	800	3.0	-

*The GPC operating temperature for all column combinations was $24 \pm 2^{\circ}C$.

TABLE II-2

Mn and Mw - ABSOLUTE AND INFINITE RESOLUTION VALUES

RUN	STD	Mn(t) ±4 ×10	Mw(t) ±4 ×10	P(t)	Mn(∞) ±4 ×10	Mw(∞) ±4 ×10	P(∞)
CODE 8							
08201	108	24.7	26.7	1.08	14.3	21.9	1.53
08202	108	24.7	26.7	1.08	13.7	22.1	1.61
08203	41984	16.4	17.3	1.06	11.0	15.4	1.41
08204	41984	16.4	17.3	1.06	11.2	15.9	1.42
08205	103	11.8	12.5	1.05	9.52	12.6	1.33
08206	103	11.8	12.5	1.05	8.62	12.7	1.49
08207	4A	9.76	9.62	<1.06	7.97	10.7	1.34
08208	7A	5.01	5.05	<1.06	4.55	6.17	1.36
08209	4190039	1.97	1.99	1.01	1.70	2.35	1.38
08210	8A	1.09	1.00	1.06	0.850	1.13	1.33
CODE 5							
05108	3A	39.2	39.4	<1.06	33.3	43.0	1.29
05109	3A	39.2	39.4	<1.06	37.9	53.3	1.41
05110	108	24.7	26.7	1.08	23.8	31.4	1.32
05101	108	24.7	26.7	1.08	19.7	25.0	1.26
05112	103	11.8	12.5	1.05	10.0	12.6	1.26
05102	CST30	3.48	6.14	1.76	3.29	6.49	1.97
05113	7A	5.01	5.05	<1.06	4.80	5.46	1.14
05105	CST29	1.48	3.62	2.45	1.41	3.81	2.72
05115	2A	1.98	1.98	<1.06	1.81	2.10	1.16
05116	4190039	1.97	1.99	1.01	1.79	2.08	1.16
05117	4190039	1.97	1.99	1.01	1.80	2.06	1.15
05107	CST31	1.02	1.46	1.42	0.982	1.52	1.55
05118	8A	1.09	1.00	<1.06	0.953	1.11	1.17
05103	8A	1.09	1.00	<1.06	0.975	1.12	1.15
05114	12A	.207	.220	<1.10	0.269	0.314	1.17
05120	15A	.0927	-	<1.10	0.211	0.252	1.20
CODE 13							
13301	3A	39.2	39.4	<1.06	22.8	34.7	1.53
13305	3A	39.2	39.4	<1.06	30.1	39.1	1.30
13303	4A	9.76	9.62	<1.06	7.96	9.04	1.14
13307	CST30	3.48	6.14	1.76	3.14	5.75	1.83
13302	4190039	1.97	1.99	1.01	1.82	2.11	1.16

TABLE II-2 Cont'd.

CODE 14							
14602	3A	39.2	39.4	<1.06	25.4	38.6	1.52
14604	41984	16.4	17.3	1.06	11.7	15.4	1.31
14611	4A	9.76	9.62	<1.06	7.25	9.34	1.29
14613	4A	9.76	9.62	<1.06	7.20	9.43	1.31
14601	4A	9.76	9.62	<1.06	7.23	9.03	1.25
14605	7A	5.01	5.05	<1.06	4.32	5.18	1.20
14612	CST30	3.48	6.14	1.76	2.95	6.01	2.04
14603	4190039	1.97	1.99	1.01	1.68	2.07	1.23
14616	4190039	1.97	1.99	1.01	1.66	2.05	1.23
CODE 15							
158606	3A	39.2	39.4	<1.06	24.1	38.6	1.61
158610	3A	39.2	39.4	<1.06	25.6	39.2	1.53
15811	108	24.7	26.7	1.08	13.5	22.1	1.64
15814	108	24.7	26.7	1.08	14.1	21.4	1.52
158609	41984	16.4	17.3	1.06	11.4	16.1	1.41
15806	41984	16.4	17.3	1.06	10.3	14.2	1.38
15809	41984	16.4	17.3	1.06	10.8	14.7	1.36
158608	4A	9.76	9.62	<1.06	7.35	9.66	1.31
15822	4A	9.76	9.62	<1.06	8.50	10.1	1.19
15817	CST30	3.48	6.14	1.76	3.32	5.71	1.72
15818	CST30	3.48	6.14	1.76	3.23	5.79	1.80
15819	CST30	3.48	6.14	1.76	3.22	5.82	1.81
158607	4190039	1.97	1.99	1.01	1.77	2.30	1.30
CODE 12							
12201	G35	19.00	57.00	3.00	7.86	42.5	5.40
12202	COOPA	11.60	30.40	2.62	5.00	23.0	4.60
12203	NBS706	13.65	25.78	1.89	10.9	26.0	2.41
CODE 16							
16312	61970	178.	215.	1.20	115.	165.	1.43
16321	14A	161.	170.	1.18	58.3	160.	2.74
16328	41984	16.4	17.3	1.06	13.3	16.1	1.21
16334	7A	5.01	5.05	<1.06	5.14	5.95	1.16
16335	11A	0.52	-	<1.10	0.86	1.00	1.18

TABLE II-3

DESCRIPTION OF GPC COLUMN COMBINATIONS--PHASE II

THE FLOW RATE = 2.40 ML/MIN

COLUMN COMBINATION CODE NO.	NO. OF COLUMNS IN SERIES	COLUMN PACKING DESIGNATIONS*
25	5	S5 X 10^6, S5 X 10^6, S(0.7-5) X 10^6, S10^4, S800
26	7	B2500/1500, C2000/1250, C2000/1250, C700, S10^4, S800
27	7	S800, S10^4, C700, C2000, C2000/1250, C2000/1250, B2500/1500
28	9	S350/100, S350/100, S800, S10^4, C700, C2000, C2000/1250, C2000/1250, B2500/1500

*Columns for each code are listed in the direction of THF flow.

S = Styragel

C = Corning Porous Glass

B = Bioglas

TABLE II-4

POLYMER STANDARDS FOR GPC CALIBRATION

POLYSTYRENE

STD #	NAME	SUPPLIER	Mn(t) $\times 10^{-3}$	METHOD* ±	Mv(t)× $\times 10^{-3}$	±	Mw(t) $\times 10^{-3}$	METHOD+ ±	P(t)
2	15A	Pressure Chem. Co.	1.212	9% VOS	1.220	7%			<1.10
			.927	7% VOS					
			1.06	7% VOS					
			1.13	7% VOS					
			.912	CRYO					
			1.032	CRYO					
3	12A	Pressure Chem. Co.	1.753	VOS					<1.10
			2.07	5% VOS	2.07	5%	2.20	10% KIN	<1.10
4	11A	Pressure Chem. Co.	5.2	5% VOS	4.70				<1.10
			5.2	5% MOS					
5	8A	Pressure Chem. Co.	10.9	5% MOS	10.50	4%	10.00	10% LS	<1.06
7	2B	Pressure Chem. Co.	20.4						
8	4190039	Waters Associates	19.65				19.85		1.01
9	7A	Pressure Chem. Co.	50.1	5% MOS	51.0	3%	50.5	4% LS	≤1.06
10	4A	Pressure Chem. Co.	97.6	5% MOS	98.2	3%	96.2	2% LS	≤1.06
11	S103	H. W. McCormick					127.0	UC	
			118.0				124.7		1.05
			109.0	MOS			117.0	LS	1.07
					128.0		126.0	UC	
13	S41984	Waters Associates	164.0				173.0		1.06

TABLE II-4 Cont'd.

14	NBS705	National Bureau of Stds.	170.9	MOS			179.3	LS	1.05
15	IC	Pressure Chem. Co.	200.				189.8	UC	
16	S108	H. W. McCormick	247.2	MOS			267.	LS	1.08
			236.	MOS			242.	LS	1.03
					264.		253.	UC	
17	S3A	Pressure Chem. Co.	392.	5% MOS	411.	3%	394.	2% LS	≤1.06
20	S6A	Pressure Chem. Co.	735.	5% MOS	842.	3%	862.	2% LS	1.17
			773.35	FR	.		867.	FR	1.12
21	4190038	Waters Associates	773.				867.		1.12
22	S14A	Pressure Chem. Co.	1610.	FR	1700.	4%	1900.	FR	1.18
							1700.	4% LS	
23	S61970	Waters Associates	1780.				2145.		1.20
27	NBS706	National Bureau of Stds.	<136.0				257.8	LS	1.89
							288.1	UC	
28	COOPA	Mobil	116.0				304.		2.62
POLYBUTADIENE									
41	17M	Phillips Petroleum Co.	16.1				17.		1.06
42	170M	Phillips Petroleum Co.	135.				170.		1.26
43	272 M	Phillips Petroleum Co.	206.				272.		1.32
44	332M	Phillips Petroleum Co.	226.				332.		1.47
45	423M	Phillips Petroleum Co.	286.				423.		1.48

TABLE II-4 Cont'd.

POLYVINYLCHLORIDE

46	PV-2	Pressure Chem. Co.	25.5			68.6		2.69
47	PV-3	Pressure Chem. Co.	41.0			118.2		2.88
48	PV-4	Pressure Chem. Co.	54.0			132.		2.44

POLYMETHYLMETHACRYLATE

50	RH	Rohm and Haas	50.0			290.		
51	ICI	I.C.I.	33.0	MOS	61.7	78.	LS	
			17.3	VOS				
			33.0	GPC		63.3	GPC	

*VOS = Vapor Pressure Osmometry
CRYO = Cryoscopy
MOS = Membrane Osmometry
FR = Fractionation

+LS = Light Scattering
EST = Estimated
UC = Ultracentrifugation
KIN = Kinetics

xAll Mv were determined from intrinsic viscosity measurement.

TABLE II-5

GPC CALIBRATION DATA-COLUMN CODE 25

STD.	GPC NO.	MG INJECTED	$\frac{\text{AREA}}{\text{MG INJECTED}}$	M_{RMS}	$M^{*}_{CAL\ CURVE}$	PRV
3	904(1)	1.77	7.793 E+02	1.96 E+03	2.62 E+03	43.14
3	927(1)	1.77	7.534 E+02	1.96 E+03	2.60 E+03	43.15
4	907(1)	1.86	8.566 E+02	5.20 E+03	3.90 E+03	42.54
4	930(1)	1.77	8.426 E+02	5.20 E+03	3.97 E+03	42.51
5	905	1.77	9.231 E+02	1.04 E+04	9.63 E+03	41.19
5	922	1.87	8.833 E+02	1.04 E+04	9.82 E+03	41.16
8	909	1.77	9.057 E+02	1.97 E+04	1.94 E+04	40.16
8	915	1.77	9.114 E+02	1.97 E+04	1.94 E+04	40.16
9	919	1.77	8.678 E+02	5.03 E+04	5.22 E+04	38.72
9	931	1.77	8.837 E+02	5.03 E+04	5.18 E+04	38.73
10	912	1.82	9.032 E+02	9.67 E+04	9.63 E+04	37.84
10	933	1.77	8.942 E+02	9.67 E+04	9.97 E+04	37.79
11	911	1.96	1.029 E+03	1.13 E+05	1.26 E+05	37.46
13	900	.89	8.969 E+02	1.68 E+05	1.70 E+05	37.03
13	901	.89	9.205 E+02	1.68 E+05	1.70 E+05	37.03
13	902	.89	8.411 E+02	1.68 E+05	1.71 E+05	37.02
13	910	1.77	8.903 E+02	1.68 E+05	1.60 E+05	37.12
13	916	1.77	9.000 E+02	1.68 E+05	1.60 E+05	37.12
13	926	1.77	9.036 E+02	1.68 E+05	1.64 E+05	37.08
13	937	1.77	8.774 E+02	1.68 E+05	1.57 E+05	37.14
13	939	1.77	8.865 E+02	1.68 E+05	1.55 E+05	37.16
14	928	1.94	2.845 E+02	1.75 E+05	1.92 E+05	36.86
14	936	1.94	3.450 E+02	1.75 E+05	1.86 E+05	36.90
17	941	1.77	8.722 E+02	3.93 E+05	4.17 E+05	35.77
17	942	1.77	8.710 E+02	3.93 E+05	4.11 E+05	35.79
20	925	1.74	8.721 E+02	7.96 E+05	7.73 E+05	34.91
20	935	1.74	9.015 E+02	7.96 E+05	7.67 E+05	34.92
21	906	1.77	8.511 E+02	8.19 E+05	7.45 E+05	34.96
21	914	1.77	9.739 E+02	8.19 E+05	7.40 E+05	34.97

*M calculated from calibration curve

TABLE II-5 (CONTINUED)

22	903	.89	8.994 E+02	1.75 E+06	1.94 E+06	33.64
22	938	1.77	5.317 E+02	1.75 E+06	1.99 E+06	33.61
23	929 (2)	1.82	9.240 E+02	1.95 E+06	1.75 E+06	33.78
28	932 (2)	1.77	1.032 E+03	1.88 E+05		
50	751 (2)	1.88	3.972 E+02	1.20 E+05		
50	751 (2)	1.88	3.879 E+02	1.20 E+05		

Note: GPC Sensitivity = 8X unless otherwise noted

(1) Impurity Peak Interference
(2) Polydisperse Standards

TABLE II-6

GPC CALIBRATION DATA-COLUMN CODE 26

STD.	GPC NO.	MG INJECTED	$\frac{\text{AREA}}{\text{MG INJECTED}}$	M_{RMS}	$M^{*}_{CAL\ CURVE}$	PRV
2	955(1)	1.77	5.615 E+02	1.30 E+03	2.91 E+03	60.12
2	956(1)	1.77	5.400 E+02	1.30 E+03	2.65 E+03	60.30
4	954(1)	2.00	9.147 E+02	5.20 E+03	4.94 E+03	59.03
7	952	1.82	1.110 E+03	2.04 E+04	2.09 E+04	55.59
9	951	1.74	1.098 E+03	5.03 E+04	5.07 E+04	53.01
13	953	1.89	1.119 E+03	1.68 E+05	1.55 E+05	48.98
14	960	1.68	1.080 E+03	1.75 E+05	1.70 E+05	48.60
17	949	1.78	1.034 E+03	3.93 E+05	3.96 E+05	44.82
21	959	1.82	1.137 E+03	8.19 E+05	8.06 E+05	41.30
21	965	1.77	1.073 E+03	8.19 E+05	8.22 E+05	41.20
22	958	1.84	9.911 E+02	1.75 E+06	1.92 E+06	37.10
27	961(2)	2.40	1.091 E+03	1.87 E+05		
46	852(1)	1.86	6.240 E+02	4.18 E+04	4.32 E+04	52.27
47	853	1.85	6.097 E+02	6.96 E+04	7.98 E+04	50.00
48	854	1.77	6.599 E+02	8.44 E+04	9.06 E+04	49.49

(1) Impurity Peak Interference
(2) Polydisperse Standards

Note: GPC Sensitivity = 8X unless otherwise noted.

*M calculated from calibration curve

TABLE II-7

GPC CALIBRATION DATA-COLUMN CODE 27

STD.	GPC NO.	MG INJECTED	AREA / MG INJECTED	M_{RMS}	$M^{*}_{CAL\ CURVE}$	PRV
2	969(1)	1.82	5.370 E+02	1.30 E+03	2.71 E+03	60.26
2	993(1)	3.99	2.968 E+02	1.30 E+03	2.88 E+03	60.14
3	971(1)	1.80	6.764 E+02	1.96 E+03	3.38 E+03	59.82
4	970(1)	1.80	8.775 E+02	5.20 E+03	4.92 E+03	59.04
4	992(1)	3.99	4.625 E+02	5.20 E+03	5.23 E+03	58.91
7	978	1.78	1.090 E+03	2.04 E+04	2.09 E+04	55.60
8	968	1.77	1.165 E+03	1.97 E+04	2.03 E+04	55.68
8	995	3.99	1.057 E+03	1.97 E+04	2.03 E+04	55.67
9	972	1.81	1.045 E+03	5.03 E+04	4.97 E+04	53.07
13	977	1.84	1.073 E+03	1.68 E+05	1.58 E+05	48.92
13	987	3.55	1.171 E+03	1.68 E+05	1.61 E+05	48.84
13	994	4.03	1.080 E+03	1.68 E+05	1.61 E+05	48.84
14	986(3)	3.55	1.094 E+03	1.75 E+05	1.72 E+05	48.56
15	991	3.55	5.531 E+02	1.95 E+05	1.75 E+05	48.48
17	975	1.77	1.026 E+03	3.93 E+05	4.03 E+05	44.73
20	974	1.77	1.068 E+03	7.96 E+05	8.43 E+05	41.07
21	976	1.72	1.085 E+03	8.19 E+05	8.14 E+05	41.25
21	988	3.55	1.089 E+03	8.19 E+05	8.33 E+05	41.13
22	966	1.77	1.120 E+03	1.75 E+06	1.90 E+06	37.14
22	990	3.55	1.737 E+03	1.75 E+06	1.55 E+06	38.09
23	989(2)	3.55	1.101 E+03	1.95 E+06	1.77 E+06	37.48
27	985(5)	3.55	1.111 E+03	1.87 E+05		
41	803(5)	3.55	7.650 E+02	1.65 E+04		54.20
42	801(5)	3.55	7.869 E+02	1.51 E+05		46.14
43	802(5)	3.55	7.727 E+02	2.37 E+05		44.12
44	804(5)	3.55	7.618 E+02	2.74 E+05		43.21
45	800(1)	3.55	7.588 E+02	3.48 E+05		42.22
46	857(1)	1.80	6.476 E+02	4.18 E+04	3.96 E+04	52.57

*M calculated from calibration curve

TABLE 11-7 (CONTINUED)

46	858[1]	4.04	6.147 E+02	4.18 E+04	4.47 E+04	52.15
47	859	3.99	6.260 E+02	6.96 E+04	7.39 E+04	50.30
48	860[2,4]	3.99	6.517 E+02	8.44 E+04	8.90 E+04	49.56
50	752[2]	1.82	9.977 E+02	1.20 E+05		
50	753[1,2]	3.55	5.195 E+02	1.20 E+05		
51	757	2.21	8.133 E+02	3.67 E+04		

(1) Impurity Peak Interference
(2) Polydisperse Standards
(3) Sensitivity 4X
(4) Sensitivity 16X
(5) No Mark Houwink Constants available

Note: GPC Sensitivity = 8X unless otherwise noted.

TABLE II-8

GPC CALIBRATION DATA-COLUMN CODE 28

STD.	GPC NO.	MG INJECTED	AREA / MG INJECTED	M_{RMS}	$M^{*}_{CAL\ CURVE}$	PRV
2	920(1)	3.55	7.626 E+02	1.30 E+03	1.39 E+03	69.67
2	999(1,3)	5.33	3.747 E+02	1.30 E+03	1.38 E+03	69.68
2	21(1)	3.55	7.603 E+02	1.30 E+03	1.36 E+03	69.71
3	1000(1,3)	5.33	4.600 E+02	1.96 E+03	2.15 E+03	68.82
3	12(3)	3.55	9.015 E+02	1.96 E+03	2.08 E+03	68.89
4	998(3)	5.33	5.267 E+02	5.20 E+03	4.05 E+03	67.52
4	13(3)	3.55	1.048 E+03	5.20 E+03	4.05 E+03	67.52
8	7(3)	5.33	5.531 E+02	1.97 E+04	1.88 E+04	63.84
7	6(3)	5.33	5.435 E+02	2.04 E+04	2.12 E+04	63.52
7	24(3)	3.55	1.014 E+03	2.04 E+04	2.14 E+04	63.49
10	9(3)	5.33	5.589 E+02	9.67 E+04	9.21 E+04	58.92
10	20(3)	3.55	1.108 E+03	9.67 E+04	9.37 E+04	58.86
13	1(3)	5.33	5.505 E+02	1.68 E+05	1.51 E+05	57.06
14	11	3.55	8.361 E+02	1.75 E+05	1.69 E+05	56.61
14	18(3)	3.55	1.111 E+03	1.75 E+05	1.73 E+05	56.51
15	2(3)	5.33	5.408 E+02	1.95 E+05	1.71 E+05	56.57
16	924(3)	3.55	1.105 E+03	2.57 E+05	2.46 E+05	55.04
17	8(3)	5.33	5.444 E+02	3.93 E+05	3.86 E+05	53.02
17	26(3)	3.55	1.116 E+03	3.93 E+05	4.08 E+05	52.77
21	3(3)	5.33	5.283 E+02	8.19 E+05	7.91 E+05	49.57
22	5(3)	5.33	6.020 E+02	1.75 E+06	1.70 E+06	45.82
23	4(3)	5.33	5.329 E+02	1.95 E+06	1.71 E+06	45.78
23	10(3)	5.33	5.475 E+02	1.95 E+06	1.72 E+06	45.76
23	17(2)	3.55	1.087 E+03	1.95 E+06	1.88 E+06	45.33
27	996(2)	5.33	1.065 E+03	1.87 E+05	2.15 E+05	55.62

*M calculated from calibration curve

TABLE II-8 (CONTINUED)

46	861	3.55	6.582 E+02	4.18 E+04	4.31 E+04	60.21
47	862	3.55	6.564 E+02	6.96 E+04	7.48 E+04	58.20
48	863(2)	3.55	6.520 E+02	8.44 E+04	8.76 E+04	57.58
50	754(2)	5.33	4.911 E+02	1.20 E+05		
50	755(2)	3.55	5.149 E+02	1.20 E+05		
51	756(2)	3.55	5.238 E+02	3.67 E+04		

(1) Impurity Peak Interference
(2) Polydisperse Standards
(3) Sensitivity 4X

Note: GPC Sensitivity = 8X unless otherwise noted.

TABLE II-9

MARK HOUWINK CONSTANTS

$$[\eta] = KM^a$$

POLYMER	K	a	SOURCE
Polystyrene	1.6×10^{-4}	.706	Provder, T., Rosen, E. M., Sep. Sci., 5, 437 (1970)
PVC	1.63×10^{-4}	.766	Pressure Chemical Company
PMMA			
$M \leq 31000$	21.1×10^{-4}	.406	Provder, T., Woodbrey, J. C., Clark, J. H., ACS Symposium on GPC, ACS, Houston, Texas Feb. 1970.
$M > 31000$	1.04×10^{-4}	.697	

TABLE II-10

UNIVERSAL CALIBRATION CURVES

$$\ell nV = B_1 + B_2 v + B_3 v^2 + B_4 v^3$$

COLUMN CODE	COEFFICIENT VALUE			
	B_1	B_2	B_3	B_4
25	65.04	-1.671	6.300×10^{-3}	0.0
26, 27	66.26	-3.050	6.484×10^{-2}	-5.173×10^{-4}
28	81.28	-3.403	6.267×10^{-2}	-4.281×10^{-4}

TABLE II-11

INFINITE RESOLUTION MOLECULAR WEIGHT AVERAGES

COL CODE 25

STD.	GPC #	MG INJECTED	M_n (∞)	M_w (∞)	M_z (∞)	M_{z+1} (∞)	P (∞)
3	904 (1)	1.77	2.47 E+03	2.92 E+03	3.51 E+03	4.23 E+03	1.18
3	927 (1)	1.77	2.60 E+03	2.98 E+03	3.47 E+03	4.07 E+03	1.15
4	907 (1)	1.86	3.42 E+03	4.27 E+03	5.36 E+03	6.76 E+03	1.25
4	930 (1)	1.77	3.58 E+03	4.33 E+03	5.25 E+03	6.31 E+03	1.21
5	905	1.77	7.80 E+03	1.07 E+04	1.41 E+04	1.82 E+04	1.37
5	922	1.87	8.45 E+03	1.09 E+04	1.39 E+04	1.78 E+04	1.28
8	909	1.77	1.60 E+04	2.15 E+04	2.82 E+04	3.61 E+04	1.35
8	915	1.77	1.59 E+04	2.23 E+04	3.81 E+04	1.32 E+05	1.40
9	919	1.77	4.21 E+04	5.62 E+04	7.23 E+04	9.11 E+04	1.33
9	931	1.77	4.20 E+04	5.63 E+04	7.30 E+04	9.37 E+04	1.34
10	912	1.82	7.48 E+04	1.05 E+05	1.45 E+05	2.12 E+05	1.41
10	933	1.77	7.75 E+04	1.06 E+05	1.38 E+05	1.74 E+05	1.37
11	911	1.96	7.94 E+04	1.25 E+05	1.78 E+05	2.45 E+05	1.57
13	900	.89	1.28 E+05	1.80 E+05	2.40 E+05	3.07 E+05	1.41
13	901	.89	1.25 E+05	1.82 E+05	2.48 E+05	3.28 E+05	1.45
13	902	.89	1.25 E+05	1.82 E+05	2.44 E+05	3.12 E+05	1.45
13	910	1.77	1.16 E+05	1.70 E+05	2.29 E+05	2.97 E+05	1.46
13	916	1.77	1.17 E+05	1.70 E+05	2.27 E+05	2.91 E+05	1.45
13	926	1.77	1.25 E+05	1.76 E+05	2.36 E+05	3.18 E+05	1.41
13	937	1.77	1.18 E+05	1.69 E+05	2.30 E+05	3.14 E+05	1.44
13	939	1.77	1.17 E+05	1.66 E+05	2.26 E+05	3.09 E+05	1.42
14	928	1.94	1.25 E+05	1.98 E+05	2.81 E+05	3.85 E+05	1.58
14	936	1.94	1.33 E+05	2.01 E+05	2.90 E+05	4.29 E+05	1.51
17	941	1.77	2.64 E+05	4.37 E+05	5.95 E+05	7.72 E+05	1.65
17	942	1.77	2.57 E+05	4.31 E+05	5.86 E+05	7.62 E+05	1.68
20	925	1.74	5.62 E+05	8.52 E+05	1.15 E+06	1.55 E+06	1.51
20	935	1.74	5.64 E+05	8.57 E+05	1.25 E+06	2.32 E+06	1.52

TABLE 11-11 (CONTINUED)

21	906	1.77	5.73 E+05	8.23 E+05	1.10 E+06	1.46 E+06	1.44
21	914	1.77	5.55 E+05	8.27 E+05	1.17 E+06	1.81 E+06	1.49
22	903	.89	8.51 E+05	1.99 E+06	3.70 E+06	7.29 E+06	2.34
22	938	1.77	8.84 E+05	2.00 E+06	3.29 E+06	5.06 E+06	2.26
23	929(2)	1.82	7.80 E+05	1.88 E+06	3.30 E+06	5.72 E+06	2.40
28	932(2)	1.77	8.95 E+04	3.56 E+05	1.16 E+06	3.33 E+06	3.98
50	750(2)	1.88	4.79 E+04	3.74 E+05	1.50 E+06	3.18 E+06	7.81
50	751(2)	1.88	5.68 E+04	3.91 E+05	1.82 E+06	5.67 E+06	6.88

(1) Impurity Peak Interference
(2) Polydisperse Standards

Note: GPC Sensitivity = 8X unless otherwise noted.

TABLE II-12

INFINITE RESOLUTION MOLECULAR WEIGHT AVERAGES

COL CODE 26

STD.	GPC #	MG INJECTED	M_n (∞)	M_w (∞)	M_z(∞)	M_{z+1}(∞)	P (∞)
2	955 (1)	1.77	4.02 E+03	4.58 E+03	5.40 E+03	6.52 E+03	1.14
2	956 (1)	1.77	3.98 E+03	4.50 E+03	5.26 E+03	6.28 E+03	1.13
4	954 (1)	2.00	5.16 E+03	6.33 E+03	7.95 E+03	9.99 E+03	1.22
7	952	1.82	1.75 E+04	2.28 E+04	2.86 E+04	3.45 E+04	1.31
9	951	1.74	4.06 E+04	5.26 E+04	6.47 E+04	7.70 E+04	1.29
13	953	1.89	1.29 E+05	1.63 E+05	2.04 E+05	2.61 E+05	1.27
14	960	1.68	1.37 E+05	1.81 E+05	2.25 E+05	2.78 E+05	1.32
17	949	1.78	3.30 E+05	4.05 E+05	4.78 E+05	5.55 E+05	1.23
21	959	1.82	6.17 E+05	8.08 E+05	9.73 E+05	1.16 E+06	1.31
21	965	1.77	6.50 E+05	8.17 E+05	9.70 E+05	1.13 E+06	1.26
22	958 (2)	1.84	9.97 E+05	1.69 E+06	2.31 E+06	2.94 E+06	1.70
27	961 (1)	2.40	8.95 E+04	2.77 E+05	4.88 E+05	7.05 E+05	3.10
46	852	1.86	2.91 E+04	6.60 E+04	1.24 E+05	1.99 E+05	2.27
47	853	1.85	5.11 E+04	1.02 E+05	1.68 E+05	2.38 E+05	2.00
48	854	1.77	5.67 E+04	1.27 E+05	2.29 E+05	3.63 E+05	2.25

(1) Impurity Peak Interference
(2) Polydisperse Standards

Note: GPC Sensitivity = 8X unless otherwise noted.

TABLE II-13

INFINITE RESOLUTION MOLECULAR WEIGHT AVERAGES

COL CODE 27

STD.	GPC #	MG INJECTED	Mn (∞)	Mw (∞)	Mz (∞)	Mz+1 (∞)	P (∞)
2	969(1)	1.82	4.09 E+03	4.62 E+03	5.41 E+03	6.56 E+03	1.13
2	993(1)	3.99	4.18 E+03	4.79 E+03	5.77 E+03	7.39 E+03	1.15
3	971(1)	1.80	4.33 E+03	4.98 E+03	5.93 E+03	7.24 E+03	1.15
4	970(1)	1.80	5.18 E+03	6.29 E+03	7.83 E+03	9.76 E+03	1.21
4	992(1)	3.99	5.37 E+03	6.60 E+03	8.34 E+03	1.07 E+04	1.23
7	978	1.78	1.72 E+04	2.26 E+04	2.84 E+04	3.42 E+04	1.31
8	968	1.77	1.68 E+04	2.28 E+04	2.96 E+04	3.75 E+04	1.35
8	995	3.99	1.70 E+04	2.29 E+04	2.98 E+04	3.76 E+04	1.35
9	972	1.81	4.08 E+04	5.29 E+04	6.50 E+04	7.71 E+04	1.29
13	977	1.84	1.29 E+05	1.58 E+05	1.87 E+05	2.14 E+05	1.23
13	987	3.55	1.29 E+05	1.62 E+05	1.93 E+05	2.26 E+05	1.26
13	994	4.03	1.29 E+05	1.61 E+05	1.94 E+05	2.31 E+05	1.25
14	986	3.55	1.40 E+05	1.83 E+05	2.29 E+05	2.88 E+05	1.31
15	991(3)	3.55	1.49 E+05	1.84 E+05	2.19 E+05	2.60 E+05	1.23
17	975	1.77	3.26 E+05	4.14 E+05	5.13 E+05	6.55 E+05	1.27
20	974	1.77	6.02 E+05	8.13 E+05	9.83 E+05	1.17 E+06	1.35
21	976	1.72	6.51 E+05	8.14 E+05	9.76 E+05	1.15 E+06	1.25
21	988	3.55	6.28 E+05	8.42 E+05	1.03 E+06	1.26 E+06	1.34
22	966	1.77	8.90 E+05	1.66 E+06	2.29 E+06	2.87 E+06	1.87
22	990	3.55	8.56 E+05	1.51 E+06	2.25 E+06	4.04 E+06	1.77
23	989(2)	3.55	7.93 E+05	1.56 E+06	2.18 E+06	2.78 E+06	1.96
27	985(5)	3.55	7.65 E+04	2.81 E+05	5.34 E+05	8.75 E+05	3.68
41	803(5)	3.55					
42	801(5)	3.55					
43	802(5)	3.55					
44	804(5)	3.55					
45	800(5)	3.55					

TABLE II-13 (CONTINUED)

46	857(1)	1.80	2.85 E+04	6.32 E+04	1.14 E+05	1.74 E+05	2.22
46	858(1)	4.04	2.96 E+04	6.50 E+04	1.18 E+05	1.80 E+05	2.20
47	859	3.99	5.14 E+04	1.08 E+05	1.91 E+05	3.02 E+05	2.09
48	860(2,4)	3.99	5.59 E+04	1.49 E+05	3.62 E+05	7.89 E+05	2.66
50	752(2)	1.82	4.33 E+04	3.04 E+05	9.99 E+05	1.79 E+06	7.03
50	753(1,2)	3.55	4.56 E+04	2.99 E+05	9.18 E+05	1.55 E+06	6.55
51	751	2.21	3.02 E+04	7.96 E+04	1.45 E+05	2.16 E+05	2.64

(1) Impurity Peak Interference
(2) Polydisperse Standards
(3) Sensitivity 4X
(4) Sensitivity 16X
(5) No Mark Houwink Constants Available

Note: GPC Sensitivity = 8X unless otherwise noted.

TABLE 11-14

INFINITE RESOLUTION MOLECULAR WEIGHT AVERAGES

COL CODE 28

STD.	GPC #	MG INJECTED	Mn (∞)	Mw (∞)	Mz (∞)	Mz+1 (∞)	P (∞)
2	920(1)	3.55	1.50 E+03	2.22 E+03	3.89 E+03	9.04 E+03	1.47
2	999(1,3)	5.33	1.57 E+03	2.21 E+03	3.25 E+03	4.57 E+03	1.41
2	21(1)	3.55	1.51 E+03	2.16 E+03	3.22 E+03	4.60 E+03	1.43
3	1000(1,3)	5.33	1.85 E+03	2.68 E+03	3.92 E+03	5.46 E+03	1.45
3	12(3)	3.55	1.83 E+03	2.66 E+03	3.86 E+03	5.30 E+03	1.45
4	998(3)	5.33	2.94 E+03	4.61 E+03	6.71 E+03	9.02 E+03	1.57
4	13(3)	3.55	2.92 E+03	4.58 E+03	6.67 E+03	8.97 E+03	1.57
8	7(3)	5.33	1.54 E+04	2.08 E+04	2.66 E+04	3.28 E+04	1.35
7	6(3)	5.33	1.74 E+04	2.28 E+04	2.85 E+04	3.47 E+04	1.31
7	24(3)	3.55	1.74 E+04	2.31 E+04	2.89 E+04	3.49 E+04	1.32
10	9(3)	5.33	7.64 E+04	9.75 E+04	1.18 E+05	1.38 E+05	1.27
10	20(3)	3.55	7.66 E+04	9.77 E+04	1.18 E+05	1.38 E+05	1.27
13	1(3)	5.33	1.24 E+05	1.57 E+05	1.88 E+05	2.18 E+05	1.27
14	11	3.55	1.31 E+05	1.83 E+05	2.44 E+05	3.63 E+05	1.39
14	18(3)	3.55	1.31 E+05	1.82 E+05	2.31 E+05	2.90 E+05	1.40
15	2(3)	5.33	1.39 E+05	1.78 E+05	2.14 E+05	2.52 E+05	1.28
16	924(3)	3.55	1.75 E+05	2.49 E+05	3.13 E+05	3.83 E+05	1.42
17	8(3)	5.33	3.08 E+05	4.04 E+05	4.98 E+05	6.19 E+05	1.31
17	26(3)	3.55	3.17 E+05	4.23 E+05	5.28 E+05	6.82 E+05	1.33
21	3(3)	5.33	5.94 E+05	8.04 E+05	9.82 E+05	1.18 E+06	1.35
22	5(3)	5.33	3.23 E+05	1.49 E+06	2.22 E+06	3.14 E+06	4.60
23	4(3)	5.33	8.24 E+05	1.54 E+06	2.13 E+06	2.71 E+06	1.87
23	10	5.33	7.63 E+05	1.53 E+06	2.14 E+06	2.75 E+06	2.00
23	17	3.55	8.86 E+05	1.63 E+06	2.23 E+06	2.79 E+06	1.84

TABLE II-14 (CONTINUED)

27	996[2]	5.33	8.20 E+04	2.83 E+05	5.14 E+05	7.69 E+05	3.46
46	861	3.55	2.63 E+04	6.78 E+04	1.60 E+05	3.70 E+05	2.57
47	862	3.55	4.68 E+04	1.10 E+05	2.64 E+05	8.42 E+05	2.35
48	863[2]	3.55	5.54 E+04	1.34 E+05	2.78 E+05	5.30 E+05	2.43
50	754[2]	5.33	4.46 E+04	3.16 E+05	1.05 E+06	1.93 E+06	7.09
50	755[2]	3.55	3.98 E+04	3.07 E+05	9.76 E+05	1.65 E+06	7.70
51	756[2]	3.55	2.43 E+04	7.76 E+04	1.48 E+05	2.31 E+05	3.19

(1) Impurity Peak Interference
(2) Polydisperse Standards
(3) Sensitivity 4X

Note: GPC Sensitivity = 8X unless otherwise noted.

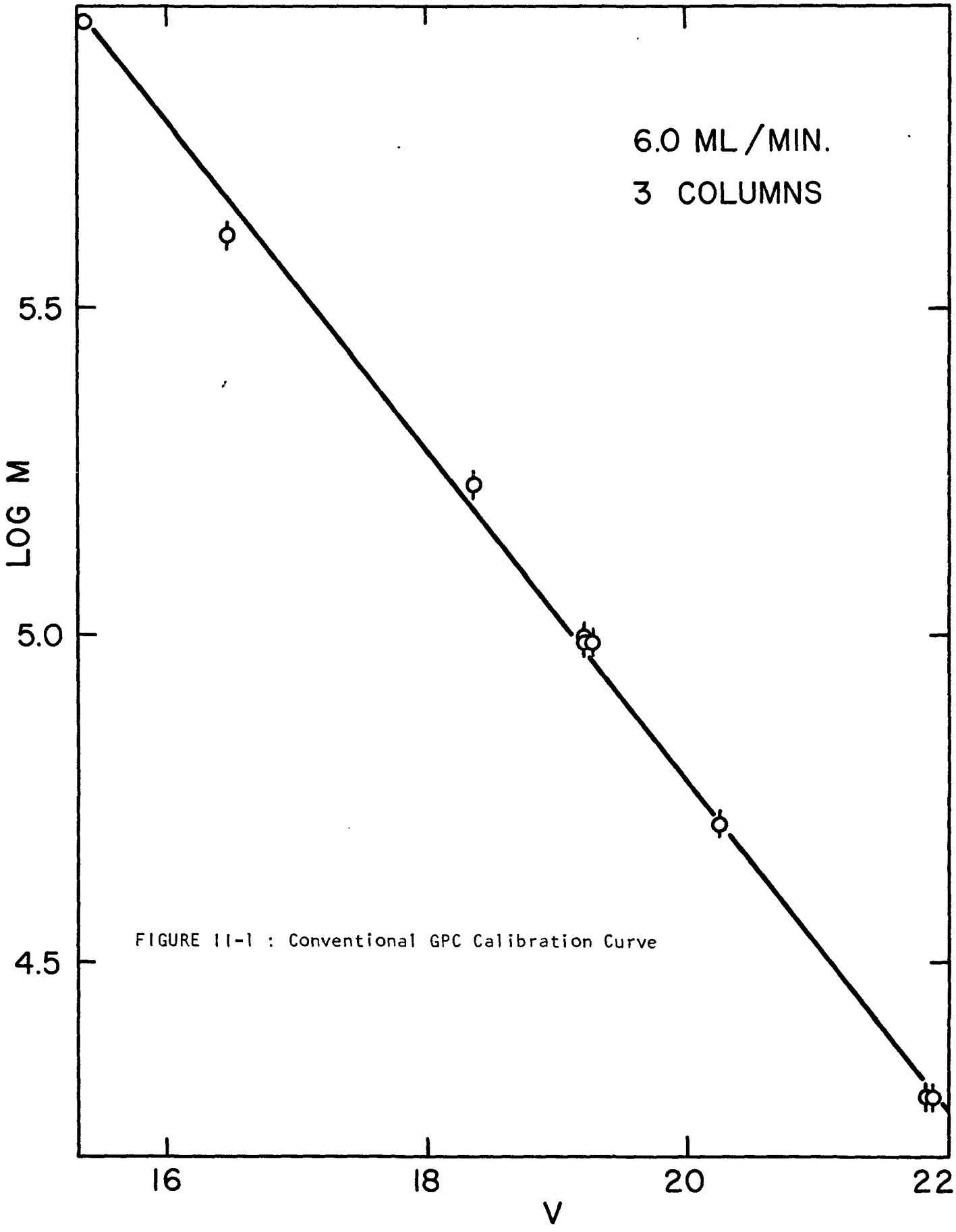

FIGURE II-1 : Conventional GPC Calibration Curve

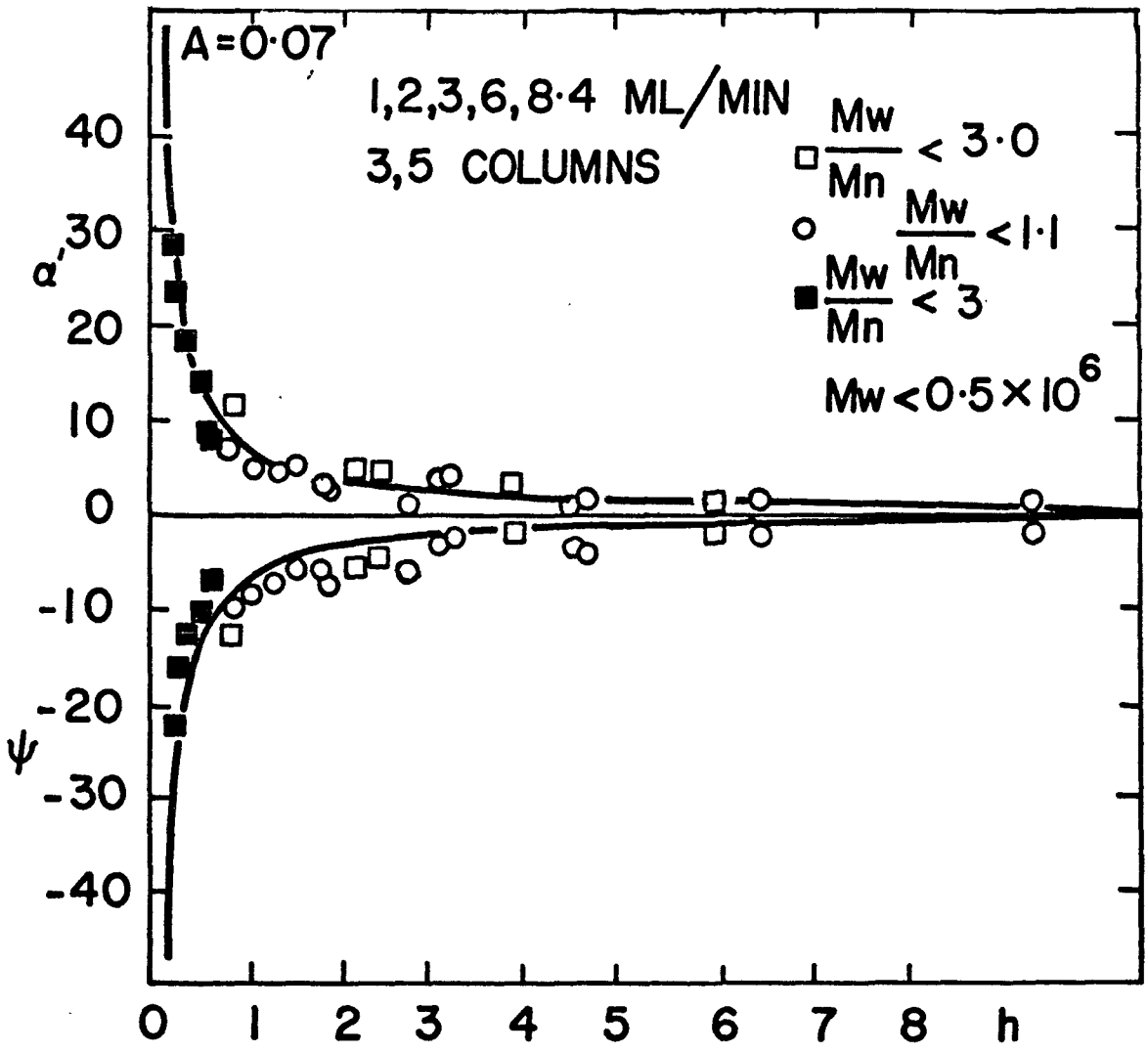

FIGURE II-2 : Percent Change in Mn ($\alpha' = \frac{Mn(h) - Mn(\infty)}{Mn(\infty)} * 100$)

and Percent Charge in Mw ($\psi = \frac{Mw(h) - Mw(\infty)}{Mw(\infty)} * 100$)

as a Function of h

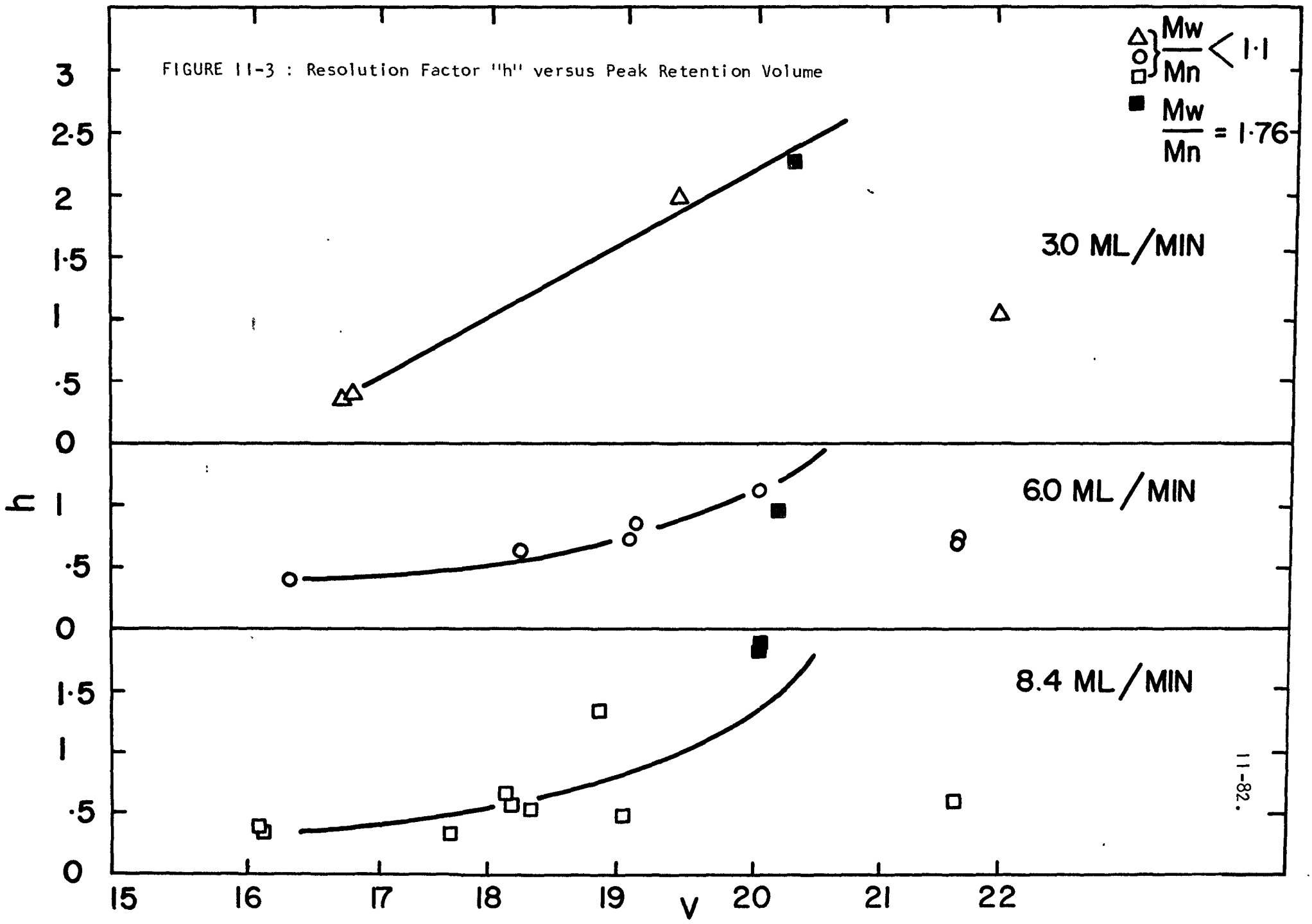
FIGURE II-3 : Resolution Factor "h" versus Peak Retention Volume
Mw/Mn < 1·1
Mw/Mn = 1·76
3.0 ML/MIN
6.0 ML/MIN
8.4 ML/MIN
h
V
3
2·5
2
1·5
1
·5
0
15
16
17
18
19
20
21
22
II-82.

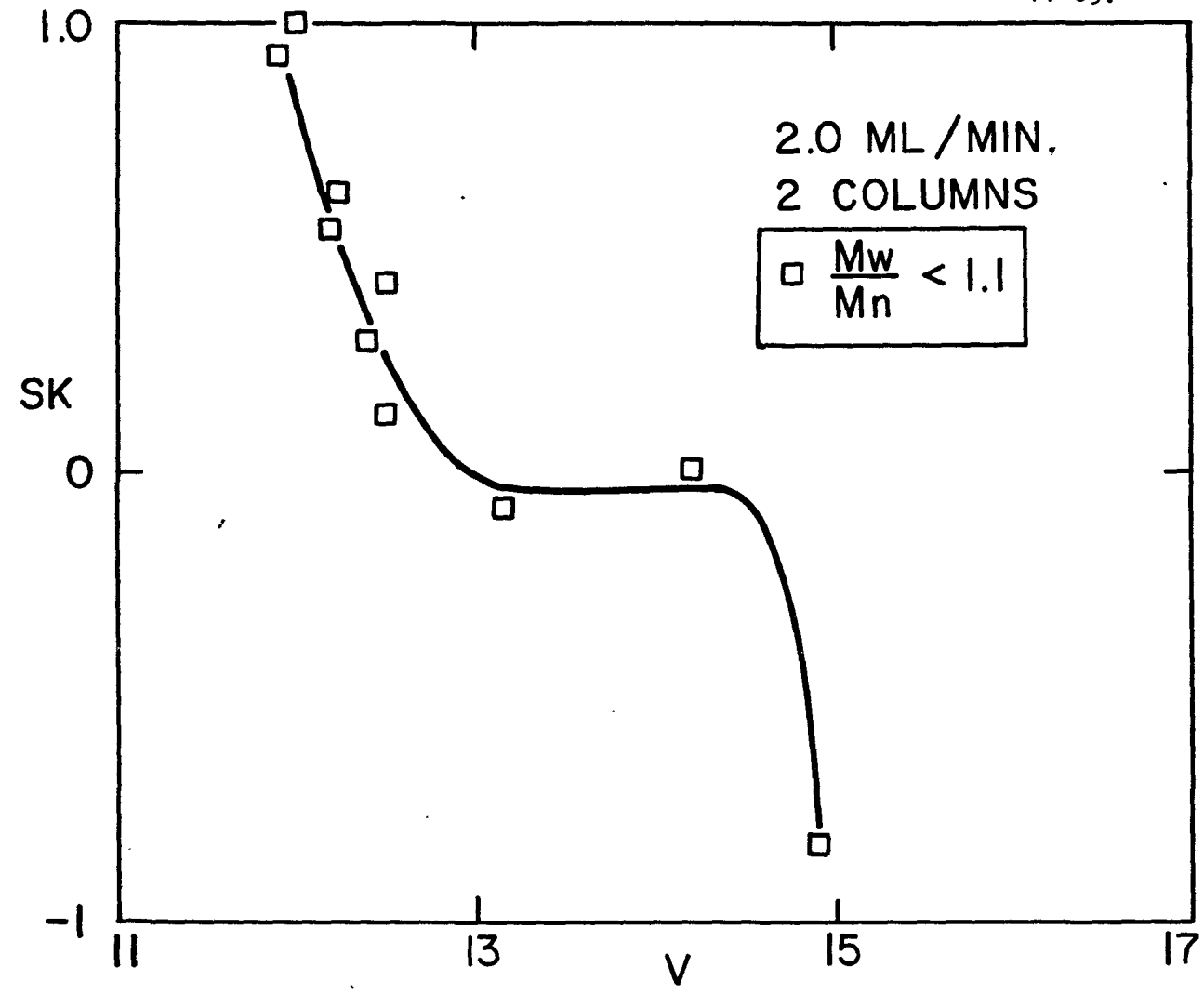

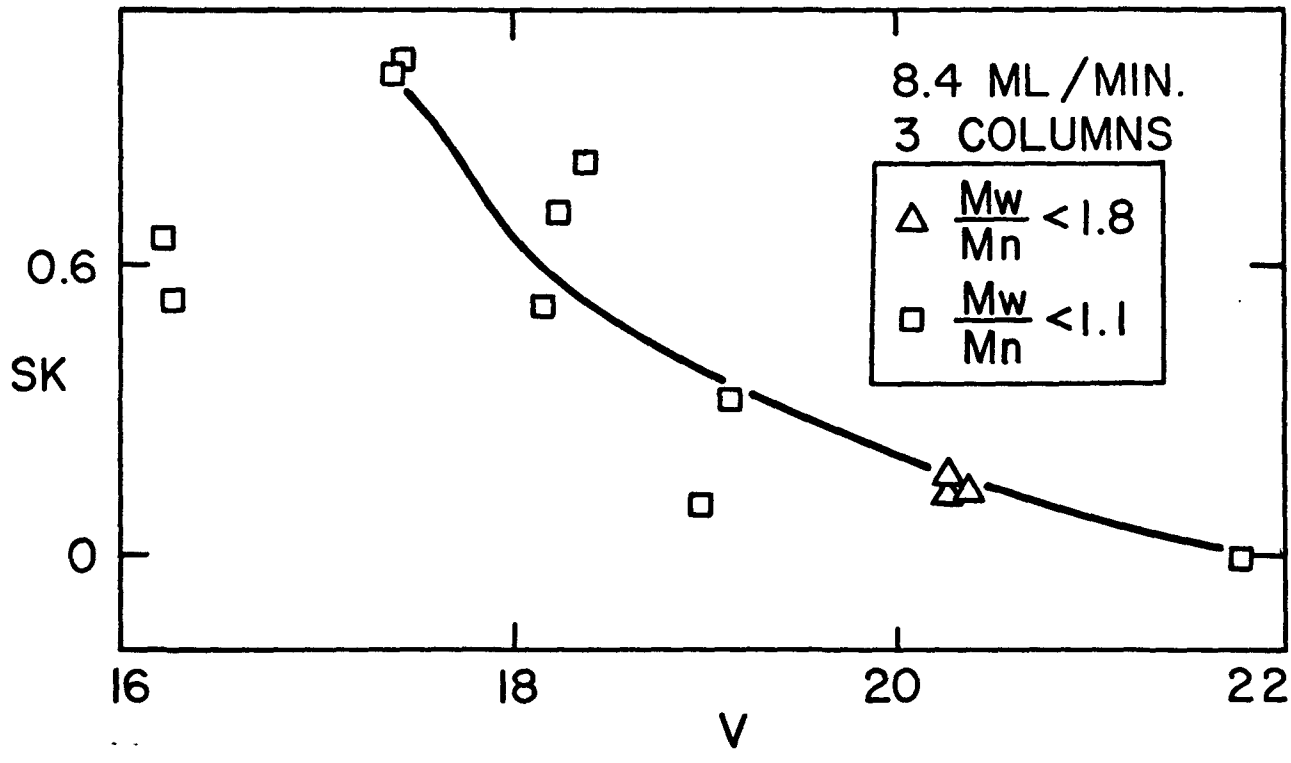

FIGURE 11-4 : Skewing Factor "SK" versus Peak Retention Volume

FIGURE II-5 : Skewing Factor "SK" versus Amount of Polymer (mg) Injected (Calculated from Data of Cantow et.al.[58])

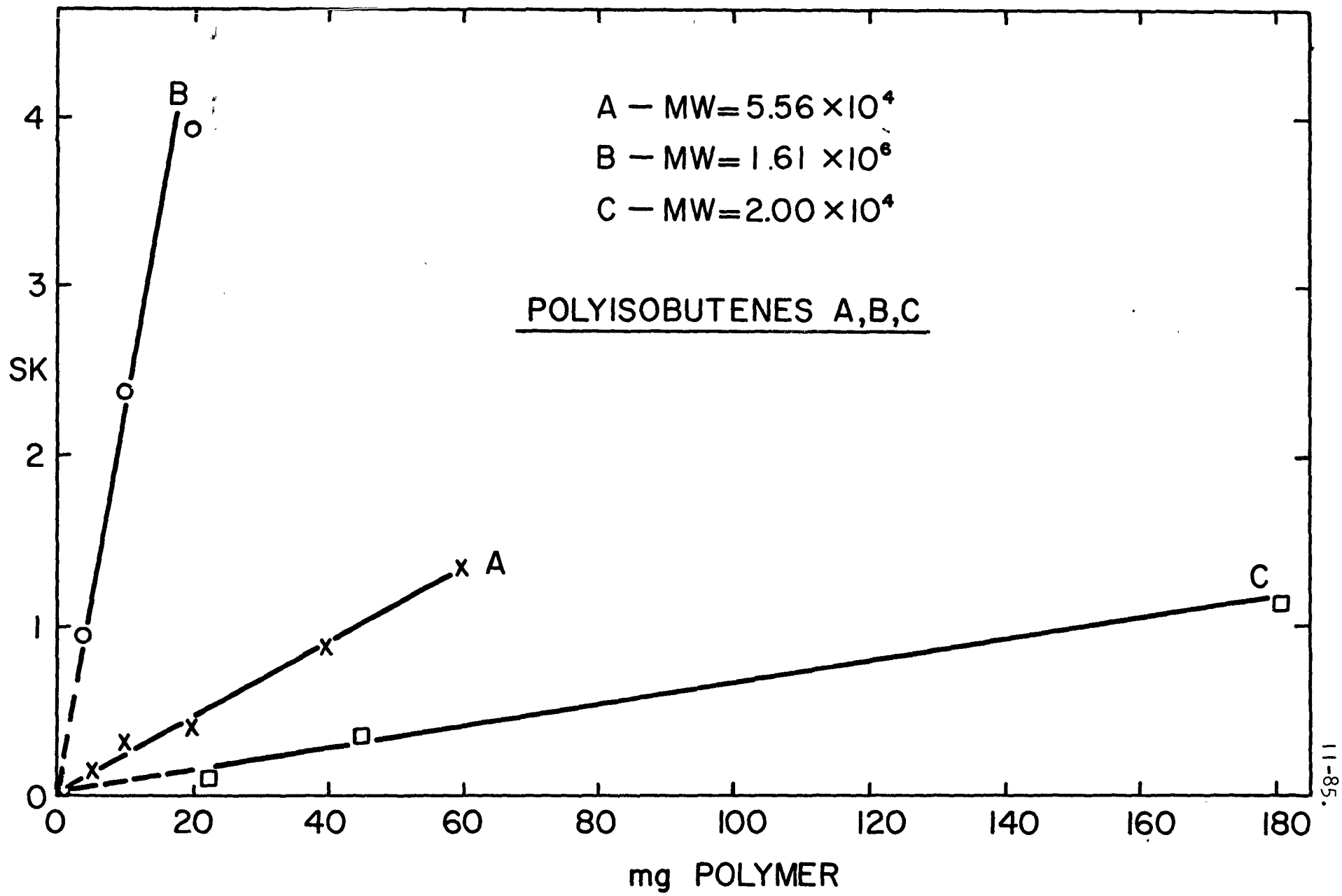
A – MW=5.56×10⁴
B – MW=1.61×10⁶
C – MW=2.00×10⁴
POLYISOBUTENES A,B,C
SK
mg POLYMER
0
1
2
3
4
0
20
40
60
80
100
120
140
160
180
A
B
C
11-85.

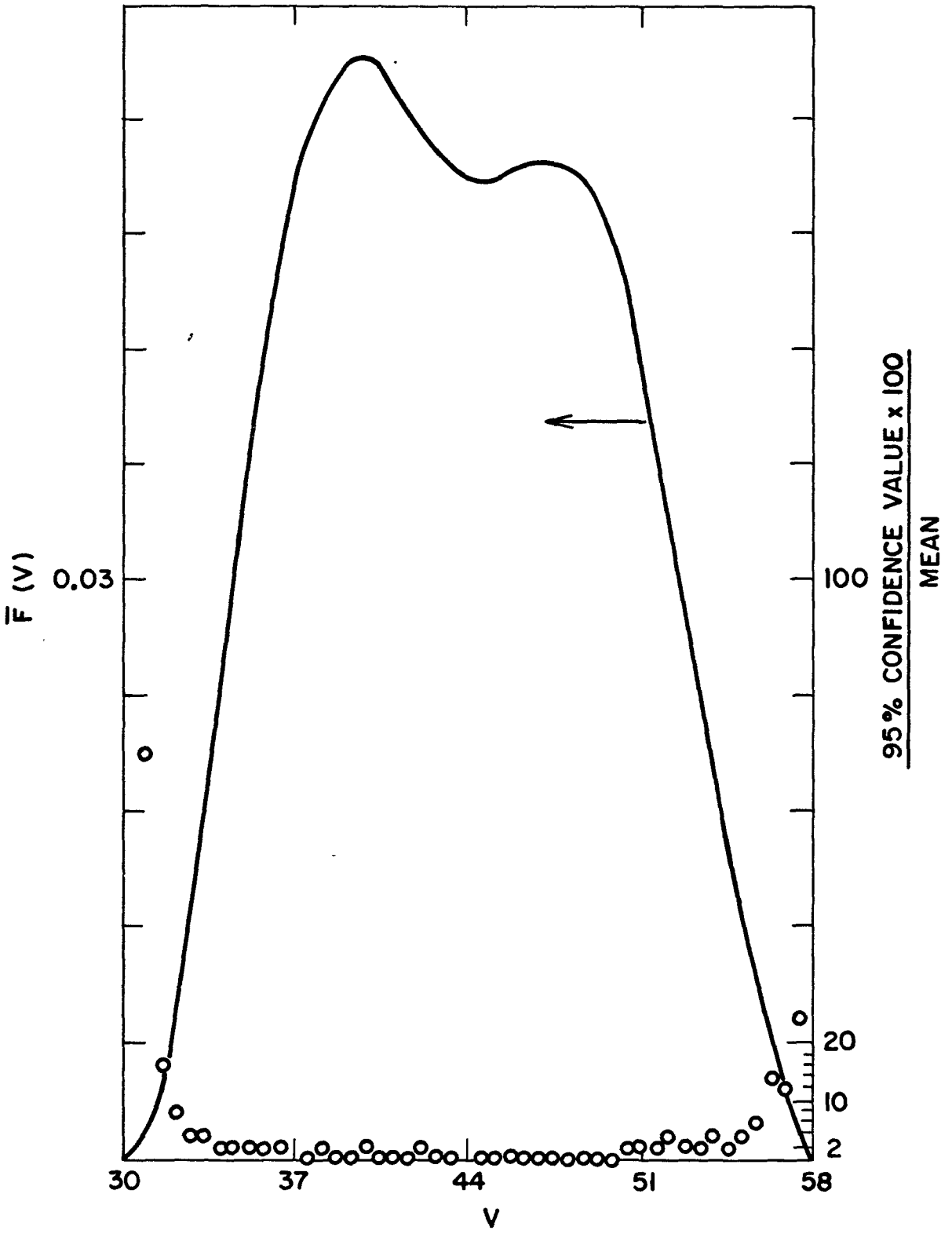

FIGURE II-6 : Mean Height Values of Chromatograms of PMMA from Sample No. 18J (GPC Numbers 610, 615 to 619) and 95% Confidence Value as a Percent of Mean versus Retention Volume

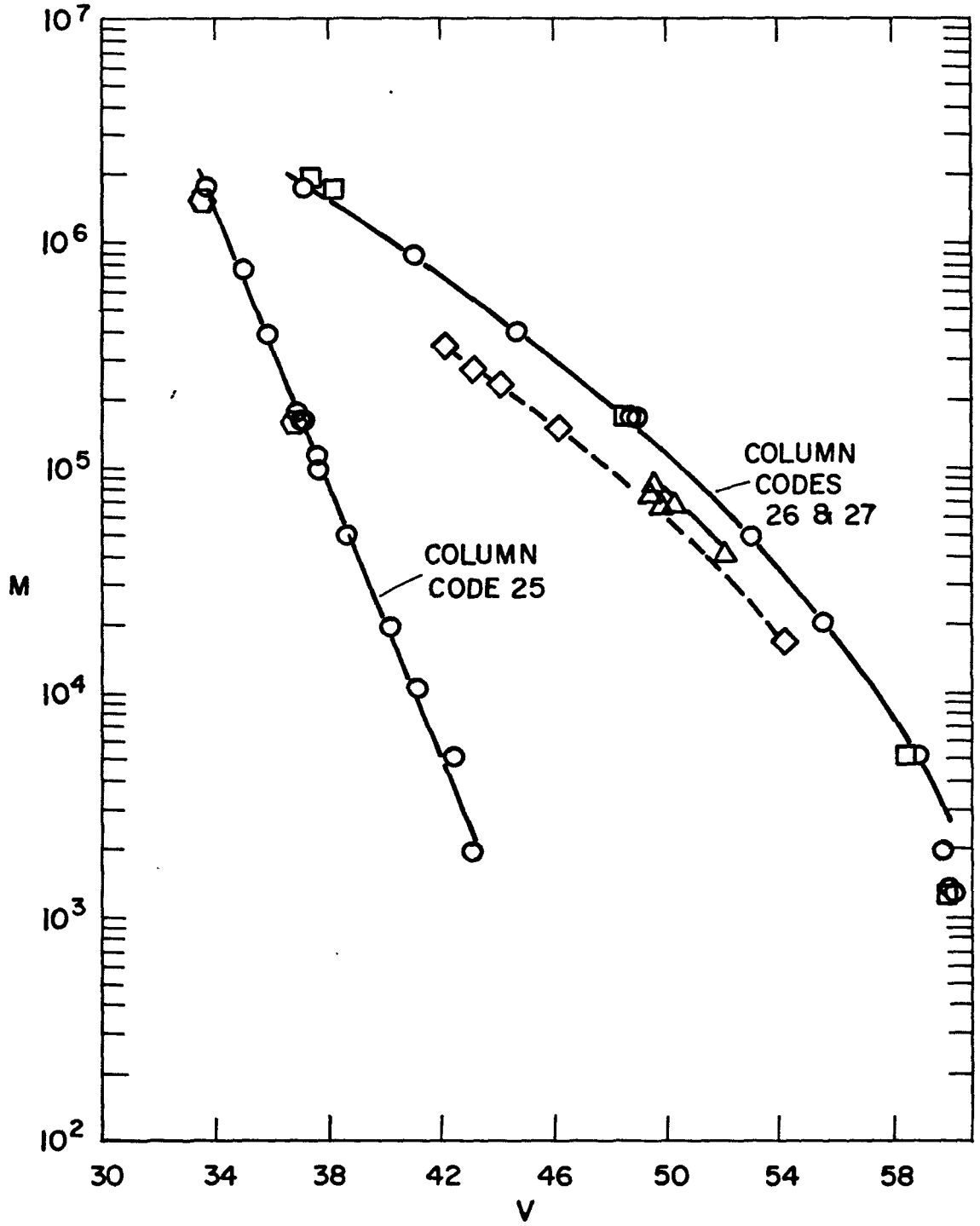

FIGURE II-7 : Calibration Curves for Polystyrene PVC and PBD, COLUMN CODES 25, 26 and 27.

Polynomial Used

0.9 mg
1.8 mg
3.6 mg
} Polystyrene

3.6 mg PBD

4.0 mg
1.8 mg
} PVC

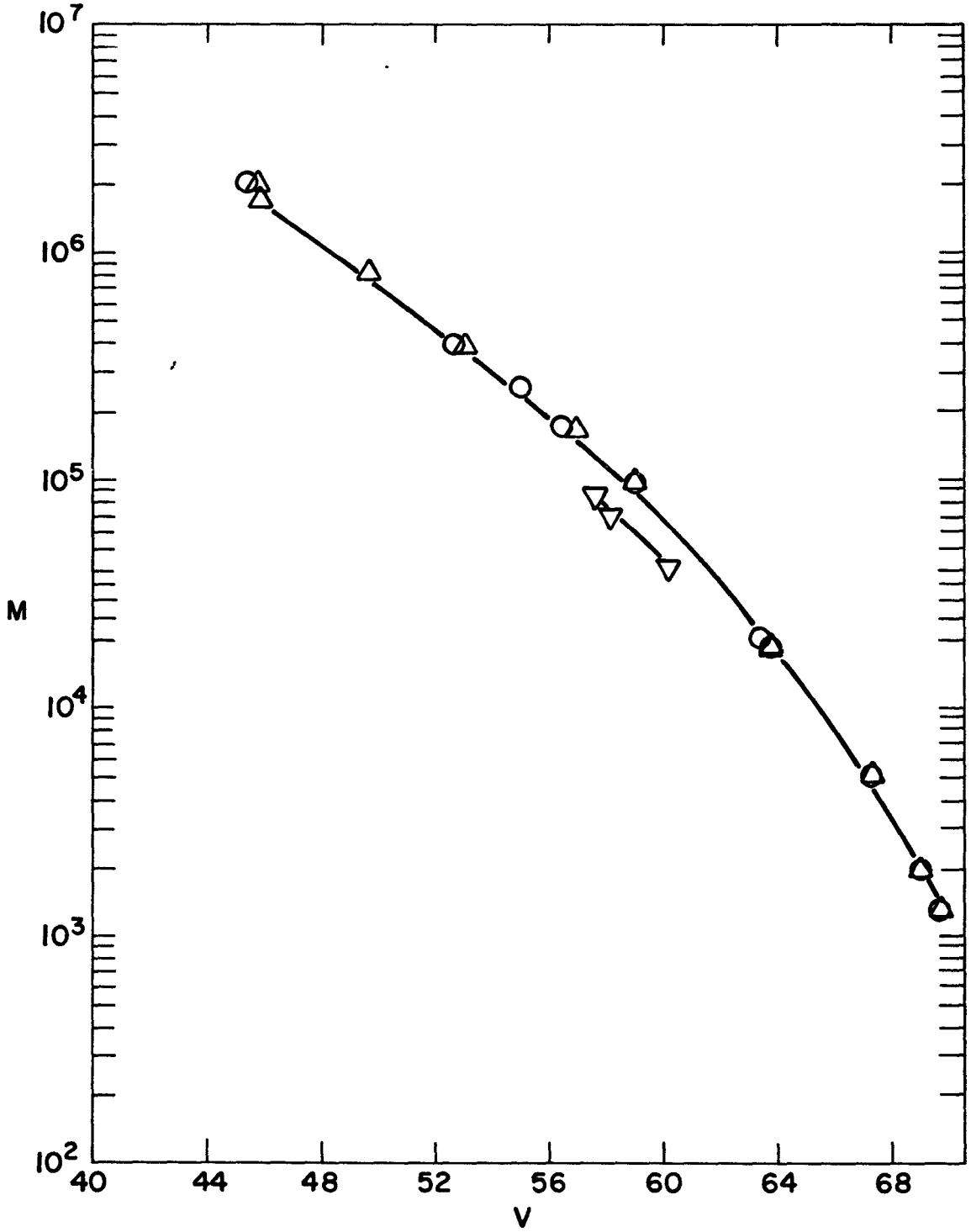

FIGURE II-8 : Calibration Curve for Polystyrene and PVC, COLUMN CODE 28.

○ Polystyrene, 3.55 mg

△ Polystyrene, 5.33 mg

▽ PVC, 3.55 mg

—— Polynomial Used

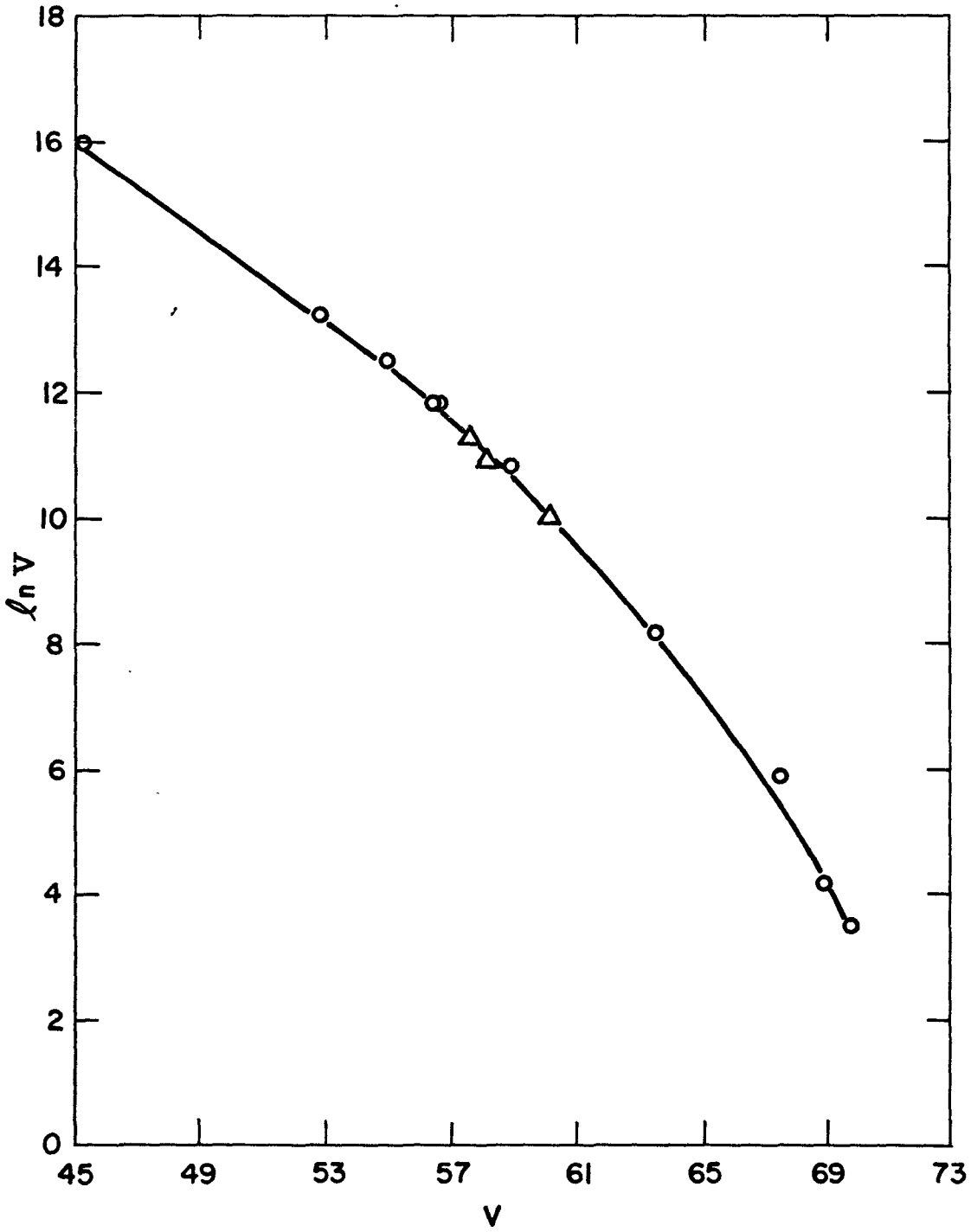

FIGURE II-9 : Universal Calibration Curve, COLUMN CODE 28

○ Polystyrene, 3.55 mg

△ PVC, 3.55 mg

—— Polynomial Used

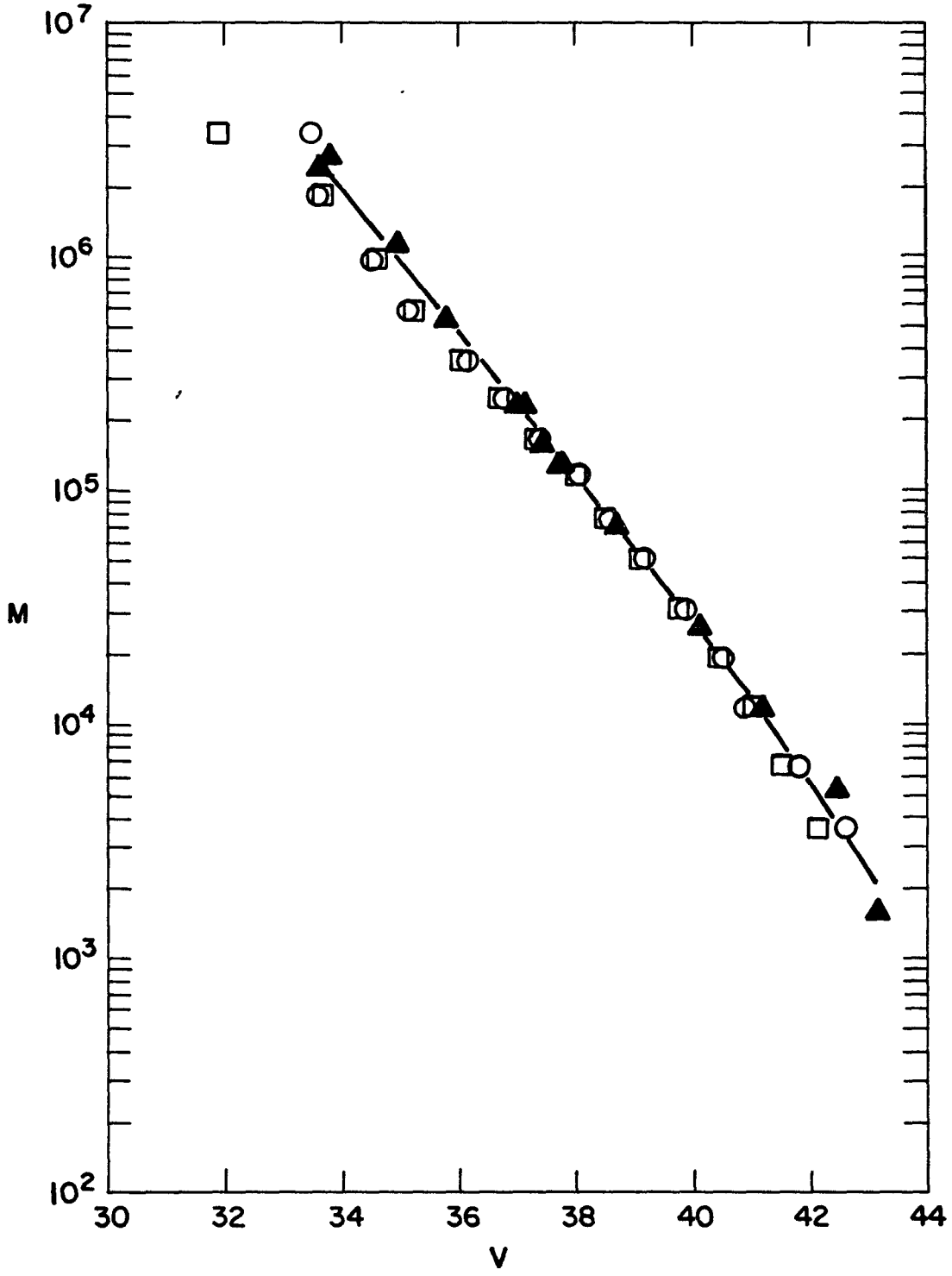

FIGURE II-10 : Calibration Curve for PMMA, COLUMN CODE 25.

——— Polynomial Used

▲ From Universal Calibration Curve

□ } From Weiss Method (1.88 mg of RH PMMA Std)

○ } (GPC Nos. 750 and 751)

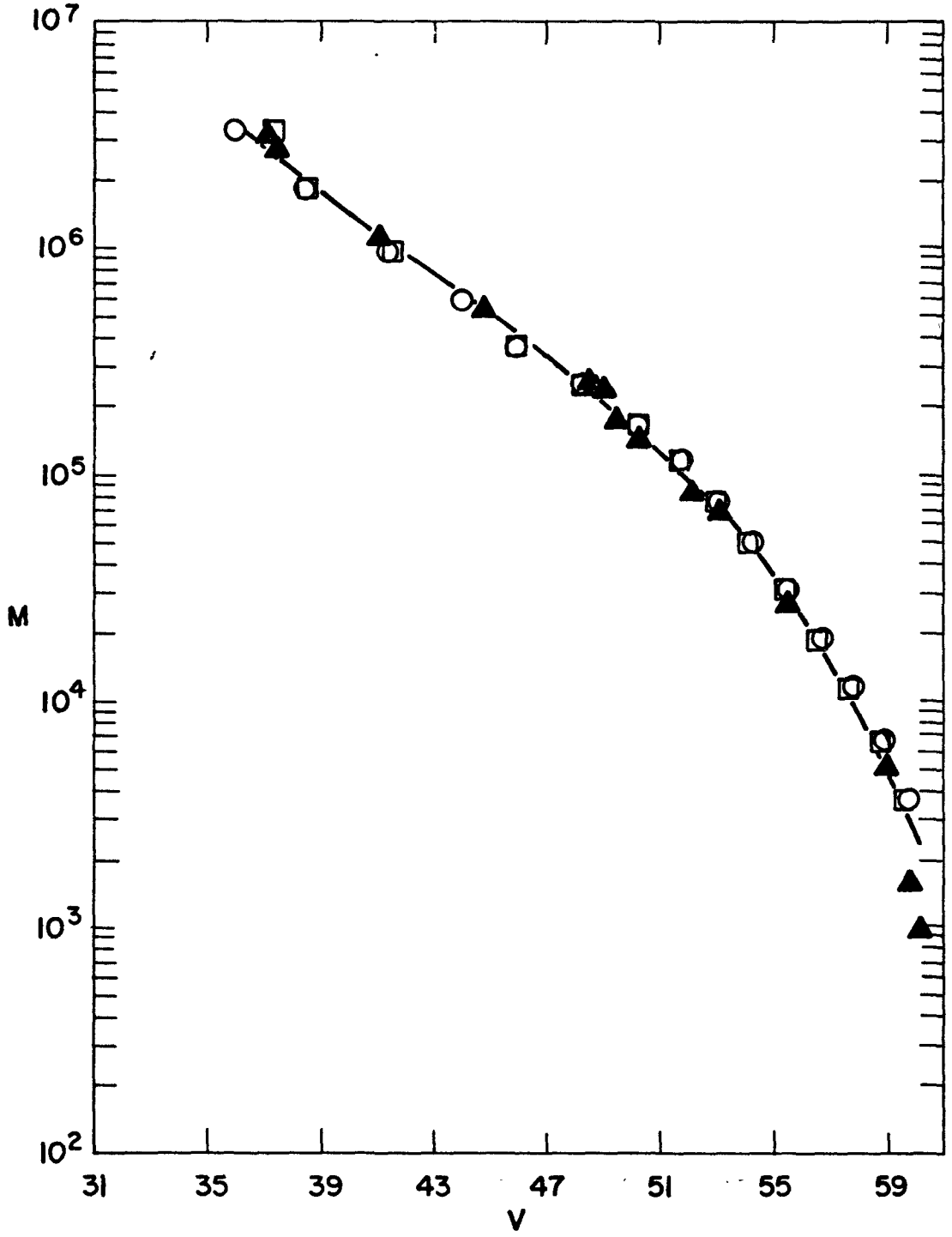

FIGURE II-11 : Calibration Curve for PMMA, COLUMN CODE 27

——— Polynomial used

▲ From universal calibration

□ From Weiss method (3.55 mg of RH PMMA std.; GPC No. 753)

○ From Weiss method (1.82 mg of RH PMMA std.; GPC No. 752)

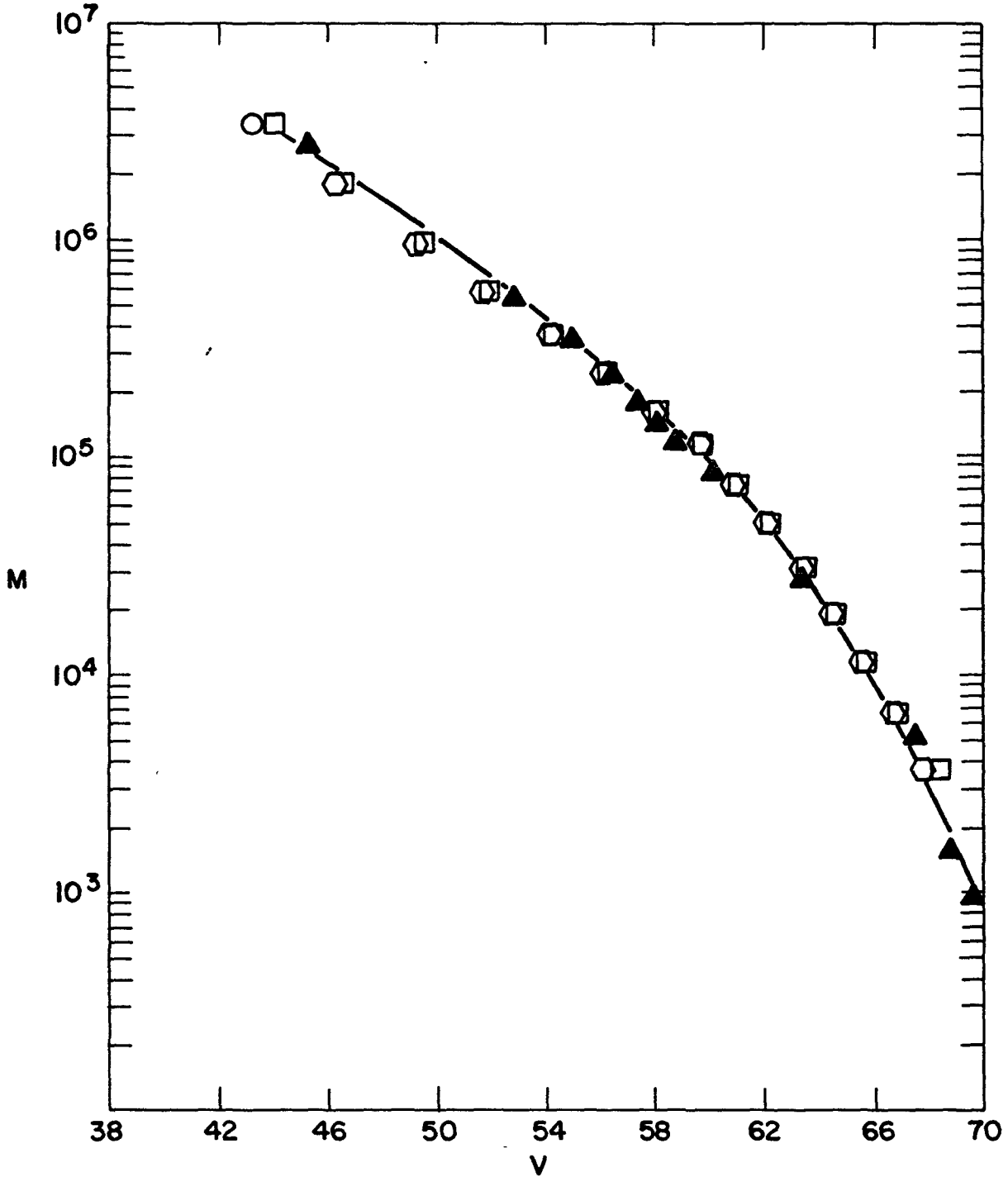

FIGURE II-12 : Calibration Curve for PMMA, COLUMN CODE 28.

——— Polynomial Used

▲ From Universal Calibration Curve

□ From Weiss Method (3.55 mg of RH PMMA Std; GPC No. 755)

⬡ From Weiss Method (5.33 mg of RH PMMA Std; GPC No. 754)

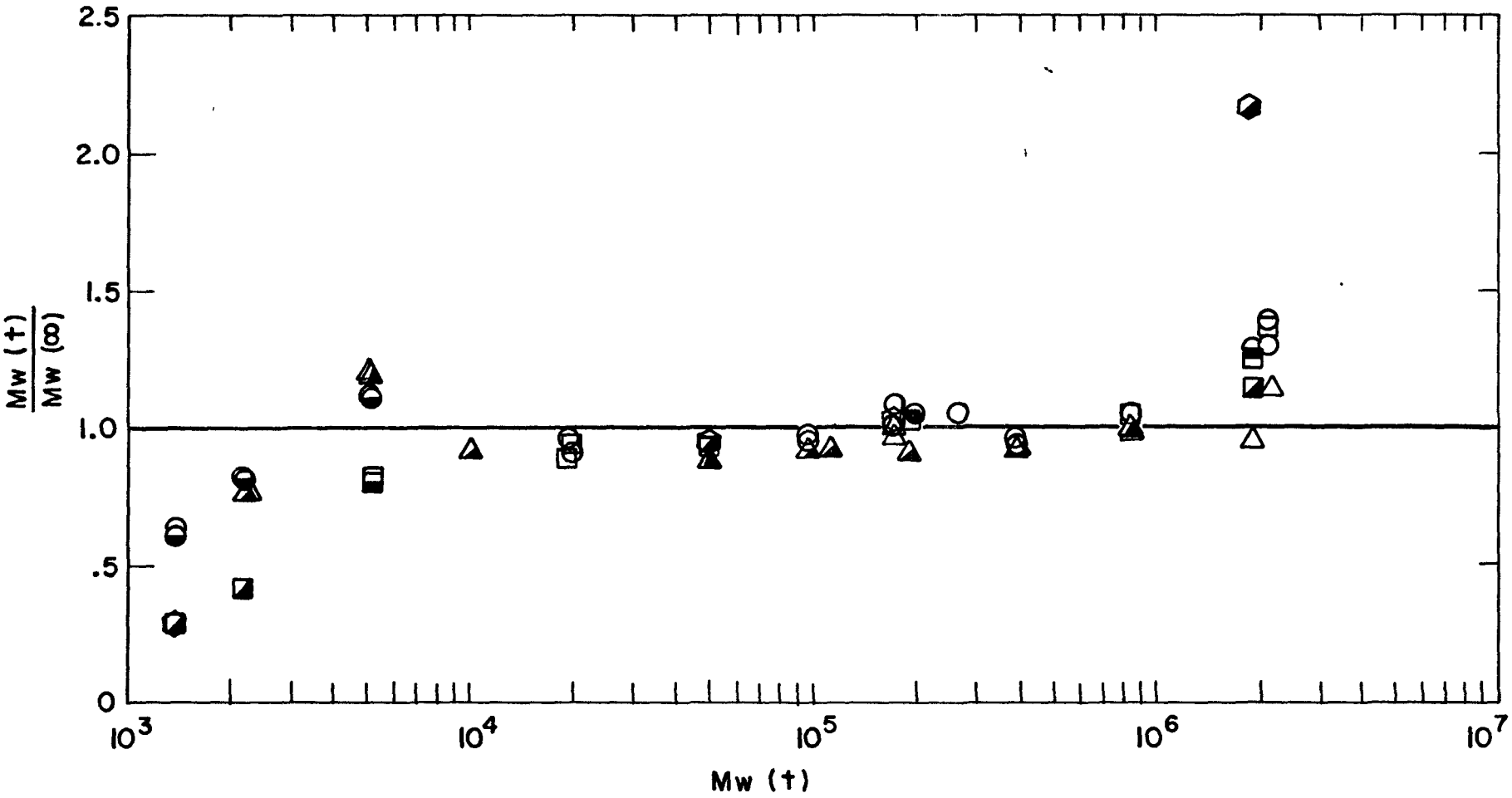

FIGURE II-14 : GPC and Absolute Mw Comparison (Polystyrene Standards) (Ref. Fig. 13 for Index)

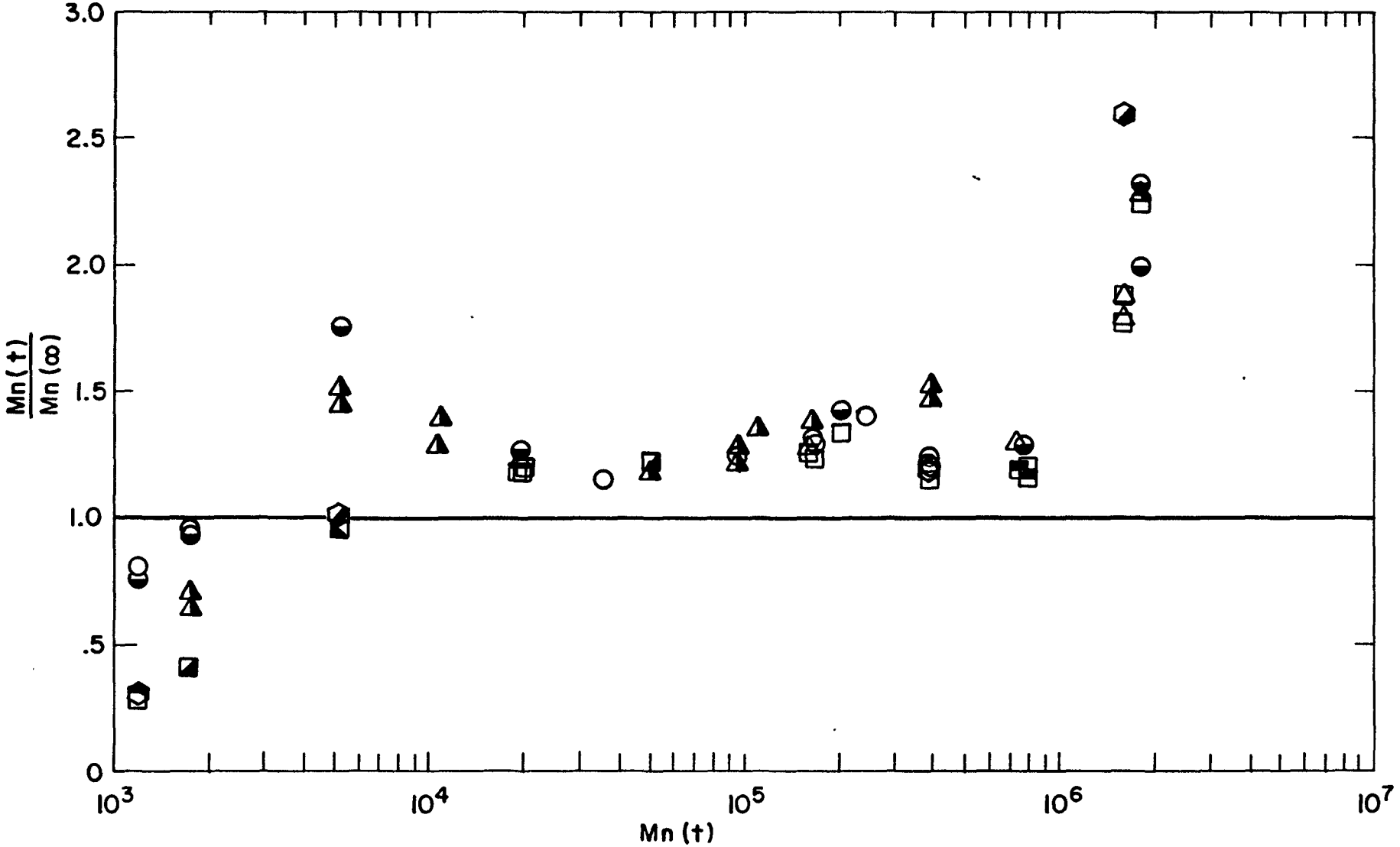

FIGURE II-13 : GPC and Absolute Mn Comparison (Polystyrene Stds)

COLUMN CODE 25:
- 1.8 mg
- .8 mg

COLUMN CODE 26:
- 1.8 mg

COLUMN CODE 27:
- 1.77 mg
- 1.81 mg
- 3.55 mg
- 3.99 mg

COLUMN CODE 28:
- 3.55 mg
- 5.33 mg

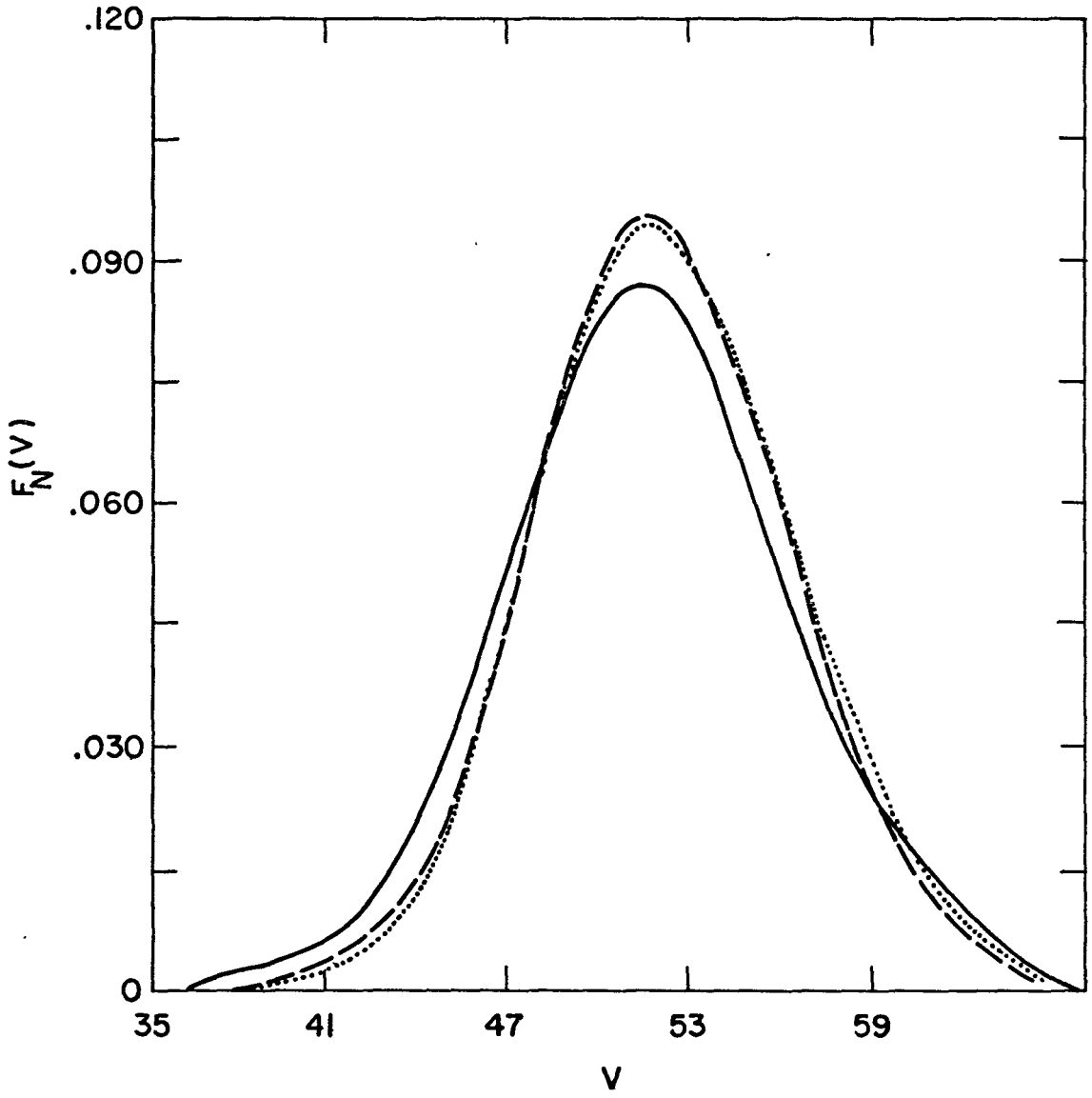

FIGURE II-15 : Experimental Chromatograms of Sample No. 41

Different Column Codes

——— CODE 25 (GPC No. 560)

— — — CODE 27 (GPC No. 626)

---------- CODE 28 (GPC No. 648)

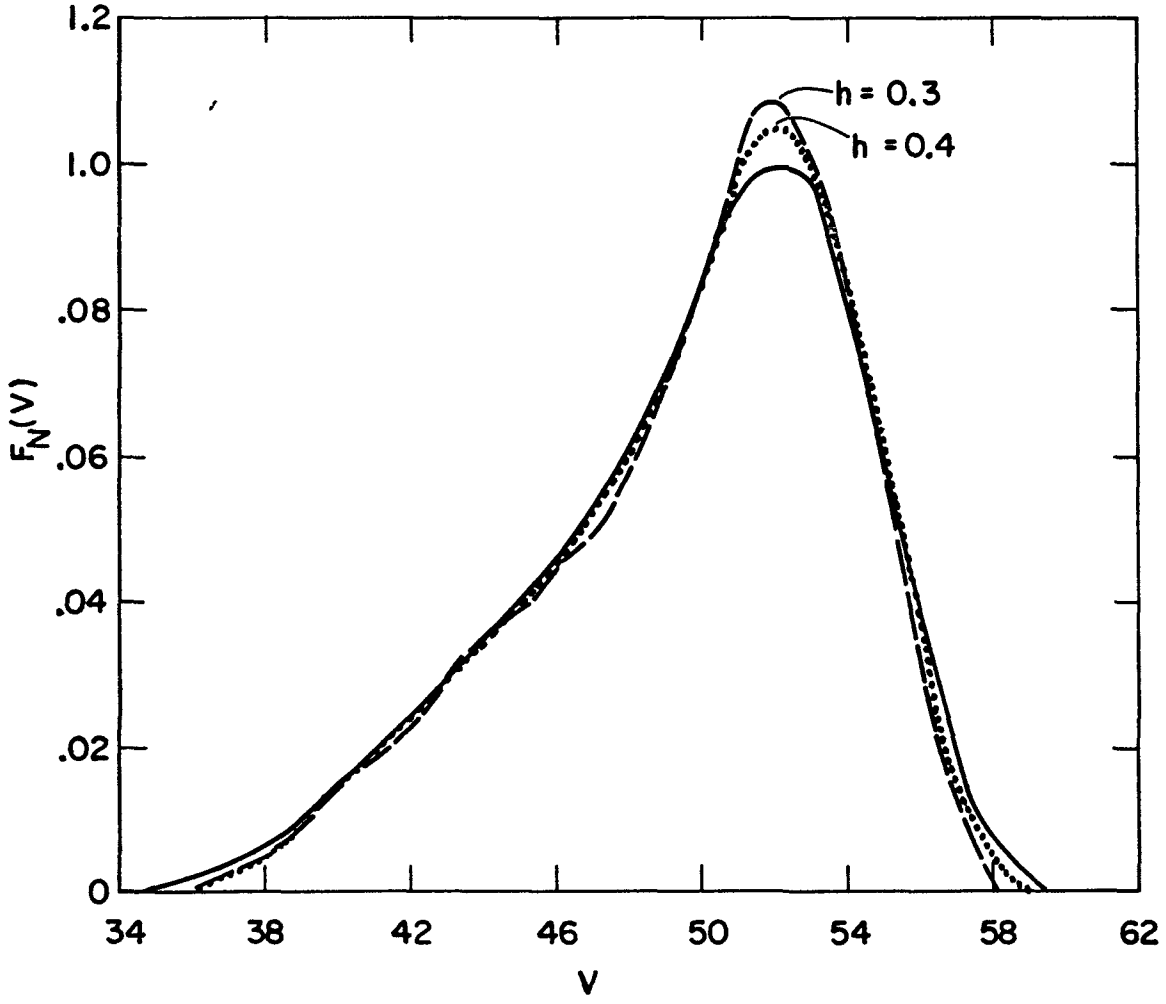

FIGURE II-16 : Effect of Symmetrical Axial Dispersion Correction on Chromatogram Heights

——— Experimental Chromatogram

-------- h = 0.3 } Chromatograms ($W_N(y)$) obtained

— — h = 0.4 } Using Method 2 with Smoothing

(Values of h = 0.2 and h = 0.1 showed oscillations due to numerical instabilities).

PART III

HIGH SHEAR VISCOMETRY

1. Introduction

In the processing of fluids, rheology is an important consideration. The constitutive equation of the fluid (the relationship between shear stress and rate of deformation) is necessary if the flow behavior is to be described through solution of the Equations of Motion. Newton's Law of Viscosity has been found to provide this relationship for some fluids at low shear conditions. However, the situation for many fluids, particularly polymers, and for all materials under very high shear conditions, can be more complicated and is much less well known, despite its industrial importance.

With polymers a basic cause of this situation is the long chain nature of their molecules. Through chain entanglements in concentrated solutions for example, non-Newtonian viscoelastic behavior can result.[1] Three reasons for the difficulties in elucidating the flow behavior of polymers at very high shear rates are: (1) polymer chains are liable to degrade and possibly react, (2) the characterization of polymers (MWD, branching and chemical composition) is difficult, and (3) instruments for measuring flow behavior, particularly at high shear, have design limitations which can cause data obtained using them to be difficult if not impossible to accurately interpret. Investigation of problems related to

the first two mentioned reasons are the subjects of Parts I and II of this thesis (i.e. polymerization kinetics and polymer analysis by GPC). This part of the work involved the initial steps in development of a suitable instrument in which to study polymer flow and polymer reactions in a shear field with emphasis on high shear. It should be noted that the study of polymer rheology includes the topics in the first two parts of this work, combined with fluid mechanics and mechanical engineering equipment design, and is a vast area for research.

2. Design Considerations

2.1 General

The object in designing an instrument to measure flow properties is usually to obtain "simple shear flow". That is, flow in which there is a significant component of velocity in only one direction.[2] Both shear stress and normal stress may be significant as a result of this velocity component. Analysis of simple shear flow is the most practical route to establishing a constitutive equation because the Equations of Motion can be solved in terms of the unknown shear stress and rate of deformation tensor components to give a relationship between these unknowns. However, the results obtained from only one instrument cannot be considered general enough to determine a complete constitutive equation, since this latter relationship must involve all of the components of the rate of deformation tensor.

Simple shear flow is often obtained by either flow through a capillary (Poiseuille Flow), flow between a cone and plate, or flow between concentric cylinders (Couette Flow). All of these instrument types have

advantages and disadvantages to a greater or lesser extent depending on their design details. A high shear concentric cylinder instrument was a reasonable choice for the work initiated here. In particular, it has the potential of giving a uniform, well defined shear field, and data which reflects no undesirable effects (notably temperature gradients).[3] Furthermore, the instrument could be based on a design which was proven practical for extremely high shear rates ($\sim 10^6 sec^{-1}$) by several investigators.[3-8] The original blueprints for the instrument were those of Porter et. al.[6]

The prime design considerations for high shear operation are discussed below with the viewpoint that the instrument will initially be used with Newtonian oils and later with polymer solutions or melts.

2.2 Fluid Mechanics

The derivation and notation which follow are largely based on that of Middleman.[2]

For Couette Flow, the velocity vector $\underline{v}$, has one component:

$$\underline{v} = (v_\theta, 0, 0) \qquad \text{(III-1)}$$

$$\text{and } v_\theta = v_\theta(r) = r\omega(r) \qquad \text{(III-2)}$$

where r is distance in the radial direction, v_θ is the tangential component of velocity and ω is the angular velocity (radians/sec). Also the rate of deformation tensor Δ has only the components

$$\Delta_{12} = \Delta_{21} = r \frac{d\omega}{dr} \equiv -\dot{\gamma} \qquad \text{(III-3)}$$

Let

$$f(\tau) \equiv -r \frac{d\omega}{dr} = \dot{\gamma} \qquad \text{(III-4)}$$

The objective in examining a fluid is to determine this relation from the experimental data: Torque and Shear Rate.

If the inner cylinder is driven with angular velocity Ω then the torque τ required to restrain the outer cylinder from moving when the gap is filled with the fluid is

$$\tau = \tau_{R_o} 2\pi R_o^2 L = \tau_{R_o} 2\pi \frac{R^2}{S^2} L \qquad \text{(III-5)}$$

where τ is shear stress

R is the radius of the inner cylinder (the rotor)

R_o is the radius of the hole in the outer cylinder (the stator)

and $S = R/R_o$

For this simple shear flow the only informative equation of motion will be the one in the θ-direction (tangential), which reduces to:

$$r^2 \tau = \text{constant}$$

Differentiation with respect to r shows that

$$\frac{d\omega}{dr} = - \frac{2\tau}{r} \frac{d\omega}{d\tau} \qquad \text{(III-6)}$$

Then

$$f(\tau) = \dot{\gamma} = - r \frac{d\omega}{dr} \qquad \text{(III-7)}$$

$$= 2\tau \frac{d\omega}{d\tau} \qquad \text{(III-8)}$$

Using the boundary condition that

$$\omega = 0 \text{ at } r = R_o \qquad \text{(III-9)}$$

and with τ_{R_o} the shear stress at the inner cylinder then at r = R by integration of Equation (III-8):

$$\Omega = \tfrac{1}{2}\int_{\tau_{R_o}}^{\tau_R} \frac{\dot{\gamma}}{\tau}\, d\tau \tag{III-10}$$

where Ω is the angular velocity of the inner cylinder.

Equation (III-10) is the basic relationship of interest. From

$$\tau_{R_o} R_o^2 = \tau_R R^2 \tag{III-11}$$

$$\frac{d\tau_{R_o}}{d\tau_R} = \left(\frac{R}{R_o}\right)^2 = \frac{\tau_{R_o}}{\tau_R} = S^2 \tag{III-12}$$

and differentiation of (Equation (III-10)) with respect to τ_R a difference equation for $f(\tau_R)$ results. Without assuming any relation for $f(\tau_R)$ the difference equation can be solved so that determination of $\frac{d\ln\Omega}{d\ln\tau_R}$ from the experimental data along with Ω, S, and τ_R yields $f(\tau_R)$.

If a power law relation is assumed

$$\tau = K\dot{\gamma}^n \tag{III-13}$$

$$= Kf(\tau)^n \tag{III-14}$$

$$f(\tau) = \frac{1}{K^{\frac{1}{n}}}\tau^{\frac{1}{n}} = a\tau^m \tag{III-15}$$

Substituting $f(\tau)$ into (III-10) and integrating using $\tau_{R_o} = S^2\tau_R$ gives

$$\Omega = \tfrac{1}{2}\, a\, \left(\frac{1-S^{2m}}{m}\right) \tau_R^m \tag{III-16}$$

$$f(\tau_R) = \frac{2\Omega m}{(1-S^{2m})} = a\,\tau_R^m \tag{III-17}$$

For a Newtonian Fluid

$$m = 1$$

$$f(\tau_R) = \dot{\gamma}_R = \frac{2\Omega}{(1-S^2)} = -r\frac{d\omega}{dr} \qquad \text{(III-18)}$$

Then, using the relationship between the measured torque and the shear stress on the surface of the outer cylinder:

$$\tau_R = \tau_{\frac{R_o}{S^2}} = \frac{\tau S^2}{S^2 R^2 2\pi L} = \frac{\tau}{R^2 2\pi L} \qquad \text{(III-19)}$$

Thus if Newtonian standards of known viscosity are used then the gap can be calculated from

$$\dot{\gamma}_R = \frac{2\Omega}{(1-S^2)} = \frac{\tau}{\mu R^2 2\pi L} \qquad \text{(III-20)}$$

$$S = \sqrt{1 - \frac{2\Omega\mu R^2 2\pi L}{\tau}}$$

Although Reches[8] used a very similar instrument to the one used here, he considered the measured torque to be

$$\tau' = \tau_R 2\pi R^2 L \qquad \text{(III-21)}$$

This is actually the torque at which the inner rotor is driven and hence the torque balanced by the fluid on the face of the inner rotor. The measured torque is actually that torque required to hold the outer cylinder stationary and hence the torque exerted by the fluid at the inner face of the outer cylinder and is given by equation III-5. The result of this was that instead of obtaining $\frac{1}{1-S^2}$ explicitly from Equation (III-20) Reches obtained $\frac{S^2}{1-S^2}$ and even approximated this by $\frac{1}{2}\left(\frac{S}{1-S}\right)$ since S was close to unity. The results of all these discrepancies are insignificant if S is very close to unity.

2.3 Viscous Heating and Temperature Rise

There are two important aspects of the results of temperature rise due to viscous dissipation: (1) the temperature at the film edges and (2) the maximum temperature rise through the film. Calculation of the first mentioned can be accomplished reliably using measured values of temperature. The second can only be estimated since it depends on the unknown constitutive equation and thus effort should be made in the instrument design to make it of probable insignificance.

2.3.1 Film Edge Temperature

As Reches[8] shows, from a straightforeward heat balance and use of Fourier's Law the temperature T_f at R_o (the radius of the hole) is calculated from the following equation when T_{R_1} (temperature at the outer radius of the outer cylinder (R_1)) and T_c (temperature at radial distance R_2) have been measured.

$$T_f = T_{R_1} + (T_{R_1} - T_c) \frac{\ln (R_o/R_1)}{\ln (R_1/R_2)} \qquad (III-22)$$

By having cooling fluid on the inside of the inner cylinder as well as the outside of the outer cylinder and having the heat path to the film the same distance in each case then the assumption that the other edge of the film (at least for a very narrow gap) is at the same temperature is reasonable. Then, if the maximum temperature rise through the film is negligible T_f is considered as the isothermal film temperature.

Often the film temperature cannot be precisely set to a constant value at all shear rates because of the inadequacy of the

temperature control system. To obtain data all at one temperature, it is then necessary to find some way of interpolating or extrapolating the result from data obtained at one or more temperatures.

Andrade's equation is often assumed for the variation of viscosity with temperature:

$$\eta = A' e^{-B'/T} \qquad \text{(III-23)}$$

where η is apparent viscosity, T is absolute temperature and A' and B' are constants.

Runs at two temperatures provide sufficient data to calculate A' and B'. Then these values can be used to calculate the viscosity at the desired temperature. If the viscosity is already known at several other temperatures for the sample (as for Newtonian Standards) a plot of log η versus $\frac{1}{T}$ can be used for interpolation. A universal plot of log η versus the reciprocal of temperature difference can also be used and is valuable once established for a type of material since it then requires only one experiment to obtain the viscosity at different temperatures if a material is a member of that type.[9]

The ratio of the viscosity at a desired temperature T to the viscosity at any temperature at which shear stress was actually measured T_m has been termed a viscosity factor and was used to change the shear stress value from T_m to that at the desired temperature, T.[8]

2.3.2 Maximum Temperature Rise

Although maximum temperature rise in the film may be estimated, if a simple form for the constitutive equation is assumed, by simultaneous solution of the momentum and energy equations,[2] since these forms are

generally uncertain except for Newtonian Standards, probably the best course of action here is to calculate the maximum temperature rise for Newtonian fluids with viscosities similar to the apparent viscosities to be encountered with non-Newtonian materials, and then to make this temperature rise negligible by altering the instrument design or operating conditions.

For Newtonian fluids the maximum temperature rise (ΔT) is given by:

$$\Delta T \approx \frac{\mu v_1^2}{8K} \qquad \text{(III-24)}$$

where μ is Newtonian viscosity, v_1 is velocity, and k is thermal conductivity of the film.

For very narrow gaps the shear rate may be approximated as follows by the assumption of a linear velocity profile:

$$\dot{\gamma} \approx \frac{v_1}{b} \qquad \text{(III-25)}$$

$$\Delta T = \frac{\mu b^2 \dot{\gamma}^2}{8K} \qquad \text{(III-26)}$$

where b is film thickness.

As already pointed out by other investigators.[2-7] Equation III-26 shows that high shear rates are best obtained by narrower gaps rather than higher RPM.

2.4 End Effects

Shear stress on the ends of the rotating cylinder can contribute significantly to the measured torque. In this instrument the film is suspended by surface tension in the annular gap. There is an air liquid interface above and below the film. It should be noted that as

with capillary rise, surface tension, not viscosity, is the important parameter in attaining suspension against the force of gravity. This design effectively eliminates end effects.

2.5 Concentricity

Concentricity of the inner cylinder in the concentric cylinder viscometer is not often considered as a problem in the rheology literature. In one case [10] it was noted that causing deliberate eccentricity in the particular apparatus resulted in no significant difference in results. The problem is not mentioned in previous publications [3-8] regarding the narrow gap high shear concentric cylinder viscometer (the instrument used in this study). The consistent and considerable discrepancies between annular gaps measured by micrometer and those calculated by running Newtonian standards in the instrument when very narrow gaps are used were always attributed to the fact that micrometer measurement tended to emphasize high spots on the surface.

Reches[8] considered the long secondary drive shaft to be a safety factor (meant to shear if the inner cylinder seized). Although he did point out that this shaft was balanced and periodically checked for alignment, he did not state how. Porter, [11] in a recent seminar at the University of Toronto, emphasized that the drive shaft was long and thin (actually a 1/8 inch O.D., 17 inch long steel drill rod) to provide self centering of the inner cylinder by the action of viscous forces in the gap. In a discussion of the Stormer Viscometer, a popular rheology text [12] mentions that two universal joints are supplied in the rotor shaft to permit self alignment by the action of viscous forces in the narrower portion of the

gap but that this sometimes resulted in an undamped pendulum-like motion of the rotor. The only reference quoted by this text on the concentricity problem is the 1939 publication of Inglis. [13]

Inglis derived an approximate relation for the effect of simple (two dimensional) eccentricity on the measured torque for a concentric cylinder viscometer containing a Newtonian fluid. Using a simplified Navier Stokes equation for the flow which neglected curvature:

$$\frac{\partial p}{\partial x} = \mu \frac{\partial^2 v_\theta}{\partial y^2} \qquad \text{(III-27)}$$

where μ = Newtonian viscosity

v_θ = velocity in the angular direction

p = pressure

x = distance in the angular direction

y = distance in the radial direction

He assumed narrow gap dimensions (compared to the radius of the inner cylinder) and solved for the pressure distribution as a function of angle due to the eccentricity. From this solution he derived the following expression for the viscous torque per unit height on the outer cylinder:

$$\frac{\tau}{L} \approx \frac{2\pi\mu v_1 R^2 (1-c^2)}{b} \qquad \text{(III-28)}$$

where v_1 = the velocity at the inner cylinder

b = the film thickness with zero eccentricity

c = the eccentricity ratio (distance between cylinder centers $\div$ b) = 0 for concentricity

R = radius of the inner cylinder

Qualitatively speaking, the eccentricity makes the channel wider in one portion than another. This results in a net decrease in fluid transport, a decrease in the average velocity of fluid and, since the finite velocity of the moving boundary and the zero velocity of the stationary boundary are fixed, an increase in shear rate near the moving boundary and a decrease near the stationary boundary. Thus shear stress on the stationary boundary is decreased while that on the moving boundary is increased.

Equation (III-28) shows that, as it should, for zero eccentricity it reduces to the expression given by Equation (III-20). However, it is clearly evident that torque measurement at high shear rates (narrow gaps and high velocities) can be severely affected by eccentricity. Since most instruments to date operate at low shear rate, or have wide gaps which cause other more obvious problems (e.g. temperature gradients) and end effects (since the film is then not suspended) it is easy to see why the problem of eccentricity has been given little attention.

A better understanding of the results and causes of eccentricity can be obtained from the Mechanical Engineering literature regarding vibration of rotating shafts[14] and lubrication of journal bearings.[15] A journal bearing may be considered as a horizontal concentric cylinder viscometer used to support a vertical load on the outer cylinder. It has been found that seizing or rough operation of the bearing can occur because of the combination of oil forces, shaft vibration and misalignment. The first mentioned topic is the main concern of lubrication

theory. The problem is dealt with by numerical solutions of the Reynolds Equation (this equation is really a momentum equation phrased in terms relevant to the thin film problem (e.g. film thickness and eccentricity) as well as velocity and pressure).[15] The pressure distributions obtained (most uncertain for non-Newtonian fluids) [16] indicate that a film force tends to center the inner cylinder for an absolutely zero load [17] situation but that this centering is unstable. This conclusion is by no means certain [18] because of the inherent complexity of the force situation, in particular the interaction of shaft vibration with oil forces. Whirl or whip (usually defined as a self perpetuating, often violent movement of the center of the inner cylinder with respect to the center of the outer cylinder) is often observed to be a problem in bearings at frequencies corresponding to one half shaft speed. The reason for this is unknown. With the concentric cylinder viscometer there is no gravitational load (unlike the usual bearing situation). The load is rotational and originates primarily from unbalancing or presence of a bend in the shaft or misalignment or interaction of the shaft movement with the oil forces. Balancing of such a shaft is still a subject of research as is the whole field of vibration in rotating shafts and lubrication of bearings.

From a polymer rheologist's point of view the state of the art is particularly unsatisfactory,since what progress there has been made towards this problem emphasizes the avoidance of actual bearing failure,or rough running,rather than exact prediction of the location of the inner cylinder center relative to the outer cylinder center. Design of bearings which encourage stable running at the expense of a well defined velocity profile is the main result.

Thus from the above discussion it is evident that eccentricity is complex, critical, and difficult to predict or eliminate for a narrow gap high shear concentric cylinder viscometer. The most practical course is either to measure it or to prove it negligible with respect to the desired torque measurement. The latter course is necessary and sufficient in the case of Newtonian fluids but uncertain for non-Newtonians. For the latter, electrical measurement[15] of eccentricity obtained is likely the best course of action.

2.6 Static Friction

"Friction is the resistance to motion which exists when a solid object is moved tangentially with respect to the surface of another which it touches or when an attempt is made to produce such a motion." [19] When movement is induced by a friction force F then the following expression may be written:

$$F = \tau_{av} * A_r \qquad \text{(III-29)}$$

where τ_{av} = average shear stress over the real area of contact

A_r = real area of contact

Thus the uncertainties of friction are lumped into A_r. The magnitude and variation of A_r is the unknown at which many explanations of friction are aimed. A_r is influenced by many factors: the nature of the materials in contact, the presence of lubricant and the time of application of the force F. It is well known that the F required to start sliding is usually greater than that required to maintain sliding. This has given rise to the simplification that a static friction and a kinetic friction exists.

With viscometers the only value of shear stress desired is that applied to the fluid whose viscosity is to be measured. Friction can add to the measured value of shear stress and therefore must either be made insignificant or measured. The main source of friction in the concentric cylinder viscometer is the contact between the support bearings and the outer cylinder. This can be made negligible by using an air bearing or by working at such high shear stresses that the frictional component is negligible.

Barber et.al.,[3] in experiments with the high shear concentric cylinder viscometer, claimed that torques measured while moving the support table in one direction and then in the other, are shearing torque plus, and shearing torque minus, support bearing friction. He mentioned that this cancellation procedure was significant only for the lowest torques. Reches[8] extrapolated the torque measured values to zero RPM to obtain estimates of static friction.

3. Development of the High Shear Viscometer

3.1 Description of the Original Instrument

The high shear viscometer constructed is basically the same as that used by Barber,[3] Reches[8] and Porter.[6] The original blueprints were those of Porter. The design considerations implemented in the instrument have already been outlined.

The apparatus can be considered to consist of the following main components:

(1) the thermostating system

(2) the transducing cell, the outer viscometer cylinder and its mountings

(3) the console containing the electronic controls

(4) the drive system

3.1.1 The Thermostating System

This system was similar to that of Reches.[8] The bath was a Blue M-Magni Whirl Model MW-1145A-1 Utility Oil Bath. Union Carbide UNICON HTF-30 heat transfer fluid was used. An Albany Model Gear Pump circulated the fluid. Control of flow rate was effected by adjusting the valves in the line. The fluid circulated around the outer cylinder in a brass retaining cup and was prevented from entering the film by a steel guard. Fluid also was sprayed into the inside of the inner cylinder.

3.1.2 Viscometer Table and Transducing Cell

The outer cylinder and its attachments were mounted on self aligning ball bearings. Shear stress was obtained by measuring the force exerted by the torque arm. This measurement was accomplished by positioning a Strathan UC3 Transducing Cell along the arm at one of seven positions. Two pulleys were mounted opposite each other on needle bearings at the end of the torque arm. They permitted calibration of the transducing cell against known weights and accurate positioning of the arm. The transducing cell permitted a range of zero to 0.5 lbs. and zero to 5 lbs. force depending on the cell adapter used. The power supply used for the cell was very similar to that used by Porter except, for these cells, a 7 volt excitation was required. Figure I-1 shows the cylinders.

Both inner and outer cylinders were originally constructed of SAE4140 carbon steel. Although a range of shear clearances were available by varying the diameter of the inner cylinder only a clearance of 1.3×10^{-3} inches (by micrometer measurement) was used here.

Samples were injected by using a glass syringe connected through a Luer-Lok fitting to the sample inlet tubes.

3.1.3 Electronic Controls

A Sargent Two Pen Recorder Model DSRG was used to record torque and temperature.RPM control was the same as Porter's. Measurement of RPM was by stroboscope.

3.1.4 Drive System

A 1 HP Reliance Electric Co. Type T DC Motor was used to drive overhead pulleys which in turn drove a secondary shaft. This secondary shaft held a chuck which attached to a 17" long 1/8 inch diameter flexible steel shaft which was in turn attached to the top of the inner cylinder. Speed control and drive ratio changes were identical to Porter's.

3.2 Development of the Instrument

The following major modifications were found to be necessary:

(1) The 1 HP drive motor was mounted on a concrete pillar to reduce vibrations (Porter's plans had called for this motor to be on the floor). Reches[8] also found this modification necessary.

(2) The material of construction was changed to Stainless Steel 430. The mild steel originally used corroded very easily. Use of the new material sacrificed some temperature control (the thermal conductivity of SS430 is 15.1 Btu/hr ft^2 at 212°F.) but use of interpolation methods (ref. section 2.3.1) were known to be necessary anyway because of the inadequacy of the temperature control system.

(3) The reservoir for coolant fluid was shortened and the fluid guard

removed (for the last run only) to permit (for future runs with polymers) cleaning of the top of the viscometer previous to removing and washing the inner cylinder with solvent for analysis by injection into the GPC (The instrument could also be run using continuous feed if necessary to obtain more material for analysis). For room temperature runs the effect of this modification is negligible. For higher temperature runs presence of an undesirable axial temperature gradient along the film is possible. Its presence would be indicated by the thermocouple measurements.

(4) The 1/8 inch O.D. 17" long drill rod used by all previous investigators gave large "measured torque" vibration which were evidently due to eccentricity, and most severe at low rpms. The inner rotor finally cocked and jammed. The shaft stretched and bent but did not shear.

Two other shafts were then tried: (1) a similar rod equipped with a universal joint at the cylinder end and (2) a completely flexible shaft made from the flexible attachment to a portable electric drill. The first provided no improvement in torque measurement--erratic vibrations were still evident. The second provided smooth measurement at low RPM's but was obviously too flexible for use at high RPM's. The shaft finally used was semi flexible. It consisted of a 29.7 cm length of 0.65cm O.D. steel tubing attached to 3.1 cm of flexible shaft at each end. It provided good results apparently for several reasons. The central rigid portion is tubular so that unbalance was less severe. The flexible end pieces allowed for imperfect alignment and provided damping of shaft vibrations. The net effect was that the rotational load to the inner cylinder was reduced. Soft iron pins at each end served as safety measures by shearing

if the inner cylinder seized in the outer.

3.3 Development of Experimental Procedure

3.3.1 Preliminary Procedure

(a) The pump in the thermostating system and the coolant flow in the heat exchangers were started up about three hours previous to the actual run.

(b) The flow rate of coolant from the spray was maintained at greater than the minimum required to obtain a true spray in the inner rotor. (33ml/min. at room temperature for the system used).

(c) The sample was injected at least 15 minutes in advance of the run. Table III-1 shows the viscosity standards used.

(d) The run was begun when all thermocouples registered no change in temperature.

3.3.2 Calibration of the Transducer Cell

(a) Sufficient weight was attached to the foreward pulley to cause a positive response on the recorder from the pressure on the transducer cell by the torque arm.

(b) Known weights were hung on the other pulley and the pen deflection of the recorder was recorded. These data provided the calibration curve.

Two points are worthy of note here: (1) More reproducible results were obtained by the above procedure than by trying to tare (balance) the torque arm in step (a) by addition of weights to both pulleys (the good linearity of response of the transducer cells combined with the nature of the static friction were the likely reasons for this situation), and (2) the rate of application of the force (both in calibration and later with non zero rpms) was kept reasonably uniform by gently easing the

torque arm on to the transducer after the weight had been hung, (or after the rpm had been set). This was accomplished by having the arm resting against the flat of a disc which was threaded to the cell mounting. The arm was applied against the cell by wheeling the disc towards the cell after force was present on the torque arm.

3.3.3 Measurement of Sample Flow Properties

(a) An rpm was set and measured by stroboscope.

(b) The force required to maintain the outer cylinder stationary was measured by allowing the torque arm to contact the transducer cell (as in calibration).

(c) All thermocouple readings were registered by one pen of the two pen recorder by using a consecutive switching arrangement.

(d) The torque arm was then moved back from the cell.

(e) The above steps (a) through (d) were repeated for another rpm.

Calibrations were carried out before and after each run. RPM's were begun low, raised into steps the highest value to be used for the run and then taken down in steps.

3.4 Testing the Instrument with Newtonian Standards

3.4.1 Temperature

From the thermocouple measurements presence of an axial temperature gradient was checked. Temperature at the edges of the film was calculated using Equation(III-22). Maximum temperature rise was estimated using Equation (III-26). Temperatures calculated from thermocouple measurements are given in Table III-2. No axial temperature gradient was observed and temperature rise across the film was low.

3.4.2 Flow Measurements ---Calculation of Annular Gap

3.4.2.1 RPM

RPM was measured directly and is shown in Table III-4.

3.4.2.2 Torque

The calculations required for torque calculation were as follows:

(a) A calibration curve for the transducer cell response for the run was obtained by a least squares fit of pen deflection, G, on the recorder chart versus weight required to obtain the deflection (placed on the back pulley) W. Response was linear so

$$G=A+B*W \qquad (III-30)$$

(b) The weight on the pan (W_o) at zero pen deflection was calculated from Equation (III-30) by setting G=0. That is, forces above this value were assumed to be sufficient to overcome both static friction of the self aligning ball bearings on the outer cylinder and the weight hung on the foreward pulley. Reches[8] approach could not be used because of the higher film temperatures at higher shear rates. Results of the above steps ((a) and (b)) are shown in Table III-3.

(c) Pen deflection at different RPM's were used along with the calibration curve (Equation (III-30)) to obtain the total measured force (=the result of shear stress exerted by the liquid in the gap on the inner wall of the outer cylinder plus the result of shear stress exerted by the ball bearings rubbing against the bottom of the outer cylinder (static friction) plus the force of the weights hung on the foreward pulley, equals the desired force $+W_o$).

(d) Torques were calculated by multiplying each measured force and W_o by the distance from the point at which the string over the pulleys was attached, to the centre of the rotor.

(e) The desired torque (that due to liquid flow) was obtained by subtracting the torque due to W_o from the measured torque at each rpm.

(f) The torque at the desired reference temperature could then be obtained by multiplying by the viscosity factor.

Results of the above steps ((c), (d) and (f)) are shown in Table III-4.

3.4.2.3 Gap Estimate

Point estimates of gap width using Equation III-20 are shown in Table III-4. The final estimate however was made by a least squares fit of Torque vs. rpm data from all runs (shown in Figure III-2). The gap width was found to be $(1.207 \pm .007) \times 10^{-3}$ in. and $(1.184 \pm .031) \times 10^{-3}$ in. using the high and low viscosity standards respectively. This agreed with micrometer measurement (1.3×10^{-3} in).

4. Summary

The main design considerations for a high shear concentric cylinder viscometer were reviewed and discussed. Attention was drawn to the importance of concentricity of the inner cylinder in the outer, a topic insufficiently considered in the rheology literature.

The viscometer was constructed and modifications in apparatus along with developments in procedure permitted successful analysis of Newtonian standards.

5. Conclusions

(1) A semi flexible shaft and other instrument modifications permitted acceptable concentricity for the Newtonian standards examined.

(2) The experimental procedure developed reproducibly accounted for static friction in torque measurement.

6. Recommendations

(1) Eccentricity should be precisely measured electrically for non Newtonian fluid testing.

(2) Effects of normal stress and evaporation of film are likely sources of future problems. A blanket of fluid maintained as the surface edge of the film is the likely solution. End effects would be negligible because of the large diameter of the top end of the cylinder.

(3) Consideration should be given to continuous fluid feed operation to obtain larger sample sizes for GPC analysis, although for concentrated polymer solutions batch experiments will likely be sufficient.

7. Nomenclature

a	constant in Power Law
A,B	constants in transducer cell calibration curve
A_r	real area of contact (cm^2)
A',B'	constants in Andrade Equation
b	film thickness (in)
c	eccentricity ratio
F	friction force (dynes)
$f(\tau)$	function of shear stress defined by Eqn. (III-4)
G	recorder pen deflection due to force
k	thermal conductivity (BTU ft/ft^2 sec^oF)
K	constant in Power Law - Eqn. (III-13)
L	length of shear area (in)
MWD	molecular weight distribution
m	constant in Power Law
n	constant in Power Law
p	pressure (psi)

r	radial coordinate (in)
R_o	inner radius of outer cylinder (radius of hole)(in)
R_1	outer radius of outer cylinder (in)
R_2	radial distance to thermocouples in outer cylinder (in)
R	radius of inner cylinder (in)
S	R/R_o
T	temperature (^oC)
T_f	temperature at R_o (^oC)
T_c	temperature at R_2 (^oC)
T_{R_1}	temperature at R_1 (^oC)
T_m	temperature at which shear stress was measured (^oC)
T_1, T_2, T_3, T_4	temperatures in outer cylinder (averaged to obtain T_c) (^oC)
$\underline{v}$	velocity vector
v_1	velocity of inner cylinder (in/sec)
v_θ	tangential component of velocity (in/sec)
W	weight (gms)
W_o	weight at zero pen deflection (gms)
x,y	cartesian co-ordinates - Eqn. (III-27)

Greek Symbols

τ_{av}	average shear stress of real area of contact (dynes(cm)$^{-2}$)
τ	shear stress (dynes(cm)$^{-2}$)
τ'	torque at inner cylinder surface ($g_f$cm)
τ	torque at outer cylinder surface ($g_f$cm)
ω	angular velocity across gap (radians/sec)
θ	angular co-ordinate (radians)
$\dot{\gamma}$	shear rate (sec)$^{-1}$
$\underline{\underline{\Delta}}$	rate of deformation tensor
ΔT	maximum temperature rise (^{o}C)
Ω	angular velocity of inner cylinder (radians/sec)
η	viscosity (poise)
μ	Newtonian viscosity (poise)

8. References

1. Graessley, W. W.,
"Molecular Aspects of Viscoelasticity in Concentrated Polymer Systems",
ACS Polymer Preprints, 13, 35 (1972).

2. Middleman, S.,
"The Flow of High Polymers",
Interscience Publishers, New York (1968).

3. Barber, E. H., Muenger, J. R., Villforth, F. J.,
Anal. Chem., 27, 3 (1955).

4. Porter, R. S., Johnson, J. F.,
J. Phys. Chem., 63, 202 (1959).

5. Porter, R. S., Johnson, J. F.,
J. Appl. Phys., 35, 3149 (1964).

6. Porter, R. S., Klaver, R. F., Johnson, J. F.,
Rev. Scientific Inst., 36, 1846 (1965).

7. Porter, R. S., Johnson, J. F., Cantow, M. J. R.,
J. Polymer Sci., 16, 1 (1967).

8. Reches, E.,
"Studies of the Flow Properties Under High Shear Rates of Selected Organic Compounds in the Molecular Weight Range of Lubricating Oils",
Ph.D. Thesis, University of Cincinatti, Cincinatti, Ohio, (1967).

9. Pierce, P. E.,
J. Paint Technology, 41, 383 (1969).

10. Harper, J. C.,
Rev. Scientific Inst., 32, 425 (1960).

11. Porter, R. S.,
Seminar,
University of Toronto, (1968).

12. Van Wazer, J. R., Lyons, J. W., Kim, K. Y., and Colwell, R. E.,
"Viscosity and Flow Measurement",
Interscience Publishers, New York (1963).

13. Inglis, D. R.,
Phys. Rev., 56, 1041 (1939).

14. Bishop, R. E. D., and Parkinson, A. G.,
Appl. Mech. Rev., 21, 439 (1968).

15. Cameron, A.,
"The Principles of Lubrication",
John Wiley and Sons Inc., New York (1966).

16. Tao, F. F., Philippoff, W.,
ASLE Trans., 10, 302 (1967).

17. Hori, Y.,
J. Appl. Mechanics, Trans. of ASME, 189 (1959).

18. Martin, F. A.,
Paper No. 63-LUBS-8,
"Steady-State Whirl in Journal Bearings for a Vertical Flexible Rotor System",
1963 ASME Lubrication Symposium.

19. Rabinowicz, E.,
"Friction and Wear of Materials",
John Wiley and Sons, Inc., New York (1965).

TABLE III-1

CALIBRATION STANDARDS FOR HIGH SHEAR VISCOMETER

SOURCE:
CANNON INSTRUMENT COMPANY
P.O. BOX 16
STATE COLLEGE, PENNSYLVANIA 16801

T(°C)	Std. # S-200-68-11 μ (c.p.)	Std. # S-20-68-2b μ (c.p.)
20.00	557.5	40.98
25.00	389.6	31.42
37.78	172.9	17.41
98.89	14.27	3.052

Table III-2

Temperature Data

SAMPLE #	T_1	T_2	T_3	T_4	T_{R_1}	T_f	ΔT
RUN SR7 STD S-200-68-11							
1	22.8	22.8	22.8	22.8	22.2	23.0	.004
2	23.2	23.2	23.2	23.2	22.2	23.5	.005
3	23.6	23.6	23.6	23.6	22.0	24.0	.007
4	23.8	23.8	23.8	23.8	22.0	24.3	.010
5	24.2	24.2	24.2	24.2	22.2	24.8	.013
6	24.8	24.8	24.8	24.8	22.5	25.4	.016
7	23.6	23.6	23.6	23.6	22.0	24.0	.005
RUN SR8 STD S-200-68-11							
1	23.3	23.3	23.2	23.2	22.9	23.3	.003
2	23.4	23.4	23.4	23.4	23.0	23.6	.005
3	23.9	23.9	23.9	23.9	23.0	24.1	.007
4	24.4	24.4	24.4	24.3	23.2	24.7	.010
5	25.1	25.2	25.2	25.2	23.4	25.6	.015
6	24.4	24.4	24.4	24.3	23.4	24.6	.007
7	24.4	24.4	24.4	24.4	23.3	24.7	.010
RUN SR9 STD S-200-68-11							
1	22.0	22.0	22.0	22.0	21.6	22.1	.004
2	22.5	22.5	22.5	22.5	21.6	22.7	.008
3	23.7	23.8	23.8	23.7	21.7	24.3	.016
4	23.6	23.7	23.7	23.7	21.8	24.2	.010
5	23.2	23.2	23.1	23.0	22.0	23.4	.005
6	23.8	23.8	23.8	23.7	22.0	24.2	.014
7	25.2	25.4	25.4	25.1	22.1	26.1	.026

Table III-2 (CONTINUED)

Temperature Data

RUN SR10 STD S-200-68-11

SAMPLE #	T_1	T_2	T_3	T_4	T_{R_1}	T_f	ΔT
1	25.6	25.7	25.8	25.5	22.5	26.5	.024
2	28.7	29.1	29.2	28.2	23.1	30.3	.049
3	32.0	32.4	32.6	31.6	24.0	34.2	.075
4	35.2	35.6	36.1	34.7	24.7	38.1	.097
5	37.8	38.7	38.8	37.2	25.0	41.4	.121
6	40.4	41.0	41.4	39.8	25.8	44.4	.147
7	43.3	44.1	44.7	42.7	26.7	48.0	.190
8	46.4	47.2	47.7	45.6	27.4	51.7	.205
9	48.8	49.7	50.2	47.7	28.1	54.5	.231
10	47.2	47.8	48.7	46.2	28.5	52.4	.203
11	45.0	45.0	46.4	44.3	28.3	49.5	.175
12	37.6	38.0	38.4	36.8	26.6	40.5	.094
RUN SR11 STD S-200-68-11							
1	28.8	28.9	28.9	28.8	28.3	29.0	.002
2	29.1	29.2	29.2	29.2	28.4	29.4	.005
3	29.5	29.6	29.6	29.5	28.5	29.8	.009
4	29.7	29.9	29.9	29.8	28.6	30.1	.011
5	29.7	29.8	29.8	29.7	28.6	30.0	.006
6	29.4	29.4	29.4	29.4	28.7	29.6	.003
SUN SR13 STD S-20-68-11							
1	17.5	17.6	17.6	17.5	16.3	17.9	.005
2	18.1	18.2	18.2	18.2	16.7	18.6	.009
3	19.1	19.3	19.3	19.0	17.5	19.6	.015
4	19.7	20.0	20.0	19.7	18.0	20.3	.019
5	19.5	19.7	19.7	19.7	18.1	20.0	.012

Table III-2 (CONTINUED)

Temperature Data

SAMPLE #	T_1	T_2	T_3	T_4	T_{R_1}	T_f	ΔT
6	19.0	18.9	18.9	18.7	17.7	19.2	.006
7	18.3	18.3	18.3	18.6	17.4	18.6	.001
8	18.1	18.1	18.1	18.1	17.2	18.4	.000
SR12A STD S-20-68-2B							
1	24.9	25.0	25.0	25.0	24.9	25.0	.003
2	25.3	25.5	25.5	25.4	24.9	25.6	.006
3	26.4	26.5	26.5	26.3	25.0	26.8	.011
4	28.1	28.2	28.3	28.1	24.7	29.1	.030
5	30.6	31.1	31.0	30.8	25.2	32.3	.046
6	33.3	33.5	33.5	32.8	25.7	35.2	.066
7	32.8	32.8	33.0	32.4	26.2	34.4	.049
RUN SR12B STD S-20-68-2B							
1	23.4	23.2	23.4	23.3	22.4	23.5	.004
2	24.5	24.4	24.4	24.2	22.5	24.9	.016
3	26.4	26.4	26.4	26.3	23.2	27.2	.028
4	27.7	27.7	27.6	27.3	23.6	28.6	.039
5	30.5	30.4	30.5	30.0	24.4	31.9	.061
6	30.2	30.2	30.3	30.2	24.5	31.7	.048
7	29.3	29.3	29.3	29.0	24.6	30.4	.036
8	28.6	28.6	28.7	29.0	24.7	29.7	.021
9	27.5	27.6	27.6	27.6	24.7	28.3	.002

TABLE III-3

CALIBRATION OF THE TRANSDUCER CELL

STD. # S-200-68-11

			PEN DEFLECTION		COEFFICIENTS OF EQN. (III-30)	
RUN SR7	NO.	WEIGHT (GMS.)	EXP	FROM FIT	A	B
	11	80.00	9.20	9.09	-41.132	0.628
	12	90.00	15.50	15.36		
	13	100.00	21.70	21.64		
	14	100.00	21.50	21.64		
	15	110.00	27.50	27.92		
	16	140.00	46.50	46.75		
	17	160.00	59.50	59.30		
	18	120.00	34.50	34.20		
RUN SR8	9	80.00	4.90	4.88	-45.231	0.626
	10	90.00	11.10	11.14		
	11	110.00	23.50	23.67		
	12	100.00	17.50	17.41		
	13	150.00	48.50	48.72		
	14	160.00	55.10	54.99		
	15	130.00	36.40	36.20		
RUN SR9	10	90.00	13.40	12.11	-45.864	0.644
	11	120.00	26.00	31.44		
	12	160.00	57.90	57.21		
	13	140.00	45.30	44.32		
	14	180.00	71.00	70.09		
	15	80.00	7.25	5.67		
RUN SR10	12	80.00	1.60	1.60	-12.490	0.176
	13	130.00	10.50	10.41		
	14	230.00	28.10	28.02		
	15	130.00	10.50	10.41		
	16	80.00	1.60	1.60		
	17	150.00	13.70	13.93		
	18	250.00	31.40	31.54		
	19	220.00	26.40	26.26		
	20	120.00	8.60	8.64		
RUN SR11	7	130.00	37.20	37.00	-43.176	0.617
	8	130.00	37.20	37.00		
	9	80.00	6.00	6.17		
	10	80.00	6.20	6.17		
	11	80.00	6.00	6.17		
	12	80.00	5.90	6.17		
	13	130.00	36.90	37.00		
	14	130.00	37.20	37.00		
	15	150.00	49.00	49.34		
	16	150.00	49.10	49.34		
	17	120.00	31.10	30.84		
	18	120.00	30.90	30.84		
	19	90.00	12.40	12.33		
	20	90.00	12.60	12.33		

TABLE III-3 (CONTINUED)

RUN SR13	10	80.00	6.40	6.73	-43.385	0.626
	11	80.00	6.40	6.73		
	12	80.00	6.00	6.73		
	13	80.00	6.00	6.73		
	14	130.00	37.30	38.06		
	15	130.00	38.00	38.06		
	16	160.00	56.40	56.85		
	17	160.00	56.60	56.85		
	18	150.00	51.00	50.59		
	19	150.00	51.10	50.59		
	20	100.00	20.00	19.26		
	21	100.00	19.90	19.26		
	22	100.00	19.90	19.26		
	23	70.00	1.20	.47		
	STD. # S-20-68-2B					
RUN SR12A	8	80.00	6.50	6.53	-43.261	0.622
	9	100.00	18.90	18.98		
	10	150.00	50.20	50.10		
	11	150.00	50.20	50.10		
	12	130.00	37.10	37.65		
	13	130.00	38.50	37.65		
	14	150.00	49.70	50.10		
RUN SR12B	4	140.00	43.50	43.75	-43.222	0.621
	5	140.00	43.60	43.75		
	6	140.00	43.30	43.75		
	7	120.00	30.90	31.32		
	8	120.00	31.40	31.32		
	9	120.00	31.10	31.32		
	10	80.00	6.20	6.48		
	11	80.00	6.30	6.48		
	12	100.00	19.50	18.90		
	13	100.00	19.20	18.90		
	14	100.00	19.30	18.90		
	15	150.00	50.40	49.96		
	16	150.00	50.40	49.96		
	17	160.00	56.10	56.17		
	18	160.00	56.30	56.17		
	19	130.00	37.40	37.54		
	20	130.00	37.30	37.54		

TABLE III-4

SHEAR RATE-SHEAR STRESS DATA

STD. # S-200-68-11

RUN		RPM	TORQUE	VISCOSITY (POISE)	GAP	$\dot{\gamma}$ ($\frac{1}{sec}$)	τ ($\frac{dynes}{cm^2}$)	VISCOSITY FACTOR	TORQUE AT 20°C
SR7	1	111	1141.6	4.5017	1.129E-03	5.130E+03	2.330E+04	1.2384	1413.8
	2	138	1347.1	4.3295	1.144E-03	6.294E+03	2.750E+04	1.2877	1734.7
	3	167	1550.2	4.1776	1.161E-03	7.505E+03	3.165E+04	1.3345	2068.8
	4	194	1768.1	4.1054	1.162E-03	8.711E+03	3.609E+04	1.3580	2401.1
	5	224	1941.5	3.9589	1.178E-03	9.918E+03	3.963E+04	1.4082	2734.0
	6	254	2139.6	3.7910	1.161E-03	1.141E+04	4.368E+04	1.4706	3146.4
	7	142	1396.7	4.1821	1.0969E-03	6.7557E+03	2.850E+04	1.3331	1861.9
SR8	1	111	1077.1	4.3802	1.165E-03	4.973E+03	2.199E+04	1.2728	1370.9
	2	137	1290.5	4.3150	1.182E-03	6.048E+03	2.635E+04	1.2920	1667.3
	3	167	1489.0	4.1484	1.200E-03	7.259E+03	3.040E+04	1.3439	2001.1
	4	196	1697.5	3.9909	1.189E-03	8.602E+03	3.466E+04	1.3969	2371.3
	5	254	2054.9	3.7347	1.191E-03	1.113E+04	4.195E+04	1.4927	3067.4
	6	170	1474.2	4.0127	1.194E-03	7.429E+03	3.010E+04	1.3894	2048.1
	7	200	1722.3	3.9804	1.192E-03	8.7500E+04	3.516E+04	1.4006	2412.3
SR9	1	111	1194.5	4.7732	1.144E-03	5.062E+03	2.438E+04	1.1680	1395.1
	2	166	1628.8	4.5879	1.206E-03	7.179E+03	3.326E+04	1.2152	1979.3
	3	249	2203.1	4.1010	1.196E-03	1.086E+04	4.498E+04	1.3594	2994.9
	4	198	1773.6	4.1341	1.191E-03	8.676E+03	3.621E+04	1.3485	2391.8
	5	138	1303.0	4.3557	1.190E-03	6.050E+03	2.660E+04	1.2799	1667.8
	6	233	2043.9	4.1167	1.211E-03	1.004E+04	4.173E+04	1.3542	2767.9
	7	336	2569.9	3.6237	1.222E-03	1.4339E+04	5.247E+04	1.5385	3953.8

TABLE III-4 (CONTINUED)

SR10	1	327	2524.3	3.5386	1.183E-03	1.443E+04	5.153E+04	1.5755	3976.9
	2	529	3124.4	2.7604	1.206E-03	2.289E+04	6.379E+04	2.0196	6310.2
	3	738	3353.9	2.1526	1.222E-03	3.150E+04	6.848E+04	2.5899	8686.1
	4	945	3468.6	1.6970	1.193E-03	4.133E+04	7.082E+04	3.2851	11395.0
	5	1165	3530.4	1.3985	1.191E-03	5.105E+04	7.209E+04	3.9864	14073.8
	6	1400	3530.4	1.1783	1.206E-03	6.073E+04	7.208E+04	4.7313	16703.4
	7	1755	3512.8	.9649	1.244E-03	7.361E+04	7.173E+04	5.7779	20296.6
	8	2018	3459.8	.7906	1.190E-03	8.849E+04	7.064E+04	7.0513	24396.2
	9	2300	3371.6	.6841	1.204E-03	9.965E+04	6.884E+04	8.1491	27475.2
	10	2040	3371.6	.7631	1.191E-03	8.935E+04	6.883E+04	7.3059	24632.1
	11	1755	3336.2	.8903	1.208E-03	7.577E+04	6.812E+04	6.2617	20890.7
	12	1002	3230.3	1.4736	1.179E-03	4.433E+04	6.595E+04	3.7834	12221.6
SR11	1	110	766.2	3.0062	1.113E-03	5.156E+03	1.564E+04	1.8545	1420.9
	2	163	1078.7	2.9288	1.142E-03	7.450E+03	2.202E+04	1.9035	2053.3
	3	220	1325.7	2.8395	1.216E-03	9.441E+03	2.707E+04	1.9634	2602.9
	4	254	1451.7	2.7866	1.258E-03	1.053E+04	2.965E+04	2.0007	2904.4
	5	183	1149.3	2.8062	1.153E-03	8.284E+03	2.346E+04	1.9867	2283.3
	6	137	877.1	2.8864	1.163E-03	6.145E+03	1.790E+04	1.9315	1694.1
SR13	1	100	1588.0	7.1365	1.159E-03	4.510E+03	3.242E+04	.7812	1240.5
	2	155	2190.9	6.1080	1.115E-04	7.256E+03	4.472E+04	.9127	1999.7
	3	208	2650.0	5.5900	1.132E-03	9.589E+03	5.409E+04	.9973	2642.9
	4	234	2798.8	5.4634	1.178E-03	1.036E+04	5.714E+04	1.0204	2856.0
	5	184	2282.7	5.5660	1.157E-03	8.295E+03	4.660E+04	1.0016	2286.4
	6	130	1771.6	5.8040	1.099E-03	6.175E+03	3.616E+04	.9606	1701.7
	7	59	918.1	6.0703	1.003E-03	3.061E+03	1.873E+04	.9184	843.1
	8	34	620.3	6.220	8.896E-04	2.019E+03	1.265E+04	.8963	556.0

TABLE III-4 (CONTINUED)

STD. # S-20-68-2B

SR12A	1	358	294.7	.3143	9.848E-04	1.898E+04	6.012E+03	1.3038	384.3
	2	550	389.6	.3060	1.114E-03	2.576E+04	7.952E+03	1.3394	521.9
	3	785	539.5	.2882	1.082E-03	3.788E+04	1.101E+04	1.4222	767.2
	4	1338	794.2	.2590	1.126E-03	6.202E+04	1.621E+04	1.5819	1256.4
	5	1800	919.1	.2230	1.127E-03	8.338E+04	1.876E+04	1.8378	1689.1
	6	2295	999.0	.1953	1.157E-03	1.035E+05	2.039E+04	2.0987	2096.7
	7	1940	879.2	.2021	1.151E-03	8.796E+04	1.795E+04	2.0272	1782.2
SR12B	1	446	392.9	.3391	9.930E-04	2.345E+04	8.014E+03	1.2085	474.8
	2	900	608.1	.3166	1.209E-03	3.883E+04	1.242E+04	1.2943	787.0
	3	1235	793.2	.2830	1.137E-03	5.669E+04	1.619E+04	1.4479	1148.5
	4	1519	933.4	.2648	1.112E-03	7.130E+04	1.905E+04	1.5475	1444.4
	5	2055	1048.5	.2272	1.149E-03	9.335E+04	2.140E+04	1.8038	1891.3
	6	1818	943.4	.2294	1.140E-03	8.318E+04	1.926E+04	1.7865	1685.3
	7	1525	858.3	.2434	1.116E-03	7.134E+04	1.752E+04	1.6837	1445.2
	8	1140	668.1	.2508	1.104E-03	5.388E+04	1.364E+04	1.6337	1091.5
	9	310	242.7	.2685	8.840E-04	1.830E+04	4.949E+03	1.5262	370.4

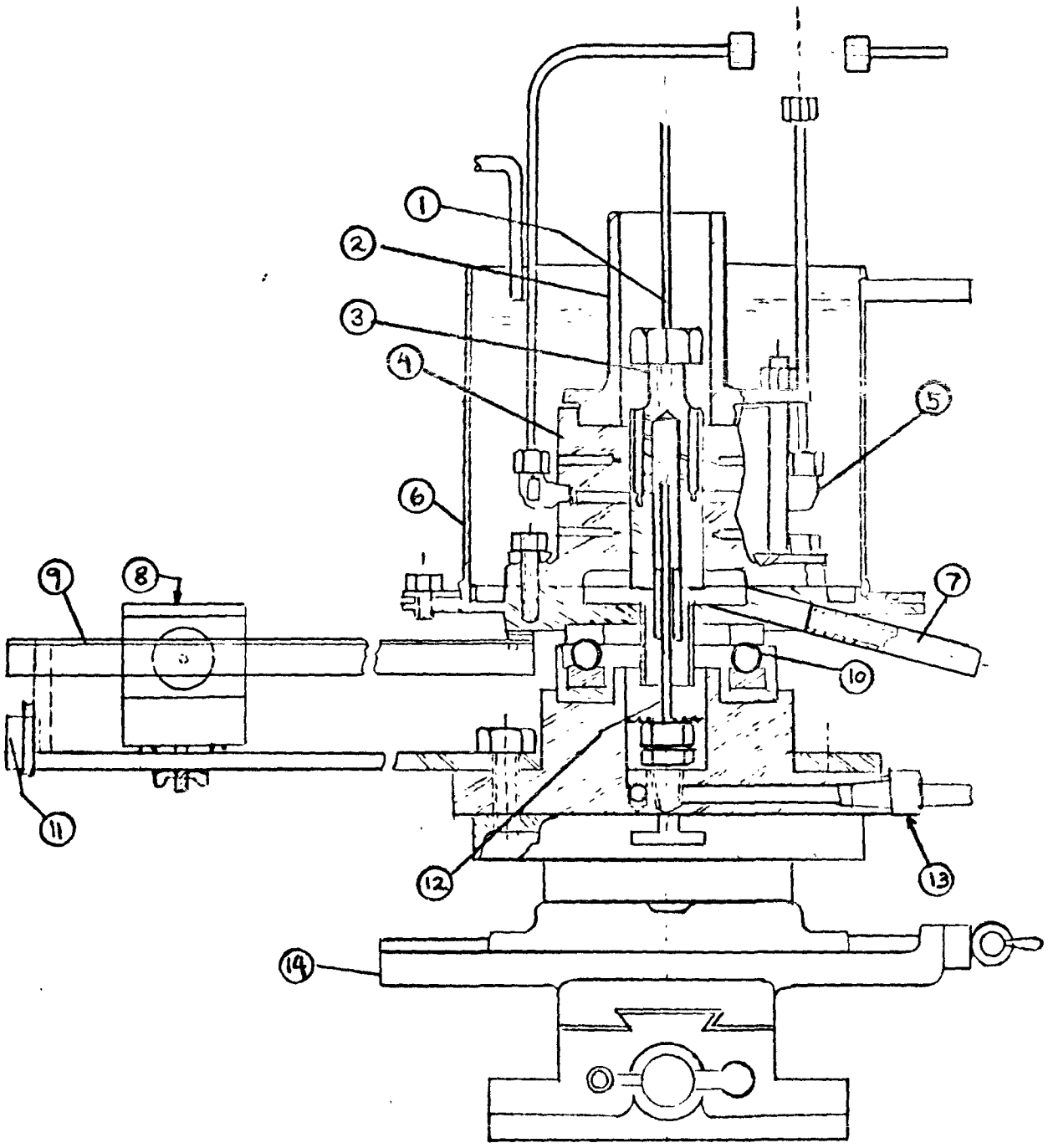

FIGURE III-1 : High Shear Viscometer

1	Flexible Drive	6	Coolant Retainer	11	Pulley
2	Cylinder Guard	7	Sample Outlet	12	Spray
3	Rotor	8	Transducer	13	Coolant Inlet
4	Stator	9	Torque Arm	14	Adjustable Table
5	Sample Inlet	10	Bearings		

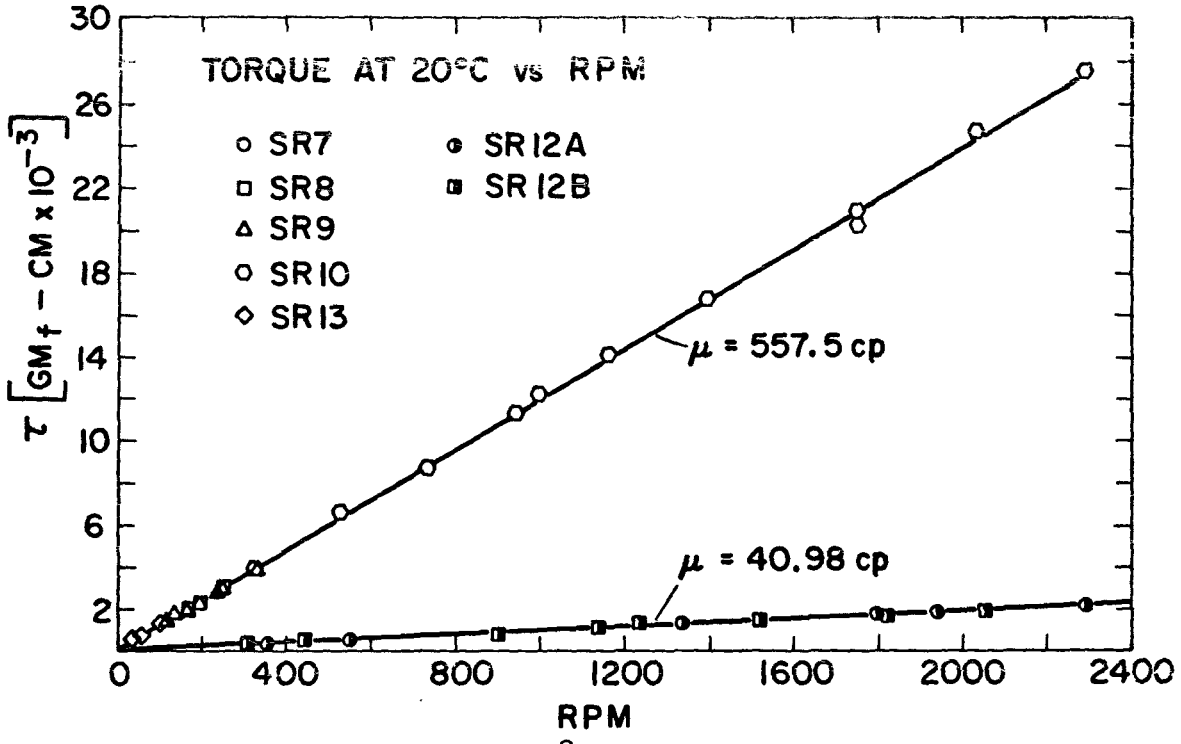

FIGURE III-2 : Torque at 20°C versus RPM for Newtonian Standards